Technology
Arts Sciences
TH Köln

HEINRICH HEINE
UNIVERSITÄT DÜSSELDORF

Pharmacological Characterization of Natural Products as Drug Candidates for the Treatment of Multidrug-Resistant Tumors

Inaugural-Dissertation

zur Erlangung des Doktorgrades
der Mathematisch-Naturwissenschaftlichen Fakultät
der Heinrich-Heine-Universität Düsseldorf

vorgelegt von

Julia Sachs
aus Wiesbaden

Köln, März 2018

aus dem Institut für Biochemie
der Heinrich-Heine-Universität Düsseldorf

durchgeführt an der Fakultät für Angewandte Naturwissenschaften,
Arbeitsgruppe „Bio-Pharmazeutische Chemie & Molekulare Pharmakologie“
der Technischen Hochschule Köln

Gedruckt mit der Genehmigung der
Mathematisch-Naturwissenschaftlichen Fakultät der
Heinrich-Heine-Universität Düsseldorf

Referent: Prof. Dr. Lutz Schmitt

Korreferent: Prof. Dr. Nicole Teusch (Technische Hochschule Köln)

Tag der mündlichen Prüfung: 16.04.2018

Meiner Familie

Abstract

Despite continuous advancements in the development and improvement of anticancer drugs and therapies, multidrug resistance (MDR) of tumor cells and tumor-associated cells constitutes a major problem for efficacious treatment of cancer patients. MDR, which describes concurrent resistance to an array of structurally and functionally unrelated drugs, leads to reduced drug efficacy and subsequent therapy failure. One mechanism of cancer MDR is the overexpression of certain ATP-binding cassette (ABC) transporters, with P-glycoprotein (P-gp, ABCB1), multidrug resistance-related protein 1 (MRP1, ABCC1) and breast cancer resistance protein (BCRP, ABCG2) being the most prominent and best studied ones. They actively translocate substrate drugs to the extracellular space, thereby preventing drugs from efficiently targeting the tumor cells. One strategy to overcome transporter-mediated MDR is inhibition of transport by non-cytotoxic small molecules. In this thesis, natural products and derivatives were screened for their ability to inhibit ABC transporters in human cancer cell lines and for their cytotoxic activity in these cells. Among the more than 200 test compounds, promising candidates were identified and further characterized.

Two derivatives of the plant secondary metabolite goniothalamin demonstrated selective inhibition of P-gp in colon carcinoma cells and were able to sensitize these cells to treatment with the chemotherapeutic drug doxorubicin. Further studies revealed an increased intracellular doxorubicin accumulation and ATPase assays as well as molecular docking studies proposed their competitive mode of P-gp inhibition. In addition, derivatives with improved cytotoxic activity compared to the natural product in different sensitive and resistant cancer cell lines were identified and structure-activity relationships (SAR) were described.

In the class of isocoumarins, three novel 3,4-dihydroisocoumarins demonstrated dual inhibition of P-gp and BCRP in colon and breast cancer cells, respectively, and could partially reverse their resistance to chemotherapy. Transporter inhibition was dependent on distinct structural features and a novel parallel SAR for both transporters was revealed.

Furthermore, novel colchicine-derived triazoles were analyzed and three derivatives with improved cytotoxicity based on increased inhibition of tubulin polymerization were identified.

Thus, these studies revealed several candidate compounds as putative starting points for future development of novel drugs for the therapy of multidrug-resistant and sensitive tumors.

Zusammenfassung

Trotz kontinuierlicher Fortschritte in der Entwicklung und Verbesserung von Medikamenten und Therapien gegen Krebs stellt die Multiresistenz von Tumorzellen und Tumor-assoziierten Zellen ein bedeutendes Problem für die effektive Behandlung von Krebspatienten dar. Multiresistenz beschreibt die gleichzeitige Resistenz gegenüber strukturell und funktionell nicht verwandten Wirkstoffen und führt zu einer reduzierten Wirkstoffeffizienz und schließlich zum Therapieversagen. Ein Mechanismus der Tumor-Multiresistenz ist die Überexpression von bestimmten ATP-Bindekassette (ABC) Transportern, wobei *P-glycoprotein* (P-gp, ABCB1), *multidrug resistance-related protein 1* (MRP1, ABCC1) und *breast cancer resistance protein* (BCRP, ABCG2) die bedeutendsten und am besten erforschten Transporter sind. Sie transportieren Wirkstoff-Substrate aktiv in den Extrazellularraum und verhindern dadurch einen wirkungsvollen Angriff auf die Tumorzellen. Eine Möglichkeit, um die durch Transporter hervorgerufene Multiresistenz pharmakologisch zu überwinden, ist die Inhibition des Transports durch nichttoxische niedermolekulare Verbindungen. In dieser Arbeit wurden Naturstoffe und Derivate bezüglich ihrer Inhibition von ABC-Transportern in humanen Tumorzelllinien sowie ihrer Zytotoxizität gescreent. Unter den über 200 Testverbindungen konnten vielversprechende Wirkstoffkandidaten identifiziert und weitergehend charakterisiert werden.

Zwei Derivate des pflanzlichen Sekundärmetaboliten Goniothalamin zeigten eine selektive Inhibition von P-gp in Darmkrebszellen und konnten diese für die Behandlung mit dem Chemotherapeutikum Doxorubicin sensitivieren. Weitere Untersuchungen zeigten eine erhöhte intrazelluläre Doxorubicin-Akkumulation und ATPase-Assays sowie molekulares Docking wiesen auf eine kompetitive Inhibition von P-gp hin. Zusätzlich wurden Derivate identifiziert, die eine verbesserte zytotoxische Aktivität als der Naturstoff in verschiedenen sensitiven und resistenten Tumorzelllinien aufwiesen und Struktur-Aktivitäts-Beziehungen konnten beschrieben werden.

In der Klasse der Isocoumarine zeigten zwei neue 3,4-Dihydroisocoumarine eine duale Inhibition von P-gp und BCRP in Darm- beziehungsweise Brustkrebszellen und konnten die Chemotherapieresistenz dieser Zellen zum Teil aufheben. Die Inhibition der Transporter war von bestimmten Strukturmerkmalen abhängig und parallele Struktur-Aktivitäts-Beziehungen für beide Transporter wurden aufgezeigt.

Des Weiteren wurden neue von Colchicin abgeleitete Triazole untersucht und drei Derivate gefunden, die im Vergleich zum Naturstoff eine erhöhte Zytotoxizität aufwiesen, welche auf einer stärkeren Inhibition der Tubulin-Polymerisation beruhte.

Somit konnten durch die im Rahmen dieser Dissertation durchgeführten Untersuchungen Kandidaten unterschiedlicher Naturstoffklassen identifiziert werden, die als mögliche Ausgangspunkte für die weitere Entwicklung von neuen Wirkstoffen zur Behandlung von multiresistenten sowie sensitiven Tumoren dienen können.

Table of Contents

List of Figures

List of Tables

List of Abbreviations

ABC	ATP-binding cassette
ADME	absorption, distribution, metabolism, excretion (of drugs)
AML	acute myeloid leukemia
ATP	adenosine triphosphate
BCRP	breast cancer resistance protein
Cdr1p	*Candida* drug resistance protein 1
Cdr2p	*Candida* drug resistance protein 2
CFTR	cystic fibrosis transmembrane conductance regulator
C_q	threshold cycle
CYP	cytochrome P450
DNA	deoxyribonucleic acid
FDA	United States Food and Drug Administration
GAPDH	glyceraldehyde 3-phosphate dehydrogenase
GSH	glutathione
MDR	multidrug resistance
MDR1	multidrug resistance protein 1
MHC	major histocompatibility complex
mRNA	messenger RNA
MRP	multidrug resistance-related protein
NBD	nucleotide-binding domain
NF-κB	nuclear factor kappa B
PCR	polymerase chain reaction
Pgh1	P-glycoprotein homologue 1
P-gp	P-glycoprotein
qPCR	quantitative real-time PCR
RNA	ribonucleic acid
ROS	reactive oxygen species
SAR	structure-activity relationship
SD	standard deviation
SEM	standard error of the mean
siRNA	short interfering RNA
TAP	transporter associated with antigen processing
TBS	*tert*-butyldimethylsilyl
TKI	tyrosine kinase inhibitor
TMD	transmembrane domain

1 Introduction

1.1 Cancer

Cancer is defined as a group of related diseases, which all involve abnormal cell growth and the potential to invade surrounding tissues and other body parts. More than 100 distinct types of cancer are known and subtypes of cancer exist in specific organs. Despite the complexity and heterogeneity, there are certain principles which lead to malignant transformation of normal cells and are possibly shared by all types of cancer: the six hallmarks of cancer as proposed by Hanahan and Weinberg in 2000 [1]. They are 1) self-sufficiency in growth signals, 2) insensitivity to anti-growth signals, 3) evading apoptosis, 4) limitless replicative potential, 5) sustained angiogenesis, and 6) tissue invasion and metastasis. During the multistep process of tumorigenesis, cells gain these capabilities by emergence of genomic instability accompanied by dynamic changes in their genome [2].

According to the latest Global Burden of Disease Study, the number of new cancer cases worldwide was 17.5 million in 2015 and there were 8.7 million cancer deaths, representing cancer the second common cause of death after cardiovascular diseases [3]. Despite emerging progress in cancer prognosis and treatment, these numbers are constantly rising, mainly due to population growth and increased life expectancy. In Germany, the number of new cancer cases was 476 120 and the number of cancer deaths was 222 972 in 2014 [4].

1.2 Multidrug Resistance (MDR)

During the last years, constant progress in developing novel drugs for effective cancer treatment has been made and especially targeted and patient-specific therapies as well as immunotherapies were in the focus of research. Nonetheless, emergence of resistance mechanisms and multidrug resistance (MDR) in tumors poses a major problem in cancer therapy. The phenomenon of MDR describes resistance to diverse drugs which are structurally and functionally not related, which leads to treatment failure and increases cancer death rates. It is estimated that MDR causes treatment failure in about 90% of patients with metastatic tumors [5]. Therapy resistance of tumors can be intrinsic or acquired during the therapy and multiple mechanism mediating resistance are known [6,7]. They include increased drug efflux or decreased drug uptake, drug sequestration, mutations in drug targets,

target overexpression, inhibition of apoptosis pathways, increased drug metabolism or activation of DNA repair mechanisms (Figure 1).

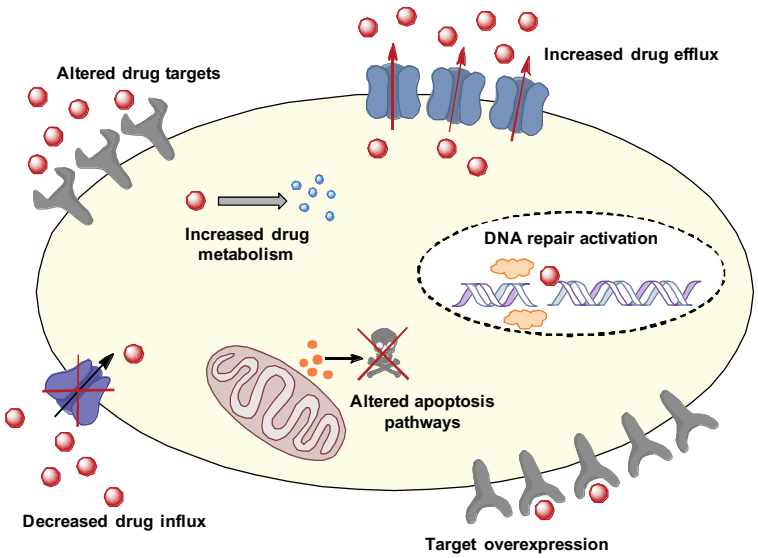

Figure 1. Mechanisms of drug resistance in cancer cells. Different mechanisms contributing to the development of drug resistance in tumors.

Probably the most important and most prevalent resistance mechanism is the overexpression of certain ATP-binding cassette (ABC) transporters, which mediate resistance by actively transporting drugs out of cells, thus inhibiting intracellular drug accumulation and impairing drug activity and efficacy [8]. This phenomenon was first described in 1973 by Danø [9].

1.3 ATP-Binding Cassette (ABC) Transporters

1.3.1 General Structure and Function

The ABC transporter superfamily represents one of the largest and oldest protein families with members in all kingdoms of life [10]. In humans, there are 49 transporters, which are divided into seven subgroups A to G based on sequence homology and gene structure [11]. The active translocation of substrates across membranes of cells and organelles coupled to ATP hydrolysis, which provides the energy for the process, is common for all ABC transporters [12]. Transport is usually against the substrate's concentration gradient. While prokaryotic ABC transporters can be divided into importers and exporters, most eukaryotic ABC transporters are exporters. The substrate spectrum of ABC transporters is broad, ranging from small molecules, like ions, amino acids or sugars, to large peptides, lipids and proteins [11].

The general structure of ABC transporters consists of four functional domains in two homologous halves, each containing one transmembrane domain (TMD) and one nucleotide-binding domain (NBD, the eponymous ATP-binding cassette). Eukaryotic full transporters encode all four units as one polypeptide, whereas half transporters express one TMD and one NBD as a single peptide and need to dimerize (homodimers or heterodimers) for functionality [13].

The NBDs bind and hydrolyze ATP and contain several highly conserved motifs, making them the hallmark of the transporter family [14,15]. The Walker A motif binds the γ-phosphate of ATP, the Walker B motif is essential for attack of the water molecule and hydrolysis, the signature motif (C-loop, LSGGQ) is involved in ATP binding and interaction between the two NBDs [16]. Two ATP molecules are positioned between the Walker A motif of one NBD and the signature motif of the second NBD, respectively [17,18]. Additional conserved motifs are involved in ATP binding and hydrolysis or communication between the NBDs or NBD and TMD [16].

In contrast to the NBDs, the TMDs of different transporters do not share significant sequence similarities. TMDs consist of six to ten α-helices and the two TMDs of a transporter form two bundles and constitute the translocation pathway, which is located at their interface and open to one side [19]. Through conformational rearrangements, the transporter switches between inward-facing and outward-facing conformation (alternating access) [20–22].

To date, the transport mechanism of ABC transporters has not been fully elucidated and there are different hypotheses concerning interplay and sequence of ATP- and substrate-binding, ATP hydrolysis, conformational changes and substrate release [23]. One is the ATP switch model [24]. According to this model, substrates enter the translocation pathway of the transporter in its inwards-facing conformation either from the cytoplasm or the inner leaflet of the membrane and bind to a high-affinity substrate-binding site. Binding causes conformational changes and a switch in the NBDs from low-affinity to high-affinity for ATP. Upon binding of two ATP molecules, the NBDs change from the open to the closed dimer configuration. Either ATP-binding or dimerization are supposed to be the “power stroke” for changes in the TMD conformation to the outward-facing conformation accompanied by lowered affinity of the substrate-binding site and in turn substrate release. ATP hydrolysis and dissociation then returns the transporter to its original state. Another model, the reciprocating twin-channel model or constant contact model, describes alternation of substrate translocation

and ATP hydrolysis between the two functionally separate halves of the transporter without complete dissociation of the NBDs [25,26].

1.3.2 Roles in Human Health and Disease

ABC transporters have important roles for human health and tissue homeostasis. They are expressed in various tissues throughout the human body, where they facilitate the transport of endogenous substrates as well as xenobiotics [27,28]. Endogenous substrates include lipids, amino acids, bile salts and sugars and their transport contributes to homeostasis. Furthermore, ABC transporters are expressed in barrier tissues, like the blood-brain barrier, placenta, liver, kidneys and the gastrointestinal tract. In these tissues, they transport endogenous as well as exogenous toxic substrates to protect the body or inhibit the penetration of drugs and toxins into sensitive compartments like the brain or the fetus. In the gastrointestinal tract, ABC transporters inhibit absorption of drugs and toxic compounds, whereas in the liver and kidney, their excretion is promoted [29]. Hence, they support a chemoimmunity defense system of the body [30]. Besides protection against harmful compounds, ABC transporters also modulate absorption, distribution, metabolism and excretion (ADME) of pharmacological agents. ABC transporters at the apical membrane of the small intestine epithelium contribute to poor absorption and low bioavailability of orally administered drugs. The major transporters there are P-gp, MRP2, MRP4 and BCRP [31]. The influence of ABC transporters on drug distribution is particularly striking at the blood-brain barrier, where transporters like P-gp, MRP1 and BCRP on one hand protect the brain from potentially toxic agents, but on the other hand limit penetration of drugs targeting the central nervous system [32]. P-gp and cytochrome P450 (CYP) 3A4, a major enzyme of phase I drug metabolism, have overlapping substrate specificities and can be induced by the same signaling pathways. A dynamic interplay between both proteins in ADME was demonstrated [33]. ABC transporters expressed in liver and kidney are important mediators of biliary and renal elimination of drugs and metabolites [34]. Having this in mind, it is not unexpected that drug-drug interactions and food-drug interactions might be mediated by ABC transporters and can lead to altered drug ADME, undesirable side effects or even toxicity. Therefore, investigation of drug-transporter interactions is critical for drug design and development and are an integral part of guidelines of drug regulatory agencies [35].

Apart from this, further functions of ABC transporters in regulating homoeostasis are known. Their expression in stem cells contributes to stem cell integrity, differentiation and tissue regeneration [36,37]. Moreover, ABC transporters play a role in immune function.

TAP1 (ABCB2) and TAP2 (ABCB3) are part of the macromolecular complex that loads peptides onto MHC class I molecules for antigen presentation to cytotoxic T-cells. Thus, TAP1 and TAP2 are indispensable for proper immune function [38]. Furthermore, their downregulation contributes to immune evasion of cancer cells [39].

Defects in ABC transporters are associated with distinct human hereditary diseases. Probably the most prominent example is cystic fibrosis, which is caused by mutations of the cystic fibrosis transmembrane conductance regulator (CFTR, ABCC7). CFTR is an atypical ABC transporter. It does not transport substrates, but is rather an ATP-gated chloride and bicarbonate channel [40,41]. Other conditions and associated transporters are Tangier disease (familial alpha-lipoprotein deficiency; ABCA1) [42], Stargardt disease (juvenile macular dystrophy; ABCA4) [43] and progressive familial intrahepatic cholestasis type 2 and 3 (ABCB11, ABCB4) [44,45].

Not only human ABC transporters affect human health. ABC transporter overexpression in pathogens like bacteria, fungi or parasites can confer drug resistance [46]. In *Plasmodium falciparum*, one of the malaria pathogens, overexpression of the P-glycoprotein homologue Pgh1 is associated with resistance to the drug mefloquine [47]. Fungi of the *Candida* genus cause opportunistic infections (candidiasis), which especially threaten immunocompromised patients. Resistance to widely used antifungal azoles is frequently caused by Cdr1p- and Cdr2p-mediated drug efflux in *Candida albicans* [48,49].

1.3.3 ABC Transporters and Cancer

As mentioned in chapter 1.2, ABC transporters are key mediators of cancer MDR. In this context, three ABC transporters are most frequently overexpressed and have therefore been in the focus of extensive studies since their discovery: P-glycoprotein (P-gp, ABCB1), multidrug resistance-associated protein 1 (MRP1, ABCC1) and breast cancer resistance protein (BCRP, ABCG2) [46]. They will be introduced in the following chapters. Upregulation of these transporters can also be observed in cancer stem cells, which are important for metastasis and recurrence of the disease, as well as tumor-associated cells of the tumor microenvironment, including tumor endothelial cells [50,51]. In cancer cell lines, upregulation of transporter expression can be induced by continuous treatment with chemotherapeutic drugs, which serves as an *in vitro* model for acquired resistance [52–54]. *In vivo*, acquired resistance can also be recapitulated by intermittent or continuous drug treatment [55].

Several more ABC transporters have been identified as anticancer drug transporters and associated with resistance, especially members of the ABCC family, but their clinical implications have not been fully clarified yet. In addition, studies focusing on profiling ABC transporter expression in cancer cell lines or patient tumor samples were performed, aiming at identifying further transporters mediating MDR [56–58].

Numerous studies have been performed with the aim of correlating ABC transporter expression in tumor samples of different entities before or after treatment with clinical drug resistance and treatment response, but the assessment proved to be difficult and results were sometimes inconsistent. Reasons are heterogeneity of clinical samples, lack of standard protocols for expression analysis and the possible cooperation of different mechanisms mediating resistance in a single tumor [59,60].

ABC transporters do not solely influence drug efflux and resistance in cancer cells. Studies have demonstrated that ABC transporters might contribute to some of the hallmarks of cancer (see 1.1), mediate tumor progression and influence tumor metabolism and the tumor microenvironment by controlling the release of signaling molecules and metabolites [61,62]. In several studies, ABC transporter expression in tumors of different origin could be associated with differentiation status of cancer cells and disease progression and aggressiveness independent from drug efflux [63–65].

1.4 P-glycoprotein (P-gp)

P-gp (MDR1, ABCB1), the first eukaryotic ABC transporter described and probably the best studied one to date, is a 170 kDA protein (1280 amino acids) expressed in the cell membrane. It was discovered in 1976 by Juliano and Ling in colchicine-resistant Chinese hamster ovary cells, which exhibited cross-resistance to several other anticancer drugs [66]. The structure of P-gp is depicted in Figure 2. It has two homologues halves with one TMD and one NBD each, which are encoded as one single polypeptide. Each TMD is composed of six α-helices [67,68]. The translocation pathway between TMD1 and TMD2 is open to the cytoplasm and the inner leaflet of the membrane. The crystal structure of human P-gp has not been obtained yet. In February 2018, the structure of a human-mouse chimeric P-gp in complex with the monoclonal antibody UIC2 and two molecules of the inhibitor zosuquidar was resolved [69]. The chimeric transporter consists of the human extracellular region and the mouse intracellular region and shares around 90% sequence identity with the human protein.

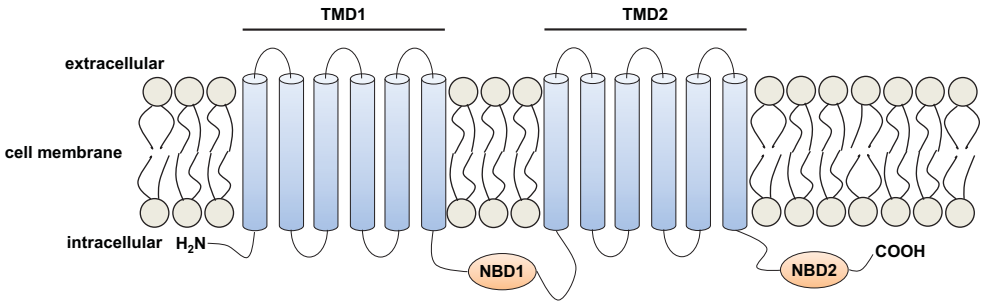

Figure 2. Topology model of human P-gp. The full transporter P-gp consists of one polypeptide divided into two TMDs and two NBDs.

In the drug-binding pocket of P-gp, proposed as a central cavity at the interface of TMD1 and TMD2, at least four distinct drug-binding sites have been identified [67,70,71]. Their partial overlapping and poly-specificity might help to explain the broad range of compounds that interact with P-gp. Furthermore, a substrate-induced fit mechanism was supposed with flexible binding sites that adjust to the bound molecule [72]. P-gp substrates are in general organic molecules with a molecular weight between 200 Da and 1900 Da. Substrates can be aromatic, linear or circular, neutral or cationic. Most substrates are weakly amphiphatic and relatively hydrophobic [73,74]. Regarding this great molecular variety, it is not surprising that P-gp transports a wide variety of commonly used drugs and that its overexpression in tumor cells mediates MDR against a broad spectrum of anticancer drugs. A selection of P-gp drug substrates is listed in Table 1.

Table 1. Selection of clinically relevant P-gp drug substrates. Example drugs were taken from [75] and [76].

Drug type	Examples
Anticancer drugs	Cisplatin
	Daunorubicin
	Doxorubicin
	Etoposide
	Gefitinib
	Imatinib
	Mitoxantrone
	Paclitaxel
	Vinblastine
Immunosuppressants	Cyclosporine A
	Sirolimus
	Tacrolimus
	Valspodar (PSC833)
Statins	Lovastatin
	Simvastatin
Antibiotics	Erythromycin
	Rifampin

	Tetracycline
Antivirals	Ritonavir
	Saquinavir
Antidepressants	Fluoxetine
Antiarrhythmics	Digoxin
	Propafenone
	Verapamil
Antimycotics	Ketoconazole
Opioids	Methadone
	Morphine

In healthy tissues, P-gp is normally highly expressed at apical membranes in organs with barrier function, including liver, kidneys, small intestine, colon, blood-brain barrier and placenta, where its main role is protection against toxic xenobiotics and endogenous compounds, such as lipids, bile acids, bilirubin and steroids [77,78].

Overexpression of P-gp in cancer cells confers strong resistance to the widest variety of chemotherapeutic drugs, including anthracyclines, taxanes, *Vinca* alkaloids, epipodophyllotoxins and tyrosine kinase inhibitors (Table 1). Regarding the clinical relevance of P-gp expression, early studies in the 1980s revealed frequent overexpression associated with treatment failure in tumors of the liver, kidney and colon, tissues with an intrinsically high P-gp expression [79,80]. In acute myeloid leukemia (AML), P-gp expression in leukemia cells was found in about 30% of patients with initial disease and in about 50% of patient with relapsed disease and has been associated with reduced treatment response and poor survival. In addition, the P-gp expression increased with patient age [81,82]. In solid tumors like breast or lung cancer, study results about P-gp as a prognostic factor were often inconsistent and no clear correlations to tumor response and patient survival could be identified [60].

1.5 Multidrug Resistance-Related Protein 1 (MRP1)

In 1992, MRP1 (ABCC1) was discovered in a multidrug-resistant small cell lung cancer cell line selected by continuous doxorubicin treatment [83]. MRP1 is a 190 kDa protein (1531 amino acids) with a structure similar to that of P-gp, but it has an additional N-terminal TMD (TMD0) composed of five α-helices (Figure 3). TMD0 does not contribute to substrate translocation; it rather seems to be necessary for membrane localization of the transporter [84,85]. In 2017, the crystal structure of bovine MRP1, which shares 91% sequence identity with human MRP1, was obtained by Johnson and Chen, leading to the observation of a single

bipartite drug-binding site, which is able to recognize diverse substrates and is only accessible from the cytoplasm [86].

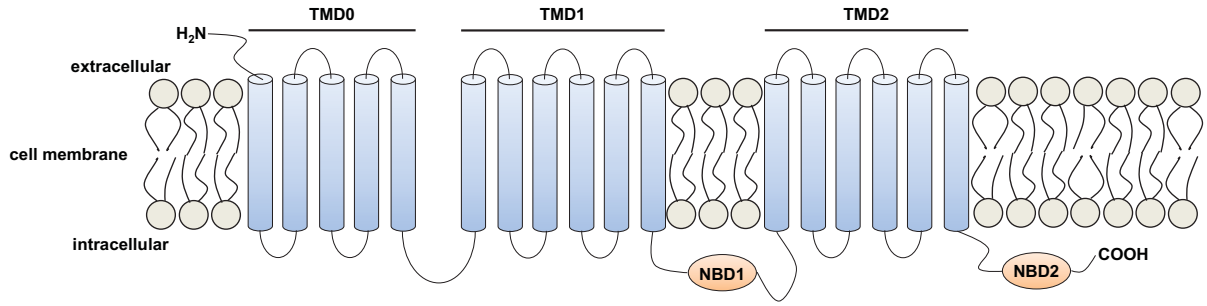

Figure 3. Topology model of human MRP1. The full transporter MRP1 consists of one polypeptide divided into three TMDs and two NBDs.

MRP1 is ubiquitously expressed, with highest levels at basolateral membranes of kidney, colon, small intestine, lung, blood-brain barrier, heart and skeletal muscles, breast, testes and placenta [87]. Like P-gp, physiological role of MRP1 is protection against xenobiotics, but the substrate spectrum of both transporters is different. MRP1 is able to transport organic anions and compounds conjugated with glutathione (GSH), glucuronic acid or sulfate, which are typical products of phase II metabolizing enzymes [88]. Furthermore, efflux of some substrates by MRP1 is only possible in co-transport with GSH [89]. Clinically relevant drug substrates of MRP1 are listed in Table 2.

Table 2. Selection of clinically relevant MRP1 drug substrates. Example drugs were taken from [90] and [91].

Drug type	Examples
Anticancer drugs	Daunorubicin
	Doxorubicin
	Etoposide
	Imatinib
	Methotrexate
	Vinblastine
Statins	Atorvastatin
	Rosuvastatin
Antibiotics	Ciprofloxacin
	Grepafloxacin
Antivirals	Ritonavir
	Saquinavir

Similar to P-gp, overexpression of MRP1 in cancer cells leads to resistance against different chemotherapeutic drugs. Several studies have revealed a high expression rate of MRP1 in lung and breast cancer samples, but as for P-gp, correlation of expression and

clinical prognosis has been difficult and often controversial [92–95]. Only in primary untreated pediatric neuroblastoma, MRP1 serves as a prognostic factor. Here, high levels of MRP1 are an independent indicator for therapy resistance and poor outcome [96].

1.6 Breast Cancer Resistance Protein (BCRP)

BCRP, the "youngest" of the three ABC transporters discussed here, is a 72 kDA protein (655 amino acids) and was discovered independently by three groups in the late 1990s. In 1998, it was identified in multidrug-resistant MCF-7 breast cancer cells generated by treatment with doxorubicin and verapamil as well as in the placenta [97,98]. One year later, BCRP was found in tumor cell lines resistant to mitoxantrone [99]. In June 2017, the crystal structure of human BCRP was resolved by Taylor and colleagues [100]. BCRP is a half transporter and is composed of one TMD with six membrane-spanning α-helices and one NBD (Figure 4). In contrast to P-gp and MRP1, the NBD of BCRP is at the N-terminal end of the peptide. Transporter dimerization is required for functionality.

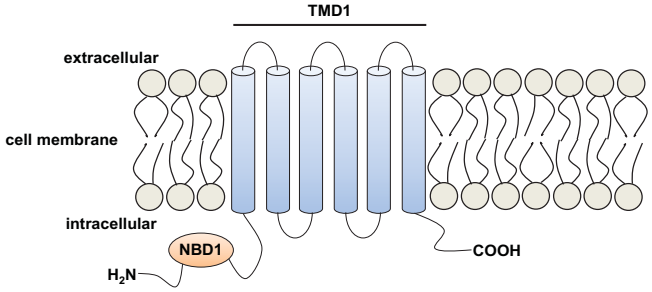

Figure 4. Topology model of human BCRP. The half transporter BCRP consists of one TMD and one NBD. Transporter dimerization is necessary for functionality.

The translocation pathway consists of two cavities, but only cavity 1 is accessible from the cytoplasm and the inner leaflet of the membrane in the inward-facing state. It was proposed that the substrate enters cavity 1 and upon binding of ATP and conformational change to the outward-facing state, the substrate moves to cavity 2 and gets expelled [100]. As for P-gp, BCRP is supposed to possess multiple poly-specific substrate-binding sites, but in contrast, it was proposed that they are symmetric in each monomer and demonstrate allosteric communication between them [101]. Latest molecular docking studies from October 2017 verified this symmetry and revealed three distinct drug-binding sites [102].

In normal human tissues, BCRP is highly expressed in apical membranes in placenta, liver, small intestine, colon, breast and blood-brain barrier, where it is involved in tissue defense

and protection [29,103]. In addition, hematopoietic progenitor cells and stem cells of other organs express BCRP [36]. BCRP has a broad substrate spectrum, partially overlapping with P-gp and MRP1 and transports a wide variety of endogenous compounds and xenobiotics. They can be unmodified or sulfate and glucuronide conjugates [104]. Some clinically relevant drug substrates are listed in Table 3.

Table 3. Selection of clinically relevant BCRP drug substrates. Example drugs were taken from [75] and [104].

Drug type	Examples
Anticancer drugs	Bisantrene
	Doxorubicin
	Imatinib
	Methotrexate
	Mitoxantrone
	SN-38
	Topotecan
Statins	Pravastatin
	Rosuvastatin
Antibiotics	Ciprofloxacin
	Norfloxacin
Antivirals	Lamivudine
	Nelfinavir
	Zidovudine

Overexpression of BCRP in cancer cells mediates resistance to various drugs used in cancer treatment (Table 3). As for P-gp and MRP1, correlation of transporter expression with therapy response or outcome in tumors has been difficult and controversial [105]. BCRP is expressed in different stem cells and was also detected in putative cancer stem cells, which are usually therapy-resistant [106]. However, it remains unclear if BCRP plays a role in maintaining stemness of cancer cells [107].

1.7 Modulation of ABC Transporters

Since the discovery of ABC transporters and the characterization of their roles in cancer MDR, the search for therapies to treat multidrug-resistant tumors has been in the focus of anticancer research.

1.7.1 Inhibition of ABC Transporter Activity

The first strategy to overcome transporter-mediated MDR was the development of ideally non-toxic, selective inhibitors of transport activity. Combination of these inhibitors with

chemotherapeutic drugs would enhance intracellular drug accumulation and efficacy, thereby reversing the resistance of the tumors.

The largest number of inhibitors has been described against P-gp. The calcium channel blocker verapamil, widely used for treatment of hypertension, arrhythmia and coronary heart disease, was the first drug identified as P-gp inhibitor in 1981 [108]. It competitively inhibits P-gp as an alternative substrate in the low micromolar range with an inhibitory constant 4- to 5-times lower compared to its primary target, the L-type calcium channel [109,110]. Other so-called first generation inhibitors, established pharmacological agents, are cyclosporine A (immunosuppressant) and quinidine (antiarrhythmic) [111,112]. Although they exhibited promising activities in preclinical studies, most clinical trials were not successful and had to be stopped in phase II [113,114]. This was due to toxic side effects, immunosuppression, low efficacy and unspecific inhibition of other ABC transporters. The second generation P-gp inhibitors were mainly derivatives of the first generation compounds, for example, valspodar (PSC833), a non-immunosuppressive analogue of cyclosporine A, and biricodar (VX-710) [115,116]. They proved to be more selective for P-gp and inhibit its transport activity in the high nanomolar range combined with less cytotoxic activity. Nevertheless, they did not improve outcome of patients with, for example, leukemia, lung, breast, ovarian or prostate cancer in clinical trials and failed because of unfavorable pharmacokinetic interactions caused by inhibition of CYP enzymes and subsequent systemic toxicity [117–120]. Third generation inhibitors were designed based on quantitative structure-activity relationship (SAR) studies and combinatorial chemistry to improve P-gp selectivity and reduce interaction with CYP enzymes with the aim to overcome the limitations of the previous generations. Examples are zosuquidar (LY335979), tariquidar (XR-9576) and laniquidar (R101933) [121–123]. Despite promising results of *in vitro* and *in vivo* studies, clinical trials revealed only limited or no clinical activity in the treatment of cancer patients [124,125]. Latest P-gp inhibiting compounds, the fourth generation, are mostly compounds derived from natural sources (see 1.8) and approved anticancer drugs like tyrosine kinase inhibitors (TKIs), for example, imatinib and nilotinib [126,127].

As for P-gp, the search for inhibitors of MRP1-mediated and BCRP-mediated drug efflux has been going on since their discovery. In case of MRP1, no candidate compound to enter clinical studies has been identified so far. Most inhibitors lack specificity for MRP1 and display cross-inhibition of other ABC transporters or organic anion transporters or their potency of inhibition is not sufficient for clinical application [91]. Examples are biricodar, the

quinoline derivative MK-571, which inhibits most MRP homologs, general inhibitors of organic anion transporters, like probenecid and sulfinpyrazone, and tricyclic isoxazoles (LY402913, LY475776) [128–131].

One of the first specific BCRP inhibitors was the mycotoxin fumitremorgin C, but its use in patients is hindered by its intrinsic neurotoxic effects [132]. Derivatives of fumitremorgin C were synthesized and Ko143 was identified as a highly potent and specific inhibitor with minimal toxicity [133]. Unspecific BCRP inhibitors include the P-gp inhibitors elacridar and tariquidar and the P-gp and MPR1 inhibitor biricodar [134–136]. Furthermore, several natural products (see 1.8) and TKIs have been identified as inhibitors of MRP1 and BCRP transport function in recent years [126,127]. In a clinical trial in 2014, the TKI sorafenib showed promising activities when combined with irinotecan in patients with metastatic colorectal cancer, which can in part be attributed to the inhibition of BCRP [137].

1.7.2 Alternative Approaches to Target MDR

Besides direct inhibition of ABC transporter function, several other approaches to reverse cancer MDR and to target resistant cancer cells have been proposed and evaluated *in vitro* and *in vivo*.

One strategy is targeting ABC transporters by using monoclonal antibodies. Especially several P-gp targeting antibodies have been evaluated. On the one hand, it has been demonstrated that binding of these antibodies to extracellular epitopes of the transporter inhibits its transport function by interfering with conformational changes crucial for substrate translocation [138–140]. On the other hand, attraction of immune cells for cell killing has been shown in cervical carcinoma cells *in vitro* and *in vivo* [141].

Another approach is to interfere with ABC transporter expression via different mechanisms, including microRNAs, RNA interference with siRNAs or compounds, which inhibit or down-regulate expression, for example, by targeting certain signaling pathways [142]. Inhibitors of expression might as well be useful to prevent the development of MDR when applied already at the beginning of chemotherapy [55].

Several studies focused on the development of novel cancer therapeutics, which are not substrates of ABC transporters and might therefore successfully target resistant cancer cells. Examples are the microtubule-targeting epothilones and second generation taxanes [143–146]. Another possibility to evade efflux or to specifically target MDR cells is encapsulation

of anticancer drugs or drug-inhibitor combinations in nanoparticles or liposomal formulations [147].

Noteworthy, ABC transporter overexpressing cancer cells exhibit the phenomenon of collateral sensitivity, which describes hypersensitivity of these cells to certain compounds compared to sensitive tumor cells [148–150]. It has been hypothesized that overexpression of ABC transporters renders cancer cells more sensitive to reactive oxygen species (ROS), changes in energy levels, membrane perturbation or to extrusion of endogenous substrates [151]. Therefore, identification and further development of drugs that specifically target resistant cancer cells might be another useful strategy to overcome MDR.

1.8 Natural Products in Drug Discovery and Development

Nature represents a vast source of compounds for the development of therapeutics against different conditions. Organisms, such as plants, bacteria, marine invertebrates or fungi, produce secondary metabolites mainly for defense, interaction or attraction of other organisms [152]. For centuries, traditional herbal medicine has been used to treat various conditions and in certain regions and cultures, they still play an important role. In modern drug research, natural products often serve as lead structure for further drug development and optimization [153,154]. Of all small-molecule drugs approved worldwide between 1981 and 2014, only 35% were not inspired by a natural product. Regarding exclusively small-molecule anticancer drugs, the percentage of truly synthetic ones even drops to 17%, highlighting the importance of natural products in cancer drug discovery [155]. Successful and widely used anticancer agents derived from natural products include paclitaxel [156], *Vinca* alkaloids [157] and doxorubicin [158].

The search for inhibitors of ABC transporters mediating resistance in cancer revealed several natural products as potent drug candidates [159,160]. Curcuminoids from turmeric powder of *Curcuma longa* and derivatives, especially curcumin, demonstrate inhibitory activity towards P-gp, MRP and BCRP [161–163]. Noteworthy, curcumin is one of the most extensively studied natural compounds with anticancer activities and is currently evaluated in several clinical trials. Cyclosporin A is an immunosuppressive peptide drug produced by the fungus *Tolypocladium inflatum* [164,165]. In addition, it was identified as an early P-gp inhibitor with high-affinity binding capacity to P-gp (see 1.7.1). Fumitremorgin C, a mycotoxin produced by *Aspergillus fumigatus*, was one of the first identified inhibitors of

BCRP [166]. Moreover, numerous nutritional components have been screened for their ability to inhibit ABC transporter activity [167–169].

In the present thesis, different classes of natural compounds were studied. They are briefly introduced in the following sections.

1.8.1 Goniothalamin

The secondary metabolite goniothalamin (Figure 5), a six-membered styryl-lactone, was first isolated from the plant *Cryptocarya caloneura* in 1967 by Hlubucek and Robertson [170]. It can primarily be found in Southeast Asian plants of the *Goniothalamus* genus [171,172]. *Goniothalamus* is a large genus of paleotropical Annonaceae and comprises over 160 species. In traditional medicine, *Goniothalamus* species have long been used to treat various conditions, for example, fever, scabies, swellings and rheumatism [173].

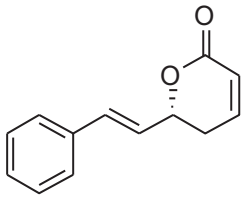

Figure 5. Structure of (*R*)-(+)-goniothalamin.

Since the late 1990s, the pharmacological activities of goniothalamin have been studied and activities against bacteria [174], fungi [175], *Trypanosoma* [176], *Plasmodium* [177] and various cancer types were identified [178–182].

Effects in cancer cells and mechanisms of action have been further elucidated. In different cancer cell lines, induction of apoptosis through caspase activation and cell cycle arrest were shown [181,183]. In addition, goniothalamin inhibits migration of lung cancer cells and induces production of ROS [179,184]. *In vivo*, delay of tumor development and tumor progression were demonstrated in mouse models of transgenic prostate carcinoma and of colitis-induced and sporadic colon carcinomas [185,186]. In both models, goniothalamin mainly repressed tumorigenesis by decreasing expression of pro-inflammatory mediators in tumor tissue and microenvironment. Anti-inflammatory activities of goniothalamin have been demonstrated *in vitro* in cancer cells as well as immune cells [187,188].

Goniothalamin and its activities have primarily been studied in sensitive cancer cell lines. Regarding MDR, only two P-gp expressing cell lines were employed in cytotoxicity assays. Tian and colleagues analyzed the cytotoxicity of goniothalamin and two additional styryl-

lactones on parental HepG2 and doxorubicin-resistant HepG2-R hepatocellular carcinoma cells. They demonstrated goniothalamin to be equally effective in killing both cell lines [189]. The resistant ovarian carcinoma cell line NCI-ADR/RES was used in several studies, in which goniothalamin and novel derivatives were analyzed for cytotoxicity or antiproliferative activity [178,180,190,191]. They demonstrated the toxicity of goniothalamin in this cell line and identified derivatives with improved potency. Derivatives with improved cytotoxic activity were also identified in sensitive cancer cell lines, for example, N-acylated aza-goniothalamin derivatives [191].

Studies on goniothalamin and derivatives in this thesis focused on one hand on the elucidation of cytotoxicity in different sensitive and resistant cancer cell lines with overexpression of P-gp, MRP1 and BCRP. Moreover, the influence of goniothalamins on the transport function of these ABC transporters was analyzed for the first time [192,193].

1.8.2 Isocoumarins

Isocoumarins are isomers of coumarin, possessing an inverted lactone ring (Figure 6). These secondary metabolites are abundant in bacteria, fungi, lichens, marine sponges and to a lesser extent in higher plants. To date, around 400 isocoumarins and dihydroisocoumarins have been isolated from natural sources, many of them exhibiting diverse biological and pharmacological activities [194]. Recently isolated isocoumarins and dihydroisocoumarins are flavoroseoside from the fungus *Malbranchea flavorosea* and orychophramarin A-D from seeds of *Orychophragmus violaceus* [195,196]. Orychophramarin A demonstrated induction of apoptosis and cell cycle arrest in HCT-116 colon carcinoma cells *in vitro* [196].

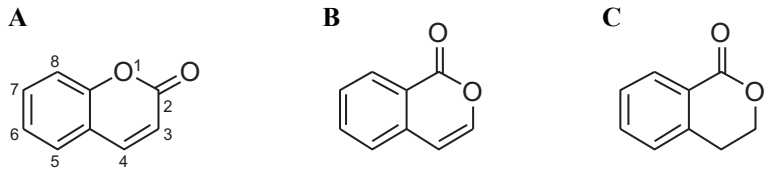

Figure 6. Structures of (A) coumarin, (B) isocoumarin and (C) 3,4-dihydroisocoumarin.

Due to the large structural diversity of natural and synthetic isocoumarin compounds, a great variety of activities has been observed. Among them are anticancer effects, such as cytotoxicity and inhibition of metastasis [197–200], antibacterial, antifungal and antimalarial activities [201–203], enzyme inhibition [204,205] and inhibition of inflammation [206,207].

One isocoumarin compound, whose anticancer properties have been extensively studied, is NM-3, a synthetic derivative of cytogenin from *Streptomyces eurocidicus* [208]. It acts anti-angiogenetic *in vitro* and *in vivo* by inhibiting proliferation and migration of endothelial cells as well as tube formation [209,210]. Furthermore, it potentiates the antitumor effects of radiotherapy and chemotherapeutic agents, such as paclitaxel, 5-fluoruracil and carboplatin [210–213]. In 2002, NM-3 entered a phase I clinical trial, encompassing adult patients with advanced solid tumors (ClinicalTrials.gov identifier: NCT00046696; results not published yet).

Several coumarins with P-gp and BCRP inhibiting activities have been identified and characterized yet. Both, natural as well as synthetic coumarins, demonstrated inhibitory activity against P-gp [214–217]. Synthetic 4-arylcoumarins and the indolylcoumarin COUFIN were identified as dual inhibitors of P-gp and BCRP activity [218,219]. In contrast, isocoumarins have not been in the focus of the search for MDR reversing drug candidates so far.

Here, the cytotoxicity of natural compound isocoumarins as well as novel compounds in sensitive and resistant cancer cell lines was analyzed. In addition, their inhibitory potential towards P-gp, MRP1 and BCRP transport activity was evaluated.

1.8.3 Colchicine

Colchicine (Figure 7) is an alkaloid from the autumn crocus *Colchicum autumnale*. It was isolated from the seeds of the plant and named colchicine by Geiger in 1833 [220]. Interestingly, although colchicine has been used for the treatment of gout for a long period of time, with its first use being attributed to Byzantine Christian physician Alexander of Tralles in the sixth century AD [221], it was approved by the United States Food and Drug Administration (FDA) only in 2009.

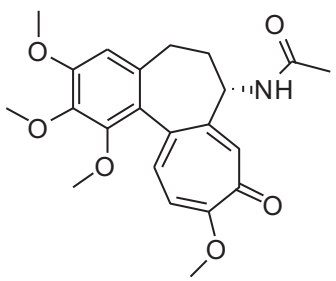

Figure 7. Structure of colchicine.

Regarding the mechanism of action, colchicine binds to tubulin heterodimers at the interphase of the α- and β-subunits, resulting in a curved tubulin-colchicine complex [222,223]. This conformational change inhibits tubulin polymerization and microtubule formation, which in turn blocks mitosis and leads to apoptotic cell death [224]. Microtubules, a part of the cytoskeleton, play key roles in, for example, cell division, intracellular transport, signaling and motility, making them an interesting target in cancer therapy [225]. Microtubule-targeting taxanes and *Vinca* alkaloids are widely used in cancer chemotherapy. Due to its high toxicity not only in cancer cells, but also in healthy cells, colchicine is currently not used in cancer treatment. Despite its potent cytotoxicity, the natural product and various novel derivatives are in the focus of lead compound identification programs within anticancer drug research [226–229]. Optimization of colchicine-derived derivatives focuses on more favorable pharmacological profiles with less toxicity in healthy tissues by applying, for example, prodrug, codrug or nanoformulation approaches [230].

Colchicine is a substrate of P-gp. Moreover, treatment of cancer cell lines with colchicine induces P-gp overexpression [231,232]. In addition, up-regulation of expression of P-gp or other ABC transporters represents a common mechanism of resistance development against microtubule-targeting chemotherapeutic drugs in clinical practice [233]. Therefore, it will be advantageous, if novel colchicine derivatives lack this feature [234].

In this thesis, novel colchicine-derived triazoles were examined regarding cytotoxicity and inhibition of microtubule assembly in different human cancer cell lines [235].

1.9 Aims

The development of MDR in cancer patients remains a large problem in effective tumor treatment and cure, as it does not only confer resistance against one drug, but against a variety of unrelated drugs. This leads to reduced therapy efficacy and loss of treatment options. Although constant progress is achieved in the improvement of anticancer therapies, resistance might evolve against classic cytotoxic chemotherapy as well as novel types of targeted and patient-specific therapy. Thus, as illustrated before, it is of utmost importance to find novel treatment strategies effective against multidrug-resistant tumors. This work focuses on overcoming MDR mediated by the overexpression of ABC transporters by using natural products and their derivatives. ABC transporters actively transport drugs out of cells, thereby preventing them from efficiently attacking tumor cells [8,76].

As part of an interdisciplinary project, the aims of the thesis were 1) to analyze the ability of natural products and derivatives to inhibit the transport function of the endogenously expressed human ABC transporters P-gp, MRP1 and BCRP in colon, lung and breast cancer cell lines with intrinsic or acquired therapy resistance, and 2) to assess their cytotoxic activity in sensitive as well as resistant cancer cell lines, thereby identifying novel lead compounds for the treatment of multidrug-resistant tumors. The test compounds were either isolated from plant material or derived by chemical syntheses by the *Institute of Bioorganic Chemistry, Heinrich-Heine-Universität Düsseldorf* and by *MicroCombiChem GmbH, Wiesbaden* and altogether, more than 300 compounds were provided for *in vitro* testing. To accomplish the objectives of the thesis, a variety of cell-based assays had to be developed and optimized to allow miniaturized and semi-automated high-throughput screening of compounds in 96-well and 384-well microtiter plate format, respectively. Promising compounds among the goniothalamin derivatives and the isocoumarins were identified and further explored regarding their molecular mechanism of action.

Furthermore, novel colchicine derivatives from the *Department of Chemistry, Universität zu Köln* were characterized regarding cytotoxicity in leukemia and solid tumor cells and inhibition of microtubule formation in order to identify potential lead structures for the development of new microtubule-targeting drugs, which in addition might have the potential to overcome resistance to clinically used tubulin inhibitors.

2 Publications

2.1 Chapter I

Title:	Synthesis and cytotoxic activities of goniothalamin and derivatives
Authors:	Anja Weber, Katja Döhl[1], **Julia Sachs**[1], Anja C.M. Nordschild, Dennis Schröder, Andrea Kulik, Thomas Fischer, Lutz Schmitt, Nicole Teusch, Jörg Pietruszka
	[1]: These authors contributed equally for the paper
Journal:	Bioorganic & Medicinal Chemistry, 2017 (Impact factor: 2.930)
Reference:	Weber A, Döhl K, Sachs J, Nordschild ACM, Schröder D, Kulik A, Fischer T, Schmitt L, Teusch N, Pietruszka J. Synthesis and cytotoxic activities of goniothalamins and derivatives. Bioorg Med Chem 2017;25:6115–25.
DOI:	10.1016/j.bmc.2017.02.004
Contribution:	cytotoxicity assay, data analysis, contribution to manuscript writing

Bioorganic & Medicinal Chemistry 25 (2017) 6115–6125

Contents lists available at ScienceDirect

Bioorganic & Medicinal Chemistry

journal homepage: www.elsevier.com/locate/bmc

Synthesis and cytotoxic activities of goniothalamins and derivatives

Anja Weber [a], Katja Döhl [b,1], Julia Sachs [c,1], Anja C.M. Nordschild [a], Dennis Schröder [d], Andrea Kulik [c], Thomas Fischer [e], Lutz Schmitt [b], Nicole Teusch [c], Jörg Pietruszka [a,d,*]

[a] Institut für Bioorganische Chemie (IBOC), Heinrich-Heine-Universität Düsseldorf im Forschungszentrum Jülich, Stetternicher Forst, Geb. 15.8, 52426 Jülich, Germany
[b] Institut für Biochemie, Heinrich-Heine-Universität Düsseldorf, Universitätsstr. 1, 40225 Düsseldorf, Germany
[c] Bio-Pharmaceutical Chemistry and Molecular Pharmacology, Faculty of Applied Science, Technische Hochschule Köln, CHEMPARK, E39 51368 Leverkusen, Germany
[d] IBG-1: Biotechnologie, Forschungszentrum Jülich, 52428 Jülich, Germany
[e] BIO-MAR im Augenzentrum Friedrichstadt, Friedrichstraße 140, 40217 Düsseldorf, Germany

ARTICLE INFO

Article history:
Received 31 October 2016
Revised 26 January 2017
Accepted 2 February 2017
Available online 6 February 2017

Keywords:
Natural product
Asymmetric synthesis
Stereoselectivity
Cytotoxicity
Multidrug exporter

ABSTRACT

Substituted goniothalamins containing cyclopropane-groups were efficiently prepared in high yields and good selectivity. Antiproliferative activity was measured on three human cancer cell lines (A549, MCF-7, HBL-100), to show which of the structural elements of goniothalamins is mandatory for cytotoxicity. We found that the configuration of the stereogenic centre of the δ-lactone plays an important role for cytotoxicity. In our studies only (*R*)-configured goniothalamins showed antiproliferative activity, whereby (*R*)-configuration accords to natural goniothalamin (*R*)-**1**. Additionally, the δ-lactone needs to be unsaturated whereas our results show that the vinylic double bond is not mandatory for cytotoxicity. Furthermore, with a two-fold *in vitro* and *in vivo* strategy, we determined the inhibitory effect of the compounds to the yeast protein Pdr5. Here, we clearly demonstrate that the configuration seems to be of minor influence, only, while the nature of the substituent of the phenyl ring is of prime importance.

1. Introduction

In the past, the natural product (*R*)-(+)-goniothalamin and its derivatives were shown to display biological activity against a broad range of cell lines,[1–5] bacteria[6] and fungi.[6,7] Goniothalamin can be isolated from plants of the genus of *Goniothalamus*, which grow in tropic and subtropic areas of Asia and Oceania.[8] In 1967 Hlubucek et al. isolated goniothalamin for the first time from *Cryptocarya caloneura* and determined the stereogenic centre to be (*S*)-configured.[9] This was revealed in 1979, when Meyer elucidated the structure of natural occurring goniothalamin as (*R*)-configured by the synthesis of both enantiomers.[10]

Goniothalamin, (*R*)-**1**, and its derivatives have an α,β-unsaturated δ-lactone as a central element, which can be used as a *Michael*-acceptor system with corresponding nucleophiles. Furthermore it seems, that the vinylic double bond and the configuration of the stereogenic centre in the lactone is essential for its cytotoxicity (Fig. 1).

In addition to the naturally-occurring (*R*)-(+)-goniothalamin (**1**), Fátima et al. showed that the (*S*)-enantiomer [(*S*)-**1**] and the two derivatives, (*S*,*E*)-6-(2-cyclohexylvinyl)-5,6-dihydro-2*H*-pyran-2-one [(*S*)-**2**] and (*S*,*E*)-6-(4-methoxystyryl)-5,6-dihydro-2*H*-pyran-2-one [(*S*)-**3**], have a higher potential towards the inhibition of kidney cell proliferation in comparison to the natural goniothalamin (*R*)-**1**, with IC_{50}-values in the micromolar range (Fig. 2).[1–5] They could also show, that the fully hydrogenated derivatives (*R*)-6-phenethyltetrahydro-2*H*-pyran-2-one and (*S*)-6-phenethyltetrahydro-2*H*-pyran-2-one have no cytotoxic effect.[1]

Further biological studies were reported by Wach et al. in 2010: They showed that naturally occurring (*R*)-goniothalamin [(*R*)-**1**] can inhibit the nucleocytoplasmatic transport.[11] In 2013 Bruder et al. synthesized new goniothalamin derivatives, with an additional methyl groups at the now quaternary stereogenic centre of γ- and δ-lactones and substituents at the phenyl group. No increase in anti-proliferative activity of (*E*)-6-methyl-6-styryl-5,6-dihydro-2*H*-pyran-2-one and (*E*)-5-methyl-5-styrylfuran-2(5*H*)-one relative to natural product (*R*)-**1** was observed. By adding a trifluoromethyl groups to the phenyl group of the methylated compounds, they could improve biological activity.[12] Pilli et al. synthesized 29 novel goniothalamin analogues and reported that aza-analogues and γ-pyrones had no increased antiproliferative activity, while tri- and tetra-methoxylated goniothalamin derivatives showed a promising increase in cytotoxicity.[13] All in all goniothalamin and its derivatives show a wide variety of biological effects,

* Corresponding author.
E-mail address: j.pietruszka@fz-juelich.de (J. Pietruszka).
[1] These authors contributed equally for the paper.

http://dx.doi.org/10.1016/j.bmc.2017.02.004
0968-0896/

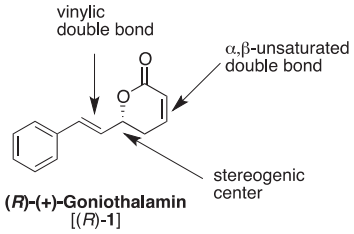

Fig. 1. Structure of the natural (*R*)-(+)-goniothalamin and its structural elements.

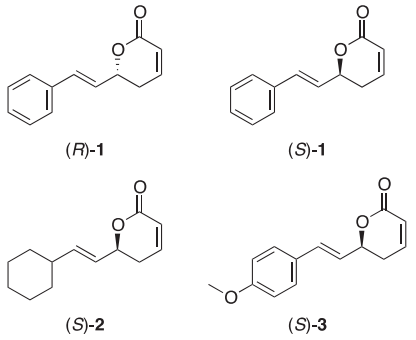

Fig. 2. Structure of goniothalamin (*R*)-**1** and some derivatives.

e.g., anti-inflammatory,[14] anti-nociceptive[14] anti-tumour activity[15] as well as plant growth inhibition.[15,16]

Here we would like to present our enantioselective synthetic route towards goniothalamin and derivatives. In addition, the corresponding results of cytotoxicity tests of these compounds on human lung adenocarcinoma cell line A549, human breast adenocarcinoma cell line MCF-7 as well as on the triple negative human breast cancer cell line HBL-100 demonstrate a first hint for a structure-activity relationship. With these cytotoxicity tests, we want to elucidate, which structural elements of the vinyl-lactone are essential for biological activity. Furthermore, we also performed assays with the *Saccharomyces cerevisiae* multidrug exporter Pdr5. Pdr5 is a functional homologue of Cdr1, an important drug efflux pump of the clinical relevant fungi *Candida albicans.* Consequently, the development of new inhibitors against these multidrug exporter proteins plays an important role in our daily fight against resistance fungi. Therefore, we analyzed goniothalamin derivatives with respect to their inhibitory capacity against Pdr5.

2. Results

2.1. Synthesis of cyclopropane derivatives

To show the importance of different structural elements of goniothalamin, we decided to synthesize different derivatives and demonstrate the influence of the vinylic double bond on the cytotoxicity of the compound; more specifically, we synthesized cyclopropane derivatives **4** with the cyclopropyl unit instead of the vinylic double bond.

Synthesis of goniothalamin derivatives **4** was performed starting from cyclopropyl alcohol **5**, which can be synthesized from corresponding cinnamic alcohol using a previously reported enzymatic kinetic resolution (Scheme 1).[17] Both diastereoisomers of cyclopropyl alcohol **5** could readily be converted into the corresponding aldehydes (*S,S*)-**6** and (*R,R*)-**6** with the use of *Dess-Martin-*

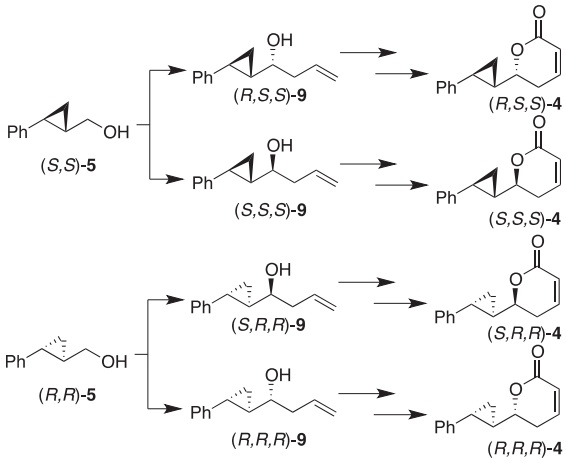

Scheme 1. Synthesis scheme for cyclopropane derivatives **4**.

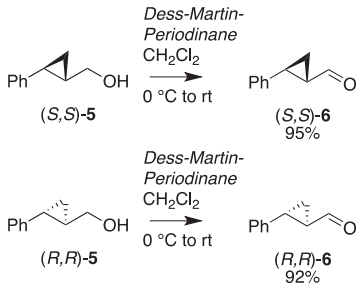

Scheme 2. Oxidation of alcohol **5** to the corresponding aldehydes **6**.

periodinane[18–22] in very good yields of 95% and 92% (Scheme 2). It has to be mentioned that the cyclopropyl aldehydes (*S,S*)-**6** and (*R,R*)-**6** are not stable against oxygen and directly oxidize to the corresponding acids under air, they have to be stored under an argon atmosphere.

Stereoselective allyl addition of the enantiomerically-pure aldehydes **6** with allylboronic acid ester **7**[24,25] and Leighton reagent **8**[26,27] gave the homoallylic alcohols **9** in good yields (Scheme 3). Using the allylboronate **7** from Roush et al., we found a 78:22-mixture of diastereoisomers (*R,S,S*)-**9** and (*S,S,S*)-**9** in 93% yield (Table 1, entry 1), with the anti-product (*R,S,S*)-**9** being the major product, due to the control of reagent **7**. To improve the diastereomeric ratio we used the Leighton reagent **8**, which gave the anti-product (*R,S,S*)-**9** > 99:1 in 75% yield (Table 1, entry 2). Due to the fact of good separation of diastereoisomers (*R,S,S*)-**9** and (*S,S,S*)-**9** by column chromatography and shorter reaction times, we decided to use allylboronic acid ester **7** for the synthesis of homoallylic alcohols (*S,R,R*)-**9** and (*R,R,R*)-**9**. With the allylboronic acid ester **7** from Roush et al. we could obtain the major *syn*-product (*R,R,R*)-**9** in a diastereomeric ratio of 77:23 and a yield of 72%.

Additionally, we started an alternative synthesis furnishing homoallylic alcohols (*S,R,R*)-**9** and (*R,R,R*)-**9** from enantiomerically-pure ethyl ester (*R,R*)-**10**,[23] also assessable by kinetic resolution:[28] First we converted enantiomerically pure ethyl ester (*R,R*)-**10** (>98% ee) into the corresponding *Weinreb*-amide (*R,R*)-**11** in 99% yield, followed by a *Grignard* reaction to the ketone (*R,R*)-**12**.[29–32] As a side product we obtained the alcohol, (1*R*,2*R*)-4-(2-phenylcyclopropyl)hepta-1,6-dien-4-ol (**16**), from a reaction of

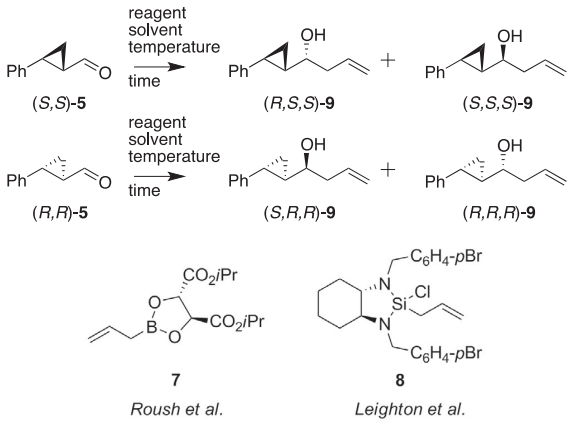

Scheme 3. Stereoselective allyl addition towards homoallylic alcohols **9**.

Table 1
Conditions for stereoselective allyl addition of aldehydes **6** towards homoallylic alcohols **9**.

Starting-material	Reagent	Conditions	d.r. (*anti:syn*)	Yield
(*S,S*)-**6**	**7**	Toluene −78 °C to rt 5 h	78:22 (*R,S,S*)-**9**:(*S,S,S*)-**9**	93%
(*S,S*)-**6**	**8**	CH_2Cl_2 −12 °C, 20 h	>99:1 (*R,S,S*)-**9**:(*S,S,S*)-**9**	75%
(*R,R*)-**6**	**7**	Toluene −78 °C to rt 5 h	23:77 (*S,R,R*)-**9**:(*R,R,R*)-**9**	72%

ketone **12** with two equivalents of *Grignard*-reagent. Subsequently, the ketone (*R,R*)-**12** could be reduced by CBS-reagent (*R*)-**13** or (*S*)-**13** in the presence of catecholborane to the homoallylic alcohols (*S,R,R*)-**9** and (*R,R,R*)-**9**.[33–36] In the reaction with (*S*)-**13** the *syn*-product (*R,R,R*)-**9** is preferred (d.r. 12:88). The anti-product (*S,R,R*)-**9** as the major product can be obtained by use of (*R*)-CBS reagent (*R*)-**13** (d.r. 94:6) (Scheme 4).

We used the homoallylic alcohols **9** as perfect precursors for the synthesis of natural products like constanolactone A-F,[37,38] halicholactone,[39] neohalicholactone,[39] and solandelactone A-H.[40] Accordingly we had no use for homoallylic alcohol (*S,S,S*)-**9**, but we could readily convert it into the desired homoallylic alcohol (*R,S,S*)-**9** by the previously established method. Starting from (*S,S,S*)-**9** (>98% ee), the reaction pathway was performed for the (*S,S*)-configured homoallylic alcohols (*R,S,S*)-**9** and (*S,S,S*)-**9**: First the (*S,S,S*)-**9** alcohol was oxidized to the corresponding ketone (*S,S*)-**12** by *Dess-Martin* periodinane (**14**) (42% yield); as a side-product upon prolonged reaction time and acid formation, the ring-opening product **15** could be identified. Subsequent CBS-reduction was conducted with the (*S*)-**13** enantiomer of the CBS-reagent, to obtain the anti-diastereomer (*R,S,S*)-**9** (d.r. 89:11) in 48% yield (Scheme 5). Homoallylic alcohols (*R,S,S*)-**9** and (*S,S,S*)-**9** could readily be separated by flash column chromatography.

To establish the unsaturated lactone unit, we focused on a ring closing metathesis starting from the homoallylic alcohols **9**. The first step was the esterification with acryloyl chloride (**16**) providing dienes **17** in very good yields (89–95%) (Scheme 6).[41]

Subsequently, dienes **17** were converted into the corresponding α,β-unsaturated δ-lactones **4** with Grubbs 1st generation catalyst (Scheme 7). We used titaniumtetraisopropylate[41] as a Lewis acid to avoid the formation of a ruthenium-chelate complex, which

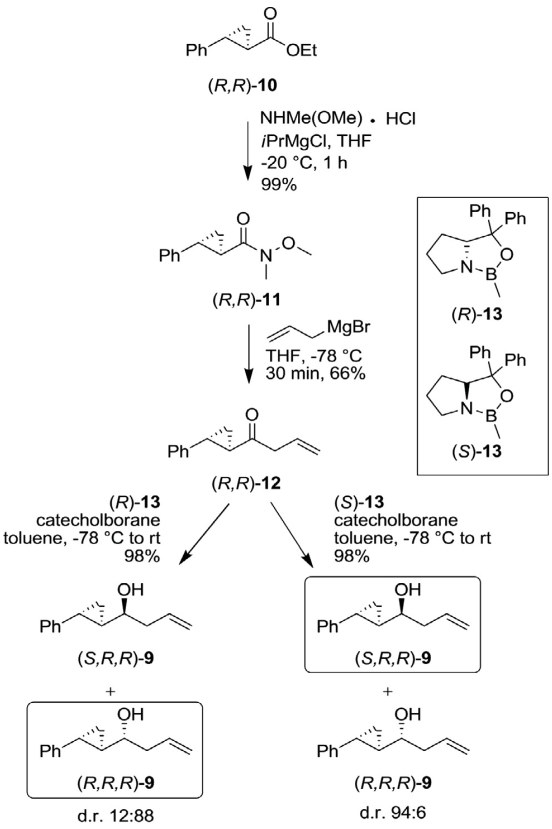

Scheme 4. Reaction scheme for the synthesis of homoallylic alcohols (*S,R,R*)-**9** and (*R,R,R*)-**9** *via* CBS-reduction.

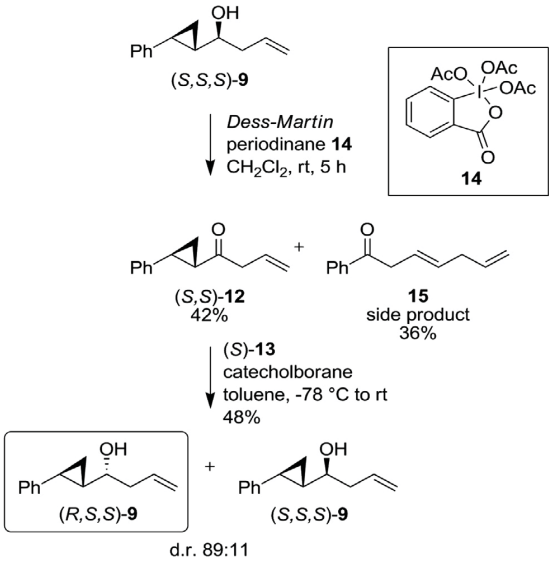

Scheme 5. Reaction scheme for the synthesis of homoallylic alcohols (*R,S,S*)-**9** and (*S,S,S*)-**9** *via* oxidation-reduction sequence.

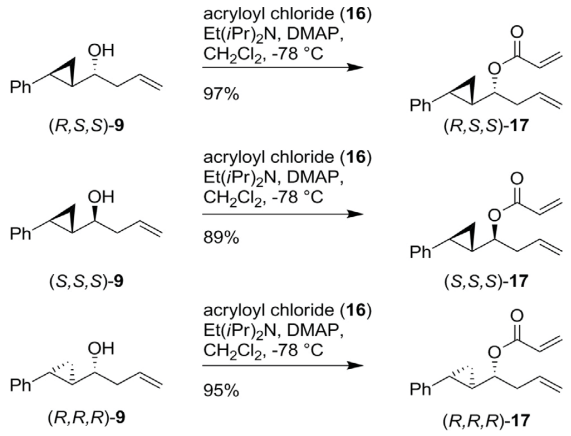

Scheme 6. Esterification of alcohols **9** with acryloyl chloride (**16**).

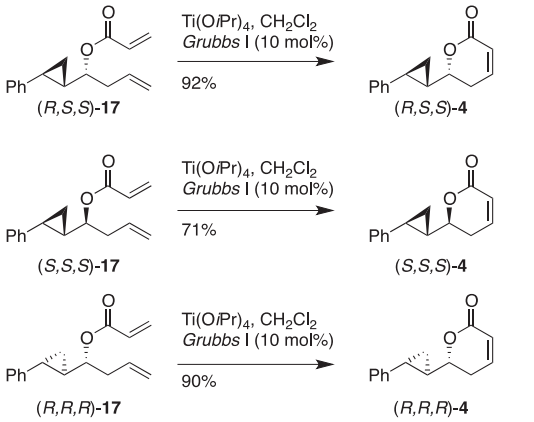

Scheme 7. Ring closing metathesis towards the desired cyclopropyl goniothalamin derivatives **4**.

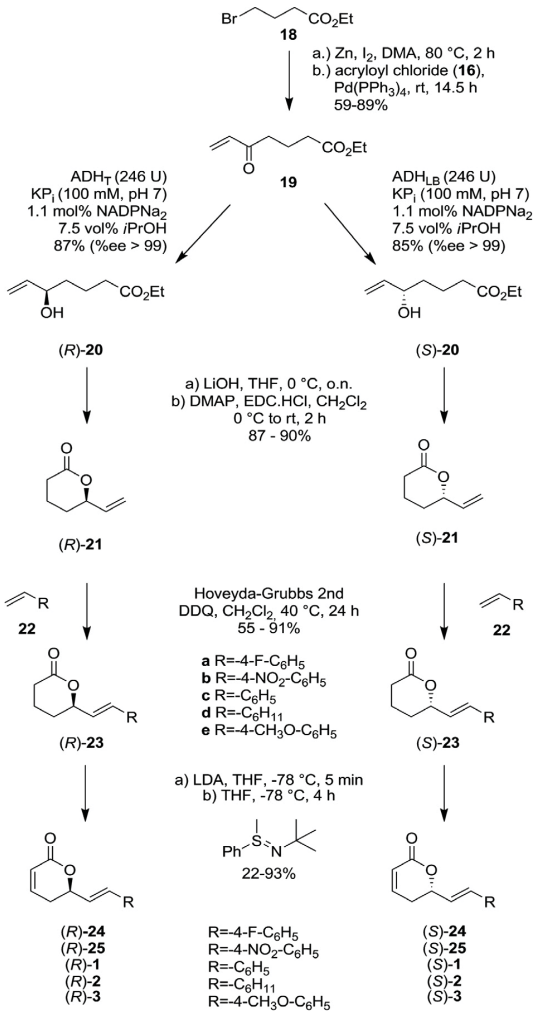

Scheme 8. Chemoenzymatic route towards goniothalamin derivatives **24, 25, 1, 2** and **3**.

makes the catalyst unavailable for the metathesis. The ring closing metathesis was conducted in moderate to excellent yields (71–92%),[42] providing the target cyclopropyl lactones **4**, which are versatile precursors for the synthesis of other natural products.[37–40]

2.2. Synthesis of substituted goniothalamins

To show the influence of different substituents on the aromatic ring and of a cyclohexane derivatives, we synthesized the compounds according to a previously reported chemoenzymatic approach.[43,44] The synthesis started with a *Negishi*-coupling of bromide **18** to acid chloride **16** yielding the corresponding vinylketone **19**. This was followed by a stereoselective alcoholdehydrogenase [from *Lactobacillus brevis* (ADH_{LB}) and *Thermoanaerobacter sp.* (ADH_T)] based reduction furnishing the two enantiomerically alcohols **20**. Cyclisation yielded the desired lactones **21**. Subsequent cross-metathesis with different styrene derivatives **22** led to saturated goniothalamin derivatives **23**. Finally, oxidation to the α,β-unsaturated lactones **1**, **2**, **3**, **24** and **25** was performed by using *N-tert*-butylphenylsulfinimidoyl chloride (Scheme 8). With this approach, we could synthesize the ten enantiomerically pure goniothalamin derivatives depicted in Fig. 3.

2.3. Biological activities of goniothalamin derivatives

(a) Inhibition of the multidrug exporter Pdr5: With the *in vivo* liquid drug assay we demonstrated that all of the tested compounds are cytotoxic to yeast up to a concentration of 100 μg/mL except for compound *(R)*-**3** which showed no cytotoxicity at all (data not shown). First, we compared a *S. cerevisiae* strain containing the *wild-type* protein (Pdr5 *wt*) to a yeast strain expressing the dead mutant (Pdr5 EQ). We were able to show that with compound *(R)*- and *(S)*-**2** the Pdr5 *wt* strain was more resistant than the mutant strain. For *(R)*-**1**, *(R)*-**3**, *(R)*-**24** and *(S)*-**25** there was no obvious difference detectable between both strains (Table 2).

In the transport assay the tested compounds were compared to Pdr5 *wt* without additives, which was set to 100% transport activity. All of them displayed inhibitory effects at the highest tested concentration (Table 3). The test with lower concentrations showed that only compounds (*R*)-**1** and (*R*)-**3** were able to inhibit the transport activity clearly. (*R*)- and (*S*)-**2** only inhibit the transport efficiency with the 500 μg/mL. However, the lowest concentration did not affect the transport activity. Compound (*S*)-**24**

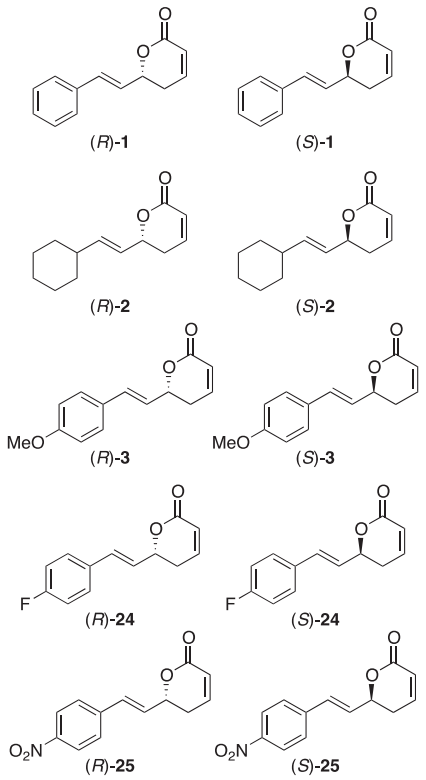

Fig. 3. Synthesized enantiomerically-pure goniothalamin derivatives.

Table 2
Relative transport activity of Pdr5 *wt*.

Compound	Relative fluorescence intensity [%]		
	500 μg/mL (∗125 μg/mL)	50 μg/mL	5 μg/mL (∗13 μg/mL)
(R)-1	−2	10	60
(R)-2	−8	18	91
(S)-2	0	37	86
(R)-3	0	4	44
(R)-25	∗21	–	∗54
(S)-24	10	75	99

Table 3
ATPase activity of Pdr5 wt.

Compound	[%] ATPase activity		
	500 μg/mL (∗250 μg/mL)	50 μg/mL (∗125 μg/mL)	5 μg/mL (∗13 μg/mL)
(R)-1	24.3 ± 6.5	30.0 ± 1.2	71.7 ± 2.1
(R)-2	56.0 ± 11.1	79.0 ± 4.4	98.0 ± 1.0
(S)-2	53.0 ± 2.6	74.7 ± 9.0	88.0 ± 1.7
(R)-3	0.0 ± 0	8.7 ± 2.1	25.7 ± 3.1
(R)-25	∗50.0 ± 1.0	∗51.0 ± 0	∗79.3 ± 7.6
(S)-24	26.3 ± 2.5	40.7 ± 1.5	71.0 ± 0.0

Data represent mean values ± SD of at least three independent experiments.

showed the same behavior, while (*R*)-**25** showed an inhibition to 50% transport activity with the 500 μg/mL and 50 μg/mL and no inhibitory effect with the lowest concentration.

Only compound *(R)*-**3** was able to inhibit the ATPase activity of Pdr5 completely and the lowest concentration of this compound

Table 4
Cytotoxicity against human cancer cell lines after 48 h compound incubation.

Compound	IC_{50} (μM)		
	A549	MCF-7	HBL-100
rac-1	34.7 ± 0.8	>100	22.4 ± 3.8
(*R*)-1	5.7 ± 1.5	55.5 ± 6.4	20.9 ± 5.4
(*S*)-1	70.3 ± 14.4	>100	>100
(*R*)-2	31.0 ± 0.3	>100	29.0 ± 3.7
(*S*)-2	68.6 ± 0.5	>100	48.2 ± 4.8
(*R*)-25	15.4 ± 0.2	28.8 ± 2.3	6.7 ± 0.5
(*S*)-25	>100	>100	>100
(*R*)-3	>100	>100	>100
(*S*)-3	>100	88.7 ± 5.6	>100
(*R*)-24	10.2 ± 0.3	76.2 ± 6.3	14.1 ± 2.3
(*S*)-24	>100	>100	>100
(*R,S,S*)-4	11.6 ± 0.2	48.2 ± 2.0	14.4 ± 0.5
(*R,R,R*)-4	62.8 ± 1.6	>100	43.4 ± 2.8
(*S,S,S*)-4	15.2 ± 0.3	68.3 ± 9.7	34.9 ± 1.5
(*R,R,R*)-26	>100	>100	>100
(*R,R*)-27	>100	>100	>100
(*S,S,S*)-26	>100	>100	>100
(*R,S,S*)-26	>100	>100	>100
(*R,S*)-27	>100	>100	>100

Data represent mean values ± SEM of at least three independent experiments.

reduced ATPase activity by 75%. Both, *(R)*- and *(S)*-**2** showed the same inhibition profile for the ATPase activity, independently of their configuration. The highest concentration is only able to inhibit the ATPase activity to 50% and at the lowest concentration used in the assay no inhibitory effect was detected at all. *(R)*-**1**, *(R)*-**25** and *(S)*-**24** demonstrated an identical behavior. Higher concentrations inhibited ATPase activity to 30–50% while at lower concentrations nearly no influence was detected.

In summary, we demonstrated that the *(R)*- or *(S)*- configuration showed cytotoxic and inhibitory effects, respectively. No differences were detected between *(R)*- and *(S)*-**2** in all three assays using Pdr5 *wt*. The higher resistance of the *wildtype yeast* strain against this compound and a comparison of ATPase and transport assay leads to the conclusion that this compound is a substrate of Pdr5. Compound *(R)*-**1**, *(R)*-**25** and *(S)*-**24** showed only a cytotoxic effect in the *in vivo* assay and the two *in vitro* assays demonstrated no big differences concerning their behavior as an inhibitor of Pdr5. Only compound *(R)*-**3**, which showed no cytotoxicity in the *in vivo* assay, displayed a quantitative inhibition in both *in vitro* assays. This leads to the obvious conclusion that an inhibition of Pdr5 is independent of the stereogenic configuration [*(R)* or *(S)*] rather the substituent of the phenyl ring plays the dominant role.

(b) Cytotoxicity assessment: The results for the cytotoxicity assessment are summarized in Table 4. Due to different sensitivities of cancer entities towards cytotoxic compounds, we used three different cell lines of various histological origin [A549 (human lung adenocarcinoma cell line), MCF-7 (estrogen receptor positive human breast adenocarcinoma cell line), HBL-100 (triple negative human breast cancer cell line)].

First, we evaluated the racemic mixture of natural goniothalamin (**1**) (Table 4, entry 1). It displayed acceptable antiproliferative activity on the lung carcinoma cell line A549 as well as on the triple negative breast cancer cell line HBL-100. By characterizing the cytotoxicity of enantiomerically-pure (*R*)- and (*S*)-goniothalamin [(*R*)-**1** and (*S*)-**1**] (entry 2 and 3, Table 4), respectively, the natural occurring (*R*)-goniothalamin **1** demonstrated higher efficacy in all three cell lines, in comparison to its enantiomer (*S*)-goniothalamin **1**.

To explore the influence of the phenyl ring on cell viability, we synthesized the cyclohexyl derivative **2**. The (*R*)-enantiomer showed a six-fold lower cytotoxicity in A549 human lung adenocarcinoma cells in comparison to the natural goniothalamin (*R*)-**1** (Table 4, entry 4). Moreover, in the MCF-7 and HBL-100 the natural

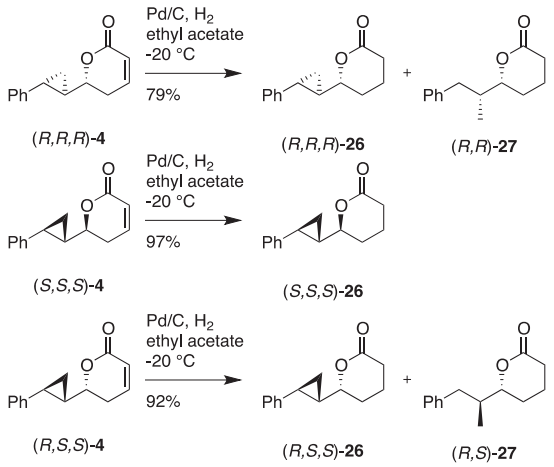

Scheme 9. Hydrogenation of unsaturated lactone **19a, 19b** and **18** to corresponding saturated lactone (*R,R,R*)-**26** (79%), (*S,S,S*)-**26** (97%) and (*R,S,S*)-**26** (92%) with methyl-compound (*R,R*)-**27** (3%) and (*R,S*)-**27** (4%) as a side product.

product displays reduced cytotoxicity. The (*S*)-**2** shows even lower cytotoxicity in comparison to the natural goniothalamin (*R*)-**1** (Table 4, entry 5). Comparing cyclohexyl derivative (*S*)-**2** with the phenyl-derivative (*S*)-**1**, the cytotoxicity is roughly on the same low level.

Antiproliferative activity of more electron-poor *p*-nitrophenyl-substituted goniothalamins **25** could not increase cytotoxicity for the (*S*)-compound **25** (Table 4, entry 7). The enantiomer (*R*)-**25** demonstrates a threefold increased cytotoxicity against human breast cancer cell line HBL-100, in contrast to the natural (*R*)-enantiomer **1** (Table 4, entry 6).

The highly-activated *p*-methoxyphenyl goniothalamins **3** did not affect cell viability in any of the tested cell lines (Table 4, entry 8 and 9). Using deactivated *para*-fluorinated goniothalamins **24** only the (*R*)-enantiomer showed notable IC_{50} values (Table 4, entry 10), which are less cytotoxic compared to the naturally-occurring (*R*)-enantiomer **1**. In summary, we demonstrated the (*R*)-configuration of the lactone ring to be mandatory for cytotoxic activity of the compound cluster. Furthermore, our data suggest that the substituent does not significantly influence the identified structure activity relationship.

Additionally, we characterized cyclopropane derivatives **4** of the natural goniothalamin. The derivatives **4** demonstrated clear cytotoxicity, except for compound (*R,R,R*)-**4**, which did not influence cell viability of breast adenocarcinoma cell line MCF-7 (Table 4, entry 13). In contrast, it displayed moderate activity on the two other cancer cell lines. Cyclopropane derivative (*R,S,S*)-**4** showed comparable biological activity to (*R*)-**1**.

Hydrogenation of lactone (*R,R,R*)-**4** and (*R,S,S*)-**4** led not only to the corresponding saturated lactone (*R,R,R*)-**26** and (*R,S,S*)-**26**, but also to compounds (*R,R*)-**27** and (*R,S*)-**27** derived from the ring-opening reaction as a side product (Scheme 9). The last entry of Table 4 shows no detectable cytotoxicity for cyclopropanes (*R,R,R*)-**26**, (*S,S,S*)-**26** and (*R,S,S*)-**26** on any cell line tested. The same holds true for the goniothalamin derivatives **(***R,R*)-**27** and (*R,S*)-**27**. In conclusion, our data demonstrate a saturated lactone moiety to be compulsory for antiproliferative activity of goniothalamins.

Furthermore, our cytotoxicity results of cyclopropane-containing goniothalamins **4** confirm the external double bond not to be mandatory for the biological activity of the compound. There is evidence that the molecule needs a certain conformational rigidity to show cytotoxic activity; however, in our case this rigidity is provided from either a cyclopropane ring or a (*E*)-double bond.

3. Conclusion

Comparing the cytotoxicity results the following three conclusions can be drawn:

First, the configuration of the stereogenic centre plays an important role for cytotoxicity. Only the (*R*)-configured goniothalamins with the vinylic double bond demonstrated cytotoxicity. The (*R*)-configuration is in accordance to natural goniothalamin (*R*)-**1**. However, looking at the inhibition of the multidrug exporter Pdr5, no pronounced configurational preference was observed, while the substitution pattern mattered.

Second, the double bond in the lactone ring is essential for the biological activity. With saturated lactones, no antiproliferative activity could be detected (derivatives **26**).

Third, the vinylic double bond is not mandatory, but a certain rigidity is required for cytotoxicity. However, this rigidity is not absolute, which is exemplified by the achieved biological activity of the cyclopropane derivatives **4**. These results are in agreement with literature, where also goniothalamin epoxides show good biological activity.[51–54] Chandraratna et al. reported in 1996, that cyclopropyl groups can be used as double bond isosteres for retinoid analogues, which show activity towards the retinoic acid receptors (RARs) and retinoid X receptors (RXRs).[55] These results show the same effect of a mandatory rigidity for biological activity and is in perfect accordance with our findings.

4. Experimental

4.1. General procedures

Unless specified, the reactions were carried out by standard *Schlenk*-technique under dry Ar/N_2 and magnetic stirring. Glassware was oven-dried at 120 °C overnight. Solvents were dried and purified by conventional methods prior to use; tetrahydrofuran (THF) was freshly distilled from sodium/benzophenone. Solvents for chromatography (petroleum ether, ethyl acetate) were distilled prior to use. Column and flash column chromatography were performed on silica gel 60, 0.040–0.063 mm (230–400 mesh). TLC was performed on pre-coated plastic sheets (Polygram SIL G/UV254, Macherey-Nagel) with detection by coloration with ceric phosphomolybdic acid solution [phosphomolybdic acid (25 g), Ce$(SO_4)_2{\cdot}H_2O$ (10 g), concentrated H_2SO_4 (60 mL), H_2O (940 mL)]. Compounds **1**–**3** and **24**–**25** were synthesized according to a reported protocol.[43,44]

4.2. Synthesis of (S,S)-(2-Phenylcyclopropyl)carbaldehyde [(S,S)-6] and (R,R)-(2-Phenylcyclopropyl)carbaldehyde [(R,R)-6]

To a solution of 3.00 g (20.2 mmol, 1.0 equiv.) enantiomerically pure (*S,S*)-(2-phenylcyclopropyl)methanol [(*S,S*)-**5**][17] (>98% ee) in 230 mL CH_2Cl_2 under a nitrogen atmosphere at 0 °C was added 12.0 g (28.3 mmol, 1.4 equiv.) *Dess-Martin*-periodinane (**14**).[18–23] The solution was stirred 1 h at 0 °C and 14 h at room temperature. After complete conversion of the starting material (TLC), the solution was hydrolysed with a 1:1-mixture of 1 M sodium thiosulfate solution and saturated sodium bicarbonate solution. The mixture was stirred until both layers were clear. The aqueous layer was extracted several times with dichloromethane. The organic layers were combined, dried with $MgSO_4$, filtered and the solvent was evaporated under reduced pressure. The crude product was purified by flash column chromatography. After purification 2.8 g

(19.2 mmol, 95%, 98% *ee*) of the (*S,S*)-aldehyde **6** could be isolated. The spectroscopic data is in agreement with literature data.[56]

(*R,R*)-(2-Phenylcyclopropyl)methanol [(*R,R*)-**5**] has been used according to the same protocol, using 1.4 g (9.3 mmol, 1.0 equiv.) (*R,R*)-(2-phenylcyclopropyl)methanol (**5**) (> 98% ee) in 106 mL CH_2Cl_2, 5.5 g (13.0 mmol, 1.4 equiv.) *Dess-Martin*-periodinane, resulting in 1.3 g (8.6 mmol, 92%) (*R,R*)-(2-phenylcyclopropyl)carbaldehyde (**6**) (> 98% ee).

R_f = 0.6 (PE:EE = 75:25). (*S,S*)-**6** $[\alpha]_D^{20}$ = +395 (c = 1.5, $CHCl_3$, >98% ee).[57] (*S,S*)-**6** $[\alpha]_D^{20}$ = +391 (c = 1.5, $CHCl_3$, >98% ee). (*R,R*)-**6** $[\alpha]_D^{20}$ = −411 (c = 1.2, $CHCl_3$, >98% ee).[58,59] MS (EI, 70 eV): *m/z* (%) = 146 (25) [$(M + H)^+$], 145 (34) [M^+], 117 (100) [$(M\text{-}CHO)^+$], 115 (68) [$(C_9H_7)^+$], 91 (26) [$(C_7H_7)^+$]. IR (ATR, film): 3032, 2832, 2732, 1702 (C=O), 1605, 1499, 1458, 1400, 1334, 1181, 1080, 1055, 1029, 965, 940, 922, 859, 759, 697 cm^{-1}. ^1H NMR ($CDCl_3$, 600 MHz): δ [ppm] = 1.53 (ddd, $^3J_{3a,1}$ = 8.3 Hz, $^3J_{3a,2}$ = 6.7 Hz, $^2J_{3a,3b}$ = 5.0 Hz, 1 H, 3-Ha), 1.75 (ddd, $^3J_{3b,2}$ = 9.2 Hz, $^3J_{3b,1}$ = 5.2 Hz, $^2J_{3b,3a}$ = 5.0 Hz, 1 H, 2-Hb), 2.18 (ddddd, $^3J_{1,3a}$ = 8.3 Hz, $^3J_{1,3b}$ = 5.2 Hz, $^3J_{1,CHO}$ = 4.6 Hz, $^3J_{1,2}$ = 4.0 Hz, 1 H, 1-H), 2.63 (ddd, $^3J_{2,3b}$ = 9.2 Hz, $^3J_{2,3a}$ = 6.7 Hz, $^3J_{2,1}$ = 4.0 Hz, 1 H, 2-H), 7.10–7.32 (m, 5 H, arom. CH), 9.33 (d, $^3J_{CHO,1}$ = 4.6 Hz, 1 H, CHO). ^{13}C NMR ($CDCl_3$, 151 MHz): δ [ppm] = 16.5 (C-3), 26.6 (C-1), 33.8 (C-2), 126.7 (o-C), 127.1 (p-C), 128.6 (m-C), 139.0 (i-C), 199.7 (CHO).

4.3. Synthesis of (1R,1'S,2'S)-1-(2-Phenylcyclopropyl)but-3-en-1-ol [(R,S,S)-9] and (1S,1'S,2'S)-1-(2-Phenylcyclopropyl)but-3-en-1-ol [(S,S,S)-9]

4.3.1. Method A: Allyl addition with Roush-reagent

In a *Schlenk*-flask was dissolved 10.8 g (38.3 mmol, 2.0 equiv.) allylboronic ester **7** in 100 mL toluene. The solution was coold to -78 °C and a solution of 2.6 g (17.7 mmol, 1.0 equiv., >98% ee) aldehyde (*S,S*)-**6** in 20 mL toluene was added *via* syringe. The solution was stirred for 5 h at −78 °C. At this temperature the reaction-mixture was washed with 50 mL of a saturated ammonium-carbonate solution. The solution was warmed to room temperature and the aqueous phase was extracted three times with Et_2O and two times with ethyl acetate. The combined organic layers were dried with $MgSO_4$, filtered and the solvent was evaporated under vacuum. The diastereomeric ratio was determined by ^1H NMR (78:22). The crude product was purified by column chromatography (PE:EE = 90:10, then 80:20). 2.5 g (13.2 mmol, 71%, >98% ee) of (*1R,1'S,2'S*)-1-(2-Phenylcyclopropyl)but-3-en-1-ol [(*R,S,S*)-**9**], 324 mg (1.7 mmol, 10%) of a diastereomeric mixture and 386 mg (2.1 mmol, 12%, 98% ee) (*1S,1'S,2'S*)-1-(2-phenylcyclopropyl) but-3-en-1-ol [(*S,S,S*)-**9**] could be isolated (93%).

4.3.2. Method B: Allyl addition with Leighton-reagent[60]

To a solution of 309.1 mg (0.6 mmol, 1.5 equiv.) of the *Leighton*-reagent (*S,S*)-**8** in 3 mL dichloromethane, 54.8 mg of aldehyde (*S,S*)-**6** dissolved in 1 mL dichloromethane was slowly added at −10 °C under an argon atmosphere. The reaction mixture was stirred 20 h at −10 °C. Afterwards at −10 °C, 5 mL of ethyl acetate and 5 mL of a 1 M HCl solution was added to hydrolyse. The mixture was stirred for 10 min at −10 °C and allowed to warm to room temperature. The reaction mixture was extracted three times with ethyl acetate. The combined organic layers were dried with $MgSO_4$, filtered and the solvent was evaporated under vacuum. The diastereomeric ratio was determined by ^1H NMR (>99:1).

After column chromatography (PE:EE 70:30) 68 mg (0.3 mmol, 75%, 98% ee) of homoallylic alcohol (*R,S,S*)-**9** could be isolated.

4.3.3. Method C: CBS-reduction[61] of ketone (S,S)-12

To a solution of 276 mg (1.48 mmol, 1.00 equiv.) of ketone (*S,S*)-**12** in 4.14 mL toluene was added under an argon atmosphere 185 mg molecular sieve (powder, 4 Å) and 3 mL (2.96 mmol, 2.0 equiv. 1 M in toluene) (*S*)-CBS-reagent (*S*)-**13**. The reaction mixture was cooled to −78 °C and 3 mL (2.96 mmol, 2.0 equiv., 1 M in toluene) of catecholborane was slowly added. The mixture was stirred overnight, where it warms to room temperature. After full conversion of starting material (TLC), the mixture was again cooled to −78 °C and 600 μL of absolute methanol was added. The mixture was warmed to room temperature and 10 mL of Et_2O and 10 mL of a 2:1 mixture of 1 M NaOH and saturated $NaHCO_3$ solution was added. The reaction mixture was extracted four times with Et_2O. The combined organic layers were washed with 1 M HCl and brine. The organic layers were dried with $MgSO_4$, filtered and the solvent was evaporated under vacuum. The crude product was purified by column chromatography (PE:EE = 90:10). 121 mg (0.64 mmol, 43%, >98% ee) of homoallylic alcohol (*R,S,S*)-**9** and 15 mg (80 μmol, 5%, 98% ee) of homoallylic alcohol (*S,S,S*)-**9** could be isolated.

R_f = 0.4 (PE:EE = 75:25). Rf = 0.6 (PE:EE = 70:30). (*R,S,S*)-**9** $[\alpha]_D^{20}$ = +84 (c = 1.0, $CHCl_3$, >98% ee). (*S,S,S*)-**9** $[\alpha]_D^{20}$ = +94 (c = 0.9 $CHCl_3$, >98% ee).

4.3.3.1. (1R,1'S,2'S)-1-(2'-Phenylcyclopropyl)but-3-en-1-ol [(R,S,S)-9]. HPLC: column: Chiracel OB (250 mm · 4.6 mm, Fa. Daicel); solvent: heptane:2-propanol = 90:10, flowrate: 0.5 mL/min; pressure: 23 bar, detection:

UV 220 nm; t_R [(*R,S,S*)-**9**] 10.8 min; t_R [(*S,R,R*)-**9**] 13.4 min. MS (EI, 70 eV): *m/z* (%) = 188 (<5) [M^+], 170 (8) [$(M\text{-}H_2O)^+$], 147 (20) [$(M\text{-}C_3H_5)^+$], 142 (7) [$(C_{11}H_{10})^+$], 129 (100) [$(C_{10}H_9)^+$], 107 (54) [$(C_8H_{11})^+$], 104 (69) [$(C_7H_4O)^+$], 91 (69) [$(C_7H_7)^+$], 77 (20) [$(C_6H_5)^+$]. Elemental analysis $C_{13}H_{16}O$ (188.27 g/mol): calc.: C 82.94 H 8.57; found: C 82.68 H 8.68. IR (ATR, film): 3387 (OH), 3072, 3002, 2978, 2903, 1641, 1604, 1497, 1464, 1431, 1413, 1277, 1090, 1067, 1047, 1030, 991, 913, 749, 697 cm^{-1}. ^1H NMR ($CDCl_3$, 600 MHz): δ [ppm] = 0.95 (m_c, 2 H, 3′-H), 1.28 (dddd, $^3J_{1',3'}$ = 8.0 Hz, $^3J_{1',1}$ = 7.6 Hz, $^3J_{1',3'}$ = 6.3 Hz, $^3J_{1',2'}$ = 4.6 Hz, 1 H, 1′-H), 1.76 (d, $^3J_{OH,1}$ = 3.6 Hz, 1 H, OH), 1.94 (ddd, $^3J_{2',3'}$ = 8.2 Hz, $^3J_{2',3'}$ = 6.0 Hz, $^3J_{2',1'}$ = 4.6 Hz, 1 H, 2′-H), 2.35 (dddt, $^2J_{2a,2b}$ = 14.0 Hz, $^3J_{2a,1}$ = 7.7 Hz, $^3J_{2a,3}$ = 7.6 Hz, $^4J_{2a,4}$ = 1.2 Hz, 2-Ha), 2.46 (dddt, $^2J_{2b,2a}$ = 14.0 Hz, $^3J_{2b,3}$ = 6.7 Hz, $^3J_{2b,1}$ = 4.6 Hz, $^4J_{2b,4}$ = 1.4 Hz, 1 H, 2-Hb), 3.26 (dddd, $^3J_{1,2a}$ = 7.7 Hz, $^3J_{1,1'}$ = 7.6 Hz, $^3J_{1,2b}$ = 4.6 Hz, $^3J_{1,OH}$ = 3.6 Hz, 1 H, 1-H), 5.1 (ddt, $^3J_{4a,3}$ = 10.2 Hz, $^2J_{4a,4b}$ = 2.0 Hz, $^4J_{4a,2}$ = 1.1 Hz, 1 H, 4-Ha), 5.17 (ddt, $^3J_{4b,3}$ = 17.1 Hz, $^2J_{4b,4a}$ = 2.0 Hz, $^4J_{4b,2}$ = 1.4 Hz, 1 H, 4-Hb), 5.90 (dddd, $^3J_{3,4b}$ = 17.1 Hz, $^3J_{3,4a}$ = 10.2 Hz, $^3J_{3,2a}$ = 7.6 Hz, $^3J_{3,2b}$ = 6.7 Hz, 1 H, 3-H), 7.07–7.27 (m, 5 H, arom. CH). ^{13}C NMR ($CDCl_3$, 151 MHz): δ [ppm] = 13.4 (C-3′), 20.9 (C-2′), 28.9 (C-1′), 41.6 (C-2), 74.4 (C-1), 118.0 (C-4), 125.6 (arom. CH), 126.1 (arom. CH), 128.3 (arom. CH), 134.6 (C-3), 142.6 (i-C).

4.3.3.2. (1S,1'S,2'S)-1-(2'-Phenylcyclopropyl)but-3-en-1-ol [(S,S,S)-9]. R_f = 0.3 (PE:EE = 75:25), m.p.: 35 °C. [(*S,S,S*)-**9**] $[\alpha]_D^{20}$ = +94 (c = 0.9 $CHCl_3$ > 98% ee); HPLC: column: Chiracel OB (250 mm·4.6 mm, Fa. Daicel); solvent: heptane:2-propanol = 90:10; flowrate 0.5 mL/min; pressure: 23 bar; detection: UV 220 nm; t_R [(*S,S,S*)-**9**]10.4 min; t_R [(*R,R,R*)-**9**] 16.2 min. MS (EI, 70 eV): *m/z* (%) = 188 (<5) [M^+], 170 (12) [$(M\text{-}H_2O)^+$], 147 (18) [$(M\text{-}C_3H_5)^+$], 142 (17) [$(C_{11}H_{10})^+$], 129 (100) [$(C_{10}H_9)^+$], 107 (54) [$(C_8H_{11})^+$], 104 (54) [$(C_7H_4O^+)$], 91 (65) [$(C_7H_7)^+$], 77 (18) [$(C_6H_5)^+$]. Elemental analysis: $C_{13}H_{16}O$ (188.27 g/mol): calc: C 82.94 H 8.57; found: C 82.32 H 8.51. IR (ATR, film): 3387 (OH), 3072, 3002, 2978, 2903, 1641, 1604, 1497, 1464, 1431, 1413, 1277, 1090, 1067, 1047, 1030, 991, 913, 749, 697 cm^{-1}. ^1H NMR ($CDCl_3$, 600 MHz): δ [ppm] = 0.97 (ddd, $^3J_{3'a,1'}$ = 8.4 Hz, $^3J_{3'a,2'}$ = 5.1 Hz, $^2J_{3'a,3'b}$ = 5.1 Hz, 1 H, 3′-Ha), 1.04 (ddd, $^3J_{3'b,2'}$ = 8.9 Hz, $^3J_{3'b,1'}$ = 5.6 Hz, $^2J_{3'b,3'a}$ = 5.1 Hz, 1 H, 3′-Hb), 1.28 (dddd, $^3J_{1',3'a}$ = 8.4 Hz, $^3J_{1',1}$ = 7.8 Hz, $^3J_{1',3'b}$ = 5.6 Hz, $^3J_{1',2'}$ = 4.5 Hz, 1 H, 1′-H), 1.69

(d, $^3J_{OH,1'}$ = 3.5 Hz, 1 H, OH), 1.84 (ddd, $^3J_{2',3'b}$ = 8.9 Hz, $^3J_{2',3'a}$ = 5.1 Hz, $^3J_{2',1'}$ = 4.5 Hz, 1 H, 2′-H), 2.37 (dddt, $^2J_{2a,2b}$ = 15.2 Hz, $^3J_{2a,3}$ = 7.8 Hz, $^3J_{2a,1}$ = 7.8 Hz, $^4J_{2a,4}$ = 1.2 Hz, 1 H, 2-Ha), 2.48 (dddt, $^2J_{2b,2a}$ = 15.2 Hz, $^3J_{2b,3}$ = 6.4 Hz, $^3J_{2b,1}$ = 4.6 Hz, $^4J_{2b,4}$ = 1.3 Hz, 1 H, 2-Hb), 3.25 (dddd, $^3J_{1,1'}$ = 7.8 Hz, $^3J_{1,2a}$ = 7.8 Hz, $^3J_{1,2b}$ = 4.6 Hz, $^3J_{1,OH}$ = 3.5 Hz 1 H, 1-H), 5.13 (ddt, $^3J_{4a,3}$ = 10.3 Hz, $^2J_{4a,4b}$ = 2.0 Hz, $^5J_{4a,2}$ = 1.0 Hz, 1 H, 4-Ha), 5.14 (ddt, $^3J_{4b,3}$ = 16.9 Hz, $^2J_{4b,4a}$ = 2.0 Hz, $^5J_{4b,2}$ = 1.4 Hz, 1 H, 4-Hb), 5.87 (dddd, $^3J_{3,4b}$ = 16.9 Hz, $^3J_{3,4a}$ = 10.3 Hz, $^3J_{3,2a}$ = 7.8 Hz, $^3J_{3,2b}$ = 6.4 Hz, 1 H, 3-H), 7.05–7.27 (m, 5 H, arom. CH). ^{13}C NMR ($CDCl_3$, 151 MHz): δ [ppm] = 13.5 (C-3′), 20.9 (C-2′), 28.9 (C-1′), 41.9 (C-2), 74.5 (C-1), 118.1 (C-4), 125.7 (arom. CH), 126.0 (arom. CH), 128.3 (arom. CH), 134.5 (C-3), 142.3 (i-C).

*4.4. Synthesis of (1S,1′R,2′R)-1-(2-Phenylcyclopropyl)but-3-en-1-ol [(S,R,R)-**9**] and (1R,1′R,2′R)-1-(2-Phenylcyclopropyl)but-3-en-1-ol [(R,R,R)-**9**]*

*4.4.1. Method C: CBS-reduction[61] of ketone (R,R)-**12***

84 mg (451 µmol, 1.0 equiv.) of ketone (*R,R*)-**12** with 0.90 mL (0.90 mmol, 2.0 equiv. 1 M in toluene) of (*S*)-CBS-reagent (*S*)-**13** and 0.90 mL (0.90 mmol, 2.0 equiv. 1 M in toluene) catecholborane have been reduced *via* method C for (*R,S,S*)-**9** and (*S,S,S*)-**9**. After purification 10 mg (53 µmol, 11%, 81% ee) of homoallylic alcohol (*S,R,R*)-**9** and 75 mg (398 µmol, 88%, 95% ee) of homoallylic alcohol (*R,R,R*)-**9** have been isolated. The diastereomeric ratio was 12:88. The spectroscopic data accords to (*R,S,S*)-**9** and (*S,S,S*)-**9**.

Analogously, 100 mg (540 mmol, 1.0 Äq) of ketone (*R,R*)-**12** was reduced with 1.08 mL (1.08 mmol, 2.0 equiv. 1 M in toluene) of (*R*)-CBS-reagent (*R*)-**13** and 0.54 mL (1.08 mmol, 2.0 equiv. 2 M in toluene) catecholborane. After purification 60 mg (319 µmol, 93%, 81% ee) of homoallylic alcohol [(*S,R,R*)-**9**] and 6.0 mg (32 µmol, 5%, 98% ee) of homoallylic alcohol (*R,R,R*)-**9** have been isolated. The spectroscopic data accords to (*S,R,R*)-**9** and (*R,R,R*)-**9**.

*4.5. Synthesis of (1S,2S)-N-Methoxy-N-methyl-2-phenylcyclopropanecarboxamide [(S,S)-**11**] and (1R,2R)-2-N-Methoxy-N-methyl-2-phenylcyclopropanecarboxamide [(R,R)-**11**]*

Under an argon atmosphere 198 mg (1.0 mmol, 1.0 equiv.) of ester (*S,S*)-**10** was dissolved in 4 mL abs·THF and 152 mg (1.6 mmol, 1.5 equiv.) *N*-methoxy-*N*-methylamino hydrochloride was added and cooled to −20 °C. With the use of a syringe pump 1.6 mL of an isopropylmagnesium chloride solution (2 M in THF, 3.1 mmol, 3.0 equiv.) was added over 45 min. After full addition the mixture stirred for 20 min at −20 °C (control *via* TLC). After full conversion, the solution was hydrolysed with saturated ammonium carbonate solution. The mixture was warmed to room temperature and diethylether and water was added until both layers were clear. The layers were separated and the aqueous layer was extracted three times with diethylether. The combined organic layers were dried with $MgSO_4$, filtered and the solvent was evaporated. After column chromatography (PE:EE 80:20, then 70:30) 160 mg (0.8 mmol, 78%) oft he *Weinreb*-amide (*S,S*)-**11** could be isolated as a colourless oil. The spectroscopic data accord to literature.[62]

Analogous to this method, 400 mg (2.1 mmol, 1.0 equiv.) of ester (*R,R*)-**10** was dissolved in 7.2 mL abs·THF. Afterwards, 312 mg (3.2 mmol, 1.5 equiv.) *N*-methoxy-*N*-methylamino hydrochloride was added. At −20 °C 3.2 mL of an isopropylmagnesium chloride solution (2 M in THF, 6.3 mmol, 3.0 equiv.) was added over 45 min. After 30 min complete conversion was detected. After workup, 426 mg (2.1 mmol, 99%) of (*R,R*)-**11** was isolated.

R_f = 0.35 (PE:EE = 70:30); (*S,S*)-**11** $[\alpha]_D^{20}$ = +228 (c = 1.0, $CHCl_3$, 97% ee); (*R,R*)-**11** $[\alpha]_D^{20}$ = −233 (c = 0.8 $CHCl_3$, 98% ee); HPLC: column: Chiracel OD-H (250 mm · 4.6 mm, Fa. Daicel); solvent: heptane:2-propanol = 98:2; flowrate: 0.5 mL/min; pressure: 33 bar; detection: UV 225 nm; t_R[(*R,R*)-**11**]: 26.2 min; t_R[(*S,S*)-**11**]: 29.1 min; MS (EI, 70 eV): *m/z* (%) = 205 (25) [M^+], 145 (100) [$(C_{10}H_9O)^+$], 127 (84) [$(C_6H_9NO_2)^+$], 117 (72) [$(C_9H_9)^+$], 115 (71) [$(C_9H_7)^+$], 91 (33) [$(C_7H_7)^+$]. HRMS (ESI, positiv-Ion): calc.: 228.1001 ($C_{12}H_{15}NO_2Na$) [$(M^+Na)^+$] found: 228.0995 ($C_{12}H_{15}NO_2$-Na) [$(M^+Na)^+$]. Elemental analysis: $C_{12}H_{15}NO_2$ (205.25 g/mol): calc.: C 70.22 H 7.37 N 6.82; found: C 69.90 H 7.48 N 6.85; IR (ATR, film): 3029, 3005, 2967, 2937, 1651 (C═O), 1605, 1498, 1460, 1439, 1421, 1394, 1368, 1174, 1119, 1097, 1022, 1004, 995, 939, 749, 698 cm^{-1}. ^{1}H NMR ($CDCl_3$, 600 MHz): δ [ppm] = 1.31 (ddd, $^3J_{3a,1}$ = 8.4 Hz, $^3J_{3a,2}$ = 6.4 Hz, $^2J_{3a,3b}$ = 4.3 Hz, 1 H, 3-Ha), 1.63 (ddd, $^3J_{3b,2}$ = 9.1 Hz, $^3J_{3b,1}$ = 5.4 Hz, $^2J_{3b,3a}$ = 4.3 Hz, 1 H, 3-Hb), 2.42 (br, 1 H, 1-H), 2.51 (ddd, $^3J_{2,3b}$ = 9.1 Hz, $^3J_{2,3a}$ = 6.4 Hz, $^3J_{2,1}$ = 4.2 H, 1 H, 2-H), 3.24 (s, 3 H, CH3), 3.69 (s, 3 H, OCH3), 7.12–7.30 (m, 5 H, arom. CH). ^{13}C NMR ($CDCl_3$, 151 MHz): δ [ppm] = 16.5 (C-3), 21.6 (C-1), 25.9 (C-2), 32.6 (NCH3), 61.7 (OCH3), 126.3 (arom. CH), 128.3 (arom. CH), 128.6 (arom. CH), 140.8 (i-C), 173.1 (NCO).

*4.6. Synthesis of (1′S,2′S)-1-(2′-Phenylcyclopropyl)but-3-en-1-on [(S,S)-**12**] and (1′R,2′R)-1-(2′-Phenylcyclopropyl)but-3-en-1-on [(R,R)-**12**]*

According to a procedure from Mohapatra and Datta[29] and Lee et al.[32] 100 mg (487 µmol, 1.0 equiv.) of *Weinreb*-amide (*S,S*)-**11** was dissolved in 2.5 mL abs·THF. The mixture was cooled to −78 °C and 0.6 mL (584 µmol, 1.2 equiv.) of a 1 M allylmagnesium bromide solution in diethylether was added slowly. The mixture was stirred for 30 min at −78 °C (reaction control by TLC). After full conversion it was hydrolysed with 5 mL of water and 0.8 mL of 1 M HCl. The mixture was warmed to room temperature and the two layers have been separated. The aqueous layer was extracted with diethylether three times. The combined organic layers were dried with $MgSO_4$, filtered and the solvent was evaporated. The crude product was purified by column chromatography (PE:EE 95:5). 70 mg (376 µmol, 77%, 97% ee) of ketone (*S,S*)-**12** could be isolated as a colourless oil.

(*R,R*)-**12** could be synthesized with the same protocol, using 119 mg (580 µmol, 1.0 equiv.) of (*1R,2R*)-*N,N*-methoxymethyl-2-phenylcyclopropancarboxamide [(*R,R*)-**11**] at −78 °C with 1.16 mL (1.16 mmol, 2.0 equiv.) of a 1 M allylmagnesium bromide solution in diethylether. The mixture was stirred for 30 min at −78 °C and hydrolysis with saturated ammonium carbonate solution at −60 °C. The mixture of two layers was warmed to room temperature and 2 mL of 1 M HCl was added. It was added water and ether until both layers were clear. The layers have been separated and the organic layer was extracted with diethylether a couple of times, followed by two times with ethyl acetate. The combined organic layers were dried with $MgSO_4$, filtered and the solvent was evaporated. The crude product was purified by column chromatography (PE:EE 95:5). 70 mg (38 µmol, 66%, 98% ee) of ketone (*R,R*)-**12** could be isolated as a colourless oil.

R_f = 0.2 (PE:EE = 70:30); (*S,S*)-**12** $[\alpha]_D^{20}$ = +475 (c = 1.2, $CHCl_3$, 97% ee); (*R,R*)-**12** $[\alpha]_D^{20}$ = −479 (c = 0.6, $CHCl_3$, >98% ee); HPLC: column: Chiracel OD-H (250 mm · 4.6 mm, Fa. Daicel); solvent: heptane : 2-propanol = 99.8:0.2; flowrate: 0.5 mL/min, pressure: 33 bar; detection: UV 225 nm; t_R[(*S,S*)-**12**]: 29.4 min; t_R[(*R,R*)-**12**]: 32.3 min. MS (EI, 70 eV): 186 (8) [M^+], 145 (91) [$(M\text{-}C_3H_5)^+$], 127 (78), 117 (100) [$(C_9H_9)^+$], 115 (85) [$(C_9H_7)^+$], 91 (45) [$(C_7H_7)^+$], 69 (19) [$(C_4H_5O)^+$]. Elemental analyse: $C_{13}H_{14}O_2$ (186.25 g/mol) calc.: C 83.83 H 7.58; found: C 83.40 H 7.63, IR (ATR, film): 3081, 3031, 1698 (C═O),

1636, 1604, 1497, 1457, 1432, 1398, 1342, 1212, 1180, 1120, 1058, 1044, 1016, 993, 918, 837, 749, 698 cm^{-1}. ^1H NMR ($CDCl_3$, 600 MHz): δ [ppm] = 1.39 (ddd, $^3J_{3'a,1'}$ = 8.1 Hz, $^3J_{3'a,2'}$ = 6.6 Hz, ^2J 3′a,3′b = 4.2 Hz 1 H, 3′-H_a), 1.69 (ddd, $^3J_{3'b,2'}$ = 9.1 Hz, $^3J_{3'b,1'}$ = 5.3 Hz, $^2J_{3'b,3'a}$ = 4.2 Hz, 1 H, 3′-H_b) 2.23 (ddd, $^3J_{1',3'a}$ = 8.1 Hz, $^3J_{1',3'b}$ = 5.3 Hz, ^3J1′,2′ = 4.0 Hz, 1 H, 1′-H), 2.53 (ddd, $^3J_{2',3'b}$ = 9.1 Hz, $^3J_{2',3'a}$ = 6.6 Hz, $^3J_{2',1'}$ = 4.0 Hz, 1 H, 2′-H), 3.36 (dt, $^3J_{2,3}$ = 6.8 Hz, $^4J_{2,4}$ = 1.4 Hz, 2 H, 2-H), 5.17 (ddt, $^3J_{4a,3}$ = 17.2 Hz, $^2J_{4a,4b}$ = 3.0 Hz, $^4J_{4a,2}$ = 1.4 Hz, 1 H, 4-H_a) 5.20 (ddt, $^3J_{4b,3}$ = 10.2 Hz, $^2J_{4b,4a}$ = 3.0 Hz, $^4J_{4b,2}$ = 1.4 Hz, 1 H, 4-H_b) 5.97 (ddt, $^3J_{3,4a}$ = 17.2 Hz, $^3J_{3,4b}$ = 10.2 Hz, $^3J_{3,2}$ = 6.8 Hz, 1 H, 3-H), 7.08–7.29 (m, 5 H, arom. CH). ^{13}C NMR ($CDCl_3$, 151 MHz): δ [ppm] = 19.2 (C-3′), 29.2 (C-2′) 31.8 (C-1′), 48.7 (C-2), 119.0 (C-4), 126.1 (arom. CH), 126.6 (arom. CH), 128.5 (arom. CH), 130.5 (C-3), 140.3 (i-C), 206.6 (C-1).

4.7. Synthesis of (1R,1′S,2′S)-1-(2′-Phenylcyclopropyl)but-3-en-1-yl acrylate [(R,S,S)-**17**]

850 mg (4.51 mmol, 1.00 equiv.) of homoallyl alcohol (*R,S,S*)-**9** was dissolved in 15 mL absolute dichloromethane under an argon atmosphere. The solution was cooled to −78 °C when 2.32 mL ethyldiisopropylamine (13.5 mmol, 3.00 equiv.) and 55 mg (0.45 mmol, 0.1 equiv.) DMAP was added. To this mixture 550 µL (6.77 mmol, 1.50 equiv.) acryloyl chloride was added slowly. The mixture was stirred 2 h at −78 °C until no starting material could be detected (TLC control). After hydrolysis with a saturated ammonium chloride-solution at −78 °C the mixture was warmed to RT and the two layers were separated. The aqueous phase was extracted three times with dichloromethane. The organic layers were combined, dried with $MgSO_4$, filtered and the solvent was evaporated under reduced pressure. The crude product was purified *via* column chromatography (PE:EE = 90:10). The clean product (*R,S,S*)-**17** could be isolated as a colourless oil [1.06 g (4.37 mmol, 97%, >98% ee)].

Dienes (*S,S,S*)-**17** and (*R,R,R*)-**17** have been synthesized according to the same protocol.

4.7.1. (1R,1′S,2′S)-1-(2′-Phenylcyclopropyl)but-3-en-1-yl acrylate [(R,S,S)-**17**]

R_f = 0.8 (PE:EE = 70:30); $[\alpha]_D^{20}$ = +147 (c = 1.0, $CHCl_3$); MS (EI, 70 eV): *m/z* (%) = 241 (<5) [M^+], 207 (<5) [$(C_{13}H_{13}O_2)^+$], 187 (<5) [$(C_{13}H_{15}O)^+$], 170 (19) [$(C_{13}H_{14})^+$], 161 (28) [$(C_{11}H_{13}O)^+$], 142 (10) [$(C_{11}H_{10}O)^+$], 129 (56) [$(C_{10}H_9)^+$], 117 [$(C_9H_9)^+$], 104 (40) [$(C_8H_8)^+$], 91 (34) [$(C_7H_7)^+$], 70 (15) [$(C_6H_7)^+$], 55 (100) [$(C_3H_5O)^+$]. Elemental analysis: $C_{16}H_{18}O_2$ (242.31 g/mol): calc.: C 79.31 H 7.49; found: C 79.22 H 7.58. IR (ATR, film): 3077, 3028, 2944, 1721 (C=O), 1619, 1638, 1605, 1498, 1404, 1295, 1270, 1195, 1092, 1047, 983, 916, 809, 751, 698 cm^{-1}. ^1H NMR (CDCl3, 600 MHz): δ [ppm] = 0.96 (ddd, $^3J_{3''a,2''}$ = 8.9 Hz, $^3J_{3''a,1''}$ = 5.5 Hz, $^2J_{3''a,3''}b$ = 5.3 Hz, 1 Hz, 3″-H_a), 1.03 (ddd, $^3J_{3''b,1''}$ = 8.7 Hz, $^3J_{3''b,2''}$ = 5.3 Hz, $^2J_{3''b,3''a}$ = 5.3 Hz, 1 H, 3″-H_b), 1.35 (dddd, $^3J_{1'',3''b}$ = 8.7 Hz, $^3J_{1'',1'}$ = 8.6 Hz, $^3J_{1'',3''a}$ = 5.5 Hz, $^3J_{1'',2''}$ = 4.5 Hz, 1 H, 1″-H), 2.07 (ddd, $^3J_{2'',3''a}$ = 8.9 Hz, $^3J_{2'',3''b}$ = 5.3 Hz, $^3J_{2'',1''}$ = 4.5 Hz, 1 H, 2″-H), 2.49 (ddddd, $^2J_{2'a,2'b}$ = 14.3 Hz, $^3J_{2'a,3'}$ = 7.5 Hz, $^3J_{2'a,1'}$ = 6.8 Hz, $^4J_{2'a,4'a}$ = 1.2 Hz, $^4J_{2'a,4'b}$ = 1.2 Hz, 1 H, 2′-H_a), 2.54 (ddddd, $^2J_{2'b,2'a}$ = 14.3 Hz, $^3J_{2'b,3'}$ = 6.6 Hz, $^3J_{2'b,1'}$ = 5.5 Hz, $^4J_{2'b,4'a}$ = 1.3 Hz, $^4J_{2'b,4'b}$ = 1.3 Hz, 1 H, 2′-H_b), 4.62 (ddd, $^3J_{1',1''}$ = 8.6 Hz, $^3J_{1',2'a}$ = 6.8 Hz, $^3J_{1',2'b}$ = 5.5 Hz, 1 H, 1′-H), 5.08 (dddd, $^3J_{4'a,3'}$ = 10.2 Hz, $^2J_{4'a,4'b}$ = 2.1 Hz, $^4J_{4'a,2'b}$ = 1.3 Hz, $^4J_{4'a,2'a}$ = 1.2 Hz, 1 H, 4′-H_a), 5.21 (dddd, $^3J_{4'b,3'}$ = 17.0 Hz, $^2J_{4'b,4'a}$ = 2.1 Hz, $^4J_{4'b,2'b}$ = 1.3 Hz, $^4J_{4'b,2'a}$ = 1.2 Hz, 1 H, 4′-H_b), 5.81 (dd, $^3J_{3a,2}$ = 10.4 Hz, $^2J_{3a,3b}$ = 1.5 Hz, 1 H, 3-H_a), 5.83 (dddd, $^3J_{3',4'b}$ = 17.0 Hz, $^3J_{3',4'a}$ = 10.2 Hz, $^3J_{3',2'a}$ = 7.5 Hz, $^3J_{3',2'b}$ = 6.6 Hz, 1 H, 3′-H), 6.11 (dd, $^3J_{2,3b}$ = 17.3 Hz, $^3J_{2,3a}$ = 10.4 Hz, 1 H, 2-H), 6.40 (dd, $^3J_{3b,2}$ = 17.3 Hz, $^2J_{3b,3a}$ = 1.5 Hz, 1 H, 3-H_b), 7.04–7.29 (m, 5 H, arom. CH). ^{13}C NMR ($CDCl_3$, 151 MHz):δ [ppm] = 13.3, 21.5, 26.3, 38.9, 76.8, 117.9,125.7, 126.1, 128.3, 128.7, 130.7, 133.4, 142.2, 165.9.

4.7.2. (1S,1′S,2′S)-1-(2′-Phenylcyclopropyl)but-3-en-1-yl acrylate [(S,S,S)-**17**] and (1R,1′R,2′R)-1-(2′-Phenylcyclopropyl)but-3-en-1-yl acrylate [(R,R,R)-**17**]

(*S,S,S*)-**17**: 514 mg (2.12 mmol, 89%), colourless oil. [(*R,R,R*)-**17**: 1.3 g (5.4 mmol, 95%), colourless oil. R_f = 0.8 (PE:EE = 70:30). [(*R,R,R*)-**17** $[\alpha]_D^{20}$ = −38 (c = 1.0, $CHCl_3$). MS (EI, 70 eV): *m/z* (%) = 242 (<5) [M^+], 201 (<5) [$(M\text{-}C_3H_5)^+$], 187 (<5) [$(C_{13}H_{15}O)^+$], 170 (26) [$(C_{13}H_{14})^+$], 161 (51) [$(C_{11}H_{13}O)^+$], 142 (13) [$(C_{11}H_{10}O)^+$], 129 (69) [$(C_{10}H_9)^+$], 104 (44) [$(C_8H_8)^+$], 91 (41) [$(C_7H_7)^+$], 55 (100) [$(C_3H_5O)^+$]. Elemental analysis: $C_{16}H_{18}O_2$ (242.31 g/mol): calc.: C 79.31 H 7.49; found: C 79.07 H 7.50. IR (ATR, film): 3078, 3028, 3008, 2942, 1720 (C=O), 1637, 1605, 1498, 1465, 1404, 1295, 1270, 1195, 1044, 983, 919, 808, 752, 697 cm^{-1}. ^1H NMR ($CDCl_3$, 600 MHz): δ [ppm] = 0.97 (ddd, $^3J_{3''a,1''}$ = 8.5 Hz, $^3J_{3''a,2''}$ = 5.3 Hz, $^2J_{3''a,3''b}$ = 5.3 Hz, 1 H, 3″-Ha), 1.12 (ddd, $^3J_{3''b,2''}$ = 8.9 Hz, $^3J_{3''b,1''}$ = 5.5 Hz, $^2J_{3''b,3''a}$ = 5.3 Hz, 1 H, 3″-Hb), 1.37 (dddd, $^3J_{1'',1'}$ = 8.6 Hz, $^3J_{1'',3''a}$ = 8.5 Hz, $^3J_{1'',3''b}$ = 5.5 Hz, $^3J_{1'',2''}$ = 4.5 Hz, 1 H, 1″-H), 1.88 (ddd, $^3J_{2'',3''b}$ = 8.9 Hz, $^3J_{2'',3''a}$ = 5.3 Hz, $^3J_{2'',1''}$ = 4.5 Hz, 1 H, 2″-H), 2.50–2.53 (m, 2 H, 2′-H), 4.61 (ddd, $^3J_{1',1''}$ = 8.6 Hz, $^3J_{1',2'}$ = 6.4 Hz, $^3J_{1',2'}$ = 5.9 Hz, 1 H, 1′-H), 5.05 (dddd, $^3J_{4'a,3'}$ = 10.2 Hz, $^2J_{4'a,4'b}$ = 2.0 Hz, $^4J_{4'a,2'}$ = 1.1 Hz, $^4J_{4'a,2'}$ = 1.1 Hz, 1 H, 4′-Ha), 5.07 (dddd, $^3J_{4'b,3'}$ = 17.1 Hz, $^2J_{4'b,4'a}$ = 2.0 Hz, $^4J_{4'b,2'}$ = 1.5 Hz, $^4J_{4'b,2'}$ = 1.5 Hz, 1 H, 4′-Hb), 5.80 (dddd, $^3J_{3',4'b}$ = 17.1 Hz, $^3J_{3',4'a}$ = 10.2 Hz, $^3J_{3',2'}$ = 7.0 Hz, $^3J_{3',2'}$ = 6.9 Hz, 1 H, 3′-H), 5.84 (dd, $^3J_{3a,2}$ = 10.4 Hz, $^2J_{3a,3b}$ = 1.4 Hz, 1 H, 3-Ha), 6.15 (dd, $^3J_{2,3b}$ = 17.3 Hz, $^3J_{2,3a}$ = 10.4 Hz, 1 H, 2-H), 6.42 (dd, $^3J_{3b,2}$ = 17.3 Hz, $^2J_{3b,3a}$ = 1.4 Hz, 1 H, 3-Hb), 7.05–7.28 (m, 5 H, arom. CH). ^{13}C NMR ($CDCl_3$, 151 MHz): δ [ppm] = 14.1 (C-3″), 21.6 (C-1″), 26.5 (C-2″), 39.2 (C-2′), 76.8 (C-1′), 117.9 (C-4′), 125.8 (arom. CH), 126.0 (arom. CH), 128.4 (arom. CH), 128.7 (C-2), 130.7 (C-3), 133.3 (C-3′), 141.8 (i-C), 165.6 (C-1).

4.8. Synthesis of (6R,1′S,2′S)-6-(2′-Phenylcyclopropyl)-5,6-dihydro-2H-pyran-2-one [(R,S,S)-**4**]

According to Ghosh et al.[41] 1.06 g (4.37 mmol, 1.00 equiv.) diene (*R,S,S*)-**17** was dissolved under an argon atmosphere in 700 mL dichloromethane. Subsequently 388 µL (1.31 mmol, 0.30 equiv.) titantetraisopropylate was added and the solution was refluxed for 30 min. Afterwards, 360 mg (0.44 mmol, 0.10 equiv.) Grubbs-I catalyst was added and the purple solution was refluxed for 16 h under absence of oxygen (control by TLC). After complete conversion the solution was distilled until 10 mL of solution were left over. The crude product was then transferred to a silica column (PE:EE = 95:5, then 90:10, then 80:20) and purified twice *via* column chromatography. The product (*R,S,S*)-**4** could be isolated as a colourless solid [859 mg (4.00 mmol, 92%)].

Lactones (*S,S,S*)-**4** and (*R,R,R*)-**4** have been synthesized according to the same protocol.

4.8.1. (6R,1′S,2′S)-6-(2′-Phenylcyclopropyl)-5,6-dihydro-2H-pyran-2-one [(R,S,S)-**4**]

R_f = 0.2 (PE:EE = 75:25). Melting point: 65 °C. $[\alpha]_D^{20}$ = +264 (c = 0.9, $CHCl_3$). MS EI (70 eV): *m/z* (%) = 214 (16) [M^+], 169 (6) [$(M\text{-}CHO_2)^+$], 145 (8) [$(C_{10}H_9O)^+$], 129 (26) [$(C_{10}H_9)^+$],117 (43) [$(C_9H_9)^+$], 103 (14) [$(C_6H_8)^+$], 97 (100) [$(C_5H_5O_2)^+$], 69 (23) [$(C_4H_4O)^+$]. IR (ATR, film): 3059, 3026, 2898, 1710 (C=O), 1605, 1498, 1415, 1381, 1246, 1152, 1062, 1021, 950, 937, 876, 816, 761, 698 cm^{-1}. ^1H NMR (CDCl3, 600 MHz): δ [ppm] = 1.02 (ddd, ^3J = 8.6 Hz, ^2J = 5.5 Hz, ^3J = 5.5 Hz, 1 H), 1.05 (ddd, ^3J = 8.9 Hz, ^2J = 5.5 Hz, ^3J = 5.5 Hz, 1 H), 1.46 (dddd, ^3J = 8.6 Hz, ^3J = 7.7 Hz, ^3J = 5.5 Hz, ^3J = 4.5 Hz, 1 H), 2.12 (ddd, ^3J = 8.9 Hz, ^3J = 5.5 Hz,

^3J = 4.5 Hz, 1 H), 2.25–2.53 (m, 2 H), 4.05 (ddd, ^3J = 7.7 Hz, ^3J = 7.7 Hz, ^3J = 7.7 Hz, 1 H), 6.05 (ddd, ^3J = 9.8 Hz, 4J3,5 = 1.9 Hz, ^4J = 1.9 Hz, 1 H), 6.90 (ddd, ^3J = 9.8 Hz, ^3J = 4.8 Hz, ^3J = 4.0 Hz, 1 H), 7.10–7.28 (m, 5 H, arom. CH). ^{13}C NMR (CDCl3, 151 MHz): δ [ppm] = 12.1, 21.3, 25.8, 29.4, 80.8, 121.7, 125.7, 126.3, 128.3, 141.4, 144.8, 164.3.

*4.8.2. (S)-6-((1S,2S)-2-Phenylcyclopropyl)-5,6-dihydro-2H-pyran-2-one [(S,S,S)-**4**]and (R)-6-((1R,2R)-2-phenylcyclopropyl)-5,6-dihydro-2H-pyran-2-one [(R,R,R)-**4**]*

[(*S,S,S*)-**4**]: (322 mg, 1.51 mmol, 71%), colourless oil. [(*R,R,R*)-**4**]: 1.04 g (4.30 mmol, 90%), colourless oil. R_f = 0.2 (PE:EE = 75:25). R_f = 0.2 (PE:EE = 80:20). (*R,R,R*)-**4** $[\alpha]_D^{20}$ = +0.7 (c = 0.9, $CHCl_3$, 97% ee). (*S,S,S*)-**4** $[\alpha]_D^{20}$ = −0.8 (c = 1.1, $CHCl_3$, 94% ee). HPLC: column: Chiralpak AS (250 mm · 4.6 mm, Fa. Daicel); solvent: heptane:2-propanol = 80:20; flowrate: 0.5 mL/min, pressure: 10 bar; detection: UV 205 nm; t_R [(*R,R,R*)-**4**] 42.2 min; t_R [(*S,S,S*)-**4**] 48.1 min. MS (EI, 70 eV): *m*/*z* (%) = 214 (10) [M^+], 169 (6) [$(M\text{-}CHO_2)^+$], 145 (8) [$(C_{10}H_9O)^+$], 129 (23) [$(C_{10}H_9)^+$], 117 (44) [$(C_9H_9)^+$], 104 (41) [$(C_6H_9)^+$], 97 (100) [$(C_5H_5O_2)^+$], 91 (32) [$(C_7H_7)^+$], 77 (10) [$(C_6H_5)^+$], 69 (25) [$(C_4H_5O)^+$], 68 (35) [$(C_4H_5O)_+$]. HRMS (ESI, positiv-Ion): calc.: 237.0886 ($C_{14}H_{14}O_2Na$) [$(M + Na)^+$] found: 237.0884 ($C_{14}H_{14}O_2Na$) [$(M + Na)_+$]. Elemental analysis: $C_{14}H_{14}O_2$ (214.26 g/mol): calc.: C 78.48 H 6.59; found: C 78.14 H 6.67. IR (ATR, film): 3027, 1713 (C=O), 1605, 1499, 1465, 1417, 1383, 1247, 1153, 1076, 1063, 1031, 938, 916, 754, 698 cm^{-1}. ^{1}H NMR ($CDCl_3$, 600 MHz): δ [ppm] = 1.11 (ddd, $^3J_{3'a,1'}$ = 8.5 Hz, $^3J_{3'a,2'}$ = 5.5 Hz, $^2J_{3'a,3'b}$ = 5.5 Hz, 1 H, 3′-Ha), 1.21 (ddd, $^3J_{3'b,2'}$ = 9.0 Hz, $^3J_{3'b,1'}$ = 5.5 Hz, $^2J_{3'b,3'a}$ = 5.5 Hz, 1 H, 3′-Hb), 1.49 (dddd, $^3J_{1',3'a}$ = 8.5 Hz, $^3J_{1',6'}$ = 8.0 Hz, $^3J_{1',3'b}$ = 5.5 Hz, $^3J_{1',2'}$ = 4.5 Hz, 1 H, 1′-H), 1.96 (ddd, $^3J_{2',3'b}$ = 9.0 Hz, $^3J_{2',3'a}$ = 5.5 Hz, $^3J_{2',1'}$ = 4.5 Hz, 1 H, 2′-H), 2.50–2.59 (m, 2 H, 5-H), 4.04 (ddd, $^3J_{6,5}$ = 9.5 Hz, $^3J_{6,1'}$ = 8.0 Hz, $^3J6_{,5}$ = 5.8 Hz, 1 H, 6-H), 6.04 (ddd, $^3J_{3,4}$ = 9.7 Hz, $^3J_{3,5}$ = 2.3 Hz, $^3J_{3,5}$ = 1.4 Hz, 1 H, 3-H), 6.89 (ddd, $^3J_{4,3}$ = 9.7 Hz, $^3J_{4,5}$ = 5.1 Hz, $^3J_{4,5}$ = 3.1 Hz, 1 H, 4-H), 7.06–7.29 (m, 5 H, arom. CH). ^{13}C NMR ($CDCl_3$, 151 MHz): δ [ppm] = 13.8 (C-3′), 20.5 (C-1′), 26.2 (C-2′), 29.6 (C-5), 80.7 (C-6), 121.6 (C-3), 125.9 (arom. CH), 126.1 (arom. CH), 128.5 (arom. CH), 141.4 (i-C), 144.9 (C-4), 164.2 (C-2).

4.9. Biological methods

4.9.1. Cell culture

Human lung adenocarcinoma cell line A549 (German Collection of Microorganisms and Cell Cultures, Braunschweig, Germany) was cultured in DMEM medium (Thermo Fisher Scientific, Waltham, MA, USA) supplemented with 10% heat inactivated fetal bovine serum (h.i. FBS; Thermo Fisher Scientific, Waltham, MA, USA), 100 U/mL penicillin and 100 μg/mL streptomycin (Thermo Fisher Scientific, Waltham, MA, USA).

Human breast adenocarcinoma cell line MCF-7 (German Collection of Microorganisms and Cell Cultures, Braunschweig, Germany) was cultured in RPMI 1640 medium (Thermo Fisher Scientific, Waltham, MA, USA) supplemented with 10% h.i. FBS, 1x MEM non-essential amino acids (Biochrom, Berlin, Germany), 1 mM sodium pyruvate (Biochrom, Berlin, Germany), 10 μg/mL human insulin (Biochrom, Berlin, Germany), 100 U/mL penicillin and 100 μg/mL streptomycin.

Triple negative human breast cancer cell line HBL-100 (Cell Lines Service, Eppelheim, Germany) was cultured in Mc Coy's 5A medium (Thermo Fisher Scientific, Waltham, MA, USA) supplemented 10% h.i. FBS, 2 mM l-glutamine, 100 U/mL penicillin and 100 μg/mL streptomycin.

Cell lines were cultured at 37 °C and 5% CO_2 in a humidified atmosphere.

4.9.2. Cytotoxicity assay

Cytotoxicity was measured using the CellTiter-Glo Luminescent Cell Viability Assay (Promega, Madison, WI, USA) according to the manufacturer's protocol. This assay is based on a luciferase reaction to determine the ATP content, which is proportional to the rate of living cells. Cells were seeded in white 384-well plates (A549, HBL-100: $2{\cdot}10^3$ cells/well; MCF-7: $5{\cdot}10^3$ cells/well) in cell culture medium with the CyBi-Well 96-channel simultaneous pipettor (Analytik Jena AG, Jena, Germany). After 24 h incubation at 37 °C and 5% CO_2, the test compounds were added and the cells were further incubated for 48 h. Afterwards, the CellTiter-Glo reagent was added and luminescence was measured using the Infinite m200 microplate reader (Tecan Group AG, Maennedorf, Switzerland).

IC_{50} values were determined by plotting the luminescence values against the logarithmic molar concentration of the compounds and subsequent curve fitting (nonlinear regression) using GraphPad Prism v. 6.07 (GraphPad Software, San Diego, CA, USA). The results are mean values of at least three independent experiments

4.9.2.1. Yeast strains. S. cerevisiae was cultured in YPD medium (10 g/liter yeast extract, 20 g/liter peptone, 2% glucose). The following *S. cerevisiae* yeast strain was used: YRE1001 (*MATa ura3-52 trp1-1 leu2-3112 his3-11,15 ade2-1 pdr1-3 pdr5pdr5promΔ::TRP1*).

4.9.2.2. Liquid drug assay. The test compounds were diluted in DMSO to final concentration of 20 mg/mL (except of **25** was diluted to a final concentration of 10 mg/mL). The assay was carried out in sterile 96-well microtiter plates (Falcon) with 6,25 μL of serial dilution of the test compounds, 193,75 μL of YPD medium and 50 μL of yeast culture at an OD_{600} of 0.15. Plates were incubated for 48 h at 30 °C, and OD_{600} was measured with an ELISA plate reader (BioRad).

4.9.2.3. Isolation of plasma membranes. Yeast cells were cultured to an OD_{600} of 1.5 in YPD at 25 °C. At this time point, the nitrogen sources was replenished by addition of a 10th volume 5x YP (50 g/liter yeast extract, 100 g/liter peptone). Cells were harvested at an OD_{600} of 3.5. The isolation of plasma membranes (PM) was performed as described.[63,68]

4.9.2.4. Rhodamine 6G transport assay. Active transport of rhodamine 6 G (R6G) was measured, using a Tecan Infinite 200 PRO reader (Tecan), according to the protocol developed by Kolaczkowski et al.[63] Isolated PM (6 μL of a 1 mg/mL stock solution) were resuspended in 200 μl of transport buffer (50 mM Hepes, pH 7.0, 5 mM $MgCl_2$, 10 mM NaN_3, and 150 nM R6G) and incubated at 30 °C in a 96-well-FIA-plate (Greiner). In addition, 5 μL of 3 different concentrations (500 μg/mL, 50 μg/mL and 5 μg/mL) (except of **25**: 125 μg/mL, 13 μg/mL) of the test compounds were added. The active transport was started by addition of 10 mM ATP and the fluorescence was recorded for 20 min (excitation at 524 nm, emission at 558 nm; number of flashes: 30, integration time 2000 μs).

4.9.2.5. Atpase activity assay. Oligomycin (OM)-sensitive ATPase activity of Pdr5 in highly enriched PM was determined by a colometric assay in 96-well microtiter plate.[64–66] 40 μL of the plasma membrane solution (20 μg/mL stock solution) were incubated with 2 mM ATP, 5 mM $MgCl_2$ in 270 mM Tris-glycine buffer (pH 9.5) and 5 μL of the indicated test compound concentrations in a total volume of 100 μL. To reduce the background activities 0.2 mM ammonium molybdate, 10 mM NaN_3 and 50 mM KNO_3, respectively, were added.[64,67] In a second assay, OM (20 μg/mL) was added to the experiment under same conditions. After incubation at 30 °C for 20 min, the reaction was stopped by adding 25 μL of the reaction to 175 μL 40 mM H_2SO_4. The amount of released inorganic

phosphate was determined by a colorimetric assay, using Na_2HPO_4 as standard. The difference of both assays corresponds to OM-sensitive ATPase activity of Pdr5.[68]

Acknowledgments

We gratefully acknowledge the *Studienstiftung des deutschen Volkes* (Scholarship to A. W.), the *AiF ('ZIM Kooperationsprojekt' KF3279X01AJ3),* the *Deutsche Forschungsgemeinschaft*, the *Heinrich-Heine-Universität Düsseldorf,* and the *Forschungszentrum Jülich GmbH* for their generous support of our project. The PhD training of J.S. and A.K. is financed by the *graduate program in Pharmacology and Experimental Therapeutics* at the University of Cologne which is financially and scientifically supported by Bayer. We thank *Birgit Henβen* for analytic support.

References

1. Ali AM, Mackeen MM, Hamid M, et al. *Planta Med*. 1997;63:81–83.
2. de Fátima A, Kohn LK, de Carvalho JE, Pilli RA. *Bioorg Med Chem*. 2006;14:622–631.
3. de Fátima A, Modolo LV, Conegero LS, et al. *Curr Med Chem*. 2006;13:3371–3384.
4. de Fátima A, Kohn LK, Antônio MA, de Carvalho JE, Pilli RA. *Bioorg Med Chem*. 2005;13:2927–2933.
5. Inayat-Hussain SH, Annuar BO, Din LB, Ali AM, Ross D. *Toxicol In Vitro*. 2003;17:433–439.
6. Mosaddik MA, Haque ME. *Phytother. Res.*. 2003;17:1155–1157.
7. de Fátima A, Martins CVB, de Resende MA, et al. *Lett Drug Des Discovery*. 2008;5:74–78.
8. Bermejo A, Lora MJ, Blázouez MA, Rao KS, Cortes D, Zafra-Polo MC. *Nat Prod Lett*. 1995;7:117–122.
9. Hlubucek JR, Robertson AV. *Aust J Chem*. 1967;20:2199–2206.
10. Meyer HH. *Liebigs Ann Chem*. 1979;484–491.
11. Wach J-Y, Güttinger S, Kutay U, Gademann K. *Bioorg Med Chem Lett*. 2010;20:2843–2846.
12. Bruder M, Vendramini-Costa DB, de Carvalho JE, Pilli RA. *Bioorg Med Chem*. 2013;21:5107–5117.
13. Barcelos RC, Pastre JC, Caixeta V, Vendramini-Costa DB, de Carvalho JE, Pilli RA. *Bioorg Med Chem*. 2012;20:3635–3651.
14. Vendramini-Costa DB, Spindola HM, de Mello GC, et al. *Science*. 2015;139:83–90.
15. Takemura T, Kamo T, Ismil R, et al. *Nat Prod Commun*. 2012;7:1197–1198.
16. Wasno N, Takemura T, Ismil R, Bakar B, Fujii Y. *Nat Prod Commun*. 2015;10:725–727.
17. Pietruszka J, Rieche ACM, Wilhelm T, Witt A. *Adv Synth Catal*. 2003;345:1273–1286.
18. Dess DB, Martin JC. *J Am Chem Soc*. 1991;113:7277–7287.
19. Dess DB, Martin JC. *J Org Chem*. 1983;48:4155–4156.
20. Boeckman RK, Shao P, Mullins JJ. *Org Synth*. 2000;77:141–146.
21. Meyer SD, Schreiber SL. *J Org Chem*. 1994;59:7549–7552.
22. Tohma H, Kita Y. *Adv Syn Catal*. 2004;346:111–125.
23. Müller D, Umbricht G, Weber B, Pfaltz A. *Helv Chim Acta*. 1991;74:232–240.
24. Roush WR, Pankowitz AD, Palmer MAJ. *J Org Chem*. 1987;52:316–318.
25. Roush WR, Hoong LK, Palmer MAJ, Park JC. *J Org Chem*. 1990;55:4109–4117.
26. Leighton JL. *Aldrichimica Acta*. 2010;43:3–12.
27. Kinnaird JWA, Ng PY, Kubota K, Wang X, Leighton JL. *J Am Chem Soc*. 2002;124:7920–7921.
28. Csuk R, Schabel MJ, von Scholz Y. *Tetrahedron Asym*. 1996;7:3505–3512.
29. Mohapatra DK, Datta A. *J Org Chem*. 1998;63:642–646.
30. Kramp GJ, Kim M, Gais H-J, Vermeeren C. *J Am Chem Soc*. 2005;127:17910–17920.
31. Lerm M, Gais H-J, Cheng K, Vermeeren C. *J Am Chem Soc*. 2003;125:9653–9667.
32. Lee HK, Im JH, Jung SH. *Tetrahedron*. 2007;63:3321–3327.
33. Corey EJ, Helal CJ. Angew. Chem. 1998, 110, 2092–2118 [Angew. Chem. Int. Ed. 1998, 37, 1986-2012].
34. Corey EJ, Bakshi RK, Shibata S. *J Am Chem Soc*. 1987;109:5551–5553.
35. Mathre DJ, Jones TK, Xavier LC, et al. *J Org Chem*. 1991;56:751–762.
36. Mathre DJ, Thompson AS, Douglas AW, et al. *J Org Chem*. 1993;58:2880–2888.
37. Pietruszka J, Rieche ACM, Schöne N. *Synlett*. 2007;16:2525–2528.
38. Eichenauer NC, Nordschild née Rieche ACM, Bischop M, et al. *Eur J Org Chem*. 2015;5620–5632.
39. Bischop M, Doum V, Nordschild née Rieche ACM, Pietruszka J, Sandkuhl D. *Synthesis*. 2010;527–537.
40. Pietruszka J, Rieche ACM. *Adv Synth Catal*. 2008;350:1407–1412.
41. Ghosh AK, Cappiello J, Shin D. *Tetrahedron Lett*. 1998;39:4651–4654.
42. Fürstner A, Langemann K. *J Am Chem Soc*. 1997;119:9130–9136.
43. Fischer T, Pietruszka J. *Adv Synth Catal*. 2012;354:2521–2530. for selected alternative early reports on the synthesis of goniothalamins see[45–50] as well as[2–7].
44. For an alternative see: Bartlett S, Böse D, Ghori D, et al. *Synthesis*. 2013;45:1106–1114.
45. Henkel B, Kunath A, Schick H. *Liebigs Ann Chem*. 1992;809–811.
46. Dixon DJ, Ley SV, Tate EW. *J Chem Soc Perkin Trans*. 1998;1:3125–3126.
47. Quitschalle M, Christmann M, Bhatt U, Kalesse M. *Tetrahedron Lett*. 2001;42:1263–1265.
48. Job A, Wolberg M, Müller M, Enders D. *Synlett*. 2001;1796–1798.
49. Ramachandran PV, Chandra JS, Reddy MVR. *J Org Chem*. 2002;67:7547–7550.
50. Pospisil J, Marko IE. *Tetrahedron Lett*. 2006;47:5933–5937.
51. Lan Y-H, Chang F-R, Yu J-H, et al. *J Nat Prod*. 2003;66:487–490.
52. Lan Y-H, Chang F-R, Liaw C-C, Wu C-C, Chiang M-Y, Wu Y-C. *Planta Med*. 2005;71:153–159.
53. Boonmuen N, Thongon N, Chairoungdua A, et al. *Eur J Pharmacol*. 2016;791:455–464.
54. Semprebon SC, Marques LA, D'Epiro GFR, et al. *Toxicol In Vitro*. 2015;30:250–263.
55. Vuligonda V, Lin Y, Chandraratna RAS. *Bioorg Med Chem*. 1996;6:213–218.
56. Theberge CR, Verbicky CA, Zercher CK. *J Org Chem*. 1996;61:8792–8798.
57. Cheeseman M, Feuillet FJP, Johnson AL, Bull SD. *Chem Commun*. 2005;2372–2374.
58. Kaye PT, Molema WE. *Chem Commun*. 1998;2479–2480.
59. Arai I, Mori A, Yamamoto H. *J Am Chem Soc*. 1985;107:8254–8256.
60. Kubota K, Leighton JL, Angew. Chem. **2003**, 115, 976–978 [Angew. Chem. Int. Ed. **2003**, 42, 946-948].
61. Corey EJ, Shibata S, Bakshi RK. *J Org Chem*. 1988;53:2861–2863. also see[33,34].
62. Kazuta Y, Abe H, Yamamoto T, Matsuda A, Shuto S. *J Org Chem*. 2003;68:3511–3521.
63. Kolaczkowski M, van der Rest M, Kolaczkowska AC, Soumillion JP, Konings WN, Andre G. *J Biol Chem*. 1996;271:31543–31548.
64. Goffeau A, Dufour JP. *Methods Enzymol*. 1988;157:528–533.
65. Decottignies A, Kolaczkowski M, Balzi E, Goffeau A. *J Biol Chem*. 1994;269:12797–12803.
66. Wada S, Niimi M, Niimi Ky, et al. *J Biol Chem*. 2002;277:46809–46821.
67. Dufour JP, Amory A, Goffeau A. *Methods Enzymol*. 1988;157:513–528.
68. Ernst R. *Proc Natl Acad Sci USA*. 2008;105:5069–5074.

2.2 Chapter II

Title: Selective inhibition of the P-gp transporter by goniothalamin derivatives sensitizes resistant cancer cells to chemotherapy

Authors: **Julia Sachs**, Onat Kadioglu, Anja Weber, Vanessa Mundorf, Janina Betz, Thomas Efferth, Jörg Pietruszka, Nicole Teusch

Journal: Phytomedicine, 2018 (Impact factor: 3.526), submitted

Contribution: cell culture, assay establishment, cytotoxicity assays, gene expression analysis, ABC transporter assays, flow cytometry, ATPase assays, data analysis, writing of the manuscript

Selective inhibition of the P-gp transporter by goniothalamin derivatives sensitizes resistant cancer cells to chemotherapy

Julia Sachs[a], Onat Kadioglu[b], Anja Weber[c], Vanessa Mundorf[a], Janina Betz[a], Thomas Efferth[b], Jörg Pietruszka[c,d], Nicole Teusch[a*]

[a] Bio-Pharmaceutical Chemistry and Molecular Pharmacology, Faculty of Applied Natural Sciences, Technische Hochschule Köln, CHEMPARK, Geb. E39, 51368 Leverkusen, Germany

[b] Department of Pharmaceutical Biology, Institute of Pharmacy and Biochemistry, Johannes Gutenberg Universität Mainz, Staudinger Weg 5, 55128 Mainz, Germany

[c] Institute of Bioorganic Chemistry, Heinrich-Heine-Universität Düsseldorf im Forschungszentrum Jülich, Stetternicher Forst, Geb. 15.8, 52426 Jülich, Germany

[d] IBG-1: Biotechnology, Forschungszentrum Jülich, 52428 Jülich, Germany

*** Corresponding author**

Prof. Dr. Nicole Teusch

Technische Hochschule Köln

Faculty of Applied Natural Sciences

CHEMPARK, Kaiser-Wilhelm-Allee, E39

51368 Leverkusen, Germany

Tel.: +49 214 32831 4623

E-Mail: nicole.teusch@th-koeln.de

Abstract

Background: Overexpression of efflux transporters of the ATP-binding cassette (ABC) transporter family, primarily P-glycoprotein (P-gp), is a frequent cause of multidrug resistance in cancer and leads to failure of current chemotherapies. Thus, identification of selective P-gp inhibitors might provide a basis for the development of novel anticancer drug candidates.

Purpose: The natural product goniothalamin and 21 derivatives were characterized regarding their cytotoxic activities in pairs of resistant cancer cell lines and corresponding sensitive parental cell lines. Moreover, the ability of goniothalamin and derivatives to inhibit ABC transporter function was analyzed for the first time.

Methods: Cytotoxicity of the natural product derivatives and reversal of resistance to chemotherapy were assessed. The influence of compounds on activity of ABC transporters was investigated by analyzing intracellular accumulation of fluorescent transporter substrates. Further insights into the mechanism of P-gp inhibition were gained by ATPase assay and molecular docking studies.

Results: Natural occurring goniothalamin **(*R*)-1** displayed comparable cytotoxicity in most sensitive and resistant cell lines tested. Two derivatives with improved cytotoxic activities were identified. Furthermore, selective inhibitors of P-gp were discovered. The two most potent and non-toxic inhibitors **(*R*)-3** and **(*S*)-3** displayed the ability to increase intracellular accumulation of doxorubicin, thereby sensitizing P-gp overexpressing tumor cells to chemotherapy by decreasing doxorubicin IC_{50} value up to 15-fold. Results of the P-gp ATPase assay and molecular docking studies revealed these compounds to inhibit P-gp by acting as transporter substrates.

Conclusion: Novel derivatives with enhanced cytotoxic efficacy compared to the natural product goniothalamin were identified. Additionally, non-toxic derivatives with selective P-gp inhibitory activity were characterized. Analyzing the mode of action revealed novel goniothalamin derivatives displaying the ability of reversing P-gp mediated chemotherapy resistance.

Keywords

Goniothalamin; multidrug resistance; P-glycoprotein; cancer chemotherapy; resistance reversal

Abbreviations

ABC, ATP-binding cassette; BCRP, breast cancer resistance protein; DMSO, dimethylsulfoxide; MDR, multidrug resistance; MRP1, multidrug resistance-associated protein 1; P-gp, P-glycoprotein; SAR, structure-activity relationship

Introduction

Despite emerging progress in the development of novel anticancer therapies, multidrug resistance (MDR) remains a major challenge in tumor treatment (Gottesman et al., 2002; Khamisipour et al., 2016). MDR describes a multifactorial phenomenon against a variety of marketed anticancer drugs (Gillet and Gottesman, 2010). Most common mechanisms of MDR encompass altered drug metabolism through the expression of phase II conjugating enzymes, including glutathione transferase P1 (Bräutigam et al., 2015), or increased expression of efflux pumps of the ATP-binding cassette (ABC) transporter superfamily in the tumor, thereby extruding chemotherapeutic drugs (Gottesman et al., 2002). To date, three ABC transporters have been most extensively studied (El-Awady et al., 2016): P-glycoprotein (P-gp, ABCB1), multidrug resistance-associated protein 1 (MRP1, ABCC1) and breast cancer resistance protein (BCRP, ABCG2). P-gp, the best characterized transporter mediating MDR, is normally expressed in the liver transport epithelium, the gastrointestinal tract and in the blood-brain barrier (Cordon-Cardo et al., 1990). Among the ABC transporters, P-gp demonstrates the strongest resistance to a variety of chemotherapeutics including anthracyclines, taxanes or tyrosine kinase inhibitors (Sharom, 2008). Besides P-gp, MRP1 and BCRP as mediators of chemotherapeutic resistance are in the focus of current research (Lu et al., 2015; Westover and Li, 2015).

The styryl-lactone goniothalamin can be found in species of the Goniothalamus genus, which is endemic in Southeast Asia (Jewers et al., 1972; Seyed et al., 2014). Over the last decades, pharmacological effects of goniothalamin have been studied against pathogens such as Trypanosoma and Plasmodium and in various tumors. Amongst its anticancer activities, inhibition of inflammation (Vendramini-Costa et al., 2015), delay of tumor progression (Kido et al., 2016; Vendramini-Costa et al., 2017), induction of apoptosis and cell cycle arrest (Innajak et al., 2016; Semprebon et al., 2015) were described. Interestingly, to date, goniothalamin has not been characterized regarding ABC transporter inhibition.

In the current study, we analyzed the cytotoxic efficacy of the natural occurring goniothalamin **(*R*)-1** and its enantiomer **(*S*)-1**, as well as 21 derivatives (Figure 1; Weber et al., 2017) on a panel encompassing sensitive and corresponding resistant human cancer cells. Moreover, their inhibitory activity towards the ABC transporters P-gp, MRP1 and BCRP was characterized for the first time.

Material and methods

Test compounds and chemicals

The chemical syntheses of goniothalamins were described before (Weber et al., 2017). Test compounds were dissolved in dimethyl sulfoxide (DMSO; Carl Roth, Karlsruhe, Germany). Calcein-AM, Hoechst 33342, PSC833, Ko143, MK-571 and doxorubicin were purchased from Sigma-Aldrich (St. Louis, MO, USA) and dissolved in DMSO, except for Hoechst 33342, which was dissolved in water. Hank's balanced salt solution was purchased from Biochrom (Berlin, Germany); hepes buffer was purchased from Lonza (Basel, Switzerland). Cell culture media and supplements were purchased from Thermo Fisher Scientific (Waltham, MA, USA), except for human recombinant insulin (Merck, Darmstadt, Germany).

Cell culture

HCT-15 colon adenocarcinoma cells (German Collection of Microorganisms and Cell Cultures [DSMZ], Braunschweig, Germany) were cultured in RPMI 1640 containing 10% fetal bovine serum (FBS), 100 U/mL penicillin and 100 µg/mL streptomycin. Small cell lung cancer cell line NCI-H69 and the multidrug-resistant progeny H69AR (American Type Culture Collection, Manassas, VA, USA) were cultured in RPMI 1640 (ATCC modification) containing 10% or 20% FBS, respectively, 100 U/mL penicillin and 100 µg/mL streptomycin. Multidrug-resistant MCF-7/MX breast cancer cells (generous gift from Dr. Erasmus Schneider, Wadsworth Center, New York State Department of Health, Albany, NY, USA) were cultured in DMEM containing 10% FBS, 100 U/mL penicillin and 100 µg/mL streptomycin. Culture of MCF-7 breast adenocarcinoma and A549 non-small cell lung adenocarcinoma cells (both DSMZ) was described in Weber et al., 2017.

Cells were maintained in a humidified atmosphere at 37 °C and 5% CO_2 and subcultured at 80 to 90% confluency.

Cell viability assay

Cytotoxicity of test compounds was determined after 48 h with the CellTiter-Glo Luminescent Cell Viability Assay (Promega, Madison, WI, USA) as described previously (Weber et al., 2017). Cell densities were as follows: A549, MCF-7/MX: 2·103 cells/well; HCT-15: 3·103 cells/well; H69AR, MCF-7: 5·103 cells/well; NCI-H69: 7·103 cells/well. Cell

seeding and addition of compounds were conducted with the CyBi-Well 96-channel simultaneous pipettor (Analytik Jena AG, Jena, Germany).

To analyze the ability of identified inhibitors of P-gp to sensitize P-gp expressing cancer cells to chemotherapy treatment, HCT-15 cells were either incubated with a serial dilution of doxorubicin alone or in combination with fixed concentrations of the test compounds. Fold change of doxorubicin IC50 was calculated with the formula IC50(doxorubicin)/IC50(doxorubicin with modulator).

P-gp transport assay

Influence on the transport activity of P-gp was analyzed in P-gp expressing HCT-15 cells by monitoring the intracellular accumulation of calcein.

Cells ($5 \cdot 10^4$ cells/well) were seeded in black 96-well plates and incubated at 37 °C and 5% CO_2. After 24 h, the culture medium was replaced by Hank's balanced salt solution containing 10 mM hepes. The cells were pre-incubated with the test compounds, positive control (2.5 µM PSC833) or negative control (0.5% DMSO) in triplicates for 30 min and afterwards the P-gp substrate calcein-AM was added (0.5 µM). The fluorescence of calcein (excitation 485 nm, emission 520 nm) was measured over a period of 3 h with the Infinite M1000 pro microplate reader (Tecan Group AG, Maennedorf, Switzerland) at 37 °C.

Inhibition of transport activity was analyzed by determining the slope of the fluorescence-time curve (0-30 min) using linear regression. Data were normalized to PSC833 (100% inhibition) and DMSO (0% inhibition).

MRP1 transport assay

As calcein-AM is also a substrate of MRP1, its transport function was determined in MRP1-expressing H69AR ($7.5 \cdot 10^4$ cells/well) cells using 20 µM MK-571 as positive control.

Inhibition of transport activity was analyzed by determining the slope of the fluorescence-time curve (0-20 min) using linear regression. Data were normalized to MK-571 (100% inhibition) and DMSO (0% inhibition).

BCRP transport assay

Activity of the BCRP transporter was analyzed in BCRP-expressing MCF-7/MX cells ($5 \cdot 10^4$ cells/well). Ko143 (1 µM) was used as positive control and Hoechst 33342 (1 µM) as fluorescent BCRP substrate (excitation 355 nm, emission 460 nm).

Inhibition of transport activity was analyzed by determining the plateau of the fluorescence-time curve using non-linear regression (one-phase exponential fit). Data were normalized to Ko143 (100% inhibition) and DMSO (0% inhibition).

Flow cytometry

Accumulation of doxorubicin in P-gp expressing HCT-15 cells was analyzed. 24 h after cell seeding, test compounds and controls were incubated for 30 min at 37 °C. 2.5 µM PSC833 and 0.5 % DMSO were used as positive or negative control. Afterwards, doxorubicin was added to a final concentration of 10 µM. After 3 h, cells were collected and washed twice with ice-cold PBS. Doxorubicin fluorescence was measured with the CyFlow Cube 8 (Sysmex Corporation, Kobe, Japan) equipped with a 590/50 bandpass filter. Data were analyzed using FlowJo 10.3 (FlowJo LLC, Ashland, OR, USA). Live cells were gated based on forward/sideward scatter. Data were normalized to DMSO-treated cells.

P-gp ATPase assay

Influence of compounds on the P-gp ATPase activity was analyzed using the SB MDR1/P-gp PREDEASY ATPase Kit (Solvo Biotechnology, Szeged, Hungary) according to manufacturer's instructions. The amount of the liberated inorganic phosphate was determined by measuring the absorbance at 610 nm using the Infinite M200 microplate reader (Tecan Group AG, Maennedorf, Switzerland). Specific P-gp related ATPase activity was measured by calculating the difference between phosphate liberation in the presence or absence of sodium orthovanadate. Data were normalized to baseline or verapamil-stimulated ATPase activity, respectively.

Molecular docking

Selected compounds were evaluated in terms of their docking pose and binding energy with AutoDock 4 (Morris et al., 2009) on the homology model of human P-gp prepared as described previously (Tajima et al., 2014) by using mouse P-gp (PDB ID: 4M1M) as template structure. PSC833 was used as positive control. For blind docking calculations, whole protein surface was covered and for defined docking, residues at the drug-binding pocket were covered (Aller et al., 2009). Three independent docking calculations were conducted with 2,500,000 energy evaluations and 250 runs using Lamarckian Genetic Algorithm. Lowest binding energies and predicted inhibition constants were obtained from the docking log files

(dlg). For visualization of the docking results, Visual Molecular Dynamics (VMD) was used. VMD software was developed with NIH support by the Theoretical and Computational Biophysics group at the Beckman Institute, University of Illinois, USA, at Urbana-Champaign.

Data analysis and statistics

All experiments were performed in at least three independent replicates. GraphPad Prism v. 6.07 (GraphPad Software Inc., La Jolla, CA, USA) was used for data analyses. Results are presented as mean ± SEM. For statistical analysis comparing different groups, one-way ANOVA followed by Dunnett's multiple comparisons test was performed. $p < 0.05$ was chosen to define statistically significant difference.

Results

Goniothalamin and derivatives demonstrate cytotoxicity against sensitive and resistant cancer cells

We have recently reported distinct structure-activity relationship (SAR) of the cytotoxicity of goniothalamin and derivatives in lung and breast cancer cell lines (Weber et al., 2017). Here, we expanded our cell panel analysis towards multidrug-resistant and corresponding sensitive tumor cell lines. For the sensitive lung cancer cell line A549, which had already been included in our previous work, the panel of test compounds was expanded.

Natural occurring goniothalamin **(*R*)-1** displayed moderate cytotoxicity in most cell lines investigated (Table 1). IC50 values varied between 29 µM and 35 µM in HCT-15, NCI-H69, H69AR and MCF-7/MX. In contrast, goniothalamin proved to be around 5-fold more efficacious in A549 (IC50 5.7 µM) and less efficacious in MCF-7 (IC50 56 µM).

Two candidates with improved cytotoxic activity on most cell lines investigated could be revealed. Compound **(*R*)-25** displayed a 1.9-fold lower IC_{50} value in HCT-15 (IC_{50} 15.9 µM) and MCF-7 (IC_{50} 28.8 µM) compared to the naturally occurring **(*R*)-1**. In NCI-H69 and H69AR, cytotoxicity of compound **(*R*)-25** was 3- and 2.6-fold lower with IC_{50} values of 10 µM and 12 µM, respectively. Regarding derivative **(*R,S,S*)-4**, IC_{50} values were around 2-fold lower in HCT-15 (IC_{50} 14.9 µM) and in H69AR (IC_{50} 15.3 µM) and 1.8-fold lower in NCI-H69 (IC_{50} 16.6 µM) compared to natural goniothalamin **(*R*)-1**. According to our previous

study, (*R*)-enantiomers displayed cytotoxicity, while in most cases (*S*)-enantiomers were not cytotoxic. Additionally, compounds with saturated lactones did not exhibit cytotoxic effects either (derivatives 23 and 26).

Moreover, we could observe that most of the compounds with cytotoxic activity in sensitive cancer cell lines showed comparable results in the multidrug-resistant cell lines tested. Comparing MRP1-overexpressing H69AR cells to the sensitive parental NCI-H69 cells, the cytotoxic compounds **(*R*)-1**, **(*R*)-2**, **(*R*)-25**, **(*R*)-24**, **(*R,S,S*)-4**, **(*R,R,R*)-4** and **(*S,S,S*)-4** demonstrated comparable IC_{50} values. Compounds **(*S*)-25**, **(*S*)-3**, **(*S*)-24** displayed efficacy merely in the sensitive cell line NCI-H69, however being rather weak.

Notably, comparing BCRP-overexpressing MCF-7/MX cells and sensitive parental MCF-7 cells, compounds with selectivity towards the resistant cells were identified. Derivative **(*R*)-2** proved the best selectivity with a 2-fold higher efficacy towards MCF-7/MX.

Analysis of sensitive and resistant cancer cell lines for distinct ABC transporter expression

To identify tumor cell lines with selectively high expression of P-gp, MRP1 or BCRP for further ABC transporter studies, a systematic screening of transporter expression by qPCR was conducted. Levels of respective mRNA in the cell lines were quantified in relation to the reference gene GAPDH (Supplementary Table S1).

Based on our in-depth comparative analysis, the cell lines HCT-15, H69AR and MCF-7/MX were selected for further evaluation of the inhibitory effects of goniothalamin and derivatives on transporter activities.

Goniothalamin and derivatives selectively inhibit P-gp transport function

The influence of the natural product goniothalamin on the transport activity of ABC transporters has not been described before. To analyze influence on P-gp activity, intracellular calcein accumulation was determined (Figure 2A). The slope of the linear part of the fluorescence-time curve and the relative inhibition rates were calculated by normalizing data of the tested compounds to the positive control PSC833 (100% inhibition) and the negative control DMSO (0% inhibition).

Goniothalamin **(*R*)-1** dose-dependently inhibited P-gp transport activity (Figure 2B). Its relative inhibition compared to the positive control PSC833 was between 19.9 ± 1.9% at 10 µM and 41.1 ± 8.2% at 50 µM (mean ± SEM). Interestingly, two derivatives with

significantly improved P-gp inhibition compared to the natural product could be identified: **(*R*)-3** and **(*S*)-3**. Highest inhibition rates were achieved by compound **(*R*)-3** with relative values between 57.4 ± 3.1% (10 µM) and 98.5 ± 2.3% (50 µM). These rates were 2.4- to 3-fold higher compared to the natural product **(*R*)-1**. Inhibition of P-gp by **(*S*)-3** was lower compared to the (*R*)-enantiomer with rates between 42.5 ± 3.1% at 10 µM and 61.8 ± 6.2% at 50 µM. Noteworthy, derivatives **(*R*)-23e** and **(*S*)-23e** with saturated lactone moiety, displayed significantly lower inhibition rates compared to the unsaturated compounds. The differences were around 9-fold between compounds **(*R*)-3** and **(*R*)-23e** and around 2.5-fold between compounds **(*S*)-3** and **(*S*)-23e**. Compound **(*R*)-24** inhibited P-gp with similar rates compared to natural goniothalamin **(*R*)-1**. Relative inhibition varied between 22.2 ± 2.1% (10 µM) and 54.6 ± 5.8% (50 µM). Here, the (*S*)-enantiomer displayed lower inhibitory activity between 4.5 ± 2.1% (10 µM) and 26.1 ± 2.2% (50 µM). Compound **(*R*)-23a** with saturated lactone moiety inhibited P-gp significantly weaker than compound **(*R*)-24**, while the inhibition of compound **(*S*)-23e** was comparable to compound **(*S*)-24**. Regarding transport activity of MRP1 in H69AR cells and BCRP in MCF-7/MX cells, no modulation by the tested goniothalamins could be observed (Figure 2C, D), proving selectivity for the inhibition capacity of goniothalamins towards P-gp.

P-gp inhibiting goniothalamins increase intracellular doxorubicin accumulation

To further confirm inhibition of P-gp transport activity, intracellular accumulation of the chemotherapeutic drug doxorubicin, a proven P-gp substrate, was analyzed by flow cytometry.

HCT-15 cells were incubated with different concentrations of the newly identified inhibitors, derivatives **(*R*)-3** and **(*S*)-3**, as well as the structurally corresponding goniothalamins with saturated lactone moiety **(*R*)-23e** and **(*S*)-23e**, exhibiting significantly weaker inhibition of P-gp in the transporter screening assay (Figure 2B). PSC833 (2.5 µM) served as positive control. Incubation with compounds **(*R*)-3** and **(*S*)-3**, lead to a dose-dependent increase in doxorubicin fluorescence intensity compared to cells treated with DMSO as negative control (Figure 3A, B). In line with the transporter inhibition data, compound **(*R*)-3** showed stronger accumulation of doxorubicin in HCT-15 compared to compound **(*S*)-3**. In comparison to treatment with DMSO, compound **(*R*)-3** dose-dependently increased the accumulation around 1.7- to 2-fold, whereas compound **(*S*)-3** could only lead to a significant increase at 50 µM (1.7-fold).

In contrast, after incubation with derivatives **(*R*)-23e** and **(*S*)-23e**, doxorubicin accumulation in HCT-15 cells was not significantly different from DMSO-treated cells (Figure 3C, D).

P-gp inhibiting goniothalamins sensitize tumor cells to doxorubicin treatment

The non-cytotoxic goniothalamins **(*R*)-3** and **(*S*)-3** were identified as the most efficacious inhibitors of P-gp (Figure 2). Doxorubicin, a clinically established chemotherapeutic drug represents a well-known P-gp substrate. Cytotoxicity of doxorubicin alone or in combination with different concentrations of selected goniothalamin derivatives was determined in HCT-15 cells, selectively expressing P-gp.

The IC_{50} value of doxorubicin on HCT-15 cells was 7.4 ± 0.8 µM (mean ± SEM; Table 3). However, co-treatment with goniothalamins **(*R*)-3** and **(*S*)-3** lead to a dose-dependent decrease in IC_{50} (Figure 4B, C; Table 2). The combination of doxorubicin with compound **(*R*)-3** resulted in an increased sensitivity towards doxorubicin treatment reflected by IC_{50} values between 2.23 ± 0.12 µM (10 µM **(*R*)-3**) and 0.47 ± 0.06 µM (50 µM **(*R*)-3**). In comparison to the treatment with doxorubicin alone, the shifts corresponded to a reduction of 3.3-fold (for 10 µM) and 15.7-fold (for 50 µM), respectively. The addition of the control PSC833 resulted in a 20.5-fold decrease to an IC_{50} of 0.36 ± 0.04 µM (Figure 4A).

The combination of doxorubicin with the weaker P-gp inhibitor compound **(*S*)-3** reduced the doxorubicin IC_{50} value 2.6- to 4.3-fold to 2.79 ± 0.21 µM (10 µM **(*S*)-3**) and 1.73 ± 0.47 µM (50 µM **(*S*)-3**). Treatment of the cells with the respective compounds alone had no effect on cell viability.

Moreover, the combination of doxorubicin and goniothalamin derivatives displaying only minor P-gp inhibiting activity, compounds **(*R*)-23e** or **(*S*)-23e**, had no significant influence on the cytotoxicity of doxorubicin in HCT-15 cells (Figure 4D, E; Table 2).

Goniothalamins influence basal and verapamil-stimulated P-gp ATPase activity

To gain insight into the mode of action of P-gp inhibitors, their influence on basal and verapamil-stimulated P-gp ATPase activity was characterized. Analyzing the basal P-gp ATPase activity revealed that both derivatives showed a stimulatory, concentration-dependent effect (Figure 4F). However, only for compound **(*R*)-3** a statistically significant increase was

noted. Here, the relative ATPase activity varied between 146.7 ± 2.7% at 5 µM and 170.4 ± 3.7% at 50 µM compared to untreated membranes. Incubation with compound **(*S*)-3**, a weaker inhibitor of P-gp (Figure 2B), resulted in relative ATPase activities varying between 104.3 ± 4.3% at 5 µM and 120.5 ± 4.3% at 50 µM, respectively.

Both derivatives dose-dependently inhibited the verapamil-stimulated ATPase activity in a similar range (Figure 4G), but statistically only significant at the highest concentration tested. The relative ATPase activity varied between 89.9 ± 6.7% at 5 µM and 69.0 ± 7.5% at 50 µM for derivative **(*R*)-3** and between 81.5 ± 6.9% at 5 µM and 69.5 ± 0.4% at 50 µM for derivative **(*S*)-3** compared to verapamil alone, which was set as 100% activity.

Molecular docking of goniothalamins

Molecular docking of the P-gp inhibiting goniothalamins **(*R*)-3** and **(*S*)-3** as well as the weak inhibitory goniothalamins **(*R*)-23e** and **(*S*)-23e** on the homology model of human P-gp was performed to gain insights into the possible binding mode.

Blind docking covering the whole protein surface revealed that the P-gp inhibiting goniothalamin derivatives were able to interact with P-gp even stronger than PSC833. Unlike PSC833, the derivatives **(*R*)-3** and **(*S*)-3** bound in close proximity of the drug-binding pocket (Figure 5A). Furthermore, compounds **(*R*)-3** and **(*S*)-3** bound slightly stronger than compounds **(*R*)-23e** and **(*S*)-23e** with lower predicted inhibition constants, confirming the P-gp inhibition data set presented in this study (Table 3). All tested derivatives formed hydrogen bonds with Phe104.

Results of the defined docking to the drug-binding domain suggested that compounds **(*R*)-23e** and **(*S*)-23e** bound slightly stronger than compounds **(*R*)-3** and **(*S*)-3**, which is in contrast to the P-gp inhibition data (Figure 5B). However, considering binding energies around -8 kcal/mol (Table 4) indicated that the goniothalamin derivatives might inhibit P-gp drug efflux by strong interaction at the drug-binding pocket of P-gp. Allocation of the amino acids responsible for interaction to the three different drug-binding sites (Ferreira et al., 2013) revealed that the newly described goniothalamin derivatives mainly interact with the substrate-binding R-site (rhodamine 123 site).

Discussion

Targeting ABC transporters provides a promising strategy to circumvent anticancer drug resistance. In the current study, the natural product goniothalamin, its enantiomer and 21 derivatives were analyzed regarding their cytotoxicity on resistant cancer cells as well as concerning their potential to inhibit P-gp transport activity.

Cytotoxicity of goniothalamin on multidrug-resistant cancer cells has been analyzed previously. Cytotoxicity assessment in the P-gp overexpressing ovarian cancer cell line NCI-ADR/RES demonstrated goniothalamin to be effective in inhibiting tumor cell proliferation including growth inhibition of the multidrug-resistant cell line (Barcelos et al., 2014; Bruder et al., 2013). This is in accordance with our results, revealing comparable IC50 values of natural occurring goniothalamin **(*R*)-1** on all cell lines tested, except for A549 lung carcinoma cells. Furthermore, our previous work revealed novel derivatives, compounds **(*R*)-25** and **(*R,S,S*)-4**, to be around 2-fold more potent than goniothalamin **(*R*)-1** against breast cancer cell lines MCF-7 and HBL-100 (Weber et al., 2017).

In the current study, we expanded the pharmacological evaluation towards MRP1- and BCRP-overexpressing cells. We confirmed superiority of the goniothalamin derivatives **(*R*)-25** and **(*R,S,S*)-4** in P-gp expressing colon carcinoma cells and MRP1-expressing small cell lung cancer cells, thus serving as a starting point for development of drug candidates inducing cytotoxicity of P-gp or MRP1-expressing cancer cells. In BCRP-expressing breast cancer cells, compounds with selective cytotoxicity towards the resistant cells were identified, derivatives **(*R*)-2**, **(*S*)-2**, **(*S*)-3** and **(*R*)-24**.

In summary, distinct SAR regarding cytotoxicity could be confirmed: (*R*)-enantiomers are more potent than (*S*)-enantiomers, the unsaturated lactone ring is essential for activity and the vinylic double bond is not mandatory.

Overexpression of P-gp in tumor cells is the best characterized mechanism of cancer MDR (Efferth and Volm, 2017; Gottesman et al., 2002), and natural products have long been in the focus of researchers to identify new anti-tumor agents and ABC transporter inhibitors (Yu et al., 2016). To date, pharmacological effects of goniothalamin against ABC transporters have not been studied. Our study demonstrates that the natural product **(*R*)-1** moderately inhibited P-gp transport function in a dose-dependent manner, but not the transport mediated by MRP1 or BCRP. Interestingly, regarding the SAR of goniothalamins in inhibiting P-gp, we did not observe any differences between the (*R*)- and (*S*)-enantiomers of the natural product 1 or for the compounds with saturated lactone moiety **23c**, **23e** and **23a**. This is in contrast to the SAR

revealed for the cytotoxic effects. Comparing the enantiomers of the substituted derivatives **3** and **24**, increased P-gp inhibition was detected for the (*R*)-enantiomers. Saturation of the lactone moiety did not affect P-gp inhibition compared to the unsaturated compounds **23c** and **23a**, whereas the activity of **23e** was markedly reduced.

To further explore the molecular mechanism of the identified P-gp inhibitors, their influence on the intracellular doxorubicin accumulation was analyzed. In accordance with the P-gp inhibition data set, both compounds **(*R*)-3** and **(*S*)-3** lead to a dose-dependent increase of intracellular doxorubicin accumulation. In line, compound **(*S*)-3** enhanced doxorubicin accumulation to a lesser extent than compound **(*R*)-3**. Both compounds dose-dependently sensitized colon carcinoma cells to doxorubicin treatment.

Inhibition of P-gp has been reported via different mechanisms (Cihalova et al., 2015; Yuan et al., 2017). Substrates of P-gp usually stimulate basal ATPase activity, whereas slowly transported substrates stimulate the basal and inhibit the drug-stimulated activity. Both goniothalamin derivatives increased the basal ATPase activity of P-gp dose-dependently, but the effect was only significant for compound **(*R*)-3**, whereas the verapamil-stimulated ATPase activity was decreased dose-dependently. Both observations suggest that goniothalamins are transported by P-gp subsequently leading to transporter inhibition, but at a slower rate than verapamil.

Molecular docking of compounds **(*R*)-3** and **(*S*)-3** to homology-modeled human P-gp demonstrated interaction close to the drug-binding domain. Applying defined docking to only the drug-binding domain of P-gp resulted in stronger interaction and lowest binding energies. Allocation of interacting amino acids to the three different drug-binding sites suggests that interaction mainly occurs at the R-(rhodamine 123) site (Ferreira et al., 2013), potentially explaining the increase of intracellular doxorubicin, as anthracyclines are presumed to bind to the R-site.

We hypothesize that goniothalamin derivatives **(*R*)-3** and **(*S*)-3** specifically inhibit P-gp by acting as alternative substrates, thereby leading to increased intracellular accumulation of chemotherapeutic drugs, which are transported by P-gp. The increased drug accumulation in turn causes improved cytotoxicity and sensitizes cancer cells to chemotherapy (Figure 6). In conclusion, our results advocate further optimization of goniothalamin derivatives representing a versatile starting point for the development of novel drugs to overcome MDR in cancer therapy.

Acknowledgements

This work was funded by the German Federal Ministry for Economic Affairs and Energy ['ZIM Kooperationsprojekt' KF3279X01AJ3] and supported by a scholarship of the Studienstiftung des deutschen Volkes for A.W. The PhD training of J.S. is financed by the graduate program in Pharmacology and Experimental Therapeutics at the University of Cologne, which is financially and scientifically supported by Bayer.

We would like to thank Dr. Erasmus Schneider (Wadsworth Center, New York State Department of Health, Albany, NY, USA) for kindly providing the MCF-7/MX cells.

Conflict of interests

The authors declare no conflict of interest.

References

Aller, S.G., Yu, J., Ward, A., Weng, Y., Chittaboina, S., Zhuo, R., Harrell, P.M., Trinh, Y.T., Zhang, Q., Urbatsch, I.L., Chang, G., 2009. Structure of P-glycoprotein reveals a molecular basis for poly-specific drug binding. Science 323, 1718–1722.

Barcelos, R.C., Pastre, J.C., Caixeta, V., Vendramini-Costa, D.B., Carvalho, J.E. de, Pilli, R.A., 2012. Synthesis of methoxylated goniothalamin, aza-goniothalamin and γ-pyrones and their in vitro evaluation against human cancer cells. Bioorg. Med. Chem. 20, 3635–3651.

Barcelos, R.C., Pastre, J.C., Vendramini-Costa, D.B., Caixeta, V., Longato, G.B., Monteiro, P.A., Carvalho, J.E. de, Pilli, R.A., 2014. Design and synthesis of N-acylated aza-goniothalamin derivatives and evaluation of their in vitro and in vivo antitumor activity. ChemMedChem 9, 2725–2743.

Bräutigam, M., Teusch, N., Schenk, T., Sheikh, M., Aricioglu, R.Z., Borowski, S.H., Neudörfl, J.-M., Baumann, U., Griesbeck, A.G., Pietsch, M., 2015. Selective inhibitors of glutathione transferase P1 with trioxane structure as anticancer agents. ChemMedChem 10, 629–639.

Bruder, M., Vendramini-Costa, D.B., Carvalho, J.E. de, Pilli, R.A., 2013. Design, synthesis and in vitro evaluation against human cancer cells of 5-methyl-5-styryl-2,5-dihydrofuran-2-ones, a new series of goniothalamin analogues. Bioorg. Med. Chem. 21, 5107–5117.

Cihalova, D., Ceckova, M., Kucera, R., Klimes, J., Staud, F., 2015. Dinaciclib, a cyclin-dependent kinase inhibitor, is a substrate of human ABCB1 and ABCG2 and an inhibitor of human ABCC1 in vitro. Biochem. Pharmacol. 98, 465–472.

Cordon-Cardo, C., O'Brien, J.P., Boccia, J., Casals, D., Bertino, J.R., Melamed, M.R., 1990. Expression of the multidrug resistance gene product (P-glycoprotein) in human normal and tumor tissues. J. Histochem. Cytochem. 38, 1277–1287.

Efferth, T., Volm, M., 2017. Multiple resistance to carcinogens and xenobiotics: P-glycoproteins as universal detoxifiers. Arch. Toxicol. 91, 2515–2538.

El-Awady, R., Saleh, E., Hashim, A., Soliman, N., Dallah, A., Elrasheed, A., Elakraa, G., 2016. The role of eukaryotic and prokaryotic ABC transporter family in failure of chemotherapy. Front. Pharmacol. 7, 535.

Fátima, A. de, Kohn, L.K., Antônio, M.A., Carvalho, J.E. de, Pilli, R.A., 2005. (R)-Goniothalamin: total syntheses and cytotoxic activity against cancer cell lines. Bioorg. Med. Chem. 13, 2927–2933.

Ferreira, R.J., Ferreira, M.-J.U., dos Santos, D.J.V.A., 2013. Molecular docking characterizes substrate-binding sites and efflux modulation mechanisms within P-glycoprotein. J. Chem. Inf. Model. 53, 1747–1760.

Gillet, J.-P., Gottesman, M.M., 2010. Mechanisms of multidrug resistance in cancer. In: Zhou, J. (Ed.), Multi-Drug Resistance in Cancer. Humana Press, Totowa, NJ, pp. 47–76.

Gottesman, M.M., Fojo, T., Bates, S.E., 2002. Multidrug resistance in cancer: role of ATP-dependent transporters. Nat. Rev. Cancer 2, 48–58.

Hlubucek, J.R., Robertson, A.V., 1967. (+)-(5S)-δ-Lactone of 5-hydroxy-7-phenylhepta-2,6-dienoic acid, a natural product from Cryptocarya caloneura (Scheff.) Kostermans. Aust. J. Chem. 20, 2199.

Innajak, S., Mahabusrakum, W., Watanapokasin, R., 2016. Goniothalamin induces apoptosis associated with autophagy activation through MAPK signaling in SK-BR-3 cells. Oncol. Rep. 35, 2851–2858.

Jewers, K., Davis, J.B., Dougan, J., Manchanda, A.H., Blunden, G., Kyi, A., Wetchapinan, S., 1972. Goniothalamin and its distribution in four Goniothalamus species. Phytochemistry 11, 2025–2030.

Khamisipour, G., Jadidi-Niaragh, F., Jahromi, A.S., Zandi, K., Hojjat-Farsangi, M., 2016. Mechanisms of tumor cell resistance to the current targeted-therapy agents. Tumor Biol. 37, 10021–10039.

Kido, L.A., Montico, F., Sauce, R., Macedo, A.B., Minatel, E., Costa, D.B.V., Carvalho, J.E. de, Pilli, R.A., Cagnon, V.H.A., 2016. Anti-inflammatory therapies in TRAMP mice: delay in PCa progression. Endocr. Relat. Cancer 23, 235–250.

Lu, J.F., Pokharel, D., Bebawy, M., 2015. MRP1 and its role in anticancer drug resistance. Drug Metab. Rev. 47, 406–419.

Morris, G.M., Huey, R., Lindstrom, W., Sanner, M.F., Belew, R.K., Goodsell, D.S., Olson, A.J., 2009. AutoDock4 and AutoDockTools4: Automated docking with selective receptor flexibility. J. Comput. Chem. 30, 2785–2791.

Semprebon, S.C., Marques, L.A., D'Epiro, G.F.R., Camargo, E.A. de, da Silva, G.N., Niwa, A.M., Macedo Junior, F., Mantovani, M.S., 2015. Antiproliferative activity of goniothalamin enantiomers involves DNA damage, cell cycle arrest and apoptosis induction in MCF-7 and HB4a cells. Toxicol. In Vitro 30, 250–263.

Seyed, M.A., Jantan, I., Bukhari, S.N.A., 2014. Emerging anticancer potentials of goniothalamin and its molecular mechanisms. Biomed. Res. Int. 2014, 536508.

Sharom, F.J., 2008. ABC multidrug transporters: structure, function and role in chemoresistance. Pharmacogenomics 9, 105–127.

Tajima, Y., Nakagawa, H., Tamura, A., Kadioglu, O., Satake, K., Mitani, Y., Murase, H., Regasini, L.O., Bolzani, V.d.S., Ishikawa, T., Fricker, G., Efferth, T., 2014. Nitensidine A, a guanidine alkaloid from Pterogyne nitens, is a novel substrate for human ABC transporter ABCB1. Phytomedicine 21, 323–332.

Vendramini-Costa, D.B., Francescone, R., Posocco, D., Hou, V., Dmitrieva, O., Hensley, H., Carvalho, J.E. de, Pilli, R.A., Grivennikov, S.I., 2017. Anti-inflammatory natural product goniothalamin reduces colitis-associated and sporadic colorectal tumorigenesis. Carcinogenesis 38, 51–63.

Vendramini-Costa, D.B., Spindola, H.M., Mello, G.C. de, Antunes, E., Pilli, R.A., Carvalho, J.E. de, 2015. Anti-inflammatory and antinociceptive effects of racemic goniothalamin, a styryl lactone. Life Sci. 139, 83–90.

Weber, A., Döhl, K., Sachs, J., Nordschild, A.C.M., Schröder, D., Kulik, A., Fischer, T., Schmitt, L., Teusch, N., Pietruszka, J., 2017. Synthesis and cytotoxic activities of goniothalamins and derivatives. Bioorg. Med. Chem. 25, 6115–6125.

Westover, D., Li, F., 2015. New trends for overcoming ABCG2/BCRP-mediated resistance to cancer therapies. J. Exp. Clin. Cancer Res. 34, 159.

Yu, J., Zhou, P., Asenso, J., Yang, X.-D., Wang, C., Wei, W., 2016. Advances in plant-based inhibitors of P-glycoprotein. J. Enzyme Inhib. Med. Chem. 31, 867–881.

Yuan, Z., Shi, X., Qiu, Y., Jia, T., Yuan, X., Zou, Y., Liu, C., Yu, H., Yuan, Y., He, X., Xu, K., Yin, P., 2017. Reversal of P-gp-mediated multidrug resistance in colon cancer by cinobufagin. Oncol. Rep. 37, 1815–1825.

	Compound	Structure	R
1	(*R*)-1	(*R*)-I	A
2	(*S*)-1	(*S*)-I	A
3	(*R*)-23c	(*R*)-II	A
4	(*S*)-23c	(*S*)-II	A
5	(*R*)-2	(*R*)-I	B
6	(*S*)-2	(*S*)-I	B
7	(*R*)-25	(*R*)-I	C
8	(*S*)-25	(*S*)-I	C
9	(*R*)-3	(*R*)-I	D
10	(*S*)-3	(*S*)-I	D
11	(*R*)-23e	(*R*)-II	D
12	(*S*)-23e	(*S*)-II	D
13	(*R*)-24	(*R*)-I	E
14	(*S*)-24	(*S*)-I	E
15	(*R*)-23a	(*R*)-II	E
16	(*S*)-23a	(*S*)-II	E
17	(*R,S,S*)-4	(*R*)-I	F
18	(*R,R,R*)-4	(*R*)-I	G
19	(*S,S,S*)-4	(*S*)-I	F
20	(*R,R,R*)-26	(*R*)-II	G
21	(*R,R*)-27	(*R*)-I	H
22	(*S,S,S*)-26	(*R*)-II	F
23	(*R,S,S*)-26	(*S*)-II	G

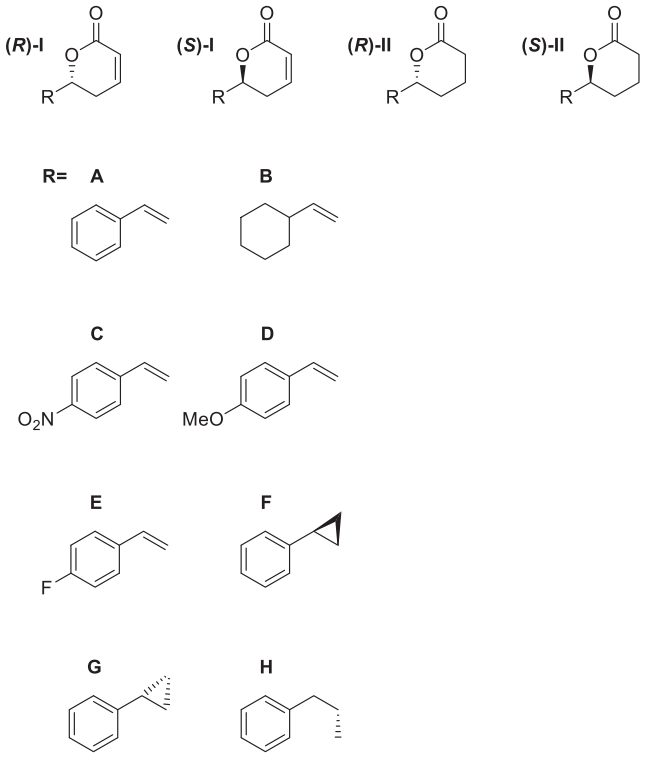

Figure 1. Structures of natural compound goniothalamin **(*R*)-1** and derivatives.

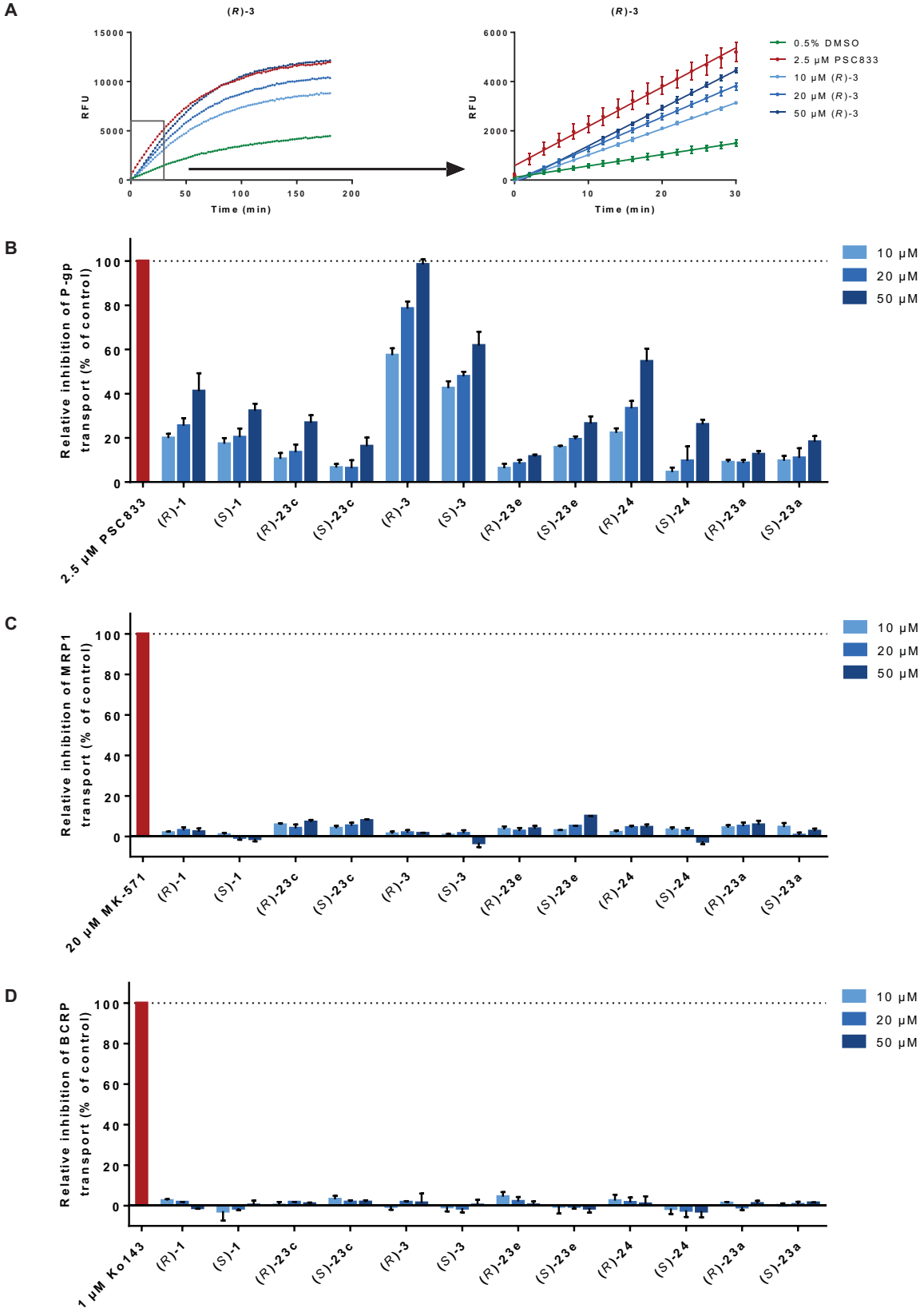

Figure 2. Influence of goniothalamins on transport activity of ABC transporters. P-gp transport activity was analyzed in HCT-15 cells **(A-C)**. Intracellular accumulation of the P-gp substrate calcein-AM was measured (**A**, left). For quantification, the slope of the linear part of

the fluorescence-time curve (grey rectangle) was determined (**A**, right). Curves represent one exemplary measurement of the compound **(*R*)-3**. Data were normalized to PSC833 (100% inhibition) and DMSO (0% inhibition; B). MRP1 transport activity was analyzed in H69AR cells using calcein-AM and MK-571 as positive control **(C)**. BCRP transport activity was analyzed in MCF-7/MX cells using Hoechst 33342 and Ko143 as positive control **(D)**. Bars indicate mean ± SEM of at least three independent experiments performed in triplicates.

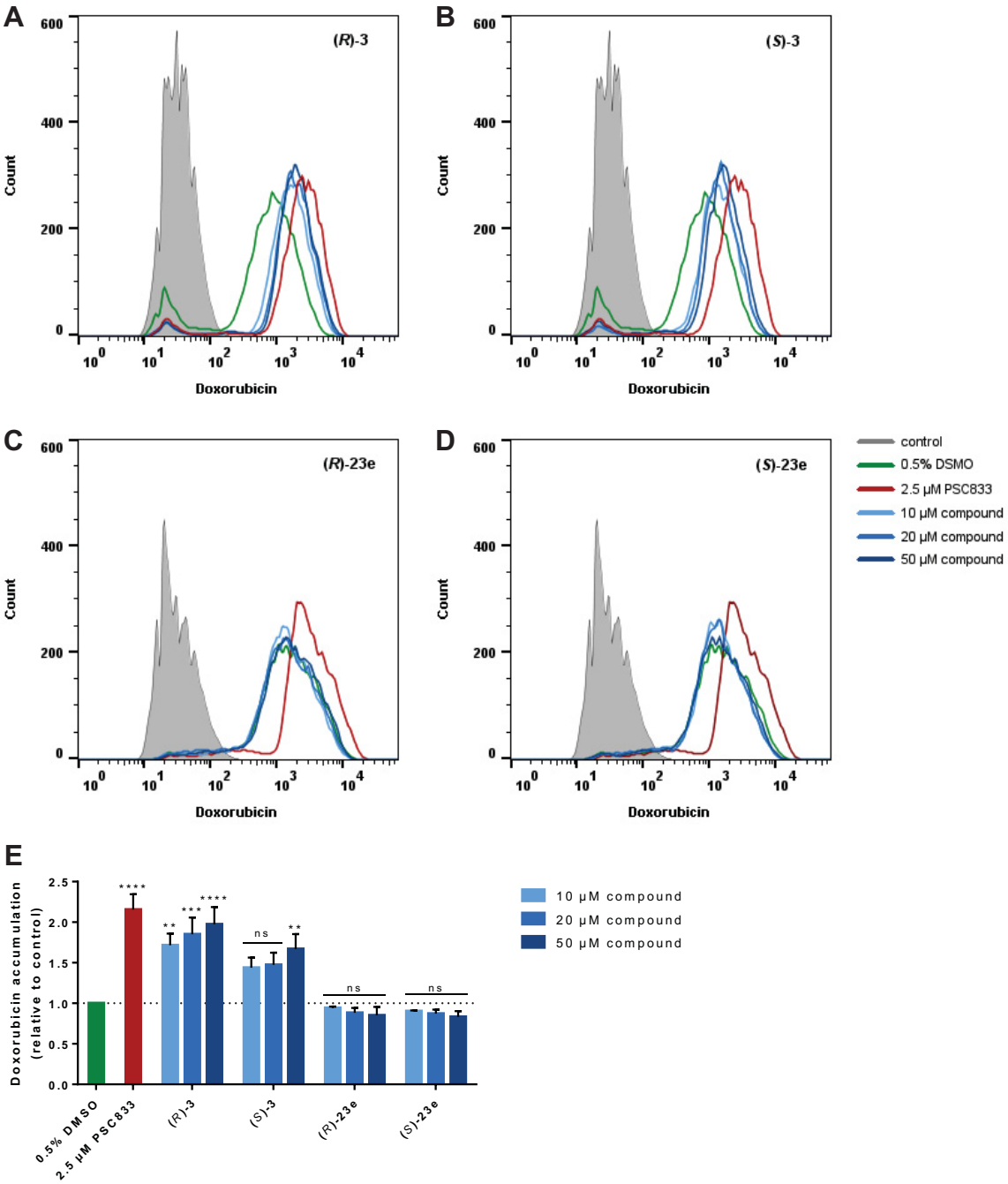

Figure 3. Influence on intracellular doxorubicin accumulation. HCT-15 cells were treated with different concentrations of goniothalamins **(*R*)-3 (A)**, **(*S*)-3 (B)**, **(*R*)-23e (C)** or **(*S*)-23e (D)** and subsequently, doxorubicin. Intracellular doxorubicin fluorescence was analyzed by flow cytometry. PSC833 and DMSO served as positive or negative control, respectively. Median fluorescence intensities were determined and normalized to DMSO **(E)**. Histograms are exemplary for three independent experiments. Bar diagram represents mean ± SEM of three independent experiments. ** $p < 0.01$; *** $p < 0.001$; **** $p < 0.0001$; ns not significant, compared to 0.5% DMSO.

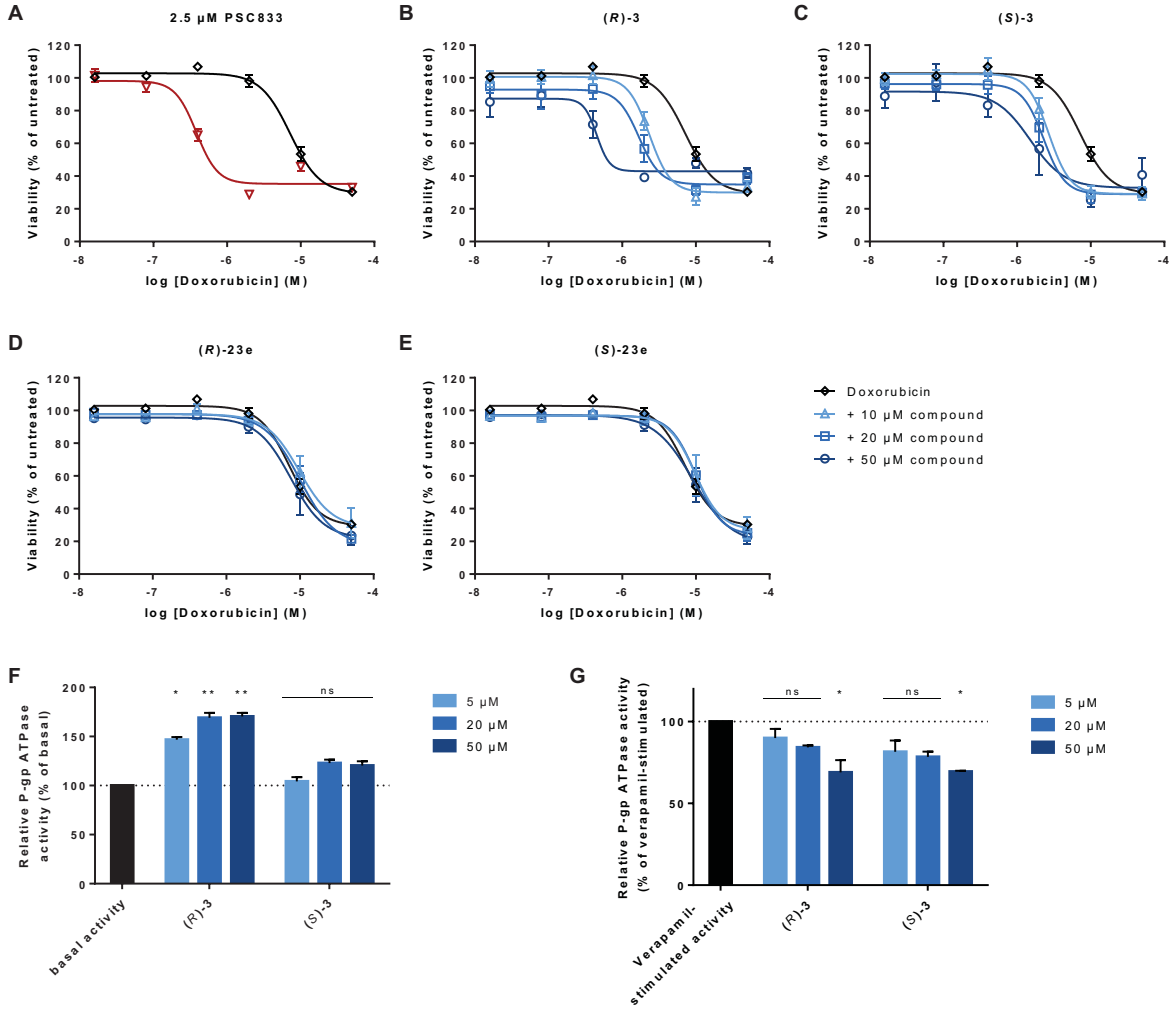

Figure 4. Sensitization of HCT-15 cells to doxorubicin treatment (A-E). HCT-15 were incubated with either doxorubicin alone (◊), doxorubicin combined with 2.5 µM PSC833 (positive control; **A**), or doxorubicin in combination with 10 µM (Δ), 20 µM (□) or 50 µM (○) of the goniothalamins **(*R*)-3 (B)**, **(*S*)-3 (C)**, **(*R*)-23e (D)** and **(*S*)-23e (E)**, respectively. Viability was determined after 48 h. Graphs represent mean values ± SEM normalized to untreated cells of at least three independent experiments performed in quadruplicates. Effect of goniothalamins **(*R*)-3** and **(*S*)-3** on P-gp ATPase activity (E, F). Vanadate-sensitive basal **(E)** and verapamil-stimulated **(F)** P-gp ATPase activities were determined in P-gp expressing cell membranes by measuring liberated inorganic phosphate. Activity of untreated membranes and verapamil-treated (40 µM) was set as 100%, respectively. Bars represent mean ± SEM of three independent experiments. * $p < 0.05$; ** $p < 0.01$; ns not significant, compared to respective control.

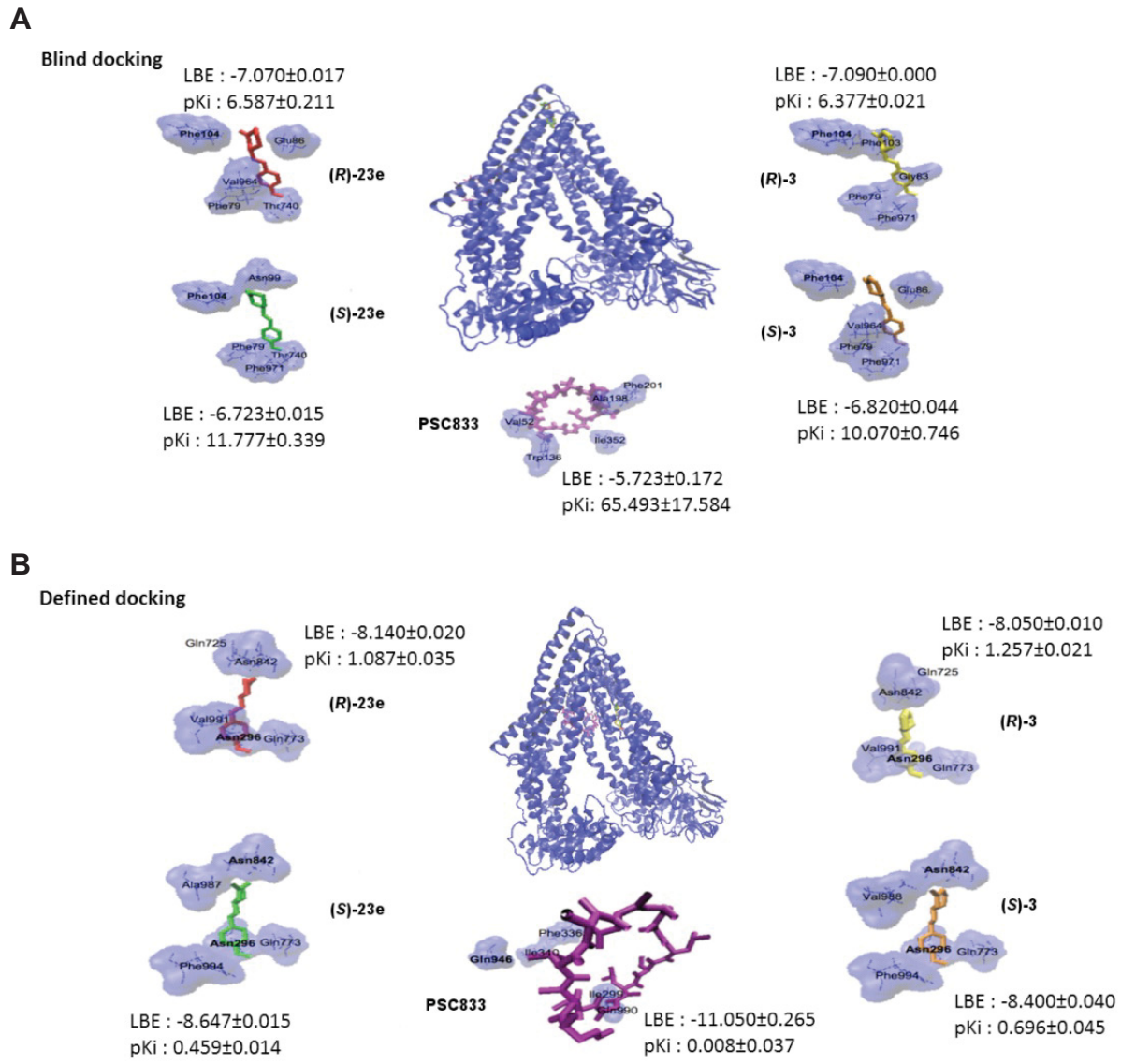

Figure 5. Molecular docking of goniothalamins on homology-modeled human P-gp. Goniothalamins **(*R*)-3**, **(*S*)-3**, **(*R*)-23e**, **(*S*)-23e** and PSC833 were docked on the whole protein surface (blind docking; **A**) or the drug-binding site (defined docking; **B**). Lowest binding energies in kcal/mol (LBE) and predicted inhibition constant in µM (pKi) were determined as well as the interacting amino acids. Data represent mean ± SD of three independent dockings with 2,500,000 energy evaluations and 250 runs each.

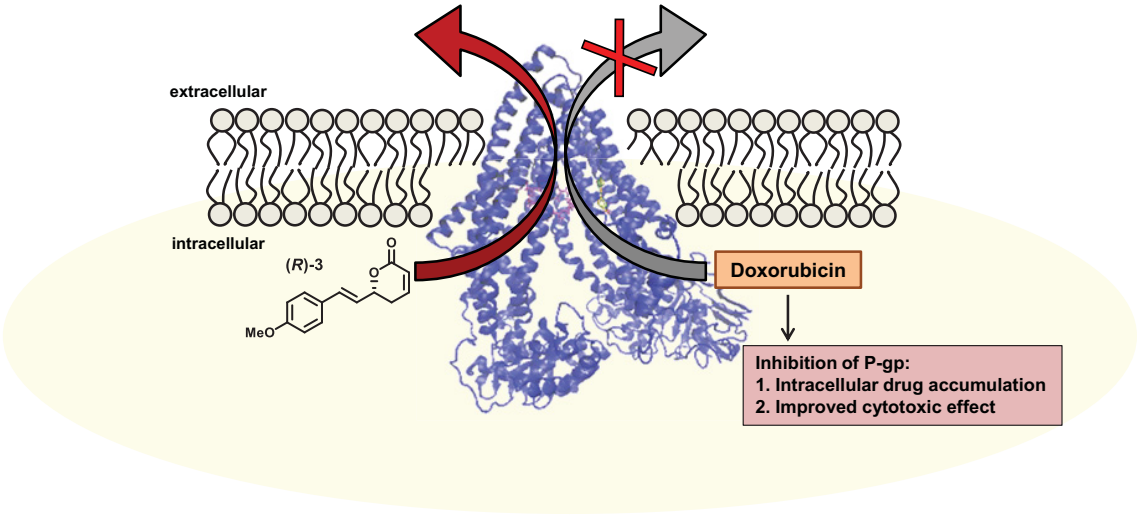

Figure 6. Hypothesized mechanism of goniothalamins reversing multidrug resistance. Goniothalamins inhibit P-gp specifically by acting as alternative P-gp substrates. Transporter inhibition leads to reduced efflux and subsequent intracellular accumulation of the chemotherapeutic drug and P-gp substrate doxorubicin. Accumulation of doxorubicin results in sensitization of cancer cells to chemotherapy.

Table 1

Cytotoxicity of goniothalamins on different human cancer cell lines.

Compound	IC_{50} (μM)					
	HCT-15	A549	MCF-7	MCF-7/MX	NCI-H69	H69AR
(*R*)-1	30.0 ± 3.2	5.7 ± 1.5[a]	55.5 ± 6.4[a]	35.5 ± 5.3	29.2 ± 0.4	>100
(*S*)-1	>100	70.3 ± 14.4[a]	>100[a]	>100	>100	>100
(*R*)-23c	>100	>100	>100	>100	>100	>100
(*S*)-23c	>100	>100	>100	>100	>100	15.3 ± 0.5
(*R*)-2	47.4 ± 1.8	31.0 ± 0.3[a]	>100[a]	48.3 ± 7.2	36.9 ± 3.3	43.6 ± 4.1
(*S*)-2	60.0 ± 2.3	68.6 ± 0.5[a]	>100[a]	54.2 ± 2.3	60.7 ± 4.6	30.3 ± 4.1
(*R*)-25	15.9 ± 1.8	15.4 ± 0.2[a]	28.8 ± 2.3[a]	37.9 ± 2.4	10.0 ± 0.7	>100
(*S*)-25	>100	>100[a]	>100[a]	>100	61.7 ± 4.6	>100
(*R*)-3	>100	>100[a]	>100[a]	>100	>100	>100
(*S*)-3	66.4 ± 4.0	>100[a]	88.7 ± 5.6[a]	64.4 ± 6.7	61.3 ± 3.3	>100
(*R*)-23e	>100	>100	>100	>100	>100	>100
(*S*)-23e	>100	>100	>100	>100	>100	>100
(*R*)-24	20.8 ± 1.3	10.2 ± 0.3[a]	76.2 ± 6.3[a]	41.6 ± 6.2	22.2 ± 3.1	>100
(*S*)-24	>100	>100[a]	>100[a]	>100	76.6 ± 7.1	15.3 ± 0.5
(*R*)-23a	>100	>100	>100	>100	>100	43.6 ± 4.1
(*S*)-23a	>100	>100	>100	>100	>100	30.3 ± 4.1
(*R,S,S*)-4	14.9 ± 2.2	11.6 ± 0.2[a]	48.2 ± 2.0[a]	62.7 ± 3.2	16.6 ± 0.6	>100
(*R,R,R*)-4	57.9 ± 3.1	62.8 ± 1.6[a]	>100[a]	>100	44.7 ± 3.1	>100

(*S,S,S*)-4	29.6 ± 3.3	15.2 ± 0.3[a]	68.3 ± 9.7[a]	44.7 ± 1.8	23.5 ± 1.4	>100
(*R,R,R*)-26	>100	>100[a]	>100[a]	>100	>100	>100
(*R,R*)-27	>100	>100[a]	>100[a]	>100	>100	>100
(*S,S,S*)-26	>100	>100[a]	>100[a]	>100	>100	>100
(*R,S,S*)-26	>100	>100[a]	>100[a]	>100	>100	>100

Data represent mean ± SEM of at least three independent experiments performed in quadruplicates.

[a] IC_{50} values published previously (Weber et al., 2017).

Table 2

Effects of selected goniothalamins on the sensitivity of HCT-15 cells to doxorubicin.

Compound	IC_{50} (μM)	*p*-value	fold change
Doxorubicin	7.37 ± 0.83	-	1.00
+ 2.5 μM PSC833	0.36 ± 0.04****	<0.0001	20.47
+ 10 μM (*R*)-3	2.23 ± 0.12**	0.0024	3.30
+ 20 μM (*R*)-3	1.63 ± 0.21***	0.0001	4.52
+ 50 μM (*R*)-3	0.47 ± 0.06****	<0.0001	15.68
+ 10 μM (*S*)-3	2.79 ± 0.21**	0.0087	2.64
+ 20 μM (*S*)-3	2.64 ± 0.49**	0.0019	2.79
+ 50 μM (*S*)-3	1.73 ± 0.47***	0.0007	4.26
+ 10 μM (*R*)-23e	9.90 ± 1.04	0.3382	0.74
+ 20 μM (*R*)-23e	9.51 ± 1.60	0.5376	0.77
+ 50 μM (*R*)-23e	7.71 ± 1.87	0.9996	0.96
+ 10 μM (*S*)-23e	9.37 ± 1.79	0.6181	0.78
+ 20 μM (*S*)-23e	9.63 ± 1.62	0.4692	0.77
+ 50 μM (*S*)-23e	8.66 ± 1.62	0.9509	0.85

PSC833 was used as positive control. Fold change of cytotoxicity was calculated by IC_{50}(doxorubicin)/IC_{50}(doxorubicin with modulator). Data represent mean ± SEM of at least three independent replicates performed in quadruplicates. ** $p < 0.01$; *** $p < 0.001$; **** $p < 0.0001$ compared to doxorubicin alone.

Table 3

Molecular docking of selected goniothalamins on the whole protein surface of homology-modeled human P-gp.

Compound	Lowest binding energy (kcal/mol)	Predicted inhibition constant (μM)	Interacting amino acids	Amino acids involved in hydrogen bonds
PSC833	-5.723 ± 0.172	65.493 ± 17.584	6	-
(*R*)-3	-7.090 ± 0.000	6.377 ± 0.021	6	Phe104
(*S*)-3	-6.820 ± 0.044	10.070 ± 0.746	9	Phe104
(*R*)-23e	-7.070 ± 0.017	6.587 ± 0.211	8	Phe104
(*S*)-23e	-6.723 ± 0.339	11.777 ± 0.339	10	Phe104

Docking simulations were performed in three independent experiments with 2,500,000 energy evaluations

Table 4

Molecular docking of selected goniothalamins on the drug-binding domain of homology-modeled human P-gp. Numbers in brackets denote shared amino acids between sites.

Compound	Lowest binding energy (kcal/mol)	Predicted inhibition constant (μM)	Interacting amino acids	Amino acids involved in hydrogen bonds	Interacting amino acids in		
					H-site	R-site	M-site
PSC833	-11.050 ± 0.265	0.008 ± 0.037	13	Gln946	2 (1)	5 (2)	4 (3)
(*R*)-3	-8.050 ± 0.010	1.257 ± 0.021	10	Asn296	-	6 (1)	1 (1)
(*S*)-3	-8.400 ± 0.040	0.696 ± 0.045	10	Asn296, Asn842	-	5	-
(*R*)-23e	-8.140 ± 0.020	1.087 ± 0.035	11	Asn296	-	6 (1)	1 (1)
(*S*)-23e	-8.647 ± 0.015	0.459 ± 0.014	9	Asn296, Asn842	-	5	-

Docking simulations were performed in three independent experiments with 2,500,000 energy evaluations and 250 runs each. Data

Supplementary material

Supplementary Table 1

Relative mRNA expression of the ABC transporters P-gp, MRP1 and BCRP in different human cancer cell lines.

Cell line	ΔC_q (C_q gene - C_q GAPDH)		
	P-gp	MRP1	BCRP
HCT-15	6.4 ± 0.2	12.3 ± 0.4	13.8 ± 0.4
H69AR	20.5 ± 0.3	6.3 ± 0.3	22.7 ± 1.3
NCI-H69	17.3 ± 0.1	12.4 ± 0.3	22.9 ± 0.3
MCF-7/MX	14.8 ± 0.4	14.3 ± 0.1	0.6 ± 0.3
MCF-7	16.7 ± 0.1	13.5 ± 0.7	10.6 ± 0.3

1 µg of total RNA was transcribed to first strand cDNA using Oligo$(dT)_{15}$ primer and the Reverse Transcription System (Promega, Madison, WI, USA). For the real-time PCR, 30 ng of cDNA, 0.75 µM of each primer and the QuantiTect SYBR Green PCR Kit (Qiagen, Hilden, Germany) were used. Primer sequences were 5'-TGCACCACCAACTGCTTAGC-3' (forward) and 5'-GGCATGGACTGTGGTCATGAG-3' (reverse) for glyceraldehyde-3-phosphate dehydrogenase (GAPDH; reference gene), 5'-CCATGCTCAGACAGGATGTGA-3' (forward) and 5'-ATCATTGGCGAGCCTGGTAG-3' (reverse) for P-gp, 5'-TTACTCATTCAGCTCGTCTTGTC-3' (forward) and 5'-CAGGGATTAGGGTCGTGGAT-3' (reverse) for MRP1, 5'-TGAGCCTACAACTGGCTTAGA-3' (forward) and 5'-CCCTGCTTAGACATCCTTTTCAG-3' (reverse) for BCRP (synthesized by Eurofins Genomics, Ebersberg, Germany). Reactions were performed in triplicates on the CFX Connect Real-Time System (Bio-Rad, Hercules, CA, USA) under the following conditions: pre-incubation at 95 °C for 15 min, amplification (45 cycles) at 94 °C for 15 s, 55 °C for 25 s and 72°C 10 s. Specificity of the PCR products was validated by melt curve analysis. The ΔC_q method was applied for data analyses. Data show mean ± SEM of three independent experiments performed in triplicates.

Graphical Abstract

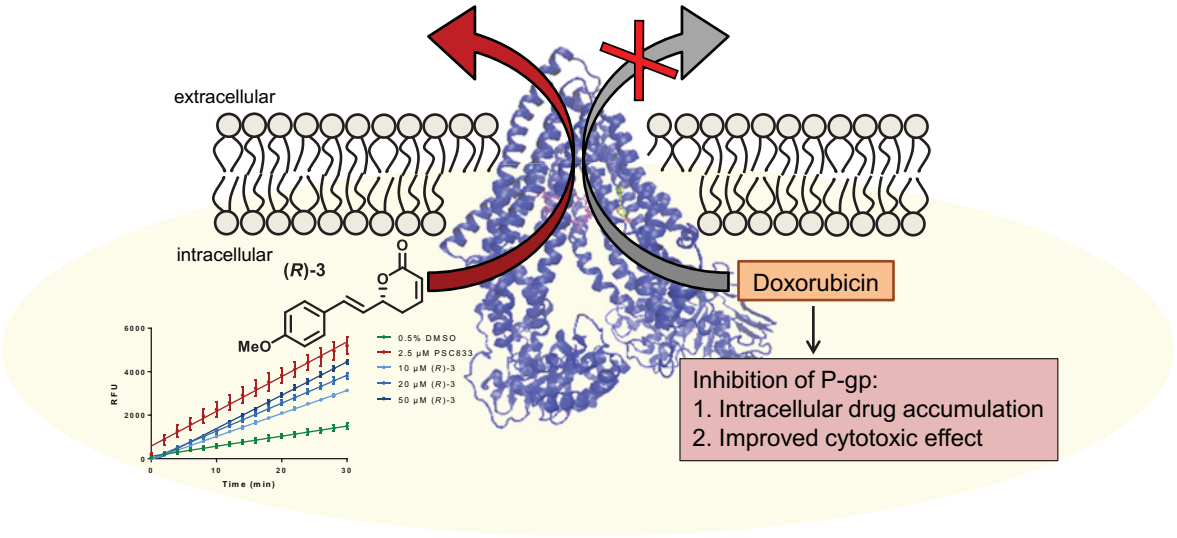

2.2.1 Appendix to Chapter II

In Chapter II (2.2), expression analysis of P-gp, MRP1 and BCRP in five sensitive and resistant cancer cell lines was performed using quantitative real-time PCR (qPCR). These data were part of a systematic screening of ABC transporter expression in a larger cell line panel comprising 16 cell lines from different tumor entities (Table 4). Relative mRNA expression levels of P-gp, MRP1 and BCRP were determined and compared to the reference gene glyceraldehyde 3-phosphate dehydrogenase (GAPDH) by the ΔC_q method ($\Delta C_q = C_q$ gene$-C_q$ GAPDH; C_q: threshold cycle). Lower ΔC_q values represent higher mRNA expression.

Table 4. Relative mRNA expression of P-gp, MRP1 and BCRP in a panel of human cancer cell lines. Expression was determined by qPCR in relation to the reference gene GAPDH. Data represent mean ± SEM of three independent experiments performed in triplicates.

Entity	Cell line	ΔC_q (C_q gene$-C_q$ GAPDH) (mean ± SEM)		
		P-gp	MRP1	BCRP
Brain	U-251 MG	18.3 ± 0.1	12.3 ± 0.5	15.5 ± 0.4
	U-87 MG	19.0 ± 0.4	13.3 ± 0.2	12.1 ± 0.4
Breast	MCF-7	16.7 ± 0.1	13.5 ± 0.7	10.6 ± 0.3
	MCF-7/MX	14.8 ± 0.4	14.3 ± 0.1	0.6 ± 0.3
	MDA-MB-231	19.08 ± 0.2	11.8 ± 0.1	10.3 ± 0.3
	SK-BR-3	18.4 ± 1.0	11.4 ± 1.7	12.8 ± 0.3
	HBL-100	22.9 ± 0.8	11.8 ± 0.3	11.3 ± 0.3
Colon	HCT-15	6.4 ± 0.2	12.3 ± 0.4	13.7 ± 0.4
	Caco-2	4.6 ± 0.1	13.4 ± 0.1	9.2 ± 0.2
	HT-29	15.1 ± 0.6	12.3 ± 0.1	7.2 ± 0.1
Liver	HepG2	8.0 ± 0.6	11.5 ± 0.5	8.9 ± 0.5
Lung	NCI-H69	17.3 ± 0.1	12.4 ± 0.3	22.9 ± 0.3
	H69AR	20.5 ± 0.3	6.3 ± 0.3	22.7 ± 1.3
	A549	15.9 ± 0.2	11.0 ± 0.5	7.8 ± 0.1
	SK MES 1	11.2 ± 0.2	12.3 ± 0.4	9.9 ± 0.5
Pancreas	Panc-1	18.5 ± 0.3	8.9 ± 0.1	7.7 ± 0.2

Data were in part obtained by Vanessa Mundorf and Janina Betz.

U-87 MG, MDA-MB-231 and SK MES 1 cell lines were obtained from the European Collection of Authenticated Cell Cultures (Salisbury, UK). U-251 MG and HBL-100 cell lines were obtained from CLS Cell Lines Service (Eppelheim, Germany). All other cell lines were obtained from the American Type Culture Collection (Manassas, VA, USA). Cell lines were cultured according to manufactures' instructions. Gene expression analysis was performed as described in Chapter II, Supplementary material.

2.3 Chapter III

Title: Novel 3,4-dihydroisocoumarins as dual inhibitors of human P-gp and BCRP in multidrug-resistant tumors

Authors: **Julia Sachs,** Anja Weber, Ferdinand Blesse, Edmond Fleischer, Anette Klinger, Jörg Pietruszka, Nicole Teusch

Journal: to be submitted

Contribution: cell culture, cytotoxicity assays, ABC transporter assays, data analysis, writing of the manuscript

Novel 3,4-dihydroisocoumarins as dual inhibitors of human P-gp and BCRP in multidrug-resistant tumors

Julia Sachs[1], Anja Weber[2], Ferdinand Blesse[1], Edmond Fleischer[3], Anette Klinger[3], Jörg Pietruszka[2,4] and Nicole Teusch[1,*]

[1]Bio-Pharmaceutical Chemistry and Molecular Pharmacology, Faculty of Applied Natural Sciences, Technische Hochschule Köln, Leverkusen, Germany

[2]Institute of Bioorganic Chemistry, Heinrich-Heine-Universität Düsseldorf im Forschungszentrum Jülich, Jülich, Germany

[3]MicroCombiChem GmbH, Wiesbaden, Germany

[4]IBG-1: Biotechnology, Forschungszentrum Jülich, Jülich, Germany

***Correspondence:**

Nicole Teusch

nicole.teusch@th-koeln.de

Abstract

Multidrug resistance (MDR) in tumors and pathogens remains a major problem in the efficacious treatment of patients by reduction of therapy options and subsequent treatment failure. Various mechanisms are known to be involved in the development of MDR with overexpression of ATP-binding cassette (ABC) transporters being the most extensively studied. These membrane transporters translocate a wide variety of substrates utilizing energy from ATP hydrolysis leading to decreased intracellular drug accumulation and impaired drug efficacy. One treatment strategy might be inhibition of transporter-mediated efflux by small molecules. Isocoumarins and 3,4-dihydrocoumarins represent a large group of natural products derived from various sources with great structural and functional variety, but have so far not been in the focus as potential MDR reversing agents. Thus, three natural products and nine novel 3,4-dihydroisocoumarins were designed and analyzed regarding cytotoxicity induction and inhibition of human ABC transporters P-glycoprotein (P-gp), multidrug resistance-associated protein 1 (MRP1) and breast cancer resistance protein (BCRP) in a variety of human cancer cell lines. Dual inhibitors of P-gp and BCRP could be identified and distinct, parallel structure-activity relationships for inhibition of both transporters were revealed. The strongest inhibitor of P-gp and BCRP, which inhibited the transporters up to between 80% to 90%, demonstrated the ability to reverse chemotherapy resistance in resistant cancer cell lines up to 5.6-fold. Thus, the novel 3,4-dihydroisocoumarins of this study might serve as a promising starting point for development of potent dual inhibitors of P-gp and BCRP for efficacious treatment of multidrug-resistant tumors.

Keywords

multidrug resistance, cancer chemotherapy, natural products, 3,4-dihydroisocoumarin, P-glycoprotein, breast cancer resistance protein

Abbreviations

MDR, multidrug resistance; ABC, ATP-binding cassette; P-gp, P-glycoprotein; MRP1, multidrug resistance-associated protein 1; BCRP, breast cancer resistance protein; TBS, *tert*-butyldimethylsilyl; LHMDS, lithium bis(trimethylsilyl)amide; DDQ, 2,3-dichloro-5,6-dicyano-1,4-benzoquinone; FBS, fetal bovine serum

Introduction

Cancer remains the second most cause of death worldwide with 8.7 million case studies in 2015 [1]. Despite constant progress in antitumor drug development, multidrug resistance (MDR) poses a major problem in effective patient treatment. MDR is estimated to cause treatment failure in about 90% of patients with recurrent tumors [2]. MDR encompasses intrinsic or acquired resistance of pathogens or cancer cells to a spectrum of drugs, finally leading to reduction of treatment options and to therapy failure. Several mechanisms mediating MDR have been described, including mutations in drug targets, alterations in drug metabolism, decreased uptake or increased efflux of the drug [3,4].

Probably the most prominent and widespread mechanism is covered by increased drug transport from the cytoplasm through overexpression of ATP-binding cassette (ABC) transporters [5]. The ABC transporter superfamily, representing one of the oldest and largest protein families, is expressed from archaea to human. The common mechanism for all ABC transporters encompasses the active membrane translocation of a broad spectrum of substrates using energy from ATP hydrolysis [6].

Regarding MDR development accompanying antitumor therapy, three ABC transporters were identified as the main contributors. P-glycoprotein (P-gp, ABCB1), multidrug resistance-associated protein 1 (MRP1, ABCC1) and breast cancer resistance protein (BCRP, ABCG2) are frequently overexpressed in chemotherapy-resistant tumors, where they facilitate resistance to wide varieties of drugs commonly used in clinical practice [7]. Furthermore, recent studies have pronounced influence of ABC transporters in drug resistance mechanisms controlled by cancer stem cells, mainly responsible for recurrence of the disease [8].

Since the discovery of ABC transporter and characterization of their significant contribution to MDR, pharmacological strategies to overcome transporter-mediated MDR have been in the focus of various drug discovery approaches [9,10]. One focus is the development of small molecule inhibitors interfering with transporter activity in combination with chemotherapeutic drugs, thereby increasing intracellular drug accumulation and efficacy by reversing resistance [11–13]. ABC transporters involved in MDR have overlapping substrate spectrums. For example, several tyrosine kinase inhibitors, including dasatinib and imatinib, were demonstrated to become translocated to the extracellular space by P-gp and BCRP [14]. This leads to reduced efficacy of those drugs and subsequent therapy failure.

In most tumors, MDR is not only mediated by overexpression of one ABC transporter, but by expression of several transporters. Furthermore, P-gp and BCRP are co-expressed at the blood-brain barrier and prevent effective treatment of brain tumors [15]. Hence, the design of dual transporter inhibitors appears to be more efficacious in mentioned cases. To date, several dual inhibitors of P-gp and BCRP have been identified, including tariquidar and derivatives, aurones and chalcones [16–18]. Tariquidar entered clinical trials up to phase II to circumvent P-gp mediated MDR, but did not reveal sufficient clinical activity [19].

In principle, natural compounds and their derivatives play an important role in drug discovery and development [20,21]. In this context, various ABC transporter inhibitors from natural sources were identified and characterized in the last decades [22]. Early natural product P-gp inhibitors like cyclosporine A or its synthetic derivative PSC833 were tested in clinical trials up to phase III, but failed due to toxicity or other unintended side effects [23,24]. Among them were several dual inhibitors of P-gp and BCRP, for example some aurones, chalcones or flavonoids [18,25–27].

Isocoumarins, isomers of coumarin, represent a large class of secondary metabolites, which can be found in bacteria, fungi, lichens, marine sponges and to a lesser extent in higher plants [28]. To date, several hundred different isocoumarins and dihydroisocoumarins from nature have been identified and derivatives have been synthesized. Owing to their great structural diversity, diverse biological and pharmacological activities of isocoumarins like cytotoxicity and antimetastatic effects against various cancer types, including breast, colon, melanoma [29–32], inhibition of inflammation [33,34] or different enzymes, such as aromatase and kallikrein peptidases as potential cancer targets [35,36], as well as antibacterial, antifungal and antimalarial activities [37–39] could be identified. Several natural or synthetic coumarins were identified as inhibitors of either P-gp, BCRP or both and activities were mostly moderate and compound concentrations between 10 μM and 100 μM had to be applied for transporter inhibition [40–44]. In contrast, isocoumarins have to our knowledge not been characterized as potential MDR-reversing agents to date.

In this study, the three natural compounds 6-methoxymellein (**3**), angelicoin B (**4**) and ellagic acid as well as nine novel 3,4-dihydroisocoumarins (Figure 1) were analyzed regarding cytotoxicity in cancer cells and inhibition of the endogenously expressed human ABC transporters P-gp, BCRP and MRP1.

Material and Methods

Chemicals and reagents

A549 and HCT-15 cells were purchased from the German Collection of Microorganisms and Cell Cultures (Braunschweig, Germany) and H69AR cells from the American Type Culture Collection (Manassas, VA, USA). Dr. Erasmus Schneider (Wadsworth Center, New York State Department of Health, Albany, NY, USA) kindly provided the MCF-7/MX cells. Cell culture media and supplements were purchased from Thermo Fisher Scientific (Waltham, MA, USA). Hoechst 33342 was purchased from Sigma-Aldrich (St. Louis, MO, USA) and dissolved in water. Calcein-AM, PSC833, Ko143, MK-571, doxorubicin and mitoxantrone (Sigma-Aldrich, St. Louis, MO, USA) were dissolved in dimethyl sulfoxide (DMSO; Carl Roth, Karlsruhe, Germany). Hepes buffer was purchased from Lonza (Basel, Switzerland). CellTiter-Glo Luminescent Cell Viability Assay was purchased from Promega (Madison, WI, USA). Microtiter plates were purchased from Greiner Bio-One (Kremsmünster, Austria).

Test compounds

3,4-dihydroisocoumarins were synthesized in three steps starting from *α,β*-unsaturated *δ*-lactones and freshly prepared Brassard's diene. The reaction was catalyzed by $AlMe_3$ as Lewis acid and Tf_2CH_2 as Brønsted acid in toluene at room temperature for 30 min leading to the major vinylogous (*E*)-configured Michael-product and the minor cyclic product. The isolated (*E*)-configured Michael-product was cyclized with the strong base lithium bis(trimethylsilyl)amide (LHMDS) at -78°C to room temperature for 16 h. Both fractions of the isochromenones from the first and second step were oxidized with 2,3-dichloro-5,6-dicyano-1,4-benzoquinone (DDQ) in toluene at room temperature for 4 h to the desired end product. Overall yields were between 30% and 84%.

Deprotection of isocoumarins **(*R*)-19** and **(*S*)-19** by boron trifluoride diethyl ether in dichloromethane at 0 °C gave **(*R*)-19a** and **(*S*)-19a** in good to moderate yields between 36–47%. The free hydroxy groups of the pentyl-derivative **16** and the unsubstituted isocoumarin **14** were protected by dimethylsulfate. This procedure gave 66% of the corresponding methyl-protected pentyl-isocoumarin **16a** and 51% of the methyl-protected isocoumarin **14a**.

Ellagic acid was provided by MicroCombiChem GmbH (Wiesbaden, Germany). All test compounds were dissolved in DMSO.

Cell culture

The human lung adenocarcinoma cell line A549 was cultured in DMEM medium supplemented with 10% fetal bovine serum (FBS), 100 U/mL penicillin and 100 µg/mL streptomycin. P-gp-expressing human colon adenocarcinoma cells HCT-15 were cultured in RPMI 1640 medium supplemented with 10% FBS, 100 U/mL penicillin and 100 µg/mL streptomycin. BCRP-expressing MCF-7/MX human breast adenocarcinoma cells were cultured in DMEM medium supplemented with 10% FBS, 100 U/mL penicillin and 100 µg/mL streptomycin. MRP1-expressing H69AR human small cell lung cancer cells were cultured in RPMI 1640 medium (ATCC modification) supplemented with 20% FBS, 100 U/mL penicillin and 100 µg/mL streptomycin.

Cells were maintained in a humidified atmosphere at 37 °C and 5% CO_2 and subcultured when confluency reached 80 to 90%.

Cell viability assay

Cytotoxic activity of test compounds was analyzed after 48 h using the CellTiter-Glo Luminescent Cell Viability Assay published previously [45] in 384-well plates with the following cell densities: A549, MCF-7/MX: $2 \cdot 10^3$ cells/well; HCT-15: $3 \cdot 10^3$ cells/well; H69AR: $5 \cdot 10^3$ cells/well. Pipetting was conducted with the CyBi-Well 96-channel simultaneous pipettor (Analytik Jena AG, Jena, Germany). For generation of dose-response curves and calculation of IC_{50} values, the four-parameter logistic model was applied.

The ability of identified inhibitors of P-gp and BCRP to sensitize HCT-15 or MCF-7/MX cells to chemotherapy was analyzed by co-treatment with test compounds and doxorubicin or mitoxantrone, respectively. Cells were incubated with a serial dilution of the chemotherapeutic drug alone or in combination with fixed concentrations of the test compounds or positive controls (2.5 µM PSC833 and 1 µM Ko143, respectively). Fold change of drug IC_{50} was calculated with the formula IC_{50} (drug alone)/IC_{50} (drug with modulator).

Inhibition of ABC transporter activities

P-gp transport assay

The transport of calcein-AM by P-gp and its modulation by test compounds was analyzed in the P-gp-expressing HCT-15 cell line. $5 \cdot 10^4$ cells were seeded in black 96-well plates and incubated at 37 °C and 5% CO_2 for 24 h. The culture medium was removed and replaced by Hank's balanced salt solution supplemented with 10 mM hepes. Test compounds, 2.5 µM PSC833 (positive control) or 0.5% DMSO (negative control) were added in triplicates and incubated for 30 min at 37°C and 5% CO_2. The substrate calcein-AM was added (final concentration 0.5 µM) and the fluorescence (excitation 485 nm, emission 520 nm) was measured over 3 h with the Infinite m1000 pro microplate reader (Tecan Group AG, Maennedorf, Switzerland) at 37 °C. The transport activity of P-gp was analyzed by determining the slope of the linear part of the fluorescence-time curve (0-30 min) using linear regression. Normalization of the data to PSC833 (100% inhibition) and DMSO (0% inhibition) was performed.

BCRP transport assay

BCRP transport activity was determined in the BCRP-expressing MCF-7/MX cell line. Hoechst 33342 was applied as transporter substrate and 1 µM Ko143 as positive control and the assay was performed according to the P-gp assay. Fluorescence was measured at excitation wavelength of 355 nm and emission wavelength of 460 nm. The transport activity of BCRP was analyzed by determining the plateau of the fluorescence-time curve by using non-linear regression (one-phase exponential fit). Normalization of the data to Ko143 (100% inhibition) and DMSO (0% inhibition) was performed.

MRP1 transport assay

Transport activity of MRP1 was determined in MPR1-expressing H69AR cells using the substrate calcein-AM and 20 µM MK-571 as the positive control. Experimental procedure was according to the P-gp assay, except that $7.5 \cdot 10^4$ cells were seeded per well. The transport activity of MRP1 was analyzed by determining the slope of the linear part of the fluorescence-time curve (0-20 min) using linear regression. Normalization of the data to MK-571 (100% inhibition) and DMSO (0% inhibition) was performed.

Data analysis and statistics

Experiments in human cancer cell lines were performed in at least three independent replicates. Data were analyzed with GraphPad Prism v. 6.07 (GraphPad Software Inc., La Jolla, CA, USA) and results are presented as mean ± SEM. Different groups were compared statistically using one-way ANOVA followed by Dunnett's multiple comparisons test. Differences were considered significant when $p < 0.05$.

Results

Cytotoxic activity of 3,4-dihydroisocoumarins in human cancer cell lines

Cytotoxicity of twelve 3,4-dihydroisocoumarins was analyzed in the sensitive lung cancer cell line A549 as well as in three resistant cell lines HCT-15 (colon carcinoma), MCF-7/MX (breast carcinoma) and H69AR (lung carcinoma) either expressing the ABC transporter P-gp, BCRP or MRP1, respectively. Cells were incubated for 48 h with test compounds and cell viability was assessed.

IC_{50} values of the tested 3,4-dihydroisocoumarins are summarized in Table 1. Most compounds did not display significant cytotoxic activities in the cancer cell lines and IC_{50} values were above the highest concentrations applied in the assay. One exception were the enantiomers **(*R*)-19** and **(*S*)-19**. Both compounds were comparably cytotoxic in sensitive A549 cells and the BCRP-overexpressing MCF-7/MX cells. In A549 cells, IC_{50} value of compound **(*R*)-19** was 47.5 ± 3.2 µM (mean ± SEM) and IC_{50} value of **(*S*)-19** was 42.0 ± 3.9 µM. In MCF-7/MX cells, both compounds were slightly more toxic with IC_{50} values of 28.1 ± 0.7 µM and 33.5 ± 7.5 µM, respectively. In contrast, in P-gp expressing HCT-15 cells, only **(*R*)-19** demonstrated a cytotoxic effect, whereas **(*S*)-19** was not toxic. Furthermore, the unprotected derivatives of **(*R*)-19** and **(*S*)-19**, **(*R*)-19a** and **(*S*)-19a**, were analyzed. In both cases, removal of the protecting *tert*-Butyldimethylsilyl (TBS) group lead to complete or near complete loss of cytotoxic activity in all cell lines.

Compound **16** was not cytotoxic in P-gp expressing HCT-15 cells and BCRP-expressing MCF-7/MX cells. In MRP1-expressing H69AR cells and sensitive A549 cells, only minor cytotoxic activity was observed. IC_{50} values were 88.5 ± 4.6 µM and 78.6 ± 2.2 µM, respectively. Remarkably, the derivative **16a**, which differs from **16** by the methoxy group

instead of the hydroxy group at position 8, displayed slightly improved activity in A549 cells with an about 1.5-fold lower IC_{50} value and a clearly improved activity in BCRP-expressing MCF-7/MX cells. In those cells, the IC_{50} value was 10.6 ± 0.9 µM. In P-gp or MRP1-expressing cell lines, no cytotoxicity could be observed.

The known natural products 6-methoxymellein (**3**), angelicoin B (**4**) and ellagic acid did not show any cytotoxic effects against the tested cancer cell lines.

Identification of 3,4-dihydroisocoumarins as dual inhibitors of P-gp and BCRP

The twelve 3,4-dihydroisocoumarins were tested for their ability to inhibit the transport activity of the human ABC transporters P-gp, BCRP and MRP1 in cell lines overexpressing the respective transporter. Therefore, intracellular fluorescence of the transporter substrates calcein-AM and Hoechst 33341 were measured over time after cells had been treated with different concentrations of the test compounds. Inhibition rates of the compounds were normalized to the positive controls 2.5 µM PSC833, 1 µM Ko143 and 20 µM MK-571, respectively. As a result, three compounds were identified as dual inhibitors of transport activity of P-gp and BCRP (Figure 2A, B).

Pentyl-derivative **16** was the strongest dose-dependent inhibitor of P-gp and BCRP among the tested compounds. Relative inhibition of P-gp was 36.3 ± 5.3% at a concentration of 10 µM, 52.6 ± 3.1 % at 20 µM and 81.2 ± 2.7% at 50 µM (mean ± SEM). Regarding inhibition of BCRP, the rates were comparable to P-gp with relative values between 35.3 ± 3.4% at 10 µM and 89.1 ± 4.6% at 50 µM. Interestingly, derivative **16a**, which differs from **16** only by the methoxy group instead of the hydroxy group at position 8, showed reduced inhibition rates against both transporters with a more pronounced effect for BCRP. Relative inhibition was between 18.4 ± 0.5% and 31.9 ± 2.2% for P-gp and 2.3 ± 0.9% and 14.9 ± 2.2% for BCRP.

Two additional compounds were identified as dual P-gp and BCRP inhibitors, **(*R*)-19** and **(*S*)-19**, but with lower activities compared to derivative **16**. Derivative **(*R*)-19** inhibited P-gp with relative rates between 23.6 ± 4.2% and 46.8 ± 5.7%. Regarding **(*S*)-19**, highest P-gp inhibition was achieved at 10 µM (37.1 ± 2.9%). Inhibition of BCRP was comparable. As both compounds bore protective groups at the hydroxy group at the ethyl chain at position 3, inhibition rates were compared to the deprotected derivatives **(*R*)-19a** and **(*S*)-19a**. In both

cases, the deprotected compounds showed clearly reduced inhibitory ability of P-gp with values between about 5% and 15% and completely abolished inhibitory ability of BCRP.

Two compounds without substitution at position 3 were analyzed, **14** and **14a**. They only differ in the substituent at position 8, which is either a hydroxy group (**14**) or methoxy group (**14a**). Both compounds did not inhibit BCRP and displayed only minor inhibitory activity against P-gp up to about 10% relative inhibition.

Furthermore, the two natural products and enantiomers 6-methoxymellein (**3**) and angelicoin B (**4**) were studied. They share the same structure with compound **14**, but are substituted with a methyl group at position 3. Relative rates of P-gp inhibition of 6-methoxymellein (**3**) and angelicoin B (**4**) did not differ significantly from those of derivative **14**. In case of BCRP, no inhibitory activity could be observed, as was the case for derivative **14**.

Compound **21**, a tricyclic derivative, weakly inhibited P-gp with a relative inhibition rate of 20.0 ± 1.2% at the highest concentration used. Its ability to inhibit BCRP could not be determined due to inherent fluorescence. The natural product ellagic acid did not display any inhibitory activity against P-gp or BCRP. It has to be noted that this compound could not be employed at a concentration of 50 µM due to its low solubility.

Regarding inhibition of MRP1 transport function in H69AR cells, none of the test compounds demonstrated any activity (Figure 2C).

Sensitization of resistant cancer cells to chemotherapy by 3,4-dihydroisocoumarins

Cancer cells overexpressing multidrug resistance related ABC transporters are characterized by reduced susceptibility to chemotherapeutic drugs, which are substrates of the respective transporters. These are for example doxorubicin and mitoxantrone. To determine if the identified P-gp and BCRP inhibitor derivative **16** is able to re-sensitize resistant cancer cells to chemotherapy, P-gp expressing HCT-15 cells and BCRP-expressing MCF-7/MX cells were co-treated with doxorubicin or mitoxantrone and different concentrations of compound **16**. IC_{50} values were determined after 48 h and compared to single treatment with the chemotherapeutic drugs. PSC833 (2.5 µM) and Ko143 (1 µM) served as respective positive controls.

In both cases, compound **16** was able to significantly sensitize the resistant cancer cells to chemotherapy. In HCT-15 cells, doxorubicin alone had an IC_{50} value of 8.5 ± 0.7 μM (mean ± SEM; Table 2, Figure 3A). Addition of 20 μM of compound **16** did not lead to a change in IC_{50}, whereas the combination with 50 μM of the compound lead to a 3.7-fold decrease in IC_{50} to 2.3 ± 0.08 μM. In contrast, the compound **14**, which displayed minor P-gp inhibiting activity, did not sensitize the cells to doxorubicin. The positive control PSC833 reduced the IC_{50} of doxorubicin around 28-fold to a value of 0.3 ± 0.08 μM.

In BCRP-expressing MCF-7/MX cells, IC_{50} value of the drug mitoxantrone alone was 19.6 ± 2.4 μM (Table 3, Figure 3B). Addition of the compound **16** revealed a dose-dependent decrease in IC_{50} up to 5.6-fold at 50 μM to 3.5 ± 0.9 μM. Like observed above, compound **14**, which did not inhibit BCRP transport function, did not have a significant influence on the sensitivity of the cells to mitoxantrone. The positive control Ko143 was able to increase the cytotoxicity of mitoxantrone around 65-fold to an IC_{50} value of 0.3 ± 0.07 μM.

Discussion

As MDR mediated by overexpression of ABC transporters remains a major issue in efficacious treatment of cancer or pathogenic diseases, it is of utmost importance to identify novel treatment strategies. One possibility is the development of inhibitors of transporter function. Although isocoumarins and 3,4-dihydroisocoumarins demonstrated various pharmacological activities, such as anticancer, anti-inflammatory, antifungal and antibacterial effects [28], to date, they have not been characterized as potential ABC transporter inhibitors. However, in previous manuscripts several natural or synthetic coumarins were described as mostly moderate inhibitors of either P-gp, BCRP or both transporters [40–44]. Thus, in this study 3,4-dihydroisocoumarins of natural or synthetic origin were evaluated for the first time as potential inhibitors of human ABC transporters.

Among the tested derivatives, three novel 3,4-dihydroisocoumarins were identified as dual inhibitors of both transporters, human P-gp and BCRP. Furthermore, the most potent inhibitor, derivative **16**, demonstrated inhibition of both transporters between 80% and 90% compared to the respective positive controls at the highest test concentration (50 μM). As proof of concept, P-gp expressing HCT-15 cells and BCRP-expressing MCF-7/MX cells were treated with derivative **16** in combination with the chemotherapeutic drugs doxorubicin and

mitoxantrone, broadly described as transporter substrates for P-gp and BCRP. Subsequently, co-treatment with 50 μM of derivative **16** sensitized chemotherapy-resistant carcinoma cells HCT-15 to doxorubicin by decreasing the IC_{50} value of doxorubicin-induced cytotoxicity by 3.7-fold and sensitized MCF-7/MX breast carcinoma cells to mitoxantrone by decreasing the IC_{50} value of mitoxantrone-induced cytotoxicity by 5.6-fold. Moreover, enantiomers **(*R*)-19** and **(*S*)-19** inhibited transport function of P-gp and BCRP, but with lower potency compared to derivative **16**. Noteworthy, distinct structure-activity relationships for transporter inhibition could be identified and they run parallel for P-gp and BCRP inhibition: our data show that the hydroxy group at position 8 is mandatory for transporter inhibition and substitution by a methoxy group clearly reduces activity. Furthermore, a hydrophobic carbon chain at position 3 is indispensable for inhibition and this substituent seems to need a certain chain length. Compounds without alkyl substituent (derivative **14**) or with a methyl group (6-methoxymellein (**3**) and angelicoin B (**4**)) as well as compounds with hydrophilic chain (derivatives **(*R*)-19a** and **(*S*)-19a**) demonstrated significantly decreased inhibition of both transporters. However, those effects were more pronounced in BCRP inhibition than in P-gp inhibition.

Regarding these results, the 3,4-dihydroisocoumarin derivatives that we identified as dual P-gp and BCRP inhibitors with moderate activity might serve as a promising starting point for further development of more efficacious inhibitors to overcome MDR in cancer patients. Here, it would be interesting to further explore the influence of prolonged alkyl groups at position 8 or the effect of substituent variations on the inhibitory activities.

In addition to transporter inhibition, the cytotoxic activities of the test compounds were analyzed in sensitive A549 lung carcinoma cells as well as in resistant HCT-15 colon carcinoma, H69AR lung carcinoma and MCF-7/MX breast carcinoma cells. Noteworthy, most compounds did not exhibit any toxic effects in cancer cells. One exception was derivative **16a**, which proved selective cytotoxicity in BCRP-expressing MCF-7/MX cells with an IC_{50} value of 10.6 μM, but not in P-gp or MRP1-expressing cells. In sensitive A549 lung carcinoma cells, cytotoxicity was significantly lower with an IC_{50} value of 53.6 μM. Future studies might involve the analysis of the cytotoxic activity of **16a** in parental, chemotherapy-sensitive MCF-7 cells. Depending on putative selectivity for multidrug resistant tumor cells, insights into the mechanism of action and target would be helpful to find out more about collateral sensitivity in BCRP-overexpressing cancer cells and how to exploit this feature in tumor therapy [46,47]. Furthermore, to our knowledge, anticancer effects of

angelicoin B (**4**) have not been studied yet. However, the high IC_{50} value of 6-methoxymellein (**3**) is in accordance with a previous study [48]. In contrast, the diverse pharmacological activities of ellagic acid have been extensively explored [49]. Although several anticancer activities of ellagic acid were identified *in vitro* and *in vivo*, including cell cycle arrest and apoptosis with moderate potency, such effects could not be recapitulated in our study.

In summary, our data reveal for the first time the potential of selected non-toxic 3,4-dihydroisocoumarins to function as dual inhibitors of the ABC transporters P-gp and BCRP, which are two of the main contributors to cancer MDR. These compounds might serve as a promising starting point for further optimization and development. In future studies, the underlying molecular mechanism of transporter inhibition will be analyzed by P-gp and BCRP ATPase assays and molecular docking studies.

Funding

This work is funded by the German Federal Ministry for Economic Affairs and Energy ('ZIM Kooperationsprojekt' KF3279X01AJ3) and supported by a scholarship of the Studienstiftung des deutschen Volkes for A.W. The PhD training of J.S. is financed by the graduate program in Pharmacology and Experimental Therapeutics at the University of Cologne which is financially and scientifically supported by Bayer.

Acknowledgments

We would like to thank Dr. Erasmus Schneider (Wadsworth Center, New York State Department of Health, Albany, NY, USA) for kindly providing the MCF-7/MX cell line and Janina Betz and Vanessa Mundorf for excellent technical assistance.

References

[1] Fitzmaurice C, Allen C, Barber RM, Barregard L, Bhutta ZA, Brenner H et al. Global, Regional, and National Cancer Incidence, Mortality, Years of Life Lost, Years Lived With Disability, and Disability-Adjusted Life-years for 32 Cancer Groups, 1990 to 2015: A Systematic Analysis for the Global Burden of Disease Study. JAMA Oncol 2017;3:524–48.

[2] Longley DB, Johnston PG. Molecular mechanisms of drug resistance. J Pathol 2005;205:275–92.

[3] Gillet J-P, Gottesman MM. Mechanisms of Multidrug Resistance in Cancer. In: Zhou J, editor. Multi-Drug Resistance in Cancer. Totowa, NJ: Humana Press; 2010. p. 47–76.

[4] Kaye KS, Kaye D. Multidrug-resistant pathogens: mechanisms of resistance and epidemiology. Curr Infect Dis Rep 2000;2:391–8.

[5] El-Awady R, Saleh E, Hashim A, Soliman N, Dallah A, Elrasheed A et al. The Role of Eukaryotic and Prokaryotic ABC Transporter Family in Failure of Chemotherapy. Front Pharmacol 2016;7:535.

[6] Szöllősi D, Rose-Sperling D, Hellmich UA, Stockner T. Comparison of mechanistic transport cycle models of ABC exporters. Biochim Biophys Acta 2017;1860:818–32.

[7] Bugde P, Biswas R, Merien F, Lu J, Liu D-X, Chen M et al. The therapeutic potential of targeting ABC transporters to combat multi-drug resistance. Expert Opin Ther Targets 2017;21:511–30.

[8] Begicevic R-R, Falasca M. ABC Transporters in Cancer Stem Cells: Beyond Chemoresistance. Int J Mol Sci 2017;18.

[9] Tillotson GS, Theriault N. New and alternative approaches to tackling antibiotic resistance. F1000Prime Rep 2013;5:51.

[10] Szakács G, Paterson JK, Ludwig JA, Booth-Genthe C, Gottesman MM. Targeting multidrug resistance in cancer. Nat Rev Drug Discov 2006;5:219–34.

[11] Zhang L, Ma S. Efflux pump inhibitors: a strategy to combat P-glycoprotein and the NorA multidrug resistance pump. ChemMedChem 2010;5:811–22.

[12] Tran-Nguyen V-K, Prasad R, Falson P, Boumendjel A. Modulators of the Efflux Pump Cdr1p of *Candida albicans*: Mechanisms of Action and Chemical Features. Curr Med Chem 2017;24:3242–53.

[13] Spengler G, Kincses A, Gajdács M, Amaral L. New roads leading to old destinations: efflux pumps as targets to reverse multidrug resistance in bacteria. Molecules 2017;22.

[14] Dohse M, Scharenberg C, Shukla S, Robey RW, Volkmann T, Deeken JF et al. Comparison of ATP-binding cassette transporter interactions with the tyrosine kinase inhibitors imatinib, nilotinib, and dasatinib. Drug Metab Dispos 2010;38:1371–80.

[15] Agarwal S, Hartz AMS, Elmquist WF, Bauer B. Breast cancer resistance protein and P-glycoprotein in brain cancer: Two gatekeepers team up. Curr Pharm Des 2011;17:2793–802.

[16] Li X-Q, Wang L, Lei Y, Hu T, Zhang F-L, Cho C-H et al. Reversal of P-gp and BCRP-mediated MDR by tariquidar derivatives. Eur J Med Chem 2015;101:560–72.

[17] Gu X, Ren Z, Peng H, Peng S, Zhang Y. Bifendate-chalcone hybrids: A new class of potential dual inhibitors of P-glycoprotein and breast cancer resistance protein. Biochem Biophys Res Commun 2014;455:318–22.

[18] Sim HM, Loh KY, Yeo WK, Lee CY, Go ML. Aurones as modulators of ABCG2 and ABCB1: Synthesis and structure-activity relationships. ChemMedChem 2011;6:713–24.

[19] Pusztai L, Wagner P, Ibrahim N, Rivera E, Theriault R, Booser D et al. Phase II study of tariquidar, a selective P-glycoprotein inhibitor, in patients with chemotherapy-resistant, advanced breast carcinoma. Cancer 2005;104:682–91.

[20] Newman DJ, Cragg GM. Natural products as sources of new drugs from 1981 to 2014. J Nat Prod 2016;79:629–61.

[21] Guo Z. The modification of natural products for medical use. Acta Pharm Sin B 2017;7:119–36.

[22] Karthikeyan S, Hoti S. Development of fourth generation ABC inhibitors from natural products: a novel approach to overcome cancer multidrug resistance. Anticancer Agents Med Chem 2015;15:605–15.

[23] Baer MR, George SL, Dodge RK, O'Loughlin KL, Minderman H, Caligiuri MA et al. Phase 3 study of the multidrug resistance modulator PSC-833 in previously untreated patients 60 years of age and older with acute myeloid leukemia: Cancer and Leukemia Group B Study 9720. Blood 2002;100:1224–32.

[24] Warner E, Tobe SW, Andrulis IL, Pei Y, Trachtenberg J, Skorecki KL. Phase I-II study of vinblastine and oral cyclosporin A in metastatic renal cell carcinoma. Am J Clin Oncol 1995;18:251–6.

[25] Yuan J, Wong ILK, Jiang T, Wang SW, Liu T, Wen BJ et al. Synthesis of methylated quercetin derivatives and their reversal activities on P-gp- and BCRP-mediated multidrug resistance tumour cells. Eur J Med Chem 2012;54:413–22.

[26] Boumendjel A, McLeer-Florin A, Champelovier P, Allegro D, Muhammad D, Souard F et al. A novel chalcone derivative which acts as a microtubule depolymerising agent and an inhibitor of P-gp and BCRP in in-vitro and in-vivo glioblastoma models. BMC Cancer 2009;9:242.

[27] Iriti M, Kubina R, Cochis A, Sorrentino R, Varoni EM, Kabała-Dzik A et al. Rutin, a Quercetin Glycoside, Restores Chemosensitivity in Human Breast Cancer Cells. Phytother Res 2017;31:1529–38.

[28] Saeed A. Isocoumarins, miraculous natural products blessed with diverse pharmacological activities. Eur J Med Chem 2016;116:290–317.

[29] Guimarães KG, Freitas RP de, Ruiz ALTG, Fiorito GF, Carvalho JE de, da Cunha EFF et al. Synthesis, antiproliferative activities, and computational evaluation of novel isocoumarin and 3,4-dihydroisocoumarin derivatives. Eur J Med Chem 2016;111:103–13.

[30] Zhang G-J, Li B, Chen L, Tian Y, Liu S-J, Cui H-M et al. Isocoumarin derivatives and monoterpene glycoside from the seeds of *Orychophragmus violaceus*. Fitoterapia 2017;125:111–6.

[31] Cichewicz RH, Valeriote FA, Crews P. Psymberin, a potent sponge-derived cytotoxin from *Psammocinia* distantly related to the pederin family. Org Lett 2004;6:1951–4.

[32] Abid O-u-R, Khalid M, Hussain MT, Hanif M, Qadeer G, Rama NH et al. Synthesis and anti-cancer, anti-metastatic evaluation of some new fluorinated isocoumarins and 3,4-dihydroisocoumarins. J Fluor Chem 2012;135:240–5.

[33] Ramanan M, Sinha S, Sudarshan K, Aidhen IS, Doble M. Inhibition of the enzymes in the leukotriene and prostaglandin pathways in inflammation by 3-aryl isocoumarins. Eur J Med Chem 2016;124:428–34.

[34] Liang Q, Wu Q, Jiang J, Duan J'a, Wang C, Smith MD et al. Characterization of sparstolonin B, a Chinese herb-derived compound, as a selective Toll-like receptor antagonist with potent anti-inflammatory properties. J Biol Chem 2011;286:26470–9.

[35] Teixeira TSP, Freitas RF, Abrahão O, Devienne KF, Souza LR de, Blaber SI et al. Biological evaluation and docking studies of natural isocoumarins as inhibitors for human kallikrein 5 and 7. Bioorg Med Chem Lett 2011;21:6112–5.

[36] Endringer DC, Guimarães KG, Kondratyuk TP, Pezzuto JM, Braga FC. Selective inhibition of aromatase by a dihydroisocoumarin from *Xyris pterygoblephara*. J Nat Prod 2008;71:1082–4.

[37] Simic M, Paunovic N, Boric I, Randjelovic J, Vojnovic S, Nikodinovic-Runic J et al. Functionalised isocoumarins as antifungal compounds: Synthesis and biological studies. Bioorg Med Chem Lett 2016;26:235–9.

[38] Lai D, Wang A, Cao Y, Zhou K, Mao Z, Dong X et al. Bioactive dibenzo-α-pyrone derivatives from the endophytic fungus *Rhizopycnis vagum* Nitaf22. J Nat Prod 2016;79:2022–31.

[39] Hoepfner D, McNamara CW, Lim CS, Studer C, Riedl R, Aust T et al. Selective and specific inhibition of the *Plasmodium falciparum* lysyl-tRNA synthetase by the fungal secondary metabolite cladosporin. Cell Host Microbe 2012;11:654–63.

[40] Raad I, Terreux R, Richomme P, Matera E-L, Dumontet C, Raynaud J et al. Structure-activity relationship of natural and synthetic coumarins inhibiting the multidrug transporter P-glycoprotein. Bioorg Med Chem 2006;14:6979–87.

[41] Sjöstedt N, Holvikari K, Tammela P, Kidron H. Inhibition of Breast Cancer Resistance Protein and Multidrug Resistance Associated Protein 2 by Natural Compounds and Their Derivatives. Mol Pharmaceutics 2017;14:135–46.

[42] Combes S, Barbier P, Douillard S, McLeer-Florin A, Bourgarel-Rey V, Pierson J-T et al. Synthesis and biological evaluation of 4-arylcoumarin analogues of combretastatins. Part 2. J Med Chem 2011;54:3153–62.

[43] Barthomeuf C, Grassi J, Demeule M, Fournier C, Boivin D, Béliveau R. Inhibition of P-glycoprotein transport function and reversion of MDR1 multidrug resistance by cnidiadin. Cancer Chemother Pharmacol 2005;56:173–81.

[44] Bisi A, Cappadone C, Rampa A, Farruggia G, Sargenti A, Belluti F et al. Coumarin derivatives as potential antitumor agents: Growth inhibition, apoptosis induction and multidrug resistance reverting activity. Eur J Med Chem 2017;127:577–85.

[45] Weber A, Döhl K, Sachs J, Nordschild ACM, Schröder D, Kulik A et al. Synthesis and cytotoxic activities of goniothalamins and derivatives. Bioorg Med Chem 2017;25:6115–25.

[46] Rao DK, Liu H, Ambudkar SV, Mayer M. A combination of curcumin with either gramicidin or ouabain selectively kills cells that express the multidrug resistance-linked ABCG2 transporter. J Biol Chem 2014;289:31397–410.

[47] Pluchino KM, Hall MD, Goldsborough AS, Callaghan R, Gottesman MM. Collateral sensitivity as a strategy against cancer multidrug resistance. Drug Resist Updat 2012;15:98–105.

[48] Snene A, Sirignano C, Rigano D, Formisano C, El Mokni R, Ercolano G et al. Antiproliferative metabolites from the Northern African endemic plant *Daucus virgatus* (Apiaceae). Phytochemistry 2017;143:194–8.

[49] Shakeri A, Zirak MR, Sahebkar A. Ellagic acid: A logical lead for drug development? Curr Pharm Des 2017;23.

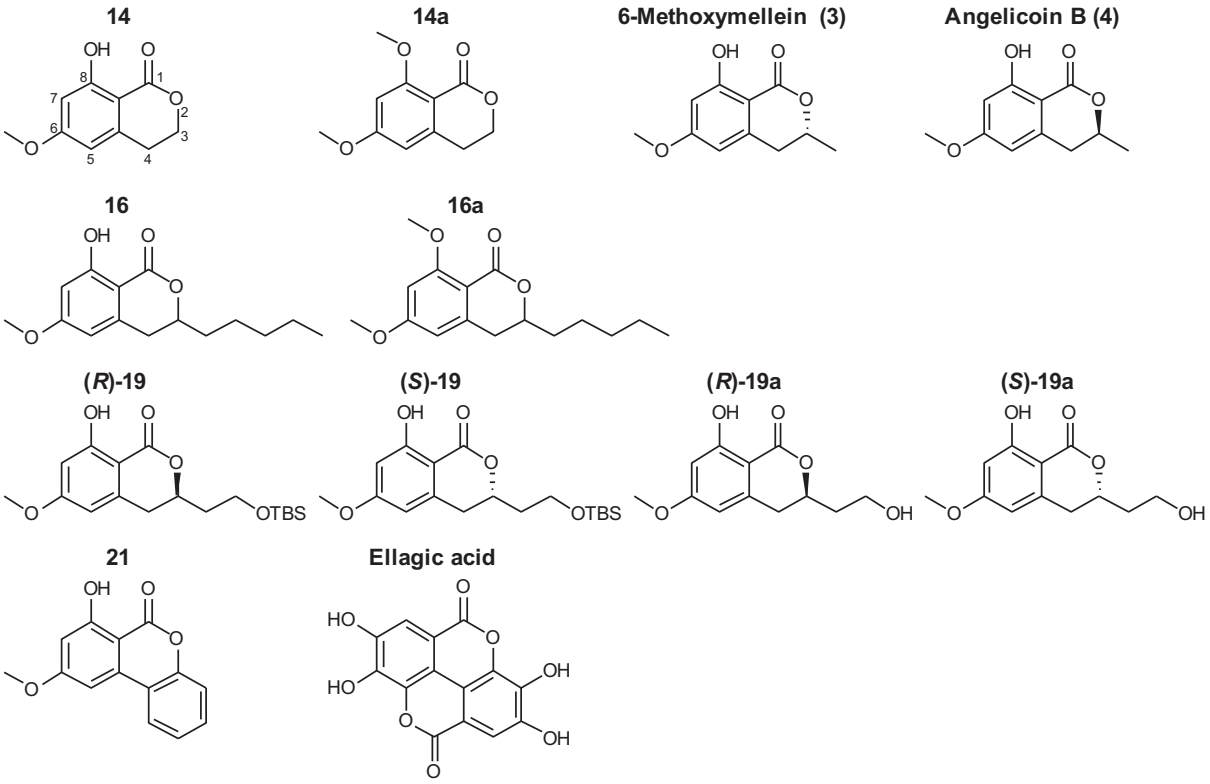

Figure 1. Structures of natural and synthetic 3,4-dihydroisocoumarins.

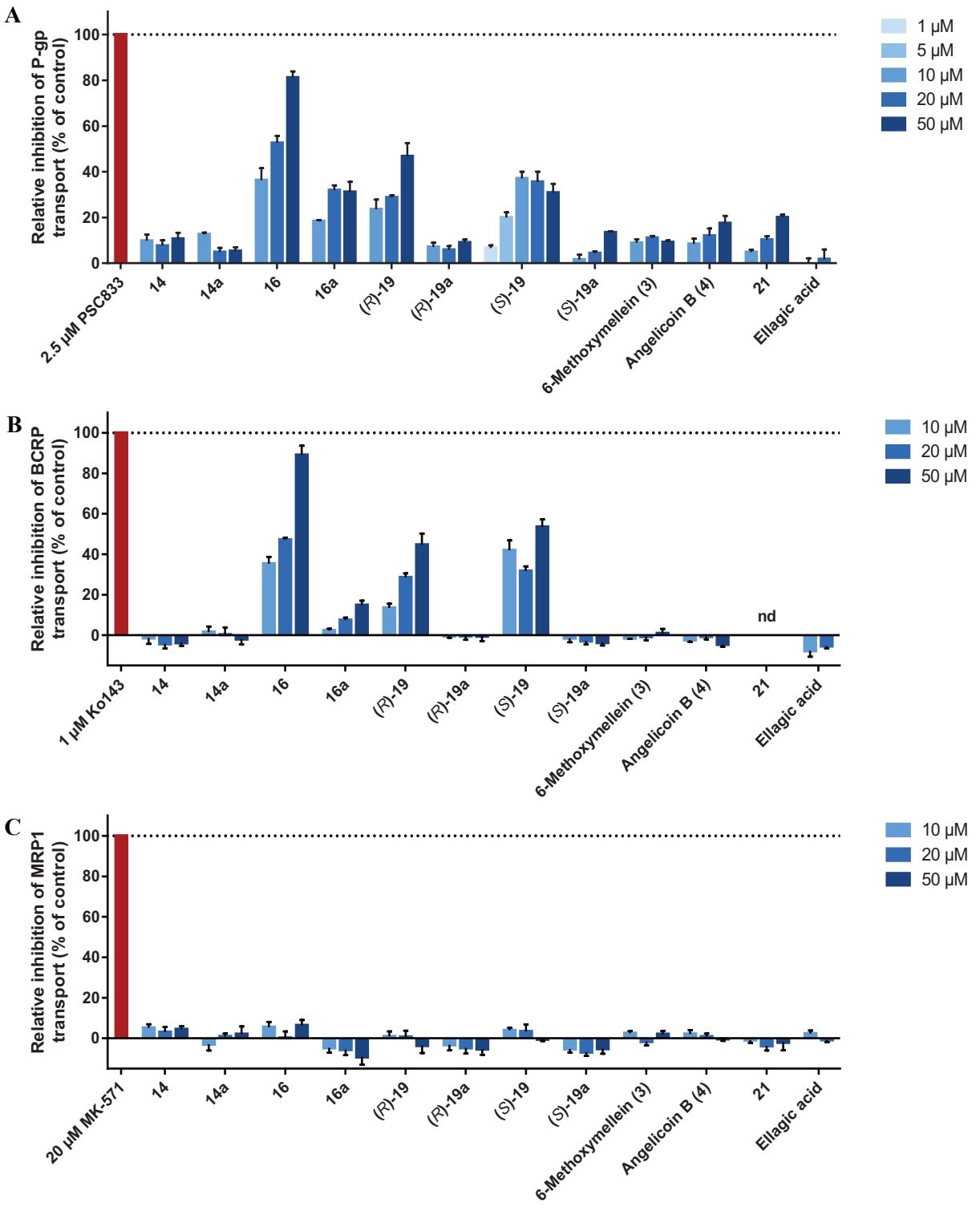

Figure 2. Influence of 3,4-dihydroisocoumarins on ABC transporter activity. Cancer cell lines overexpressing **(A)** P-gp (HCT-15), **(B)** BCRP (MCF-7/MX) or **(C)** MRP1 (H69AR) were incubated with test compounds and intracellular fluorescence of the substrates calcein-AM (P-gp, MRP1) or Hoechst 33342 (BCRP) was measured over 3 h. Data were normalized to DMSO (0% inhibition) and the positive controls PSC833, Ko143 and MK-571, respectively (100% inhibition). Bars represent mean ± SEM of at least three independent experiments. nd: not determined because of intrinsic fluorescence.

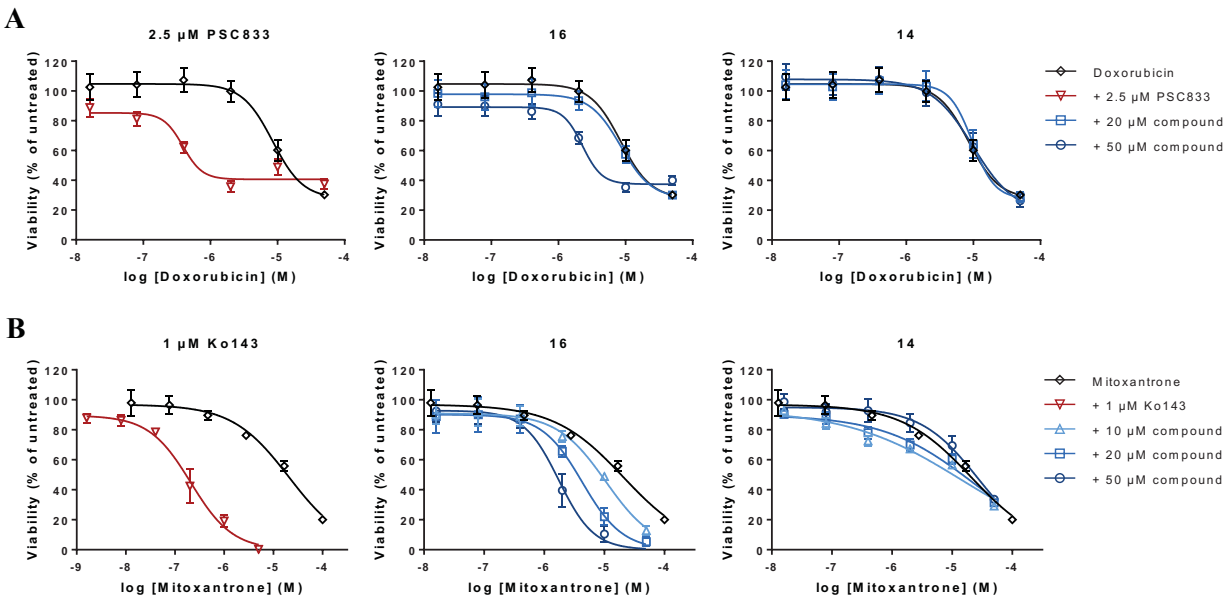

Figure 3. Sensitization of resistant cancer cells to chemotherapy by selected 3,4-dihydroisocoumarins. **(A)** P-gp expressing HCT-15 and **(B)** BCRP-expressing MCF-7/MX were treated with either doxorubicin or mitoxantrone alone, in combination with positive controls PSC833 or Ko143 or in combination with varying concentrations of test compounds **16** and **14**. Cell viability was determined after 48 h. Data represent mean ± SEM normalized to untreated cells of at least three independent experiments performed in quadruplicates.

Table 1

Cytotoxicity of 3,4-dihydroisocoumarins on human tumor cell lines.

Compound	IC_{50} (μM)			
	A549	HCT-15	MCF-7/MX	H69AR
14	>100	>100	>100	>100
14a	>100	>100	>100	>100
16	78.6 ± 2.2	>100	>100	88.5 ± 4.6
16a	53.6 ± 5.6	>100	10.6 ± 0.9	>100
(*R*)-19	47.5 ± 3.2	57.1 ± 7.5	28.1 ± 0.7	>100
(*R)*-19a	>100	>100	>100	>100
(*S*)-19	42.0 ± 3.9	>100	33.5 ± 7.5	86.8 ± 9.2
(*S*)-19a	>100	>100	89.8 ± 4.9	>100
6-Methoxymellein (3)	>100	>100	>100	>100
Angelicoin B (4)	>100	>100	>100	>100
21	>50	>50	>50	>50
Ellagic acid	>50	>50	>50	>50

Data represent mean ± SEM of at least three independent experiments performed in quadruplicates.

Table 2

Sensitization of HCT-15 cells to doxorubicin treatment by selected 3,4-dihydroisocoumarins.

Compound	IC_{50} (μM)	*p*-value	fold change
Doxorubicin	8.5 ± 0.7	-	1.00
+ 2.5 μM PSC833	0.3 ± 0.03**	0.0017	28.33
+ 20 μM 16	8.7 ± 1.6	0.9999	0.98
+ 50 μM 16	2.3 ± 0.08*	0.0129	3.70
+ 20 μM 14	9.6 ± 1.0	0.9498	0.89
+ 50 μM 14	10.6 ± 2.1	0.6313	0.80

PSC833 was used as positive control. Fold change of cytotoxicity was determined by dividing the IC_{50} value of cells treated with doxorubicin alone by the IC_{50} value of cells treated with doxorubicin in combination with the respective test compound. Data show mean ± SEM of three independent experiments performed in quadruplicates. * $p < 0.05$; ** $p < 0.01$ compared to doxorubicin alone (One-way ANOVA followed by Dunnett's multiple comparisons test).

Table 3

Sensitization of MCF-7/MX cells to mitoxantrone treatment by selected 3,4-dihydroisocoumarins.

Compound	IC_{50} (μM)	*p*-value	fold change
Mitoxantrone	19.6 ± 2.4	-	1.00
+ 1 μM Ko143	0.3 ± 0.07****	<0.0001	65.33
+ 10 μM 16	21.1 ± 1.4	0.9795	0.93
+ 20 μM 16	5.3 ± 1.1****	<0.0001	3.70
+ 50 μM 16	3.5 ± 0.9****	<0.0001	5.60
+ 10 μM 14	19.4 ± 2.6	>0.9999	1.01
+ 20 μM 14	25.5 ± 1.0	0.0942	0.77
+ 50 μM 14	25.0 ± 1.3	0.0988	0.78

Ko143 was used as positive control. Fold change of cytotoxicity was determined by dividing the IC_{50} value of cells treated with mitoxantrone alone by the IC_{50} value of cells treated with mitoxantrone in combination with the respective test compound. Data show mean ± SEM of three independent experiments performed in quadruplicates. **** $p < 0.0001$ compared to doxorubicin alone (One-way ANOVA followed by Dunnett's multiple comparisons test).

2.4 Chapter V

Title: New colchicine-derived triazoles and their influence on cytotoxicity and microtubule morphology

Authors: Persefoni Thomopoulou, **Julia Sachs**, Nicole Teusch, Aruljothi Mariappan, Jay Gopalakrishnan, Hans-Günther Schmalz

Journal: ACS Medicinal Chemistry Letters, 2016 (Impact factor: 3.746)

Reference: Thomopoulou P, Sachs J, Teusch N, Mariappan A, Gopalakrishnan J, Schmalz H-G. New colchicine-derived triazoles and their influence on cytotoxicity and microtubule morphology. ACS Med Chem Lett 2016;7:188–91.

DOI: 10.1021/acsmedchemlett.5b00418

Contribution: cytotoxicity assay, tubulin polymerization assay, data analysis, contribution to manuscript writing

ACS Medicinal Chemistry Letters

Letter

pubs.acs.org/acsmedchemlett

New Colchicine-Derived Triazoles and Their Influence on Cytotoxicity and Microtubule Morphology

Persefoni Thomopoulou,[†] Julia Sachs,[‡] Nicole Teusch,[‡] Aruljothi Mariappan,[§] Jay Gopalakrishnan,[§] and Hans-Günther Schmalz*[,†]

[†]Department of Chemistry, University of Cologne, Greinstr. 4, 50939 Cologne, Germany

[‡]Technische Hochschule Koeln, Kaiser-Wilhelm-Allee, Building E39, 51373 Leverkusen, Germany

[§]Center for Molecular Medicine and Institute of Biochemistry II of the University of Cologne, Robert-Koch-Str. 21, 50931 Cologne, Germany

Supporting Information

ABSTRACT: A series of new colchicinoids with a variable triazole unit at C-7 was synthesized through Cu(I)-catalyzed 1,3-dipolar cycloaddition (*click*-chemistry) of a colchicine-derived azide with various alkynes and the cytotoxicity against THP-1 and Jurkat cancer cell lines was used for structural optimization. Three particularly active compounds ($IC_{50} \leq 5$ nM) were additionally investigated with respect to their efficacy against relevant solid tumor cell lines (HeLa, A549, and SK MES 1). Besides distorting the microtubule morphology by tubulin depolymerization, one compound also exhibited a pronounced centrosome declustering effect in triple negative breast cancer cells (MDA-MB-231) and nonsmall cell lung cancer cells (H1975).

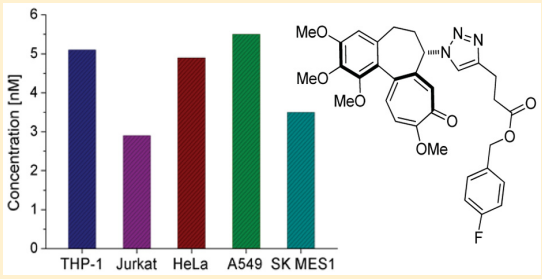

KEYWORDS: *Colchicine, click chemistry, tubulin, antitumoral compounds, resistance*

Microtubules are highly dynamic polymers of α,β-tubulin heterodimers that play a key role in essential cellular processes such as accurate cell division, intracellular transport, and cell motility.[1] Therefore, the tubulin polymerization/depolymerization equilibrium represents an attractive target for the development of anticancer drugs.[2−5] Colchicine (**1**, Figure 1) is a long-known and powerful antimitotic agent extracted from *Colchicum autumnale* and clinically used mainly in the treatment of gout.[6] It acts by destabilizing microtubules via depolymerization leading to cell cycle arrest in the metaphase and, as a consequence, apoptotic cell death. While the use of colchicine (**1**) in cancer chemotherapy is hampered by its toxicity,[7] its remarkable biological activity motivates the search for new analogues with improved pharmacological properties.[8−14]

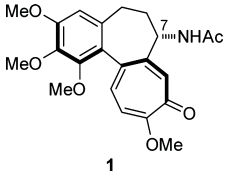

1

Figure 1. Natural product colchicine (**1**).

In this context, we recently developed a "click conjugation" approach allowing a fast and efficient variation of the C7-side chain at the colchicine core (Scheme 1).[15−17] The method is based on the microwave-assisted Cu-catalyzed 1,3-dipolar cycloaddition[18,19] of various alkynes to azide **2**, which is readily prepared from colchicine (**1**) in only four steps. Furthermore, it was shown that some of the resulting triazoles of type **3** exhibit promising levels of activity. We here report the continuation of this study, which has led to the identification of some new and highly active compounds.

Scheme 1. Synthesis of C7-Modified Colchicine Derivatives through Click-Chemistry[a]

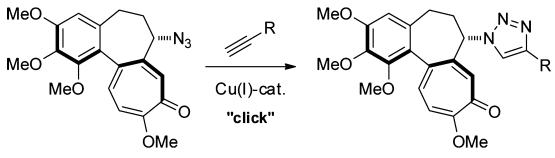

2 **3**

[a]Reagents and conditions: $CuSO_4 \cdot 5H_2O$, (5 mol %), sodium ascorbate (10 mol %), H_2O/*tert*-BuOH (1:1), μW (300 W), 85 °C, 20−45 min. See Chart 1 for structures and isolated yields.

Received: October 28, 2015
Accepted: December 29, 2015
Published: December 29, 2015

DOI: 10.1021/acsmedchemlett.5b00418
ACS Med. Chem. Lett. 2016, 7, 188−191

Following an improved protocol (see Supporting Information) the azide **2** was obtained from *N*-deacetyl-colchicin[15−17,20] through diazo transfer in 86% yield. The triazoles of type **3** were then prepared through "click chemistry" by microwave-induced heating of **2** and a terminal alkyne to 85 °C in the presence of 5 mol % of $CuSO_4 \cdot 5H_2O$ and 10 mol % of sodium ascorbate in a H_2O/*tert*-BuOH (1:1) solvent mixture. As a triazole of type **3** with an amino acid-derived side chain had shown significant activity in our previous study,[15−17] we focused on compounds derived from (*N*-protected) amino acid propargyl esters. The synthesized library of new colchicine conjugates (Chart 1), however, not only comprises compounds

Chart 1. New Colchicine-Derived Triazoles of Type 3 Synthesized According to Scheme 1[a]

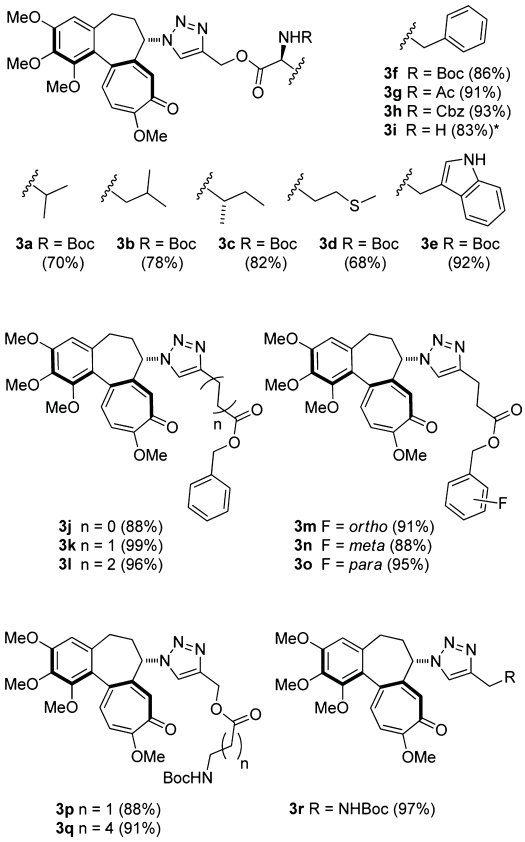

[a]Yields of purified products are given in brackets. *3i was prepared from 3f by treatment with TFA.

derived from amino acids (**3a−3i**) but also compounds with an *O*-benzylated carboxylic acid substituent (**3j−3o**) or a *N*-Boc-protected aminoalkyl side chain (**3p−3r**), respectively.

The cytotoxicity (IC_{50}) of all compounds was determined by means of a bioluminescence cell viability assay[21,22] using THP-1 acute monocytic leukemia cells as well as Jurkat T cell lymphocytes. While all compounds were found to exhibit cytotoxic activity (Table 1), the phenylalanine derivative **3f** and the *β*-alanine ester **3p** stood out in the initial screening by inhibiting cell growth even at low nanomolar concentrations (IC_{50} < 10 nM). Interestingly, these compounds carry a lipophilic moiety (phenyl or *tert*-butyl) in a certain distance to

Table 1. Cytotoxic Activity of Colchicine-Derived Compounds against THP-1 and Jurkat Cells[a]

compd	IC_{50} [nM] THP-1	IC_{50} [nM] Jurkat
1	20.4 ± 2.7	13.5 ± 4.7
2	20.9 ± 0.7	
3a	8.1 ± 1.8	
3b	6.6 ± 5.5	
3c	17.3 ± 6.6	
3d	10.6 ± 9.3	
3e	7.3 ± 2.3	
3f	4.1 ± 1.7	15.3 ± 3.5
3g	25.5 ± 0.9	84.2 ± 5.9
3h	23.3 ± 4.8	21.4 ± 3.8
3i	24.0 ± 6.1	25.1 ± 2.9
3j	139.8 ± 34.6	
3k	31.0 ± 0.8	
3l	35.2 ± 12.8	16.7 ± 7.1
3m	12.7 ± 2.4	9.7 ± 3.1
3n	9.3 ± 0.2	4.9 ± 1.4
3o	5.1 ± 1.1	2.9 ± 1.6
3p	5.7 ± 2.2	5.0 ± 1.5
3q	5.4 ± 0.3	9.4 ± 4.0
3r	23.1 ± 10.1	

[a]Values represent cytotoxic activity (IC_{50}) after 24 h (THP-1) or 48 h (Jurkat) compound incubation. Data shown are mean values ± SD from at least 3 independent experiments with biological replicates ≥3, respectively.

the colchicine core (i.e., the main pharmacophore), as does also the benzylester **3k**. Shortening or lengthening the linking unit to the lipophilic group resulted in a decrease of activity[13] as illustrated by compounds **3i−3l** or **3p−3r** (Table 1). While phenylalanine derivatives **3g−3i** differing from **3f** only in the *N*-protecting group did not exhibit improved activities as compared to **3f**, the introduction of an additional fluorine substituent in the aryl moiety of **3k** led to an increase of the cytotoxic activity (compounds **3m−3o**). These results indicate a favorable hydrophobic interaction between the side chain and a lipophilic pocket of the target protein.

The three most active compounds, that is the phenylalanine derivative **3f**, the 4-fluorobenzyl ester **3o**, and the *β*-alanine ester **3p**, were further evaluated with respect to their cytotoxic activity against solid tumor cell lines, that is HeLa cervix carcinoma cells as well as A549 and chemotherapy resistant SK MES 1 lung cancer cells (Table 2). As a reference, paclitaxel, a marketed chemotherapeutic drug, was used as a strongly mictrotubule-stabilizing compound. Interestingly, compound **3o** proved to exhibit remarkable cytotoxic efficacy by inhibiting

Table 2. Cytotoxicity and Tubulin Polymerization Inhibition Activity of Compounds 3f, 3o, and 3p[a]

compd	IC_{50} [nM] HeLa	IC_{50} [nM] A549	IC_{50} [nM] SK MES1	IC_{50} [μM] tubulin
paclitaxel	18.9 ± 1.7	13.2 ± 3.1	13.5 ± 3.2	
1	21.8 ± 1.1	23.9 ± 4.6	18.6 ± 1.8	6.7 ± 0.05
3f	70.7 ± 3.1	73.7 ± 20.5	39.2 ± 14.2	3.2 ± 0.3
3o	4.9 ± 2.7	5.5 ± 1.7	3.5 ± 0.9	2.1 ± 0.6
3p	20.0 ± 2.2	25.4 ± 4.1	9.6 ± 1.6	2.44 ± 0.4

[a]Cytotoxic activity (IC_{50}) after 48 h (n = 3). Inhibition of tubulin polymerization (n = 2). Data shown are mean values ± SD from n independent experiments.

DOI: 10.1021/acsmedchemlett.5b00418
ACS Med. Chem. Lett. 2016, 7, 188−191

cell growth already at concentrations below 6 nM clearly surpassing paclitaxel and colchicine (**1**). In addition, compounds **3f**, **3o**, and **3p** inhibited tubulin polymerization by 50% at concentrations of 2−3 μM in an *in vitro* assay. This demonstrates the strong cytotoxic activity of these compounds resulting from their microtubule-destabilizing activity, as expected.

In an additional set of experiments we explored the effect of colchicinoids **3f**, **3o**, and **3p** on the microtubule cytoskeleton morphology of MDA-MB-231 breast cancer cells by means of immune fluorescence microscopy. For this purpose, the cells were incubated with **3f**, **3o**, or **3p** at concentrations of 100 nM and microtubules, centrosomes, and DNA were visualized using fluorescence stains (Figure 2). Centrosomes are the major microtubule organizing centers of animal cells.[1,23] While untreated cells (A) showed a typical microtubule network, incubation with 100 nM of paclitaxel as a microtubule-stabilizing agent resulted in the expected segregation of the cells (B). As a second control, colchicine completely collapsed the microtubule network (C). As Figure 2 clearly shows, compounds **3f**, **3o**, and **3p** also suppressed the formation of the microtubule network (at 100 nM); however, short microtubule fragments (tending to localize around the cell nucleus) were still visible (D−F).[13,14]

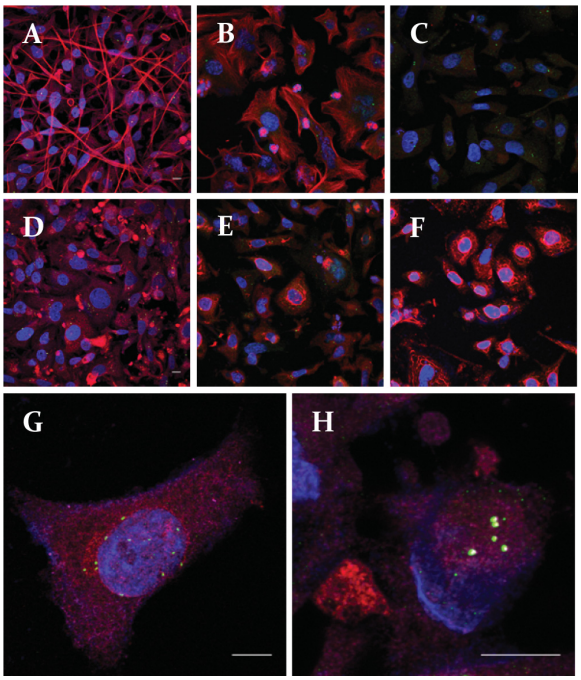

Figure 2. Microtubule morphology of MDA-MB-231 breast cancer cells after 24 h incubation with different compounds: (A) control (untreated cells); (B) paclitaxel (100 nM); (C) **1** (100 nM); (D) **3f** (100 nM); (E) **3o** (100 nM); (F) **3p** (100 nM). Centrosome declustering: (G) **3f** (100 nM) in MDA-MB-231 breast cancer cells; (H) **3f** (500 nM) in H1975 lung cancer cells. Microtubules (red) and centrosomes (green) were stained with antibodies, while DAPI (4,6-diamidino-2-phenylindole) was used to visualize DNA (blue). The white scale bars correspond to a distance of 10 μm.

In contrast to normal cells, which contain a pair of centrosomes, cancer cells exhibit extra number of centrosomes, which contributes to cancer cell invasion.[24,25] The amplified centrosomes in cancer cells are clustered together so that cancer cells are able to avoid multipolar mitosis. Thus, preventing centrosome clustering has been recognized to be an attractive cancer target.[26,27] Interestingly, the phenylalanine derivative **3f** (as the only one of the investigated compounds) was found to exhibit a strong centrosome declustering effect on MDA-MB-231 breast cancer cells (G) and also on H1975 small cell lung cancer cells (H). Notably, H1975 cells have been identified to be a therapy resistant cancer against currently available tyrosine receptor kinase inhibitors.[28]

In conclusion, we have demonstrated that readily available colchicine-derived triazoles of type **3** may exhibit remarkable biological effects in dependence of the side chain structure. Besides pronounced cytotoxic activities the remarkable centrosome-declustering effect exhibited by compound **3f** may justify further investigation. Since tubulin heterodimers are core structural components also of centrosomes,[29] targeting their regulatory mechanisms by small molecules may offer interesting new options for therapeutic intervention in cancer chemotherapy.[30]

■ ASSOCIATED CONTENT

Supporting Information

The Supporting Information is available free of charge on the ACS Publications website at DOI: 10.1021/acsmedchemlett.5b00418.

Experimental procedures, characterization of all compounds, and protocols for biological assays (PDF)

■ AUTHOR INFORMATION

Corresponding Author

*E-mail: schmalz@uni-koeln.de. Tel: +49 (0)221 470 3063. Fax: +49 (0)221 470 3064.

Author Contributions

P.T. performed the synthesis, purification, and characterization of new colchicinoids. J.S. carried out the antiproliferation and tubulin polymerization assays. A.M. performed the immune fluorescence microscopic studies. N.T., J.G., and H.G.S. initiated and supervised the project. The manuscript was written, based on a first draft by P.T., through contributions of all authors. All authors have given approval to the final version of the manuscript.

Funding

This work was supported by the Jürgen Manchot foundation (Ph.D. fellowship to P.T.), the German Science Foundation (Projects SCHM 857/18-1 and GO 2301/2-1), and the German Federal Ministry of Economy and Energy (Ph.D. fellowship to J.S.).

Notes

The authors declare no competing financial interest.

■ REFERENCES

(1) Alberts, B.; Johnson, A.; Lewis, J.; Raff, M.; Roberts, K.; Walter, P. *Mol. Biol. Cell*, 6th ed.; Garland Publishing, 2014.

(2) Dumontet, C.; Jordan, M. A. Microtubule-binding agents: a dynamic field of cancer therapeutics. *Nat. Rev. Drug Discovery* **2010**, *9*, 790−803.

(3) Seligmann, J.; Twelves, C. Tubulin: an example of targeted chemotherapy. *Future Med. Chem.* **2013**, *5*, 339−352.

DOI: 10.1021/acsmedchemlett.5b00418
ACS Med. Chem. Lett. 2016, 7, 188−191

(4) Nepali, K.; Ojha, R.; Sharma, S.; Bedi, P. M. S.; Dhar, K. L. Tubulin Inhibitors: A Patent Survey. *Recent Pat. Anti-Cancer Drug Discovery* **2014**, *9*, 176−220.
(5) Chandrasekaran, G.; Tatrai, P.; Gergely, F. Hitting the brakes: targeting microtubule motors in cancer. *Br. J. Cancer* **2015**, *113*, 693−698.
(6) Richette, P.; Bardin, T. Colchicine for the treatment of gout. *Expert Opin. Pharmacother.* **2010**, *11*, 2933−2938.
(7) Finkelstein, Y.; Aks, S. E.; Hutson, J. R.; Juurlink, D. N.; Nguyen, P.; Dubnov-Raz, G.; Pollak, U.; Koren, G.; Bentur, Y. Colchicine poisoning: the dark side of an ancient drug. *Clin. Toxicol.* **2010**, *48*, 407−414.
(8) Massarotti, A.; Theeramunkong, S.; Mesenzani, O.; Caldarelli, A.; Genazzani, A. A.; Tron, G. C. Identification of Novel Antitubulin Agents by Using a Virtual Screening Approach Based on a 7-Point Pharmacophore Model of the Tubulin Colchi-Site. Tron. *Chem. Biol. Drug Des.* **2011**, *78*, 913−922.
(9) Brossi, A.; Yeh, H. J. C.; Chrzanowska, M.; Wolff, J.; Hamel, E.; Lin, C. M.; Quin, F.; Suffness, M.; Silverton, J. Colchicine and its analogues: Recent findings. *Med. Res. Rev.* **1988**, *8*, 77−94.
(10) Nicolaou, K. C.; Valiulin, R. A.; Pokorski, J. K.; Chang, V.; Chen, J. S. Bio-inspired synthesis and biological evaluation of a colchicine-related compound library. *Bioorg. Med. Chem. Lett.* **2012**, *22*, 3776−3780.
(11) Vilanova, C.; Díaz-Oltra, S.; Murga, J.; Falomir, E.; Carda, M.; Redondo-Horcajo, M.; Díaz, J. F.; Barasoain, I.; Marco, J. A. Design and Synthesis of Pironetin Analogue/Colchicine Hybrids and Study of Their Cytotoxic Activity and Mechanisms of Interaction with Tubulin. *J. Med. Chem.* **2014**, *57*, 10391−10403.
(12) Cosentino, L.; Redondo-Horcajo, M.; Zhao, Y.; Santos, A. R.; Chowdury, K. F.; Vinader, V.; Abdallah, Q. M. A.; Abdel-Rahman, H.; Fournier-Dit-Chabert, J.; Shnyder, S. D.; Loadman, P. M.; Fang, W.-S.; Díaz, J. F.; Barasoain, I.; Burns, P. A.; Pors, K. Synthesis and Biological Evaluation of Colchicine B-Ring Analogues Tethered with Halogenated Benzyl Moieties. *J. Med. Chem.* **2012**, *55*, 11062−11066.
(13) Zefirova, O. N.; Nurieva, E. V.; Shishov, D. V.; Baskin, I. I.; Fuchs, F.; Lemcke, H.; Schröder, F.; Weiss, D. G.; Zefirov, N. S.; Kuznetsov, S. A. Synthesis and SAR requirements of adamantane−colchicine conjugates with both microtubule depolymerizing and tubulin clustering activities. *Bioorg. Med. Chem.* **2011**, *19*, 5529−5538.
(14) Zefirova, O. N.; Lemcke, H.; Lantow, M.; Nurieva, E. V.; Wobith, B.; Onishchenko, G. E.; Hoenen, A.; Griffiths, G.; Zefirov, N. S.; Kuznetsov, S. A. Unusual Tubulin-Clustering Ability of Specifically C7-Modified Colchicine Analogues. *ChemBioChem* **2013**, *14*, 1444−1449.
(15) Nicolaus, N.; Zapke, J.; Riesterer, P.; Neudörfl, J.-M.; Prokop, A.; Oschkinat, H.; Schmalz, H.-G. Azides Derived from Colchicine and their Use in Library Synthesis: a Practical Entry to New Bioactive Derivatives of an Old Natural Drug. *ChemMedChem* **2010**, *5*, 661−665.
(16) Nicolaus, N.; Reball, J.; Sitnikov, N.; Velder, J.; Termath, A.; Fedorov, A. Y.; Schmalz, H.-G. A Convenient Entry to New C-7-Modified Colchicinoids through Azide Alkyne [3 + 2]-Cycloaddition: Application of Ring-Contractive Rearrangements. *Heterocycles* **2011**, *82*, 1585−1600.
(17) Kuznetsova, N. R.; Svirshchevskaya, E. V.; Sitnikov, N. S.; Abodo, L.; Sutorius, H.; Zapke, J.; Velder, J.; Thomopoulou, P.; Oschkinat, H.; Prokop, A.; Schmalz, H.-G.; Fedorov, A. Y.; Vodovozova, E. L. Lipophilic prodrugs of a triazole-containing colchicine analogue in liposomes: Biological effects on human tumor cells. *Russ. J. Bioorg. Chem.* **2013**, *39*, 543−552.
(18) Rostovtsev, V. V.; Green, L. G.; Fokin, V. V.; Sharpless, K. B. A Stepwise Huisgen Cycloaddition Process: Copper(I)-Catalyzed Regioselective "Ligation" of Azides and Terminal Alkynes. *Angew. Chem., Int. Ed.* **2002**, *41*, 2596−2599.
(19) Meldal, M.; Tornøe, C. W. Cu-Catalyzed Azide−Alkyne Cycloaddition. *Chem. Rev.* **2008**, *108*, 2952−3015.
(20) Bagnato, J. D.; Eilers, A. L.; Horton, R. A.; Grissom, C. B. Synthesis and Characterization of a Cobalamin−Colchicine Conjugate as a Novel Tumor-Targeted Cytotoxin. *J. Org. Chem.* **2004**, *69*, 8987−8996.
(21) Kangas, L.; Grönroos, M.; Nieminen, A. L. Bioluminescence of cellular ATP: a new method for evaluating cytotoxic agents in vitro. *Med. Biol.* **1984**, *62*, 338−343.
(22) Crouch, S. P. M.; Kozlowski, R.; Slater, K. J.; Fletcher, J. The use of ATP bioluminescence as a measure of cell proliferation and cytotoxicity. *J. Immunol. Methods* **1993**, *160*, 81−88.
(23) Bornens, M. The Centrosome in Cells and Organisms. *Science* **2012**, *335*, 422−426.
(24) Godinho, S. A.; Picone, R.; Burute, M.; Dagher, R.; Su, Y.; Leung, C. T.; Polyak, K.; Brugge, J. S.; Théry, M.; Pellman, D. Oncogene-like induction of cellular invasion from centrosome amplification. *Nature* **2014**, *510*, 167−171.
(25) Ganem, N. J.; Godinho, S. A.; Pellman, D. A mechanism linking extra centrosomes to chromosomal instability. *Nature* **2009**, *460*, 278−282.
(26) Ogden, A.; Rida, P. C. G.; Aneja, R. Let's huddle to prevent a muddle: centrosome declustering as an attractive anticancer strategy. *Cell Death Differ.* **2012**, *19*, 1255−1267.
(27) Pannu, V.; Rida, P. C. G.; Celik, B.; Turaga, R. C.; Ogden, A.; Cantuaria, G.; Gopalakrishnan, J.; Aneja, R. Centrosome-declustering drugs mediate a two-pronged attack on interphase and mitosis in supercentrosomal cancer cells. *Cell Death Dis.* **2014**, *5*, 1538−1548.
(28) Laurila, N.; Koivunen, J. EGFR inhibitor and chemotherapy combinations for acquired TKI resistance in EGFR-mutant NSCLC models. *Med. Oncol.* **2015**, *32*, 1−7.
(29) Avidor-Reiss, T.; Gopalakrishnan, J. Cell cycle regulation of the centrosome and cilium. *Drug Discovery Today: Dis. Mech.* **2013**, *10*, e119−e124.
(30) Kim, S.-K.; Cho, S.-M.; Kim, H.; Seok, H.; Kim, S.-O.; Kwon, T. K.; Chang, J.-S. The colchicine derivative CT20126 shows a novel microtubule-modulating activity with apoptosis. *Exp. Mol. Med.* **2013**, *45*, e19.

DOI: 10.1021/acsmedchemlett.5b00418
ACS Med. Chem. Lett. 2016, 7, 188−191

Supporting Information

General Information

All moisture sensitive reactions were carried out under argon atmosphere using Schlenk flasks and needle / syringe techniques. Glassware was flame dried under vacuum and flushed with argon once cooled down to room temperature. Syringes and needles were dried in an oven at 80 °C and were flushed with argon directly prior use. *NMR spectra* were recorded on *Bruker* AV 300 instrument. Chemical shifts (δ) are given in ppm relative to the solvent reference as an internal standard ($CDCl_3$, δ (^1H): 7.24 ppm, δ (^{13}C): 77.0 ppm). The assignments are supported by HMBC, HMQC and H,H-COSY spectra. Data are reported as follows: chemical shift (multiplicity (s for singlet, d for doublet, dd for doublet of doublets, t for triplet, q for quartet, quint for quintet, m for multiplet), coupling constant [Hz], integration, assignment). *High resolution mass spectra (HRMS*) were recorded on a *Thermo Fisher* LTQ Orbitrap XL – FTMS Analyzer (HR-ESI-MS). *Fourier transform infrared spectra (FT-IR)* were recorded on *Perkin Elmer* FT-IR Paragon 1000 spectrometer. Absorption bands are given in wave numbers ($\tilde{\nu}$, cm^{-1}). *Melting points* (*Mp*) were measured on *Buchi* B-545 melting point apparatus and are uncorrected. *Optical rotation* $[\alpha]_D$ was measured on *Perkin-Elmer* polarimeter 343 plus at 20 °C and λ = 589 nm (cuvette length: 1.0 dm, volume: 1.0 mL). Concentration is given in g/100 mL. *Microwave* promoted reactions were carried out in a CEM Discover microwave synthesizer in sealed microwave flasks equipped with a stir bar. *Flash chromatography* was performed using *silica gel for chromatography* supplied by *Acros* (0.035-0.070 mm, 60 Å).

Experimental Procedures

Preparation of amino acid-derived alkynes:

To a 0.2 M solution of 1.00 eq. *N*-protected L-amino acid in dry CH_2Cl_2 were added 1.20 eq. of DCC or DIC (as specified below) followed by 1.20 eq. of freshly distilled propargyl alcohol. The reaction mixture was cooled to 0 °C before 0.20 eq. of DMAP were added. After stirring at room temperature for 20 h water was added and the organic phase was washed successively with 1 N aqueous HCl and saturated aqueous NaCl.* The organic layer was dried over $MgSO_4$ and concentrated under reduced pressure. Purification by column chromatography afforded the desired amino acid-derived propargyl esters as colorless oils or white solids.

*In case of DCC the resulting urea formed during the reaction was firstly filtered off bevor extraction was followed as described above.

(*S*)-Prop-2-yn-1-yl 2-((*tert*-butoxycarbonyl)amino)-3-methylbutanoate (SI-1)[1]

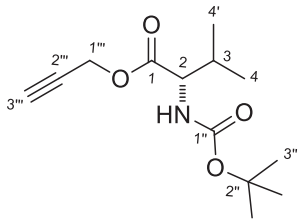

$C_{13}H_{21}NO_4$
255.31 g/mol

^{1}H NMR (300 MHz, $CDCl_3$): δ [ppm] = 0.91 (d, $^3J_{H,H}$ = 6.9 Hz, 3H, H-4), 0.98 (d, $^3J_{H,H}$ = 6.9 Hz, 3H, H-4'), 1.45 (s, 9H, H-3''), 2.09 – 2.27 (m, 1H, H-3), 2.48 (ψ-t, $^4J_{H,H}$ = 2.2 Hz, 1H, H-3'''), 4.27 (dd, $^3J_{H,H}$ = 8.5 Hz, 4.7 Hz, 1H, H-2), 4.68 (dd, $^2J_{H,H}$ = 15.6 Hz, $^4J_{H,H}$ = 2.2 Hz, 1H, H-1'''), 4.80 (dd, $^2J_{H,H}$ = 15.6 Hz, $^4J_{H,H}$ = 2.2 Hz, 1H, H-1'''), 5.00 (d, $^3J_{H,H}$ = 8.5 Hz, 1H, NH). **^{13}C NMR** (75 MHz, $CDCl_3$): δ [ppm] = 17.5 (C-4), 18.9 (C-4'), 28.3 (C-3''), 31.3 (C-3), 52.4 (C-1'''), 58.4 (C-2), 75.2 (C-3'''), 77.2 (C-2'''), 79.7 (C-2''), 155.6 (C-1''), 172.3 (C-1). **HRMS** (ESI): calcd for $[M+Na]^+$ ($C_{13}H_{21}NNaO_4$): 278.13628; found: 278.13638. **FT-IR** (ATR): $\tilde{\nu}$ [cm^{-1}] = 3294 (w), 3282 (w), 2966 (m), 2931 (w), 2874 (w), 1746 (m), 1709 (s), 1501 (m), 1462 (w), 1456 (w), 1390 (m), 1366 (m), 1350 (m), 1307 (m), 1242 (m), 1173 (s), 1154 (s), 1089 (m), 1014 (m), 992 (m), 937 (w), 866 (w), 778 (w). **R_F**: 0.28 (CyHex/EtOAc, 5/1). **Mp.**: 34 °C [Lit.[1]: Oil]. **$[\alpha]_D$** = -9.2 ($CHCl_3$, c = 1.020, 20 °C). **Yield**: 77% (reaction scale: 5.00 mmol; reagent: DCC).

(*S*)-Prop-2-yn-1-yl 2-((*tert*-butoxycarbonyl)amino)-4-methylpentanoate (SI-2)[2]

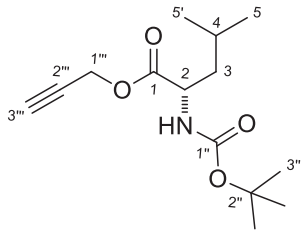

$C_{14}H_{23}NO_4$
269.34 g/mol

^{1}H NMR (300 MHz, $CDCl_3$): δ [ppm] = 0.95 (d, 6H, H-5, H-5'), 1.45 (s, 9H, H-3"), 1.48 – 1.57 (m, 1H, H-4), 1.59 – 1.81 (m, 2H, H-3), 2.48 (ψ-t, $^4J_{H,H}$ = 2.1 Hz, 1H, H-3'"), 4.29 – 4.41 (m, 1H, H-2), 4.68 (dd, $^2J_{H,H}$ = 15.6 Hz, $^4J_{H,H}$ = 2.1 Hz, 1H, H-1'"), 4.78 (dd, $^2J_{H,H}$ = 15.6 Hz, $^4J_{H,H}$ = 2.1 Hz, 1H, H-1'"), 4.87 (d, $^3J_{H,H}$ = 7.9 Hz, 1H, NH). **^{13}C NMR** (75 MHz, $CDCl_3$): δ [ppm] = 21.8 (C-5), 22.8 (C-5'), 24.8 (C-4), 28.3 (C-3"), 41.6 (C-3), 52.0 (C-2), 52.2 (C-1'"), 75.2 (C-3'"), 77.1 (C-2'"), 79.8 (C-2"), 155.4 (C-1"), 172.6 (C-1). **HRMS** (ESI): calcd for $[M+Na]^+$ ($C_{14}H_{23}NNaO_4$): 292.15248; found: 292.15190. **FT-IR** (ATR): $\tilde{\nu}$ [cm^{-1}] = 3362 (w), 2956 (m), 2931 (m), 2869 (m), 2127 (w), 1747 (s), 1700 (s), 1506 (s), 1469 (m), 1452 (m), 1437 (m), 1390 (m), 1365 (s), 1270 (m), 1250 (s), 1155 (s), 1120 (m), 1046 (m), 1021 (s), 991 (m), 953 (m), 937 (m), 870 (w), 850 (w), 779 (m). $\mathbf{R_F}$: 0.31 (CyHex/EtOAc, 5/1). $[\alpha]_D$ = -16.7 ($CHCl_3$, c = 0.890, 20 °C). **Yield**: 50% (reaction scale: 5.00 mmol; reagent: DCC).

(2*S*,3*S*)-Prop-2-yn-1-yl 2-((*tert*-butoxycarbonyl)amino)-3-methylpentanoate (SI-3)[1]

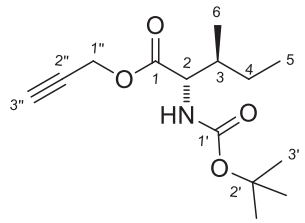

$C_{14}H_{23}NO_4$
269.34 g/mol

^{1}H NMR (300 MHz, $CDCl_3$): δ [ppm] = 0.91 – 0.97 (m, 6H, H-5, H-6), 1.10 – 1.30 (m, 2H, H-4), 1.45 (s, 9H, H-3'), 1.97 – 1.80 (m, 1H, H-3), 2.48 (ψ-t, $^4J_{H,H}$ = 2.2 Hz, 1H, H-3"), 4.25 – 4.36 (m, 1H, H-2), 4.67 (dd, $^2J_{H,H}$ = 15.6 Hz, $^4J_{H,H}$ = 2.2 Hz, 1H, H-1"), 4.79 (dd, $^2J_{H,H}$ = 15.6 Hz, $^4J_{H,H}$ = 2.2 Hz, 1H, H-1"), 5.02 (d, $^3J_{H,H}$ = 8.4 Hz, 1H, NH). **^{13}C NMR** (75 MHz, $CDCl_3$): δ [ppm] = 11.6 (C-5), 15.5 (C-6), 24.9 (C-4), 28.3 (C-3'), 38.1 (C-3), 52.3 (C-1"), 57.8 (C-2), 75.8 (C-3"), 77.3 (C-2"), 79.5 (C-2'), 155.3 (C-1'), 171.8 (C-1). **HRMS** (ESI): calcd for $[M+Na]^+$ ($C_{14}H_{23}NNaO_4$): 292.15193; found: 292.15191. **FT-IR** (ATR): $\tilde{\nu}$ [cm^{-1}] = 3379 (w), 3291 (w), 2966 (m), 2932 (m), 2876 (w), 1745 (m), 1709 (s), 1500 (m), 1455 (m), 1365 (m), 1337 (m), 1293 (m), 1247 (m), 1154 (s), 1084 (m), 1044 (m), 1018 (m), 993 (m), 937 (w), 860 (w), 778 (w). $\mathbf{R_F}$: 0.33 (CyHex/EtOAc, 5/1). $[\alpha]_D$ = +1.7 ($CHCl_3$, c = 0.650, 20 °C). **Yield**: 77% (reaction scale: 5.00 mmol; reagent: DCC).

(*S*)-Prop-2-yn-1-yl 2-((*tert*-butoxycarbonyl)amino)-4-(methylthio)butanoate (SI-4)[1]

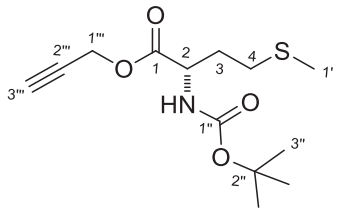

$C_{13}H_{21}NO_4S$
287.38 g/mol

^{1}H NMR (300 MHz, $CDCl_3$): δ [ppm] = 1.45 (s, 9H, H-3''), 1.90 – 2.20 (m, 1H, H-3), 2.11 (s, 3H, H-1'), 2.13 – 2.23 (m, 1H, H-3), 2.51 – 2.59 (m, 3H, H-3''', H-4), 4.37 – 4.50 (m, 1H, H-2), 4.70 (dd, $^2J_{H,H}$ = 15.6 Hz, $^4J_{H,H}$ = 2.4 Hz, 1H, H-1'''), 4.80 (dd, $^2J_{H,H}$ = 15.6 Hz, $^4J_{H,H}$ = 2.4 Hz, 1H, H-1'''), 5.24 (d, $^3J_{H,H}$ = 7.5 Hz, 1H, NH). **^{13}C NMR** (75 MHz, $CDCl_3$): δ [ppm] = 15.3 (C-1'), 28.2 (C-3''), 29.7 (C-4), 31.7 (C-3), 52.5 (C-2), 52.6 (C-1'''), 75.4 (C-3'''), 76.9 (C-2'''), 79.9 (C-2''), 155.2 (C-1''), 171.5 (C-1). **HRMS** (ESI): calcd for $[M+Na]^+$ ($C_{13}H_{21}NNaO_4S$): 310.10835; found: 310.10854. **FT-IR** (ATR): $\tilde{\nu}$ [cm^{-1}] = 3351 (w), 3290 (w), 2974 (w), 2917 (w), 1747 (m), 1706 (s), 1506 (m), 1436 (m), 1390 (m), 1506 (m), 1345 (m), 1249 (m), 1159 (s), 1049 (m), 1023 (m), 991 (m), 956 (w), 861 (w), 780 (w). **R_F**: 0.19 (CyHex/EtOAc, 5/1). **$[\alpha]_D$** = +7.3 ($CHCl_3$, c = 1.030, 20 °C). **Yield**: 82% (reaction scale: 5.00 mmol; reagent: DCC).

(*S*)-Prop-2-yn-1-yl 2-((*tert*-butoxycarbonyl)amino)-3-(1*H*-indol-3-yl)propanoate (SI-5)

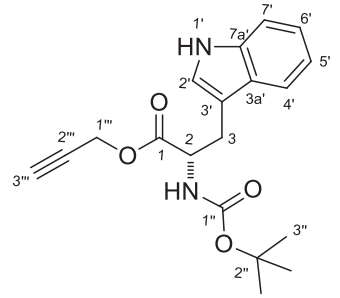

$C_{19}H_{22}N_2O_4$
342.39 g/mol

^{1}H NMR (300 MHz, $CDCl_3$): δ [ppm] = 1.42 (s, 9H, H-3''), 2.49 (ψ-t, $^4J_{H,H}$ = 2.3 Hz, 1H, H-3'''), 3.28 – 3.36 (m, 2H, H-3), 4.48 – 4.83 (m, 3H, H-2, H-1'''), 5.05 (d, $^3J_{H,H}$ = 6.8 Hz, 1H, NH), 7.01 (s, 1H, H-2'), 7.05 – 7.23 (m, 2H, H-5', H-6'), 7.33 (d, $^3J_{H,H}$ = 7.8 Hz, 1H, H-4'), 7.57 (d, $^3J_{H,H}$ = 7.5 Hz, 1H, H-7'), 8.32 (s, 1H, H-1'). **^{13}C NMR** (75 MHz, $CDCl_3$): δ [ppm] = 27.7 (C-3), 28.3 (C-3''), 52.3 (C-1'''), 54.2 (C-2), 75.4 (C-3'''), 77.1 (C-2'''), 79.9 (C-2''), 109.7 (C-3'), 111.2 (C-4'), 118.6 (C-7'), 119.6 (C-6'), 122.1 (C-5'), 123.0 (C-2'), 127.6 (C-3a'), 136.1 (C-7a'), 155.2 (C-1''), 171.5 (C-1). **HRMS** (ESI): calcd for $[M+Na]^+$ ($C_{19}H_{22}N_2NaO_4$): 365.14773; found: 365.1470. **FT-IR** (ATR): $\tilde{\nu}$ [cm^{-1}] = 3403 (w), 3295 (w), 2974 (w), 2929 (w), 2857 (w), 2127 (w), 1745 (m), 1696 (s), 1503 (m), 1456 (m), 1434 (w), 1391 (m),

1365 (m), 1273 (m), 1247 (s), 1161 (s), 1096 (w), 1059 (w), 1022 (w), 1008 (w), 991 (w), 856 (w), 778 (w), 742 (m). **R_F**: 0.08 (CyHex/EtOAc, 5/1). **Mp.**: 96 °C. **$[\alpha]_D$** = +4.9 ($CHCl_3$, c = 0.980, 20 °C). **Yield**: 62% (reaction scale: 5.00 mmol; reagent: DCC; comment: THF was used instead of CH_2Cl_2 as a solvent).

(*S*)-Prop-2-yn-1-yl 2-((*tert*-butoxycarbonyl)amino)-3-phenylpropanoate (SI-6)[2]

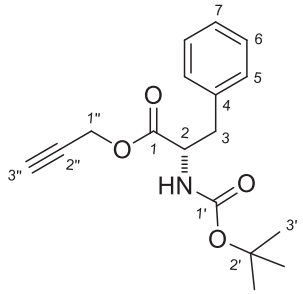

$C_{17}H_{21}NO_4$
303.35 g/mol

^{1}H NMR (300 MHz, $CDCl_3$): δ [ppm] = 1.41 (s, 9H, H-3'), 2.51 (ψ-t, $^4J_{H,H}$ = 2.1 Hz, 1H, H-3''), 3.24 – 2.98 (m, 2H, H-3), 4.57 – 4.72 (m, 2H, H-2, H-1''), 4.77 (dd, $^2J_{H,H}$ = 15.7 Hz, $^4J_{H,H}$ = 2.1 Hz, 1H, H-1''), 4.96 (d, $^3J_{H,H}$ = 7.8 Hz, 1H, NH), 7.13 – 7.19 (m, 2H, H-5), 7.25 – 7.34 (m, 3H, H-6, H-7). **^{13}C NMR** (75 MHz, $CDCl_3$): δ [ppm] = 28.2 (C-3'), 38.0 (C-3), 52.6 (C-1''), 54.3 (C-2), 75.4 (C-3'', C-2''), 80.0 (C-2'), 127.1 (C-7), 128.5 (C-6), 129.3 (C-5), 135.6 (C-4), 155.0 (C-1'), 171.1 (C-1). **HRMS** (ESI): calcd for $[M+Na]^+$ ($C_{17}H_{21}NNaO_4$): 326.13683; found: 326.13650. **FT-IR** (ATR): $\tilde{\nu}$ [cm^{-1}] = 3289 (w), 3280 (w), 2975 (w), 2931 (w), 1748 (s), 1711 (s), 1496 (s), 1454 (m), 1391 (m), 1366 (s), 1346 (m), 1249 (m), 1162 (s), 1079 (w), 1052 (m), 1022 (m), 995 (m), 950 (w), 857 (w), 778 (w), 747 (m). **R_F**: 0.32 (CyHex/EtOAc, 6/1). **$[\alpha]_D$** = +13.9 ($CHCl_3$, c = 0.890, 20 °C). **Yield**: 46% (reaction scale: 5.00 mmol; reagent: DCC).

(*S*)-Prop-2-yn-1-yl 2-acetamido-3-phenylpropanoate (SI-7)

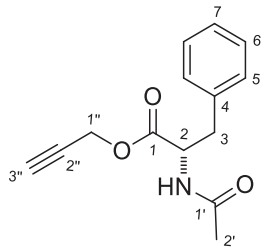

$C_{14}H_{15}NO_3$
245.28 g/mol

^{1}H NMR (300 MHz, $CDCl_3$): δ [ppm] = 1.97 (s, 3H, H-2'), 2.53 (ψ-t, $^4J_{H,H}$ = 2.4 Hz, 1H, H-3''), 3.06 – 3.23 (m, 2H, H-3), 4.68 (dd, $^2J_{H,H}$ = 15.5 Hz, $^4J_{H,H}$ = 2.4 Hz, 1H, H-1''), 4.77 (dd, $^2J_{H,H}$ = 15.5 Hz, $^4J_{H,H}$ = 2.4 Hz, 1H, H-1''), 4.87 – 5.00 (m, 1H, H-2), 5.98 (d, $^3J_{H,H}$ = 7.0 Hz, 1H, NH), 7.09 – 7.18 (m, 2H, H-5), 7.22 – 7.32 (m, 3H, H-6, H-7). **^{13}C NMR** (75 MHz, $CDCl_3$): δ [ppm] = 23.0 (C-2'), 37.6 (C-3), 52.7 (C-1''), 52.9 (C-2), 75.5 (C-3''), 75.6 (C-2''), 127.2 (C-7), 128.5 (C-6), 129.3 (C-5), 135.5 (C-4), 169.6 (C-1'), 170.9 (C-1). **HRMS** (ESI): calcd for $[M+Na]^+$ ($C_{14}H_{15}NNaO_3$): 268.09441; found: 268.09464. **FT-IR** (ATR): $\tilde{\nu}$ [cm^{-1}] = 3283 (m), 3062 (w), 3027 (w), 2942 (w), 2125 (w), 1745 (s), 1654 (s), 1538 (m), 1496 (m), 1453 (m), 1437 (m), 1373 (m), 1345 (m), 1272 (m), 1206 (m), 1174 (s), 1127 (m), 1080 (w), 1028 (w), 989 (w), 937 (w), 744 (m). **R_F**: 0.31 (CyHex/EtOAc, 4/5). **Mp.**: 68-69 °C. **[α]$_D$** = +5.6 ($CHCl_3$, c = 0.855, 20 °C). **Yield**: 88% (reaction scale: 0.20 mmol; reagent: DIC).

(*S*)-Prop-2-yn-1-yl 2-(((benzyloxy)carbonyl)amino)-3-phenylpropanoate (SI-8)[2]

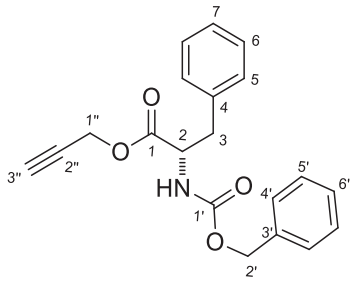

$C_{20}H_{19}NO_4$
337.37 g/mol

^{1}H NMR (300 MHz, $CDCl_3$): δ [ppm] = 2.51 (s, 1H, H-3''), 3.06 – 3.21 (m, 2H, H-3), 4.64 – 4.78 (m, 3H, H-2, H-1''), 5.09 (s, 2H, H-2'), 5.20 (d, $^3J_{H,H}$ = 7.9 Hz, 1H, NH), 7.09 – 7.15 (m, 2H, H-5), 7.22 – 7.39 (m, 8H, H-6, H-7, H-4', H-5', H-6'). **^{13}C NMR** (75 MHz, $CDCl_3$): δ [ppm] = 37.9 (C-3), 52.7 (C-1''), 54.6 (C-2), 67.0 (C-2'), 75.5 (C-3''), 75.6 (C-2''), 127.2 (C-7), 128.1 (C-6), 128.2 (C-6'), 128.5 (C-5'), 128.6 (C-4'), 129.3 (C-5), 135.3 (C-4), 136.1 (C-3'), 155.6 (C-1'), 170.7 (C-1). **HRMS** (ESI): calcd for $[M+Na]^+$ ($C_{20}H_{19}NNaO_4$): 360.12063; found: 360.12046. **FT-IR** (ATR): $\tilde{\nu}$ [cm^{-1}] = 3289 (w), 3062 (w), 3029 (w), 2948 (w), 2127 (w), 1745 (s), 1710 (s), 1505 (m), 1496 (m), 1453 (m), 1383 (w), 1341 (m), 1252 (m), 1204 (w), 1173 (s), 1079 (m), 1051 (s), 1026 (s), 993 (m), 907 (m), 729 (s). **R_F**: 0.14 (CyHex/EtOAc, 5/1). **Mp.**: 63-64 °C [Lit.[2]: 64-66 °C]. **[α]$_D$** = +17.3 ($CHCl_3$, c = 0.930, 20 °C). **Yield**: 78% (reaction scale: 0.20 mmol; reagent: DIC).

Preparation of *N*-Boc protected aminoalkanoic acid-derived alkynes:

The propargyl esters of *N*-Boc protected aminoalkanoic acids were prepared as described for the synthesis of the amino acid-derived propargyl esters (see page 3). The resulting products were isolated as colorless oils after purification by column chromatography.

Prop-2-yn-1-yl 3-((*tert*-Butoxycarbonyl)amino)propanoate (SI-9)[1]

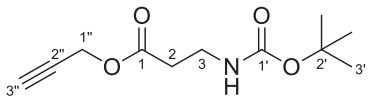

$C_{11}H_{17}NO_4$
227.26 g/mol

^{1}H NMR (300 MHz, $CDCl_3$): δ [ppm] = 1.41 (s, 9H, H-3'), 2.50 (ψ-t, $^4J_{H,H}$ = 2.4 Hz, 1H, H-3''), 2.57 (t, $^3J_{H,H}$ = 6.1 Hz, 2H, H-2), 3.33 – 3.44 (m, 2H, H-3), 4.68 (d, $^4J_{H,H}$ = 2.4 Hz, 2H, H-1''), 5.10 (s, 1H, NH). **^{13}C NMR** (75 MHz, $CDCl_3$): δ [ppm] = 28.2 (C-3'), 34.3 (C-2), 35.9 (C-3), 51.9 (C-1''), 75.0 (C-2''), 77.3 (C-3''), 79.3 (C-2'), 155.6 (C-1'), 171.5 (C-1). **HRMS** (ESI): calcd for $[M+Na]^+$ ($C_{11}H_{17}NNaO_4$): 250.10498; found.: 250.10510. **FT-IR** (ATR): $\tilde{\nu}$ [cm^{-1}] = 3379 (w), 3295 (w), 2975 (w), 2933 (w), 1736 (m), 1702 (s), 1679 (s), 1692 (s), 1513 (m), 1503 (s), 1453 (w), 1391 (m), 1365 (m), 1270 (m), 1264 (s), 1157 (vs), 1065 (m), 1027 (m), 984 (m), 966 (m), 857 (w), 781 (w), 727 (w). **R_F**: 0.35 (CyHex/EtOAc, 5/1). **Yield**: 89% (reaction scale: 0.50 mmol; reagent: DIC).

Prop-2-yn-1-yl 6-((*tert*-butoxycarbonyl)amino)hexanoate (SI-10)

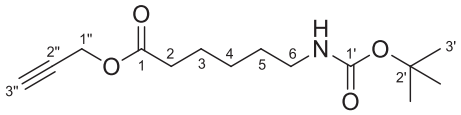

$C_{14}H_{23}NO_4$
269.34 g/mol

^{1}H NMR (300 MHz, $CDCl_3$): δ [ppm] = 1.23 – 1.40 (m, 2H, H-4), 1.44 (s, 9H, H-3'), 1.47 – 1.56 (m, 2H, H-5), 1.66 (quint, $^3J_{H,H}$ = 7.5 Hz, 2H, H-3), 2.36 (t, $^3J_{H,H}$ = 7.5 Hz, 2H, H-2), 2.51 (ψ-t, $^4J_{H,H}$ = 2.4 Hz, 1H, H-3''), 3.06 – 3.19 (m, 2H, H-6), 4.67 (d, $^4J_{H,H}$ = 2.4 Hz, 2H, H-1''), 4.70 (s, 1H, NH). **^{13}C NMR** (75 MHz, $CDCl_3$): δ [ppm] = 24.3 (C-3), 25.0 (C-4), 28.3 (C-3'), 29.6 (C-5), 33.6 (C-2), 40.2 (C-6), 51.6 (C-1''), 74.7 (C-2''), 77.6 (C-3''), 78.8 (C-2'), 155.8 (C-1'), 171.5 (C-1). **HRMS** (ESI): calcd for $[M+Na]^+$ ($C_{14}H_{23}NNaO_4$): 292.15193; found: 292.15186. **FT-IR** (ATR): $\tilde{\nu}$ [cm^{-1}] = 3369 (w), 3290 (w), 2972 (w), 2933 (w), 2858 (w), 1735 (m), 1708 (s), 1693 (s), 1681 (s), 1518 (m), 1503 (m), 1451 (w), 1389 (w), 1365 (m), 1268 (m), 1264 (s), 1156 (vs), 1100 (w), 999 (w), 934 (w), 863 (w), 779 (w). **R_F**: 0.31 (CyHex/EtOAc, 5/1). **Yield**: 91% (reaction scale: 0.50 mmol; reagent: DIC).

Preparation of 4-pentynoic acid fluorobenzyl esters:

20.0 mg (0.20 mmol, 1.00 eq.) of 4-pentynoic acid and 42.0 mg (0.30 mmol, 1.50 eq.) of K_2CO_3 were dissolved in 0.20 mL dry DMF. Then, 30.0 µL (45.0 mg, 0.24 mmol, 1.20 eq.) of *ortho*-, *meta*- or *para*-substituted fluorobenzyl bromide was added dropwise and the reaction mixture was allowed to stir at room temperature for 20 h. Water was added followed by the extraction of the aqueous phase with MTBE (4x). The combined organic layers were dried over $MgSO_4$, filtered

and concentrated under reduced pressure. Purification by column chromatography afforded the desired products as colorless oils in 88-94% yield as specified below.

2-Fluorobenzyl pent-4-ynoate (SI-11)

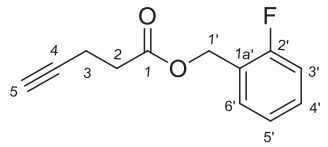

$C_{12}H_{11}FO_2$
206.22 g/mol

^{1}H NMR (300 MHz, $CDCl_3$): δ [ppm] = 1.97 (t, $^4J_{H,H}$ = 2.5 Hz, 1H, H-5), 2.47 – 2.57 (m, 2H, H-3), 2.58 – 2.65 (m, 2H, H-2), 5.22 (s, 2H, H-1'), 7.02 – 7.11 (m, 1H, H-3'), 7.11 – 7.18 (m, 1H, H-5'), 7.28 – 7.35 (m, 1H, H-4'), 7.35 – 7.43 (m, 1H, H-6'). **^{13}C NMR** (75 MHz, $CDCl_3$): δ [ppm] = 14.3 (C-3), 33.3 (C-2), 60.4 (C-1'), 69.1 (C-4), 82.3 (C-5), 115.5 (d, $^2J_{C,F}$ = 21.1 Hz, C-3'), 122.9 (d, $^2J_{C,F}$ = 14.6 Hz, C-1a'), 124.1 (d, $^4J_{C,F}$ = 2.6 Hz, C-5'), 130.3 (d, $^3J_{C,F}$ = 8.1 Hz, C-4'), 130.6 (d, $^3J_{C,F}$ = 2.8 Hz, C-6'), 161.0 (d, $^1J_{C,F}$ = 248.6 Hz, C-2'), 171.4 (C-1). **HRMS** (ESI): calcd for $[M+Na]^+$ ($C_{12}H_{11}FNaO_2$): 229.06353; found: 229.06357. **FT-IR** (ATR): $\tilde{\nu}$ [cm^{-1}] = 3295 (w), 2966 (w), 1737 (s), 1619 (w), 1587 (w), 1493 (m), 1455 (m), 1418 (w), 1385 (w), 1353 (w), 1284 (m), 1232 (m), 1186 (m), 1159 (s), 1110 (w), 1031 (w), 990 (w), 966 (w), 940 (w), 840 (w), 757 (s), 645 (m). **R_F**: 0.31 (CyHex/EtOAc, 5/1). **Yield**: 93%.

3-Fluorobenzyl pent-4-ynoate (SI-12)

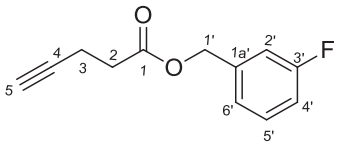

$C_{12}H_{11}FO_2$
206.22 g/mol

^{1}H NMR (300 MHz, $CDCl_3$): δ [ppm] = 1.97 (t, $^4J_{H,H}$ = 2.5 Hz, 1H, H-5), 2.48 – 2.57 (m, 2H, H-3), 2.57 – 2.66 (m, 2H, H-2), 5.13 (s, 2H, H-1'), 6.95 – 7.15 (m, 3H, H-2', H-4', H-6'), 7.27 – 7.37 (m, 1H, H-5'). **^{13}C NMR** (75 MHz, $CDCl_3$): δ [ppm] = 14.3 (C-3), 33.3 (C-2), 65.6 (C-1'), 69.2 (C-4), 82.3 (C-5), 114.9 (d, $^2J_{C,F}$ = 18.0 Hz, C-2'), 115.2 (d, $^2J_{C,F}$ = 18.0 Hz, C-4'), 123.5 (d, $^4J_{C,F}$ = 2.2 Hz, C-6'), 130.1 (d, $^3J_{C,F}$ = 8.3 Hz, C-5'), 138.2 (d, $^3J_{C,F}$ = 7.8 Hz, C-1a'), 162.9 (d, $^1J_{C,F}$ = 246.3 Hz, C-3'), 171.4 (C-1). **HRMS** (ESI): calcd for $[M+Na]^+$ ($C_{12}H_{11}FNaO_2$): 229.06353; found: 229.06378. **FT-IR** (ATR): $\tilde{\nu}$ [cm^{-1}] = 3291 (w), 2956 (w), 1736 (s), 1618 (w), 1591 (m), 1487 (m), 1452 (m), 1382 (m), 1352 (m), 1254 (s), 1203 (m), 1154 (s), 1013 (w), 973 (w), 920 (m), 867 (m), 783 (s), 748 (m), 682 (s), 640 (s). **R_F**: 0.35 (CyHex/EtOAc, 5/1). **Yield**: 88%.

4-Fluorobenzyl pent-4-ynoate (SI-13)

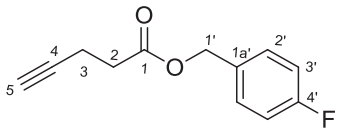

$C_{12}H_{11}FO_2$
206.22 g/mol

^{1}H NMR (300 MHz, $CDCl_3$): δ [ppm] = 1.97 (t, $^4J_{H,H}$ = 2.4 Hz, 1H, H-5), 2.47 – 2.56 (m, 2H, H-3), 2.56 – 2.64 (m, 2H, H-2), 5.11 (s, 2H, H-1'), 7.01 – 7.09 (m, 2H, H-3'), 7.30 – 7.38 (m, 2H, H-2'). **^{13}C NMR** (75 MHz, $CDCl_3$): δ [ppm] = 14.3 (C-3), 33.3 (C-2), 65.8 (C-1'), 69.1 (C-4), 82.3 (C-5), 115.5 (d, $^2J_{C,F}$ = 21.5 Hz, C-3'), 130.3 (d, $^3J_{C,F}$ = 8.3 Hz, C-2'), 131.6 (d, $^4J_{C,F}$ = 2.5 Hz, C-1a'), 161.3 (d, $^1J_{C,F}$ = 247.1 Hz, C-4'), 171.5 (C-1). **HRMS** (ESI): calcd for $[M+Na]^+$ ($C_{12}H_{11}FNaO_2$): 229.06353; found: 229.06376. **FT-IR** (ATR): $\tilde{\nu}$ [cm^{-1}] = 3296 (w), 2930 (w), 1731 (s), 1605 (w), 1510 (s), 1420 (w), 1382 (w), 1352 (w), 1281 (w), 1222 (s), 1166 (s), 1153 (s), 1098 (w), 1014 (w), 966 (w), 850 (w), 824 (m), 765 (w), 624 (m). **R_F**: 0.37 (CyHex/EtOAc, 5/1). **Yield**: 94%.

Preparation of alkynoic acid benzyl esters:

Note: The known benzyl esters of propynoic acid, 4-pentynoic acid and 6-heptynoic acid were prepared as described above for the fluorobenzyl esters using benzyl bromide (1.20 eq.) instead of fluorobenzyl bromide.

Improved protocol for the synthesis of the colchicine-derived azide 2:

I. Preparation of triflyl azide:

To a solution of 1.02 g (15.69 mmol, 8.00 eq.) of NaN_3 in 8.45 mL of water were added 3.60 mL of toluene. The resulting suspension was cooled to 0 °C before 1.90 mL (3.19 g, 11.30 mmol, 5.77 eq.) of Tf_2O were added dropwise. The reaction mixture was stirred at 0 °C for 2 h followed by the addition of saturated aqueous $NaHCO_3$ until the gas evolution had ceased. The phases were separated and the aqueous phase extracted with 3.50 mL of toluene (2x). The combined organic layers (containing triflyl azide) were used directly in the next step.

II. Diazo transfer:

A solution of 700 mg (1.96 mmol, 1.00 eq.) of *N*-deacetylcolchicine in 5.25 mL of H_2O was diluted with 5.25 mL of methanol before 691 mg (8.23 mmol, 4.20 eq.) of $NaHCO_3$ and 25.0 mg (0.10 mmol, 5.00 mol%) $CuSO_4 \cdot 5H_2O$ were added. Then, the solution of triflyl azide (prepared as described above) was added dropwise. The reaction mixture was diluted with additional 15.0 mL of methanol and stirred at room temperature for 24 h before the organic solvent was removed under reduced pressure. The remaining residue was poured into 20.0 mL of water and

extracted with EtOAc (4x). The combined organic layers were washed with brine, dried over $MgSO_4$ and concentrated. Purification of the crude product by column chromatography (CyHex/EtOAc, 1/10) yielded 650 mg (1.69 mmol, 86%) of the desired azide **2** as a yellow solid.

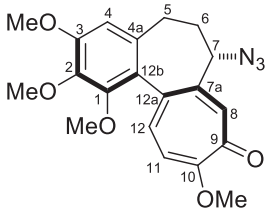

$C_{20}H_{21}N_3O_5$
383.40 g/mol

^{1}H NMR (300 MHz, $CDCl_3$): δ [ppm] = 1.82 – 1.95 (m, 1H, H-6), 2.30 – 2.51 (m, 2H, H-6, H-5), 2.51 – 2.61 (m, 1H, H-5), 3.69 (s, 3H, OMe), 3.92 (s, 6H, 2xOMe), 4.01 (s, 3H, OMe), 4.30 (dd, $^3J_{H,H}$ = 11.1 Hz, 5.6 Hz, 1H, H-7), 6.56 (s, 1H, H-4), 6.87 (d, $^3J_{H,H}$ = 10.7 Hz, 1H, H-11), 7.23 (d, $^3J_{H,H}$ = 10.7 Hz, 1H, H-12), 7.67 (s, 1H, H-8). **^{13}C NMR** (75 MHz, $CDCl_3$): δ [ppm] = 29.7 (C-5), 36.8 (C-6), 56.0 (OMe), 56.6 (OMe), 61.1 (2xOMe), 62.9 (C-7), 107.1 (C-4), 111.7 (C-11), 124.8 (C-12b), 132.6 (C-8), 134.0 (C-4a), 134.9 (C-12a), 135.0 (C-12), 141.3 (C-3), 147.3 (C-7a), 150.7 (C-1), 153.6 (C-2), 164.0 (C-10), 179.3 (C-9). **HRMS** (ESI): calcd for $[M+Na]^+$ ($C_{20}H_{21}N_3NaO_5$): 406.13730; found: 406.13700. **FT-IR** (ATR): $\tilde{\nu}$ [cm^{-1}] = 2930 (br, w), 2832 (w), 2102 (s), 1707 (w), 1612 (m), 1568 (vs), 1484 (m), 1452 (m), 1395 (m), 1344 (m), 1316 (m), 1247 (s), 1174 (m), 1136 (s), 1087 (s), 1065 (m), 1021 (m), 1000 (m), 983 (m), 919 (m), 844 (m), 609 (w). **R_F**: 0.16 (CyHex/EtOAc, 1/10). **Mp.**: 155 °C [Lit.[3]: 159 °C]. **[α]$_D$** = -244.6 ($CHCl_3$, c = 0.605, 20 °C).

General Procedure for the Cu(I)-catalyzed 1,3-dipolar cycloaddition (click-conjugation):

In a microwave vial 50.0 mg (0.13 mmol, 1.00 eq.) of azide **2** were dissolved in 0.25 mL of *t*-BuOH. To this solution were subsequently added 0.25 mL of water and 0.14 mmol (1.10 eq.) of the respective alkyne. Then, 1.6 mg (6.50 µmol, 5.00 mol%) of $CuSO_4 \cdot 5\ H_2O$ (dissolved in 20 µL of water) and 2.6 mg (13.0 µmol, 10.0 mol%) of sodium ascorbate were added. The microwave vial was sealed, placed into a microwave reactor and heated to 85°C for 20-45 min (300 W). After cooling the reaction vessel to room temperature the reaction mixture was poured into water followed by extraction with EtOAc (4x). The combined organic layers were washed with brine, dried over $MgSO_4$ and concentrated under reduced pressure. Purification by column chromatography afforded the desired triazoles in 68-99% yield as specified below.

Compound 3a:

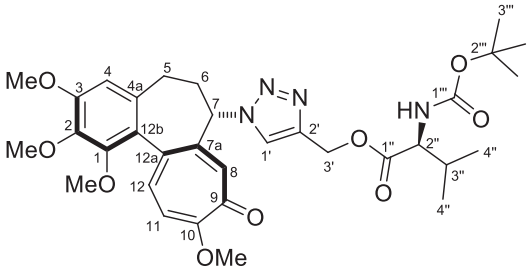

$C_{33}H_{42}N_4O_9$
638.71 g/mol

^{1}H NMR (300 MHz, $CDCl_3$): δ [ppm] = 0.82 (d, $^3J_{H,H}$ = 6.9 Hz, 3H, H-4''), 0.91 (d, $^3J_{H,H}$ = 6.8 Hz, 3H, H-4''), 1.41 (s, 9H, H-3'''), 2.08 – 2.19 (m, 1H, H-3''), 2.49 – 2.69 (m, 2H, H-5, H-6), 2.70 – 2.88 (m, 2H, H-5, H-6), 3.77 (s, 3H, OMe), 3.92 (s, 3H, OMe), 3.94 (s, 3H, OMe), 3.98 (s, 3H, OMe), 4.17 – 4.25 (m, 1H, H-2''), 4.99 (d, $^3J_{H,H}$ = 8.6 Hz, 1H, NH), 5.31 (s, 2H, H-3'), 5.39 (dd, $^3J_{H,H}$ = 11.7 Hz, 4.5 Hz, 1H, H-7), 6.46 (s, 1H, H-8), 6.60 (s, 1H, H-4), 6.81 (d, $^3J_{H,H}$ = 10.7 Hz, 1H, H-11), 7.29 (d, $^3J_{H,H}$ = 10.7 Hz, 1H, H-12), 7.68 (s, 1H, H-1'). **^{13}C NMR** (75 MHz, $CDCl_3$): δ [ppm] = 17.4 (C-4''), 18.9 (C-4''), 28.6 (C-3'''), 29.6 (C-5), 31.0 (C-3''), 35.3 (C-6), 56.1 (OMe), 56.4 (OMe), 58.1 (C-3'), 59.5 (C-2''), 61.2 (OMe), 61.3 (OMe), 62.7 (C-7), 79.7 (C-2'''), 107.4 (C-4), 111.7 (C-11), 124.4 (C-1'), 124.8 (C-12b), 131.7 (C-8), 133.5 (C-4a), 134.3 (C-12a), 135.4 (C-12), 141.6 (C-3), 142.8 (C-2'), 147.4 (C-7a), 151.0 (C-1), 153.9 (C-2), 155.6 (C-1'''), 164.3 (C-10), 172.3 (C-1''), 178.7 (C-9). **HRMS** (ESI): calcd for $[M+Na]^+$ ($C_{33}H_{42}N_4NaO_9$): 661.28440; found: 661.28439. **FT-IR** (ATR): $\tilde{\nu}$ [cm^{-1}] = 3351 (br, w), 2966 (m), 2933 (m), 1736 (m), 1707 (s), 1617 (m), 1586 (s), 1570 (s), 1487 (s), 1461 (m), 1397 (m), 1349 (m), 1320 (m), 1252 (s), 1176 (s), 1153 (s), 1094 (s), 1018 (m), 1001 (m), 983 (w), 922 (w), 843 (w), 751 (s), 666 (w). **R_F**: 0.19 (CyHex/EtOAc/EtOH, 4/1/1). **Mp.**: 105 °C. **Yield**: 70% (reaction time: 35 min).

Compound 3b:

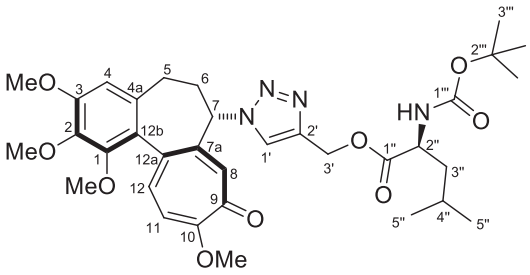

$C_{34}H_{44}N_4O_9$
652.73 g/mol

^{1}H NMR (300 MHz, $CDCl_3$): δ [ppm] = 0.90 (d, $^3J_{H,H}$ = 2.7 Hz, 3H, H-5''), 0.92 (d, $^3J_{H,H}$ = 2.7 Hz, 3H, H-5''), 1.40 (s, 9H, H-3'''), 1.45 – 1.77 (m, 3H, H-4'', H-3''), 2.49 – 2.68 (m, 2H, H-5, H-6), 2.68 – 2.91 (m, 2H, H-5, H-6), 3.77 (s, 3H, OMe), 3.92 (s, 3H, OMe), 3.94 (s, 3H, OMe), 3.98 (s, 3H, OMe), 4.23 – 4.37 (m, 1H, H-2''), 4.96 (d, $^3J_{H,H}$ = 8.3 Hz, 1H, NH), 5.31 (s, 2H, H-3'), 5.39 (dd, $^3J_{H,H}$ = 11.9 Hz, 5.0 Hz, 1H, H-7), 6.47 (s, 1H, H-8), 6.61 (s, 1H, H-4), 6.83 (d, $^3J_{H,H}$ = 10.7 Hz, 1H, H-11), 7.30 (d, $^3J_{H,H}$ = 10.7 Hz, 1H, H-12), 7.71 (s, 1H, H-1'). **^{13}C NMR** (75 MHz, $CDCl_3$): δ [ppm] = 21.5 (C-5''), 22.7 (C-5''), 24.6 (C-4''), 28.1 (C-3'''), 29.5 (C-5), 35.2 (C-6), 41.1 (C-3''), 52.0 (C-2''), 56.0 (OMe), 56.3 (OMe), 58.2 (C-3'), 61.0 (OMe), 61.1 (OMe), 62.6 (C-7), 79.7 (C-2'''), 107.2 (C-4), 111.6 (C-11), 124.2 (C-1'), 124.7 (C-12b), 131.7 (C-8), 133.4 (C-4a), 134.2 (C-12a), 135.3 (C-12), 141.5 (C-3), 142.7 (C-2'), 147.4 (C-7a), 150.8 (C-1), 153.8 (C-2), 155.3 (C-1'''), 164.1 (C-10), 173.2 (C-1''), 178.6 (C-9). **HRMS** (ESI): calcd for $[M+Na]^+$ ($C_{34}H_{44}N_4NaO_9$): 675.30005; found: 675.30004. **FT-IR** (ATR): $\tilde{\nu}$ [cm^{-1}] = 3363 (br, w), 2955 (m), 2286 (w), 1734 (m), 1706 (s), 1616 (m), 1585 (s), 1487 (s), 1457 (m), 1429 (m), 1398 (m), 1365 (m), 1348 (m), 1320 (m), 1252 (s), 1160 (s), 1138 (s), 1095 (s), 1045 (m), 1018 (m), 1001 (m), 982 (w), 923 (w), 900 (w), 844 (m), 788 (w), 710 (w), 667 (w). **R_F**: 0.28 (CyHex/EtOAc/EtOH, 4/1/1). **Mp.**: 108 °C. **Yield**: 78% (reaction time: 30 min).

Compound 3c:

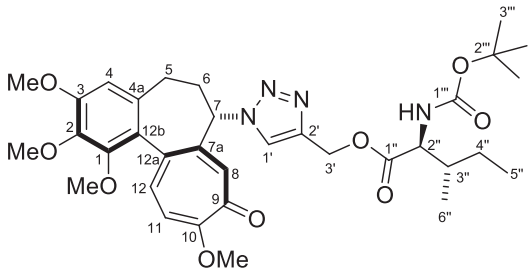

$C_{34}H_{44}N_4O_9$
652.73 g/mol

^{1}H NMR (300 MHz, $CDCl_3$): δ [ppm] = 0.81 – 0.92 (m, 6H, H-5'', H-6''), 1.05 – 1.24 (m, 1H, H-4''), 1.25 – 1.38 (m, 1H, H-4''), 1.41 (s, 9H, H-3'''), 1.85 (m, 1H, H-3''), 2.47 – 2.70 (m, 2H, H-5, H-6), 2.70 – 2.90 (m, 2H, H-5, H-6), 3.77 (s, 3H, OMe), 3.92 (s, 3H, OMe), 3.94 (s, 3H, OMe), 3.98 (s, 3H, OMe), 4.25 (dd, $^3J_{H,H}$ = 8.4 Hz, 4.7 Hz, 1H, H-2''), 5.00 (d, $^3J_{H,H}$ = 8.4 Hz, 1H, NH), 5.31 (s, 2H, H-3'), 5.39 (dd, $^3J_{H,H}$ = 12.0 Hz, 5.2 Hz, 1H, H-7), 6.47 (s, 1H, H-8), 6.60 (s, 1H, H-4), 6.81 (d, $^3J_{H,H}$ = 10.6 Hz, 1H, H-11), 7.29 (d, $^3J_{H,H}$ = 10.6 Hz, 1H, H-12), 7.68 (s, 1H, H-1'). **^{13}C NMR** (75 MHz, $CDCl_3$): δ [ppm] = 11.5 (C-5''), 15.5 (C-6''), 25.0 (C-4''), 28.2 (C-3'''), 29.7 (C-5), 35.3 (C-6), 37.8 (C-3''), 56.1 (OMe), 56.4 (OMe), 57.3 (C-2''), 58.1 (C-3'), 61.2 (OMe), 61.3 (OMe), 62.7 (C-7), 79.7 (C-2'''), 107.4 (C-4), 111.7 (C-11), 124.3 (C-1'), 124.8 (C-12b), 131.8 (C-8), 133.5 (C-4a), 134.4 (C-12a),

135.4 (C-12), 141.7 (C-3), 142.8 (C-2'), 147.4 (C-7a), 151.0 (C-1), 153.9 (C-2), 155.5 (C-1'''), 164.2 (C-10), 172.2 (C-1''), 178.7 (C-9). **HRMS** (ESI): calcd for $[M+Na]^+$ ($C_{34}H_{44}N_4NaO_9$): 675.30005; found: 675.30016. **FT-IR** (ATR): $\tilde{\nu}$ [cm^{-1}] = 3365 (br, w), 2965 (m), 2933 (m), 1736 (m), 1706 (s), 1616 (m), 1585 (s), 1573 (s), 1487 (s), 1457 (s), 1398 (m), 1364 (m), 1321 (m), 1252 (s), 1150 (s), 1095 (s), 1046 (m), 1018 (m), 1002 (m), 983 (w), 922 (w), 843 (w), 752 (s), 665 (w). $\mathbf{R_F}$: 0.20 (CyHex/EtOAc/EtOH, 4/1/1). **Mp.**: 102 °C. **Yield**: 82% (reaction time: 45 min).

Compound 3d:

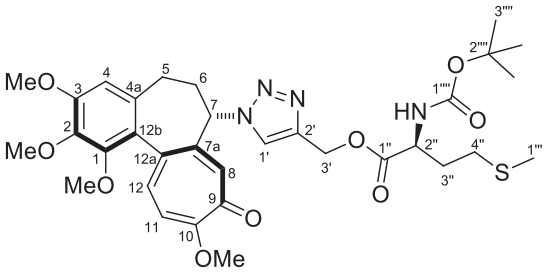

$C_{33}H_{42}N_4O_9S$
670.77 g/mol

^{1}H NMR (300 MHz, $CDCl_3$): δ [ppm] = 1.41 (s, 9H, H-3''''), 1.86 – 1.99 (m, 2H, H-3''), 2.05 (s, 3H, H-1'''), 2.50 (t, $^3J_{H,H}$ = 7.3 Hz, 2H, H-4''), 2.28 – 2.55 (m, 2H, H-5, H-6), 2.69 – 2.89 (m, 2H, H-5, H-6), 3.77 (s, 3H, OMe), 3.92 (s, 3H, OMe), 3.94 (s, 3H, OMe), 3.98 (s, 3H, OMe), 4.36 – 4.47 (m, 1H, H-2''), 5.18 (d, $^3J_{H,H}$ = 7.4 Hz, 1H, NH), 5.32 (s, 2H, H-3'), 5.39 (dd, $^3J_{H,H}$ = 11.8 Hz, 4.4 Hz, 1H, H-7), 6.45 (s, 1H, H-8), 6.60 (s, 1H, H-4), 6.82 (d, $^3J_{H,H}$ = 10.8 Hz, 1H, H-11), 7.30 (d, $^3J_{H,H}$ = 10.8 Hz, 1H, H-12), 7.69 (s, 1H, H-1'). **^{13}C NMR** (75 MHz, $CDCl_3$): δ [ppm] = 15.4 (C-1'''), 28.2 (C-3''''), 29.7 (C-5), 29.9 (C-4''), 31.7 (C-3''), 35.3 (C-6), 52.7 (C-2''), 56.1 (OMe), 56.4 (OMe), 58.5 (C-3'), 61.2 (OMe), 61.3 (OMe), 62.8 (C-7), 79.9 (C-2''''), 107.4 (C-4), 111.8 (C-11), 124.5 (C-1'), 124.8 (C-12b), 131.8 (C-8), 133.5 (C-4a), 134.4 (C-12a), 135.5 (C-12), 141.7 (C-3), 142.6 (C-2'), 147.5 (C-7a), 151.0 (C-1), 154.0 (C-2), 155.3 (C-1''''), 164.3 (C-10), 172.2 (C-1''), 178.7 (C-9). **HRMS** (ESI): calcd for $[M+Na]^+$ ($C_{33}H_{42}N_4NaO_9S$): 693.25647; found: 693.25592. **FT-IR** (ATR): $\tilde{\nu}$ [cm^{-1}] = 3348 (br, w), 2971 (w), 2933 (w), 1740 (m), 1707 (s), 1617 (m), 1585 (s), 1570 (s), 1486 (s), 1457 (m), 1397 (m), 1364 (m), 1348 (m), 1320 (m), 1282 (m), 1251 (s), 1162 (s), 1136 (s), 1095 (s), 1048 (m), 1019 (m), 1001 (m), 982 (w), 922 (w), 844 (w), 750 (s), 666 (w). $\mathbf{R_F}$: 0.16 (CyHex/EtOAc/EtOH, 4/1/1). **Mp.**: 98-100 °C. **Yield**: 68% (reaction time: 40 min).

Compound 3e:

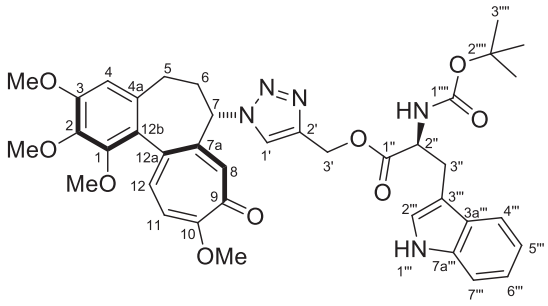

$C_{39}H_{43}N_5O_9$
725.79 g/mol

^{1}H NMR (300 MHz, $CDCl_3$): δ [ppm] = 1.47 (s, 9H, H-3''''), 2.15 – 2.32 (m, 2H, H-6), 2.49 – 2.57 (m, 2H, H-5), 3.13 (dd, $^2J_{H,H}$ = 14.0 Hz, $^3J_{H,H}$ = 8.3 Hz, 1H, H-3''), 3.46 (dd, $^2J_{H,H}$ = 14.0 Hz, $^3J_{H,H}$ = 3.3 Hz, 1H, H-3''), 3.75 (s, 3H, OMe), 3.91 (s, 3H, OMe), 3.94 (s, 3H, OMe), 4.06 (s, 3H, OMe), 4.77 – 4.87 (m, 1H, H-2''), 4.98 (d, $^2J_{H,H}$ = 13.4 Hz, 1H, H-3'), 5.20 (d, $^2J_{H,H}$ = 13.4 Hz, 1H, H-3'), 5.26 (d, $^3J_{H,H}$ = 8.3 Hz, 1H, NH), 5.37 (dd, $^3J_{H,H}$ = 11.0 Hz, 7.1 Hz, 1H, H-7), 6.43 (s, 1H, H-1'), 6.54 (s, 1H, H-8), 6.58 (s, 1H, H-4), 6.96 (s, 1H, H-2''') 6.97 (d, $^3J_{H,H}$ = 10.6 Hz, 1H, H-11), 7.03 – 7.20 (m, 3H, H-4''', H-5''', H-6'''), 7.44 (d, $^3J_{H,H}$ = 10.6 Hz, 1H, H-12), 7.70 (d, $^3J_{H,H}$ = 6.6 Hz, 1H, H-7'''), 10.20 (s, 1H, H-1'''). **^{13}C NMR** (75 MHz, $CDCl_3$): δ [ppm] = 28.3 (C-3''''), 29.1 (C-3''), 29.6 (C-5), 35.3 (C-6), 54.3 (C-2''), 56.1 (OMe), 56.5 (OMe), 58.7 (C-3'), 61.1 (OMe), 61.3 (OMe), 62.5 (C-7), 79.9 (C-2''''), 107.3 (C-4), 109.2 (C-3'''), 111.1 (C-4'''), 112.9 (C-11), 118.9 (C-7'''), 119.1 (C-6'''), 121.1 (C-5'''), 122.5 (C-1'), 123.4 (C-2'''), 124.5 (C-12b), 127.6 (C-3a'''), 131.1 (C-8), 133.4 (C-4a), 135.1 (C-12a), 136.2 (C-7a'''), 136.3 (C-12), 141.6 (C-2'), 142.7 (C-3), 148.2 (C-7a), 150.9 (C-1), 154.1 (C-2), 155.1 (C-1''''), 164.4 (C-10), 172.2 (C-1''), 179.1 (C-9). **HRMS** (ESI): calcd for $[M+Na]^+$ ($C_{39}H_{43}N_5NaO_9$): 748.29580; found: 748.29500. **FT-IR** (ATR): $\tilde{\nu}$ [cm^{-1}] = 3326 (br, w), 2966 (w), 2932 (w), 1734 (m), 1707 (m), 1615 (w), 1584 (m), 1559 (m), 1486 (m), 1456 (m), 1429 (m), 1397 (m), 1349 (m), 1321 (m), 1250 (vs), 1164 (s), 1137 (s), 1096 (s), 1044 (s), 1018 (m), 1000 (m), 983 (m), 922 (w), 899 (w), 845 (m), 814 (w), 743 (m), 609 (w). **R_F**: 0.35 (CyHex/EtOAc/EtOH, 2/1/1). **Mp.**: 191 °C. **Yield**: 92% (reaction time: 45 min).

Compound 3f:

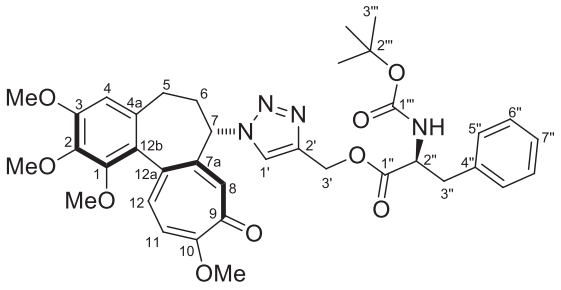

$C_{37}H_{42}N_4O_9$
686.75 g/mol

^{1}H NMR (300 MHz, $CDCl_3$): δ [ppm] = 1.38 (s, 9H, H-3'''), 2.44 – 2.69 (m, 2H, H-5, H-6), 2.70 – 2.87 (m, 2H, H-5, H-6), 2.97 – 3.16 (m, 2H, H-3''), 3.78 (s, 3H, OMe), 3.93 (s, 3H, OMe), 3.95 (s, 3H, OMe), 3.98 (s, 3H, OMe), 4.50 – 4.64 (m, 1H, H-2''), 5.01 (d, $^3J_{H,H}$ = 8.1 Hz, 1H, NH), 5.28 (s, 2H, H-3'), 5.37 (dd, $^3J_{H,H}$ = 11.7 Hz, 5.4 Hz, 1H, H-7), 6.48 (s, 1H, H-8), 6.61 (s, 1H, H-4), 6.82 (d, $^3J_{H,H}$ = 10.7 Hz, 1H, H-11), 7.05 – 7.26 (m, 5H, H-5'', H-6'', H-7''), 7.30 (d, $^3J_{H,H}$ = 10.7 Hz, 1H, H-12), 7.52 (s, 1H, H-1'). **^{13}C NMR** (75 MHz, $CDCl_3$): δ [ppm] = 28.2 (C-3'''), 29.6 (C-5), 35.3 (C-6), 38.0 (C-3''), 54.4 (C-2''), 56.1 (OMe), 56.4 (OMe), 58.5 (C-3'), 61.1 (OMe), 61.3 (OMe), 62.7 (C-7), 79.8 (C-2'''), 107.3 (C-4), 111.7 (C-11), 124.3 (C-1'), 124.8 (C-12b), 126.8 (C-7''), 128.4 (C-6''), 129.3 (C-5''), 131.8 (C-8), 133.5 (C-4a), 134.3 (C-12a), 135.4 (C-12), 138.9 (C-4''), 141.6 (C-3), 142.5 (C-2'), 147.4 (C-7a), 150.9 (C-1), 153.9 (C-2), 155.0 (C-1'''), 164.2 (C-10), 171.7 (C-1''), 178.7 (C-9). **HRMS** (ESI): calcd for $[M+Na]^+$ ($C_{37}H_{42}N_4NaO_9$): 709.2844; found: 709.2855. **FT-IR** (ATR): $\tilde{\nu}$ [cm^{-1}] = 3376 (br, w), 2926 (m), 2846 (w), 1740 (m), 1706 (s), 1616 (m), 1585 (s), 1486 (s), 1455 (m), 1397 (m), 1349 (m), 1320 (m), 1252 (s), 1165 (s), 1136 (s), 1085 (m), 1048 (m), 1018 (m), 1000 (w), 844 (w), 701 (w). **R_F**: 0.32 (CyHex/EtOAc/EtOH, 1/15/2). **Mp.**: 120 °C. **Yield**: 86% (reaction time: 30 min).

Compound 3g:

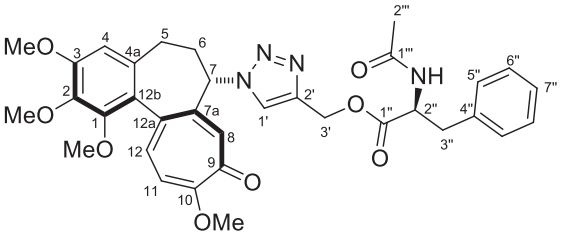

$C_{34}H_{36}N_4O_8$
628.68 g/mol

^{1}H NMR (300 MHz, $CDCl_3$): δ [ppm] = 1.97 (s, 3H, H-2'''), 2.51 – 2.70 (m, 2H, H-5, H-6), 2.71 – 2.87 (m, 2H, H-5, H-6), 3.00 – 3.19 (m, 2H, H-3''), 3.78 (s, 3H, OMe), 3.93 (s, 3H, OMe), 3.95 (s, 3H, OMe), 3.98 (s, 3H, OMe), 4.82 – 4.92 (m, 1H, H-2''), 5.26 – 5.32 (m, 2H, H-3'), 5.33 – 5.44 (m, 1H, H-7), 6.15 (d, $^3J_{H,H}$ = 7.8 Hz, 1H, NH), 6.42 (s, 1H, H-8), 6.61 (s, 1H, H-4), 6.83 (d, $^3J_{H,H}$ = 10.8 Hz, 1H, H-11), 7.04 – 7.12 (m, 2H, H-5''), 7.13 – 7.25 (m, 3H, H-6'', H-7''), 7.31 (d, $^3J_{H,H}$ = 10.8 Hz, 1H, H-12), 7.56 (s, 1H, H-1'). **^{13}C NMR** (75 MHz, $CDCl_3$): δ [ppm] = 23.0 (C-2'''), 29.6 (C-5), 35.3 (C-6), 37.5 (C-3''), 53.2 (C-2''), 56.1 (OMe), 56.4 (OMe), 58.5 (C-3'), 61.2 (OMe), 61.3 (OMe), 62.7 (C-7), 107.4 (C-4), 111.9 (C-11), 124.5 (C-1'), 124.8 (C-12b), 126.9 (C-7''), 128.5 (C-6''), 129.2 (C-5''), 131.7 (C-8), 133.5 (C-4a), 134.5 (C-12a), 135.5 (C-12), 135.9 (C-4''), 141.7 (C-3), 142.5 (C-2'), 147.5 (C-7a), 151.0 (C-1), 154.0 (C-2), 164.3 (C-10), 168.8 (C-1'''), 171.4 (C-1''), 178.7 (C-9). **HRMS** (ESI): calcd for $[M+Na]^+$ ($C_{34}H_{36}N_4NaO_8$): 651.24253; found: 651.24205. **FT-IR** (ATR): $\tilde{\nu}$ [cm^{-1}] = 3291 (br, w), 2929 (w), 2847 (w), 2237 (w), 1741 (m), 1708 (m), 1659 (m), 1613 (m), 1584 (s), 1566 (s), 1486 (m), 1454 (m), 1397 (m), 1348 (m), 1320 (m), 1283 (m), 1251 (s), 1178 (s), 1136 (s), 1084 (s), 1042 (m), 1018 (m), 1000 (m), 981 (m), 919 (m), 844 (m), 816 (w), 729 (s), 701 (s), 675 (w), 645 (w). **R_F**: 0.19 (CyHex/EtOAc/EtOH, 2/4/1). **Mp.**: 99 °C. **Yield**: 91% (reaction time: 30 min).

Compound 3h:

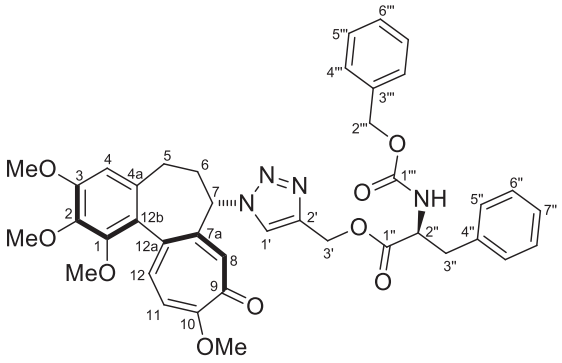

$C_{40}H_{40}N_4O_9$
720.28 g/mol

^{1}H NMR (300 MHz, $CDCl_3$): δ [ppm] = 2.44 – 2.68 (m, 2H, H-5, H-6), 2.68 – 2.84 (m, 2H, H-5, H-6), 3.04 – 3.15 (m, 2H, H-3''), 3.77 (s, 3H, OMe), 3.92 (s, 3H, OMe), 3.94 (s, 3H, OMe), 3.96 (s, 3H, OMe), 4.60 – 4.70 (m, 1H, H-2''), 5.24– 5.31 (m, 3H, H-2''', NH), 5.29 (s, 2H, H-3'), 5.36 (dd, $^3J_{H,H}$ = 11.7 Hz, 5.3 Hz, 1H, H-7), 6.46 (s, 1H, H-8), 6.60 (s, 1H, H-4), 6.81 (d, $^3J_{H,H}$ = 10.8 Hz, 1H, H-11), 7.02 – 7.08 (m, 2H, H-5''), 7.13 – 7.25 (m, 3H, H-6'', H-7''), 7.37 – 7.35 (m, 6H, H-4''', H-5''', H-6''', H-12), 7.51 (s, 1H, H-1'). **^{13}C NMR** (75 MHz, $CDCl_3$): δ [ppm] = 29.6 (C-5), 35.3 (C-6), 37.9 (C-3''), 54.8 (C-2''), 56.1 (OMe), 56.4 (OMe), 58.6 (C-3'), 61.2 (OMe), 61.3 (OMe), 62.7 (C-7), 69.9 (C-2'''),

107.4 (C-4), 111.8 (C-11), 124.4 (C-1'), 124.8 (C-12b), 127.0 (C-7''), 128.0 (C-5'''), 128.1 (C-6'''), 128.5 (C-6'', C-4'''), 129.3 (C-5''), 131.8 (C-8), 133.5 (C-4a), 134.4 (C-12a), 135.4 (C-12), 135.6 (C-4''), 136.2 (C-3'''), 141.7 (C-3), 142.5 (C-2'), 147.4 (C-7a), 151.0 (C-1), 154.0 (C-2), 155.6 (C-1'''), 164.3 (C-10), 171.3 (C-1''), 178.7 (C-9). **HRMS** (ESI): calcd for $[M+Na]^+$ ($C_{40}H_{40}N_4NaO_9$): 743.26875; found: 743.26799. **FT-IR** (ATR): $\tilde{\nu}$ [cm^{-1}] = 3430 (br, w), 2936 (w), 2837 (w), 2231 (w), 1711 (s), 1613 (m), 1573 (s), 1566 (s), 1536 (m), 1486 (m), 1454 (s), 1433 (m), 1396 (m), 1348 (m), 1320 (m), 1251 (vs), 1177 (s), 1137 (s), 1083 (s), 1018 (m), 1000 (m), 982 (m), 910 (m), 843 (m), 727 (vs), 697 (vs), 666 (m), 644 (m). $\mathbf{R_F}$: 0.24 (CyHex/EtOAc/EtOH, 3/1/1). **Mp.**: 86 °C. **Yield**: 93% (reaction time: 30 min).

Compound 3j:

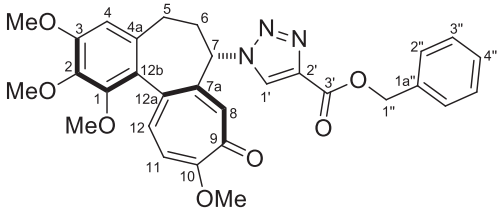

$C_{30}H_{29}N_3O_7$
543.57 g/mol

^{1}H NMR (300 MHz, $CDCl_3$): δ [ppm] = 2.46 – 2.67 (m, 2H, H-5, H-6), 2.67 – 2.82 (m, 2H, H-5, H-6), 3.77 (s, 3H, OMe), 3.91 (s, 3H, OMe), 3.94 (s, 3H, OMe), 3.97 (s, 3H, OMe), 5.38 (s, 2H, H-1''), 5.42 – 5.52 (m, 1H, H-7), 6.41 (s, 1H, H-8), 6.60 (s, 1H, H-4), 6.82 (d, $^3J_{H,H}$ = 10.8 Hz, 1H, H-11), 7.30 – 7.51 (m, 6H, H-12, H-2'', H-3'', H-4''), 8.20 (s, 1H, H-1'). **^{13}C NMR** (75 MHz, $CDCl_3$): δ [ppm] = 29.5 (C-5), 35.3 (C-6), 56.0 (OMe), 56.4 (OMe), 61.1 (OMe), 61.2 (OMe), 62.9 (C-7), 66.9 (C-1''), 107.3 (C-4), 111.8 (C-11), 124.6 (C-12b), 128.0 (C-1'), 128.3 (C-4''), 128.4 (C-3''), 128.5 (C-2''), 131.5 (C-8), 133.2 (C-4a), 134.1 (C-12a), 135.2 (C-1a''), 135.5 (C-12), 139.9 (C-2'), 141.6 (C-3), 146.8 (C-7a), 150.9 (C-1), 154.0 (C-2), 160.1 (C-3'), 164.2 (C-10), 178.5 (C-9). **HRMS** (ESI): calcd for $[M+Na]^+$ ($C_{30}H_{29}N_3NaO_7$): 566.18977; found: 566.18963. **FT-IR** (ATR): $\tilde{\nu}$ [cm^{-1}] = 3093 (w), 2936 (w), 2837 (w), 2238 (w), 1731 (s), 1614 (m), 1584 (s), 1566 (s), 1485 (s), 1454 (s), 1429 (m), 1397 (s), 1348 (s), 1320 (s), 1282 (m), 1250 (s), 1194 (s), 1162 (s), 1137 (s), 1094 (s), 1046 (m), 1033 (s), 1019 (s), 999 (s), 982 (m), 908 (s), 843 (m), 773 (m), 726 (s), 696 (s), 673 (m). $\mathbf{R_F}$: 0.63 (CyHex/EtOAc/EtOH, 2/1/1). **Mp.**: 124-127 °C. **Yield**: 88% (reaction time: 20 min).

Compound 3k:

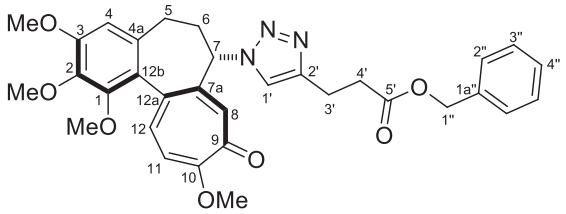

$C_{32}H_{33}N_3O_7$
571.62 g/mol

^{1}H NMR (300 MHz, $CDCl_3$): δ [ppm] = 2.41 – 2.66 (m, 2H, H-5, H-6), 2.67 – 2.76 (m, 2H, H-5, H-6), 2.80 (t, $^3J_{H,H}$ = 7.0 Hz, 2H, H-4'), 3.08 (t, $^3J_{H,H}$ = 7.0 Hz, 2H, H-3'), 3.76 (s, 3H, OMe), 3.91 (s, 3H, OMe), 3.94 (s, 3H, OMe), 3.97 (s, 3H, OMe), 5.11 (s, 2H, H-1''), 5.32 (dd, $^3J_{H,H}$ = 11.8 Hz, 5.4 Hz, 1H, H-7), 6.49 (s, 1H, H-8), 6.60 (s, 1H, H-4), 6.82 (d, $^3J_{H,H}$ = 10.8 Hz, 1H, H-11), 7.24 – 7.33 (m, 6H, H-12, H-2'', H-3'', H-4''), 7.35 (s, 1H, H-1'). **^{13}C NMR** (75 MHz, $CDCl_3$): δ [ppm] = 20.9 (C-3'), 29.6 (C-5), 33.4 (C-4'), 35.2 (C-6), 56.0 (OMe), 56.3 (OMe), 61.1 (OMe), 61.2 (OMe), 62.4 (C-7), 66.2 (C-1''), 107.3 (C-4), 111.8 (C-11), 121.8 (C-1'), 124.8 (C-12b), 128.0 (C-4''), 128.1 (C-3''), 128.4 (C-2''), 131.8 (C-8), 133.5 (C-4a), 134.4 (C-12a), 135.3 (C-12), 135.8 (C-1a''), 141.5 (C-3), 146.4 (C-2'), 147.7 (C-7a), 150.9 (C-1), 153.8 (C-2), 164.1 (C-10), 172.4 (C-5'), 178.7 (C-9). **HRMS** (ESI): calcd for $[M+Na]^+$ ($C_{32}H_{33}N_3NaO_7$): 594.22107; found: 594.22068. **FT-IR** (ATR): $\tilde{\nu}$ [cm^{-1}] = 3461 (br, w), 3133 (w), 2936 (m), 2838 (w), 2233 (w), 1730 (s), 1708 (s), 1615 (s), 1569 (s), 1485 (s), 1455 (s), 1427 (s), 1397 (s), 1347 (s), 1320 (s), 1282 (s), 1249 (s), 1177 (s), 1136 (s), 1093 (s), 1046 (s), 1017 (s), 1000 (s), 981 (s), 929 (m), 843 (m), 817 (m), 729 (s), 698 (s), 676 (m). **R_F**: 0.26 (CyHex/EtOAc/EtOH, 2/1/1). **Mp.**: 82 °C. **Yield**: 99% (reaction time: 20 min).

Compound 3l:

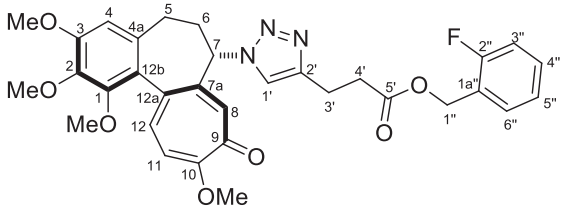

$C_{32}H_{32}FN_3O_7$
589.62 g/mol

^{1}H NMR (300 MHz, $CDCl_3$): δ [ppm] = 2.43 – 2.67 (m, 2H, H-5, H-6), 2.67 – 2.76 (m, 2H, H-5, H-6), 2.80 (t, $^3J_{H,H}$ = 6.8 Hz, 2H, H-4'), 3.08 (t, $^3J_{H,H}$ = 6.8 Hz, 2H, H-3'), 3.76 (s, 3H, OMe), 3.92 (s,

3H, OMe), 3.94 (s, 3H, OMe), 3.97 (s, 3H, OMe), 5.18 (s, 2H, H-1''), 5.34 (dd, $^{3}J_{H,H}$ = 11.6 Hz, 5.4 Hz, 1H, H-7), 6.50 (s, 1H, H-8), 6.60 (s, 1H, H-4), 6.80 (d, $^{3}J_{H,H}$ = 10.8 Hz, 1H, H-11), 6.98 – 7.15 (m, 2H, H-3'', H-5''), 7.24 – 7.36 (m, 3H, H-4'', H-6'', H-12), 7.38 (s, 1H, H-1'). **^{13}C NMR** (75 MHz, $CDCl_3$): δ [ppm] = 21.0 (C-3'), 29.7 (C-5), 33.4 (C-4'), 35.3 (C-6), 56.1 (OMe), 56.4 (OMe), 60.2 (C-1''), 61.2 (2xOMe), 62.5 (C-7), 107.4 (C-4), 111.7 (C-11), 115.3 (d, $^{2}J_{C,F}$ = 21.3 Hz, C-3''), 121.2 (C-1'), 124.1 (d, $^{4}J_{C,F}$ = 2.3 Hz, C-5''), 125.0 (C-12b), 130.1 (d, $^{3}J_{C,F}$ = 7.7 Hz, C-4''), 130.6 (d, $^{3}J_{C,F}$ = 2.5 Hz, C-6''), 131.8 (C-8), 133.6 (C-4a), 134.4 (C-12a), 135.3 (C-12), 138.6 (C-1a'')*, 141.6 (C-3), 145.8 (C-2'), 147.7 (C-7a), 151.0 (C-1), 154.0 (C-2), 162.5 (d, $^{1}J_{C,F}$ = 238.4 Hz, C-2''), 164.2 (C-10), 172.3 (C-5'), 178.8 (C-9). **HRMS** (ESI): calcd for $[M+H]^+$ ($C_{32}H_{33}FN_3O_7$): 590.22971; found: 590.22980. **FT-IR** (ATR): $\tilde{\nu}$ [cm^{-1}] = 2935 (w), 2837 (w), 2227 (w), 1733 (m), 1731 (m), 1614 (m), 1585 (s), 1573 (s), 1566 (s), 1487 (m), 1454 (m), 1427 (m), 1397 (m), 1347 (m), 1321 (m), 1281 (m), 1250 (vs), 1193 (m), 1178 (m), 1137 (s), 1094 (s), 1083 (s), 1047 (m), 1018 (m), 1001 (m), 982 (m), 906 (m), 842 (m), 816 (w), 759 (m), 726 (s), 674 (w), 644 (m). **R_F**: 0.17 (CyHex/EtOAc/EtOH, 3/1/1). **Mp.**: 58-59 °C. **Yield**: 91% (reaction time: 25 min). *Due to a very low signal intensity no $^{2}J_{C,F}$-coupling could be observed.

Compound 3m:

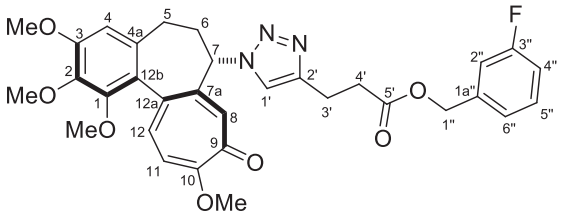

$C_{32}H_{32}FN_3O_7$
589.62 g/mol

^{1}H NMR (300 MHz, $CDCl_3$): δ [ppm] = 2.44 – 2.66 (m, 2H, H-5, H-6), 2.67 – 2.79 (m, 2H, H-5, H-6), 2.82 (t, $^{3}J_{H,H}$ = 7.1 Hz, 2H, H-4'), 3.08 (t, $^{3}J_{H,H}$ = 7.1 Hz, 2H, H-3'), 3.75 (s, 3H, OMe), 3.92 (s, 3H, OMe), 3.94 (s, 3H, OMe), 3.97 (s, 3H, OMe), 5.10 (s, 2H, H-1''), 5.34 (dd, $^{3}J_{H,H}$ = 11.7 Hz, 5.6 Hz, 1H, H-7), 6.49 (s, 1H, H-8), 6.59 (s, 1H, H-4), 6.80 (d, $^{3}J_{H,H}$ = 10.9 Hz, 1H, H-11), 6.91 – 7.12 (m, 3H, H-2'', H-4'', H-6''), 7.23 – 7.31 (m, 2H, H-5'', H-12), 7.37 (s, 1H, H-1'). **^{13}C NMR** (75 MHz, $CDCl_3$): δ [ppm] = 21.0 (C-3'), 29.7 (C-5), 33.4 (C-4'), 35.3 (C-6), 56.1 (OMe), 56.4 (OMe), 61.2 (2xOMe), 62.5 (C-7), 65.5 (C-1''), 107.4 (C-4), 111.7 (C-11), 114.5 (d, $^{2}J_{C,F}$ = 21.4 Hz, C-2'', C-4''), 121.7 (C-1'), 123.5 (d, $^{4}J_{C,F}$ = 2.2 Hz, C-6''), 124.9 (C-12b), 130.0 (d, $^{3}J_{C,F}$ = 8.6 Hz, C-5''), 131.8 (C-8), 133.6 (C-4a), 134.4 (C-12a), 135.3 (C-12), 138.4 (C-1a'')*, 141.6 (C-3), 146.3 (C-2'), 147.7 (C-7a), 151.0 (C-1), 153.9 (C-2), 160.5 (d, $^{1}J_{C,F}$ = 220.7 Hz, C-3''), 164.2 (C-10), 172.3 (C-5'), 178.8 (C-9). **HRMS** (ESI): calcd for $[M+H]^+$ ($C_{32}H_{33}FN_3O_7$): 590.22971; found: 590.22980. **FT-IR** (ATR): $\tilde{\nu}$ [cm^{-1}] = 2935 (w), 2837 (w), 2234 (w), 1733 (m), 1616 (m), 1584 (s), 1569 (s), 1486 (m), 1457 (m), 1429 (m), 1397 (m), 1348 (m), 1320 (m), 1281 (m), 1250 (vs), 1177 (m), 1137 (s), 1094 (s), 1083 (s), 1046 (m), 1018 (m), 1001 (m), 982

(m), 907 (m), 843 (m), 787 (m), 726 (s), 683 (w), 644 (w). **R_F**: 0.19 (CyHex/EtOAc/EtOH, 3/1/1). **Mp.**: 54-55 °C. **Yield**: 88% (reaction time: 25 min). *Due to a very low signal intensity no $^3J_{C,F}$-coupling could be observed.

Compound 3n:

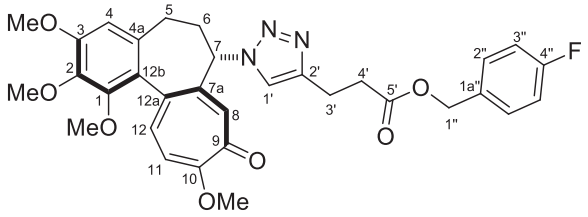

$C_{32}H_{32}FN_3O_7$
589.62 g/mol

^{1}H NMR (300 MHz, $CDCl_3$): δ [ppm] = 2.41 – 2.68 (m, 2H, H-5, H-6), 2.69 – 2.76 (m, 2H, H-5, H-6), 2.79 (t, $^3J_{H,H}$ = 6.8 Hz, 2H, H-4'), 3.07 (t, $^3J_{H,H}$ = 6.8 Hz, 2H, H-3'), 3.76 (s, 3H, OMe), 3.92 (s, 3H, OMe), 3.94 (s, 3H, OMe), 3.98 (s, 3H, OMe), 5.08 (s, 2H, H-1''), 5.34 (dd, $^3J_{H,H}$ = 11.7 Hz, 5.4 Hz, 1H, H-7), 6.48 (s, 1H, H-8), 6.59 (s, 1H, H-4), 6.81 (d, $^3J_{H,H}$ = 10.8 Hz, 1H, H-11), 6.99 (d, $^3J_{H,H}$ = 8.6 Hz, 1H, H-3''), 7.02 (d, $^3J_{H,H}$ = 8.6 Hz, 1H, H-3''), 7.27 – 7.32 (m, 3H, H-2'', H-12), 7.37 (s, 1H, H-1'). **^{13}C NMR** (75 MHz, $CDCl_3$): δ [ppm] = 21.0 (C-3'), 29.7 (C-5), 33.4 (C-4'), 35.3 (C-6), 56.1 (OMe), 56.3 (OMe), 61.2 (2xOMe), 62.5 (C-7), 65.6 (C-1''), 107.3 (C-4), 111.7 (C-11), 115.3 (d, $^2J_{C,F}$ = 21.5 Hz C-3''), 121.6 (C-1'), 124.9 (C-12b), 130.2 (d, $^3J_{C,F}$ = 8.0 Hz, C-2''), 131.8 (C-8), 133.5 (C-4a), 134.2 (C-1a'')*, 134.4 (C-12a), 135.3 (C-12), 141.6 (C-3), 146.1 (C-2'), 147.7 (C-7a), 150.9 (C-1), 153.9 (C-2), 162.5 (d, $^1J_{C,F}$ = 255.5 Hz, C-4''), 164.1 (C-10), 172.4 (C-5'), 178.8 (C-9). **HRMS** (ESI): calcd for $[M+H]^+$ ($C_{32}H_{33}FN_3O_7$): 590.22971; found: 590.22978. **FT-IR** (ATR): $\tilde{\nu}$ [cm^{-1}] = 2935 (w), 2832 (w), 2234 (w), 1730 (m), 1614 (m), 1572 (s), 1510 (m), 1486 (m), 1460 (m), 1427 (m), 1397 (m), 1347 (m), 1320 (m), 1282 (m), 1250 (vs), 1221 (s), 1177 (m), 1137 (s), 1094 (s), 1083 (s), 1046 (m), 1017 (m), 1001 (m), 981 (m), 907 (m), 824 (m), 726 (s), 676 (w), 643 (m). **R_F**: 0.20 (CyHex/EtOAc/EtOH, 3/1/1). **Mp.**: 58-59 °C. **Yield**: 95% (reaction time: 25 min). *Due to a very low signal intensity no $^4J_{C,F}$-coupling could be observed.

Compound 3o:

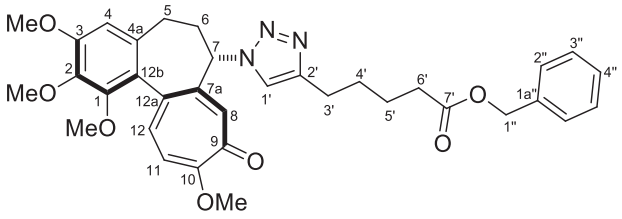

$C_{34}H_{37}N_3O_7$
599.62 g/mol

^{1}H NMR (300 MHz, $CDCl_3$): δ [ppm] = 1.67 – 1.76 (m, 4H, H-4', H-5'), 2.40 (t, $^3J_{H,H}$ = 6.5 Hz, 2H, H-6'), 2.48 – 2.64 (m, 2H, H-5, H-6), 2.68 – 2.81 (m, 4H, H-5, H-6, H-3'), 3.76 (s, 3H, OMe), 3.92 (s, 3H, OMe), 3.94 (s, 3H, OMe), 3.97 (s, 3H, OMe), 5.10 (s, 2H, H-1''), 5.37 (dd, $^3J_{H,H}$ = 11.6 Hz, 5.3 Hz, 1H, H-7), 6.53 (s, 1H, H-8), 6.59 (s, 1H, H-4), 6.80 (d, $^3J_{H,H}$ = 10.8 Hz, 1H, H-11), 7.28 (d, $^3J_{H,H}$ =10.8 Hz, 1H, H-12), 7.31 – 7.37 (m, 6H, H-1', H-2'', H-3'', H-4''). **^{13}C NMR** (75 MHz, $CDCl_3$): δ [ppm] = 24.4 (C-5'), 25.3 (C-3'), 28.5 (C-4'), 29.7 (C-5), 33.9 (C-6'), 35.3 (C-6), 56.1 (OMe), 56.3 (OMe), 61.2 (2xOMe), 62.4 (C-7), 66.1 (C-1''), 107.4 (C-4), 111.7 (C-11), 121.1 (C-1'), 124.9 (C-12b), 126.1 (C-2'', C-4''), 128.5 (C-3''), 131.9 (C-8), 133.6 (C-4a), 134.4 (C-12a), 135.2 (C-12), 136.0 (C-1a''), 141.6 (C-3), 147.8 (C-7a), 147.9 (C-2'), 150.9 (C-1), 153.9 (C-2), 164.2 (C-10), 173.3 (C-7'), 178.8 (C-9). **HRMS** (ESI): calcd for $[M+H]^+$ ($C_{34}H_{38}N_3O_7$): 600.27042; found: 600.27075. **FT-IR** (ATR): $\tilde{\nu}$ [cm^{-1}] = 3493 (w), 2857 (w), 2232 (w), 1730 (m), 1614 (m), 1584 (s), 1573 (s), 1566 (s), 1485 (m), 1454 (m), 1396 (m), 1347 (m), 1320 (m), 1250 (vs), 1191 (m), 1177 (m), 1137 (s), 1094 (s), 1083 (s), 1046 (m), 1018 (m), 1001 (m), 982 (m), 919 (m), 902 (m), 843 (w), 816 (w), 728 (s), 689 (m), 674 (w), 644 (w). **R_F**: 0.20 (CyHex/EtOAc/EtOH, 3/1/1). **Mp.**: 58 °C. **Yield**: 96% (reaction time: 25 min).

Compound 3p:

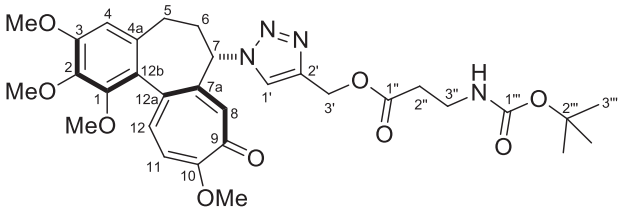

$C_{31}H_{38}N_4O_9$
610.66 g/mol

^{1}H NMR (300 MHz, $CDCl_3$): δ [ppm] = 1.41 (s, 9H, H-3'''), 2.50 – 2.68 (m, 4H, H-5, H-6, H-2''), 2.70 – 2.87 (m, 2H, H-5, H-6), 3.33 – 3.44 (m, 2H, H-3''), 3.77 (s, 3H, OMe), 3.91 (s, 3H, OMe), 3.94

(s, 3H, OMe), 3.99 (s, 3H, OMe), 5.17 (s, 1H, NH), 5.26 (s, 2H, H-3'), 5.42 (dd, $^3J_{H,H}$ = 11.8 Hz, 4.9 Hz, 1H, H-7), 6.47 (s, 1H, H-8), 6.61 (s, 1H, H-4), 6.83 (d, $^3J_{H,H}$ = 10.8 Hz, 1H, H-11), 7.30 (d, $^3J_{H,H}$ = 10.8 Hz, 1H, H-12), 7.72 (s, 1H, H-1'). **^{13}C NMR** (75 MHz, $CDCl_3$): δ [ppm] = 28.2 (C-3'''), 29.6 (C-5), 34.5 (C-2''), 35.3 (C-6), 36.0 (C-3''), 56.0 (OMe), 56.3 (OMe), 57.6 (C-3'), 61.1 (OMe), 61.2 (OMe), 62.7 (C-7), 79.1 (C-2'''), 107.3 (C-4), 111.8 (C-11), 124.2 (C-1'), 124.7 (C-12b), 131.7 (C-8), 133.4 (C-4a), 134.3 (C-12a), 135.4 (C-12), 141.6 (C-3), 142.7 (C-2'), 147.4 (C-7a), 150.9 (C-1), 153.9 (C-2), 155.7 (C-1'''), 164.2 (C-10), 172.1 (C-1''), 178.7 (C-9). **HRMS** (ESI): calcd for $[M+Na]^+$ ($C_{31}H_{38}N_4NaO_9$): 633.25310; found: 633.25165. **FT-IR** (ATR): $\tilde{\nu}$ [cm^{-1}] = 3359 (w), 2967 (w), 2935 (w), 2838 (w), 1730 (m), 1702 (m), 1616 (w), 1584 (s), 1567 (s), 1486 (m), 1456 (m), 1428 (m), 1397 (m), 1364 (m), 1348 (m), 1249 (s), 1164 (s), 1136 (s), 1092 (s), 1084 (s), 1048 (m), 1017 (m), 1000 (m), 980 (m), 920 (w), 843 (w), 728 (vs). **R_F**: 0.20 (CyHex/EtOAc/EtOH, 3/1/1). **Mp.**: 92 °C. **Yield**: 88% (reaction time: 30 min).

Compound 3q:

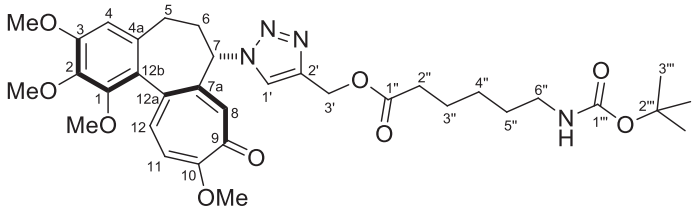

$C_{34}H_{44}N_4O_9$
652.75 g/mol

^{1}H NMR (300 MHz, $CDCl_3$): δ [ppm] = 1.29 – 1.38 (m, 2H, H-4''), 1.43 (s, 9H, H-3'''), 1.44 – 1.54 (m, 2H, H-5''), 1.56 – 1.69 (m, 2H, H-3''), 2.33 (t, $^3J_{H,H}$ = 7.4 Hz, 2H, H-2''), 2.49 – 2.69 (m, 2H, H-5, H-6), 2.69 – 2.88 (m, 2H, H-5, H-6), 3.02 – 3.14 (m, 2H, H-6''), 3.77 (s, 3H, OMe), 3.92 (s, 3H, OMe), 3.94 (s, 3H, OMe), 3.98 (s, 3H, OMe), 4.65 (s, 1H, NH), 5.23 (s, 2H, H-3'), 5.40 (dd, $^3J_{H,H}$ = 11.8 Hz, 5.1 Hz, 1H, H-7), 6.48 (s, 1H, H-8), 6.60 (s, 1H, H-4), 6.82 (d, $^3J_{H,H}$ = 10.9 Hz, 1H, H-11), 7.30 (d, $^3J_{H,H}$ = 10.9 Hz, 1H, H-12), 7.68 (s, 1H, H-1'). **^{13}C NMR** (75 MHz, $CDCl_3$): δ [ppm] = 24.3 (C-3''), 26.1 (C-4''), 28.3 (C-3'''), 29.6 (C-5, C-5''), 33.9 (C-2''), 35.3 (C-6), 40.2 (C-6''), 56.1 (OMe), 56.3 (OMe), 57.4 (C-3'), 61.1 (OMe), 61.2 (OMe), 62.6 (C-7), 79.1 (C-2'''), 107.4 (C-4), 111.7 (C-11), 124.3 (C-1'), 124.8 (C-12b), 131.8 (C-8), 133.4 (C-4a), 134.3 (C-12a), 135.4 (C-12), 141.6 (C-3), 143.0 (C-2'), 147.4 (C-7a), 150.9 (C-1), 153.9 (C-2), 155.9 (C-1'''), 164.2 (C-10), 173.4 (C-1'''), 178.7 (C-9). **HRMS** (ESI): calcd for $[M+Na]^+$ ($C_{34}H_{44}N_4NaO_9$): 675.30005; found: 675.29835. **FT-IR** (ATR): $\tilde{\nu}$ [cm^{-1}] = 3373 (w), 2933 (w), 2853 (w), 2238 (w), 17305 (m), 1697 (m), 1614 (w), 1584 (m), 1573 (m), 1503 (w), 1486 (m), 1461 (m), 1397 (w), 1365 (w), 1348 (w), 1321 (w), 1250 (s), 1162 (s), 1138 (s), 1095 (s), 1047 (w), 1018 (m), 983 (w), 907 (s), 843 (w), 724 (vs). **R_F**: 0.16 (CyHex/EtOAc/EtOH, 3/1/1). **Mp.**: 70-72 °C. **Yield**: 91% (reaction time: 30 min).

Compound 3r:

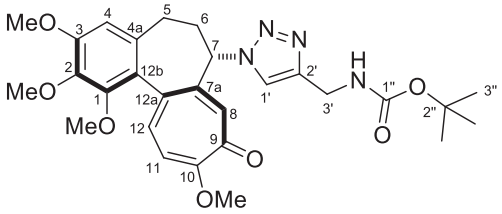

$C_{28}H_{34}N_4O_7$
538.59 g/mol

^{1}H NMR (300 MHz, $CDCl_3$): δ [ppm] = 1.43 (s, 9H, H-3''), 2.47 – 2.68 (m, 2H, H-5, H-6), 2.68 – 2.85 (m, 2H, H-5, H-6), 3.76 (s, 3H, OMe), 3.92 (s, 3H, OMe), 3.94 (s, 3H, OMe), 3.98 (s, 3H, O-Me), 4.41 (d, $^3J_{H,H}$ = 6.0 Hz, 2H, H-3'), 5.16 (br s, 1H, NH), 5.38 (dd, $^3J_{H,H}$ = 11.4 Hz, 4.8 Hz, 1H, H-7), 6.49 (s, 1H, H-8), 6.60 (s, 1H, H-4), 6.81 (d, $^3J_{H,H}$ = 10.6 Hz, 1H, H-11), 7.29 (d, $^3J_{H,H}$ = 10.6 Hz, 1H, H-12), 7.57 (s, 1H, H-1'). **^{13}C NMR** (75 MHz, $CDCl_3$): δ [ppm] = 28.3 (C-3''), 29.7 (C-5), 35.3 (C-6), 36.1 (C-3'), 56.1 (OMe), 56.4 (OMe), 61.1 (OMe), 61.2 (OMe), 62.6 (C-7), 79.6 (C-2''), 107.3 (C-4), 111.7 (C-11), 122.4 (C-1'), 124.9 (C-12b), 131.8 (C-8), 133.5 (C-4a), 134.4 (C-12a), 135.3 (C-12), 141.6 (C-3), 145.7 (C-2'), 147.6 (C-7a), 150.4 (C-1), 153.5 (C-2), 164.2 (C-10), 169.6 (C-1''), 178.8 (C-9). **HRMS** (ESI): calcd for $[M+Na]^+$ ($C_{28}H_{34}N_4NaO_7$): 561.23197; found: 561.23184. **FT-IR** (ATR): $\tilde{\nu}$ [cm^{-1}] = 3346 (br, w), 2966 (w), 2935 (w), 2233 (w), 1705 (m), 1616 (m), 1585 (s), 1570 (s), 1486 (m), 1458 (m), 1398 (m), 1348 (m), 1321 (m), 1251 (s), 1168 (s), 1138 (s), 1095 (m), 1047 (m), 1018 (m), 919 (m), 836 (w), 729 (s). **R_F**: 0.27 (CyHex/EtOAc/EtOH, 2/1/1). **Mp.**: 107 °C. **Yield**: 97% (reaction time: 45 min).

Preparation of compound 3i:

70 mg (0.10 mmol, 1.0 eq.) of **3f** were dissolved in 2.0 mL neat trifluoroacetic acid (TFA) and stirred at room temperature for 30 min. TFA was then removed under vacuum to yield a crude sample of the desired product. Addition of saturated aqueous citric acid followed by MTBE allowed for the extraction of **3i** into the aqueous phase and the isolation of unreacted **3f** in the organic phase. Pure **3i** was isolated by adjusting the aqueous layer pH to 10 with saturated aqueous Na_2CO_3 and extracting with several portions of CH_2Cl_2. The organic phase was died over $MgSO_4$, filtered and concentrated under reduced pressure. The desired product **3i** was isolated in 83% yield as a pale yellow foam.

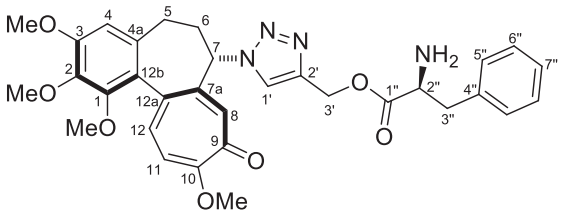

$C_{32}H_{34}N_4O_7$
586.63 g/mol

^{1}H NMR (300 MHz, $CDCl_3$): δ [ppm] = 1.80 (br s, 2H, NH_2), 2.46 – 2.69 (m, 2H, H-5, H-6), 2.70 – 2.91 (m, 3H, H-5, H-6, H-3"), 3.06 (dd, $^2J_{H,H}$ = 13.5 Hz, $^3J_{H,H}$ = 5.4 Hz, 1H, H-3"), 3.73 – 3.76 (m, 1H, H-2"), 3.78 (s, 3H, OMe), 3.92 (s, 3H, OMe), 3.94 (s, 3H, OMe), 3.98 (s, 3H, OMe), 5.30 (s, 2H, H-3'), 5.38 (dd, $^3J_{H,H}$ = 11.7 Hz, 5.4 Hz, 1H, H-7), 6.46 (s, 1H, H-8), 6.60 (s, 1H, H-4), 6.81 (d, $^3J_{H,H}$ = 10.8 Hz, 1H, H-11), 7.11 – 7.26 (m, 5H, H-5", H-6", H-7"), 7.29 (d, $^3J_{H,H}$ = 10.8 Hz, 1H, H-12), 7.55 (s, 1H, H-1'). **^{13}C NMR** (75 MHz, $CDCl_3$): δ [ppm] = 29.6 (C-5), 35.3 (C-6), 40.8 (C-3"), 55.7 (C-2"), 56.1 (OMe), 56.4 (OMe), 58.0 (C-3'), 61.1 (OMe), 61.2 (OMe), 62.7 (C-7), 107.3 (C-4), 111.7 (C-11), 124.4 (C-1'), 124.8 (C-12b), 126.7 (C-7"), 128.4 (C-6"), 129.3 (C-5"), 131.8 (C-8), 133.5 (C-4a), 134.3 (C-12a), 135.4 (C-12), 138.1 (C-4"), 141.7 (C-3), 142.7 (C-2'), 147.4 (C-7a), 151.0 (C-1), 154.0 (C-2), 164.3 (C-10), 171.7 (C-1"), 178.7 (C-9). **HRMS** (ESI): calcd for $[M+Na]^+$ ($C_{32}H_{34}N_4NaO_7$): 609.23197; found: 609.23190. **FT-IR** (ATR): $\tilde{\nu}$ [cm^{-1}] = 3375 (br, m), 2936 (w), 2831 (w), 2231 (w), 1736 (m), 1613 (m), 1584 (s), 1566 (s), 1486 (m), 1454 (m), 1397 (m), 1348 (m), 1320 (m), 1252 (s), 1192 (s), 1137 (s), 1094 (m), 1018 (m), 1000 (m), 982 (m), 910 (m), 843 (w). **R_F**: 0.29 (CH_2Cl_2/MeOH, 15/1). M**p.**: 97 °C.

Biological Data

Materials and Methods

Cell cultures:

The human tumour cell lines Jurkat (T cell leukemia), THP-1 (acute monocytic leukemia), Hela (cervix carcinoma) and A549 (lung adenocarcinoma) were obtained from the German Collection of Microorganisms and Cell Cultures (DSMZ, Braunschweig, Germany). MDA-MB-231 (triple negative breast adenocarcinoma) and H1975 (non-small cell lung adenocarcinoma) were obtained from the American Type Culture Collection.

Jurkat cells were cultivated in RPMI 1640 medium supplemented with 10% heat inactivated fetal calf serum, 2 mM L-glutamine, 100 U/mL penicillin and 100 µg/mL streptomycin.

THP-1 cells were cultivated in RPMI 1640 medium supplemented with 10% heat inactivated fetal calf serum, 100 U/mL penicillin and 100 µg/mL streptomycin.

Hela cells were cultivated in RPMI 1640 medium supplemented with 5% heat inactivated fetal calf serum, 100 U/mL penicillin and 100 µg/mL streptomycin. .

A549, MDA-MB-231 and H1975 cells were cultivated in DMEM medium (Gibco) supplemented with 10% heat inactivated fetal calf serum, 100 U/mL penicillin and 100 µg/mL streptomycin.

SK MES 1 cells, a human lung squamous carcinoma cell line, were obtained from the European Collection of Cell Cultures (ECACC, Salisbury, UK). Cells were cultivated in EMEM medium supplemented with 10% heat inactivated fetal calf serum, 2 mM L-glutamine, 1x Non Essential Amino Acids, 100 U/mL penicillin and 100 µg/mL streptomycin.

All cell lines were maintained at 37°C, 5% CO_2. Subconfluent cells were passaged two times per week.

Cell viability assay:

For determination of the IC_{50} values of the compounds, the cell viability was measured by quantitation of ATP with the CellTiter-Glo Luminescent Cell Viability Assay (Promega, Madison, WI, USA) according to the manufacturer's protocol. In short, cells were seeded at the desired concentration in white 384-well plates (Jurkat: $2.8 \cdot 10^5$ cells/mL; THP-1: $4.4 \cdot 10^5$ cells/mL; Hela, A549, SK MES 1: $8 \cdot 10^4$ cells/mL). After 2 h (suspension cells) or after 24 h (adherent cells), 5 µl of the test compounds were added, each concentration in quadruples. After the desired incubation time, the CellTiter-Glo reagent was added and the luminescence was measured with the Infinite m200 microplate reader (Tecan Group AG, Maennedorf, Switzerland).

Microtubule polymerization assay:

Inhibition of tubulin polymerization *in vitro* was analyzed with a fluorescence-based tubulin polymerization kit using >99% pure porcine tubulin (Cytoskeleton Inc., Denver, CO, USA). 5 µl of the compounds in a 10x higher concentration than desired as well as the negative control were pipetted into the wells of a pre-warmed black 96-well plate in duplicates. After incubation of the plate at 37°C for 1 min, 50 µL of the tubulin reaction mix was added (100 µg tubulin in 80 mM PIPES pH 6.9, 2 mM MgCl2, 0.5 mM EGTA, 1 mM GTP, 20% glycerol). Fluorescence intensity (excitation 360 nM, emission 450 nM) was measured at 37°C every minute over a period of 60 min using the Infinite m1000 pro microplate reader (Tecan Group AG, Maennedorf, Switzerland).

Data analysis:

Data were obtained from three or more independent experiments performed in triplicates and represent mean ± SEM. For calculation of IC_{50} values, the concentrations of test compounds were plotted against maximum bioluminescence change after stimulation. Curve fitting was performed in GraphPad Prism v. 6.0 (GraphPad Software, San Diego, CA, USA) using nonlinear re-

gression. The IC50 values of the tubulin polymerization inhibition were calculated from the area under the curve with GraphPad Prism 6 using nonlinear regression.

Microtubule morphology:

MDA-MB-231 and H1975 cells were grown to 80% confluency in DMEM medium containing 10% FBS. Compounds were treated with different concentrations for 24 hours. After the treatment, the cells were fixed using ice-cold methanol for 10 minutes followed by 30 minutes of blocking with blocking solution. The blocked cells can be stored at 4 degrees until immunofluorescence staining is carried out.

Blocking:
1 mL blocking solution was added and left at least for one hour at RT or overnight in 4 °C.

Adding of primary antibodies:
Blocking solution was removed, the primary antibody was added and incubated for one hour at RT (CPAP overnight in 4 °C).

Washing step:
Some of the primary antibodies were collected back for reuse. After this step, the cells were washed with solution D for the interval of 3 minutes three times.

Adding of secondary antibody:
Blocking solution was removed, the secondary antibody was added and incubated for one hour at RT. The same steps were repeated as above for the remaining of primary and secondary antibodies, DAPI was added in the last used secondary antibody.

Mounting:
After the last washing, the blocking solution was removed and distilled H_2O was added. The slides were labelled with cell type, staining and date.

The coverslips were removed from the water and put on paper to dry. 8µL Mowiol® was applied onto the slide the coverslip placed upside down on top of it. After drying, nail polish was applied to the edges of the coverslip, stored in a box at 4 °C till imaging. Confocal images were collected using Olympus Fluoview FV 1000 scanning confocal microscope. The images were further processed by Fiji and Adobe Photoshop.

Medium: DMEM (1X) + GlutaMax™-I, 10 % FBS HI, 1 % 100X MEM NEAA, 1 % Pen/Strep. For all cell lines only one medium was used, which was prepared in the hood under sterile conditions and kept at 4 °C until usage.

Blocking solution: 0.5 % Gelatine from cold water fish skin in 1X PBS.

Influence on microtubule morphology:

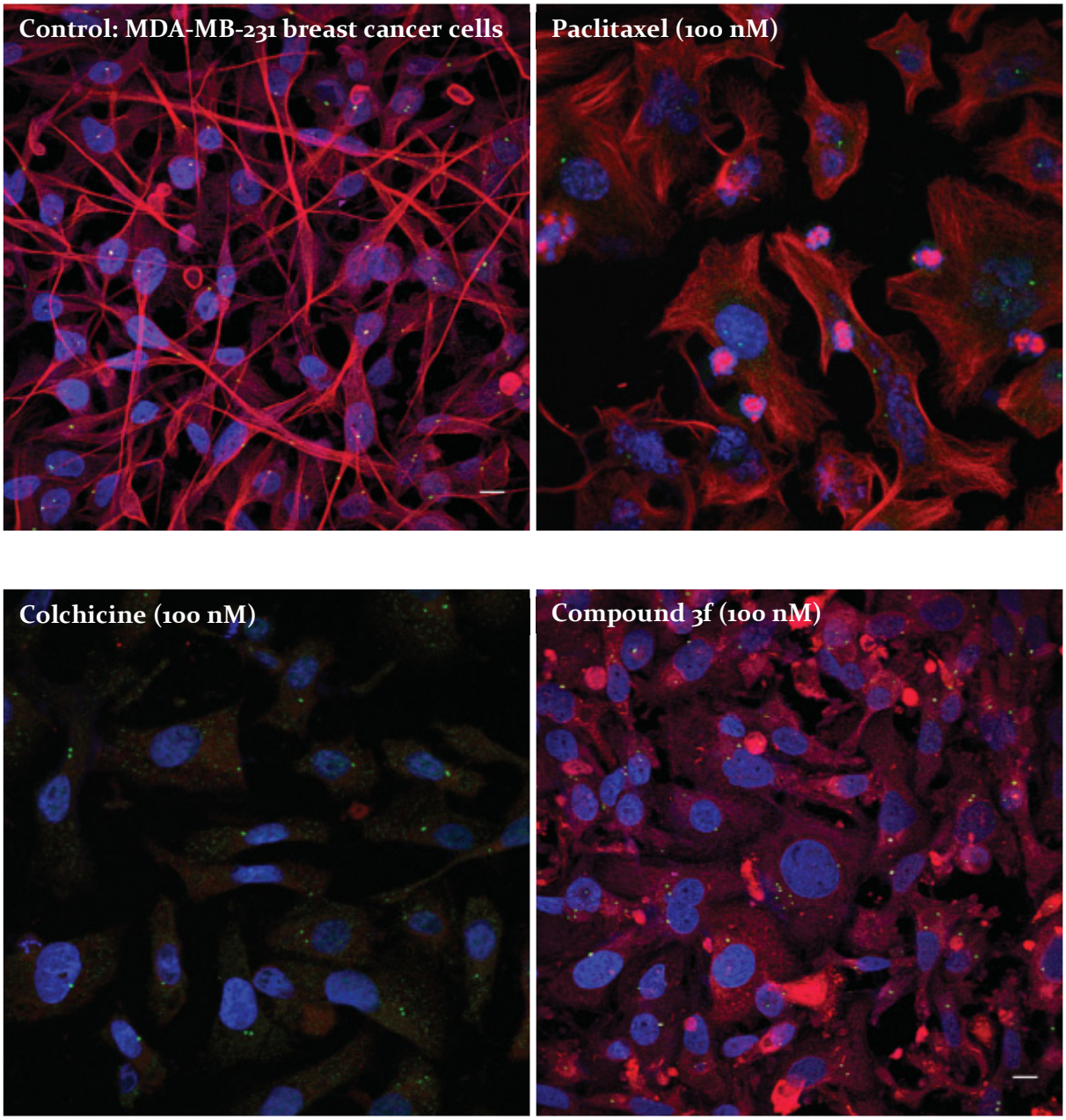

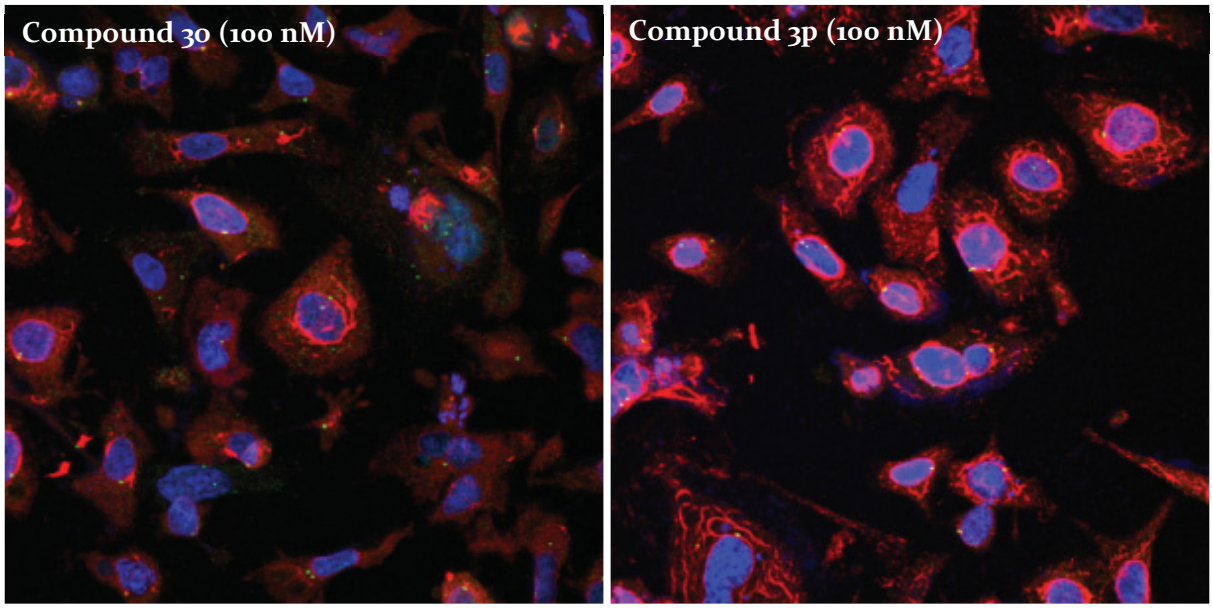

Influence on centrosomes (declustering effect):

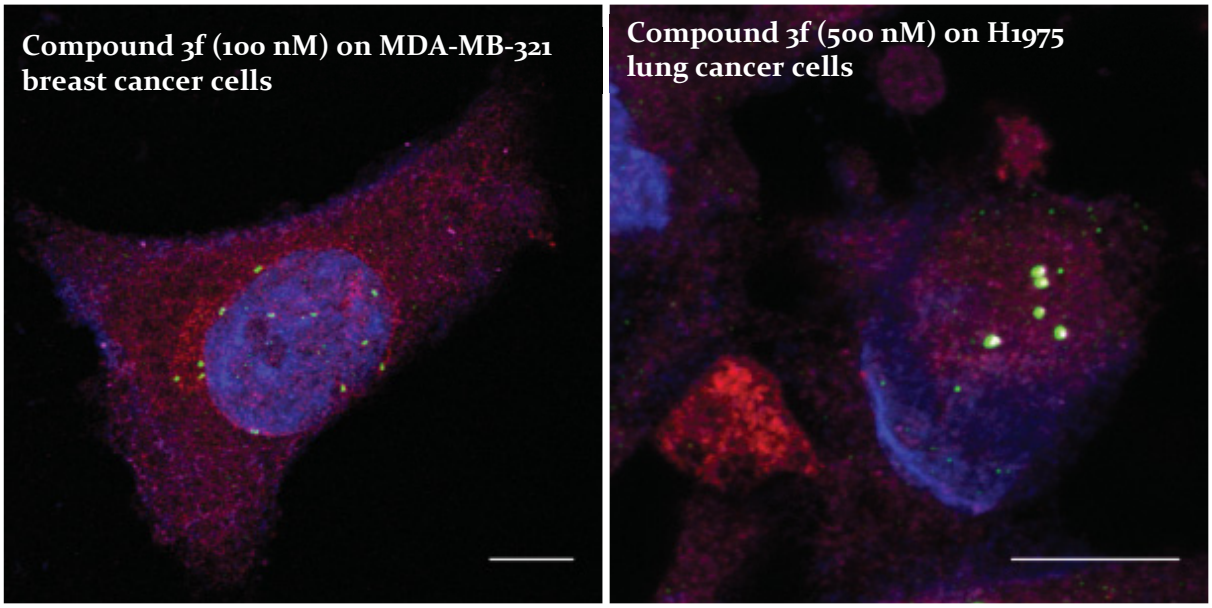

References

(1) Compounds **SI-1**, **SI-3**, **SI-4** and **SI-9** are literature-known but were synthesized following a different protocol: Ramapanicker, R.; Gupta, R.; Megha, R.; Chandrasekaran, S. Application of Propargyl Esters of Amino Acids in Solution-Phase Peptide Synthesis. *Int. J. Pept.* **2011**, *2011*, Article ID 854952, 10 pages.

(2) Compounds **SI-2**, **SI-6** and **SI-8** are literature-known but were synthesized following a different protocol: Bew, S. P.; Hiatt-Gipson, G. D. Synthesis of C-Propargylic Esters of N-Protected Amino Acids and Peptides. *J. Org. Chem.* **2010**, *75*, 3897-3899.

(3) Nicolaus, N; Zapke, J.; Riesterer, P.; Neudörfl, J.-M.; Prokop, A.; Oschkinat, H.; Schmalz, H.-G. Azides Derived from Colchicine and their Use in Library Synthesis: a Practical Entry to New Bioactive Derivatives of an Old Natural Drug. *ChemMedChem* **2010**, *5*, 661-665.

3 Discussion

In recent years, great advances have been made in the development of innovative therapies and drugs to treat cancer, the second most common cause of death worldwide, especially in the field of targeted therapy, cancer immunotherapy and most recently, gene therapy. In spite of the steady progress, MDR remains a major problem in the effective treatment of cancer and it is estimated that MDR causes treatment failure in about 90% of patients with metastatic tumors [5]. MDR not only affects tumor therapy with conventional chemotherapy, but also the more recent targeted therapies [7]. Thus, it is of urgent need to find novel therapies to overcome therapy resistance of cancer cells and cells of the tumor microenvironment. Here, one strategy is inhibition of ABC transporters, which actively efflux drugs to the extracellular space, by small molecules.

As natural products or natural product derived compounds display an immense spectrum of biological and pharmacological activities and have long been an integral part of drug development, it is obvious to focus on natural products for the search of candidate compounds to treat multidrug-resistant tumors. Therefore, different classes of natural compounds from plants were examined in this thesis and their potential to either inhibit ABC transporter-mediated efflux of drugs or to efficiently kill sensitive or ABC transporter-overexpressing cancer cells was evaluated. Promising compounds were further evaluated regarding their mechanism of ABC transporter inhibition. In total, more than 300 compounds from different classes were provided by cooperation partners and screened for pharmacological activities, including the here discussed goniothalamins, isocoumarins and colchicines as well as steroids, diverse natural products, fruit extracts and building blocks derived from natural products.

3.1 Goniothalamin Derivatives as Cytotoxic Compounds and Inhibitors of P-gp Activity

In 1967, the natural product goniothalamin was first isolated from plants endemic in Southeast Asia and since the late 1990s, its promising biological and pharmacological activities, especially in the field of cancer regarding cytotoxic activity, have been studied [170,172,236]. Therefore, natural occurring (*R*)-goniothalamin, its (*S*)-enantiomer and 21 novel derivatives, which were synthesized by our project partners from the *Institute of Bioorganic Chemistry, Heinrich-Heine Universität Düsseldorf* (*M.Sc. Anja Weber, Prof. Dr.*

Jörg Pietruszka) were characterized regarding cytotoxicity in triple-negative and progesterone and estrogen receptor positive breast cancer cell lines and a non-small cell lung cancer cell line (Chapter I, 2.1) and in sensitive and multidrug-resistant, ABC transporter expressing lung, colon and breast cancer cell lines as well as inhibitory activity against P-gp, MRP1 and BCRP (Chapter II, 2.2) [192,193]. The potential of goniothalamin and derivatives to inhibit ABC transporters and to circumvent cancer MDR had not been examined before.

3.1.1 Cytotoxic Activities of Goniothalamin Derivatives

In Chapter I, results of the cytotoxicity assays were used to describe distinct SARs of goniothalamin derivatives, which influence toxic activities in triple-negative and progesterone and estrogen receptor positive breast cancer cell lines and a non-small cell lung cancer cell line. In addition, derivatives could be identified which were more cytotoxic than the natural product **(*R*)-1** in selected cell lines, for example, the *para*-nitrophenyl goniothalamin **(*R*)-25** with an IC_{50} value of 6.7 µM and the cyclopropyl derivative **(*R,S,S*)-4** with an IC_{50} value of 14.4 µM in triple-negative breast cancer cells HBL-100 compared to **(*R*)-1** with an IC_{50} value of 20.9 µM (Figure 8A). Regarding the SAR, the data showed that (*R*)-enantiomers are more potent than (*S*)-enantiomers, which were mostly non-toxic, an unsaturated lactone ring is essential for activity and the vinylic double bond of the molecule is not mandatory for activity, but the molecule needs a certain rigidity, which can also be established by a cyclopropyl group (Figure 8B). Substituents at the phenyl group have only minor impact on cytotoxicity.

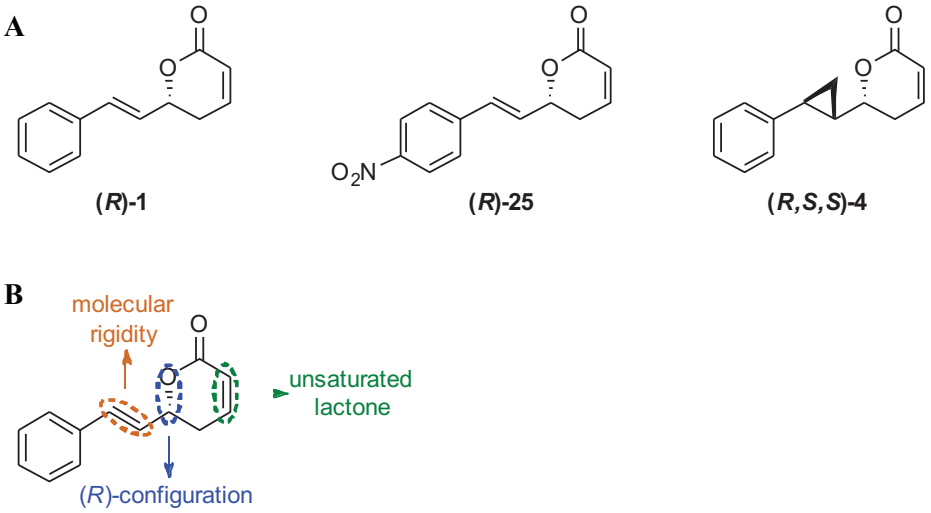

Figure 8. Goniothalamin derivatives which are cytotoxic in cancer cell lines. (A) Two derivatives of the natural product goniothalamin **(*R*)-1** were identified as more potent inducers of cytotoxicity in different human cancer cell lines, the *para*-nitrophenyl derivative **(*R*)-25** and the cyclopropyl derivative **(*R,S,S*)-4**. **(B)** Structural elements which are essential for cytotoxic activity of goniothalamin derivatives are the (*R*)-configuration, the unsaturated lactone moiety and the molecular rigidity.

Various derivatives with improved cytotoxicity compared to the natural product goniothalamin have been demonstrated before in several studies. One example is the naturally occurring derivative 5-acetyl goniothalamin, which has been shown to be 2-fold more efficacious in human breast cancer cell lines with IC_{50} values between 1.7 µM and 8.7 µM [182]. In another study, synthesized N-acylated aza-goniothalamin derivatives displayed up to 4-fold improved cytotoxicity compared to the naturally occurring product in P-gp expressing NCI-ADR/RES ovarian cancer cells [191]. With this resistant cell line as well as with P-gp overexpressing HepG2-R liver cancer cells, it could be shown that the natural product goniothalamin can efficiently inhibit proliferation and tumor cell growth of these multidrug-resistant cell lines [178,180,189,190].

As MRP1- and BCRP-overexpressing cell lines have not been included in previous pharmacological tests of goniothalamin, the pharmacological evaluation of the natural product and its derivatives were expanded towards these multidrug-resistant cells in Chapter II, which focused on overcoming cancer MDR and examined cytotoxicity and ABC transporter inhibition. In the cytotoxicity assays, the SAR from Chapter I could be confirmed. Like in Chapter I, derivatives **(*R*)-25** and **(*R,S,S*)-4** demonstrated an about 2-fold increased activity in P-gp expressing HCT-15 colon carcinoma cells, MRP1-expressing H69AR small cell lung cancer cells and sensitive NCI-H69 small cell lung cancer cells. Hence, these goniothalamin derivatives might provide a good starting point for further optimization towards novel cytotoxic compounds with activity in sensitive as well as P-gp and MRP1-expressing resistant tumor cells. Moreover, comparing sensitive and resistant MCF-7 and MCF-7/MX breast cancer cell lines, derivatives were identified to possess selective toxicity in the BCRP-expressing MCF-7/MX cells, especially **(*R*)-2** and **(*S*)-2**.

3.1.2 Inhibition of P-gp Activity by Goniothalamin Derivatives

Besides cytotoxicity, the potential of the natural product goniothalamin and derivatives to inhibit the ABC transporters P-gp, MRP1 and BCRP was analyzed for the first time in Chapter II. It could be shown that goniothalamin **(*R*)-1** slightly inhibited P-gp transport activity up to around 40% relative inhibition compared to the positive control. The non-toxic *para*-methoxy derivatives **(*R*)-3** and **(*S*)-3** (Figure 9A) displayed the strongest inhibitory activity against P-gp and relative inhibition was up to around 98% and 62%, respectively. For all compounds, inhibition of P-gp was dose-dependent and selective, no effects were observed against MRP1 and BCRP. Considering the SAR of P-gp inhibition in contrast to cytotoxicity, there was no difference between the (*R*)- and (*S*)-enantiomers of compound **1** and the

saturated derivatives **23a**, **23c** and **23e**. In contrast, increased activity of the (*R*)-enantiomers of derivatives **3** and **24** was observed. Furthermore, a saturated lactone ring had no impact on P-gp inhibition in case of the derivatives **23a** and **23c** compared to unsaturated compounds, but decreased P-gp inhibition in case of derivative **23e**. In summary, it seems that ability of goniothalamin derivatives to inhibit P-gp transport function is mainly subject to the functional group at the phenyl group (Figure 9B).

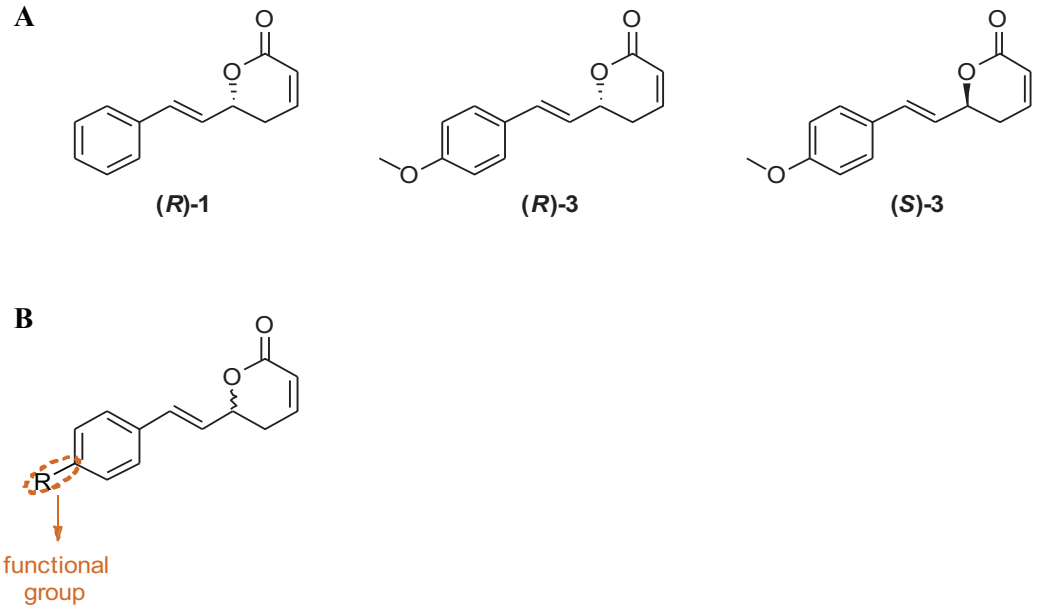

Figure 9. Goniothalamin derivatives which selectively inhibit P-gp transport. (A) Two derivatives of the natural product goniothalamin **(*R*)-1** were identified as selective and non-toxic inhibitors of P-gp transport function, the *para*-methoxy derivatives **(*R*)-3** and **(*S*)-3**. **(B)** P-gp inhibition is mainly influenced by the substituent at the phenyl ring.

Notably, inhibitory activity of kavalactones from the Kava plant, which are structurally related to the methoxylated goniothalamins **(*R*)-3** and **(*S*)-3** that were identified as P-gp inhibitors, have been previously analyzed towards P-gp by Weiss and colleagues [237]. They observed a concentration-dependent inhibition of P-gp in P388/dx cells by all natural compounds tested with desmethoxyyangonin and yangonin being the strongest inhibitors in the test set. For desmethoxyyangonin, an f_2 value (concentration needed to double baseline fluorescence of calcein) of about 17 µM was reported. However, the mechanism of inhibition of kavalactones as well as their selectivity towards P-gp remains elusive.

In addition to cell-based transporter inhibition assays, the identified inhibitors **(*R*)-3** and **(*S*)-3** were further characterized *in vitro*. Using flow cytometry, it could be shown that by inhibiting P-gp both compounds significantly increased intracellular accumulation of the chemotherapeutic drug and P-gp substrate doxorubicin up to 2-fold compared to the negative control. In line with this, P-gp expressing HCT-15 cells were sensitized to doxorubicin when

treated in combination with **(*R*)-3** or **(*S*)-3** and resistance was reversed by reducing the IC_{50} value of doxorubicin up to around 15-fold.

In general, P-gp inhibitors can act via different mechanisms and competitive or non-competitive. The mode of action can be characterized by analyzing basal and drug-stimulated ATPase activity in presence of the inhibitor [238,239]. To obtain first insights into the mechanism of inhibition of **(*R*)-3** or **(*S*)-3**, P-gp ATPase activity was analyzed. Results revealed that **(*R*)-3** or **(*S*)-3** are potential substrates of P-gp as they stimulated basal ATPase activity and inhibited verapamil-stimulated ATPase activity of P-gp. Furthermore, molecular docking to homology-modeled P-gp was performed at the *Department of Pharmaceutical Biology, Institute of Pharmacy and Biochemistry, Johannes Gutenberg Universität Mainz* (*Dr. Onat Kadioglu, Prof. Dr. Thomas Efferth*). Derivatives **(*R*)-3** and **(*S*)-3** were both demonstrated to strongly interact with the drug-binding domain of the transporter. According to amino acid allocation to different drug-binding sites of P-gp as classified by Ferreira and colleagues, both compounds primarily interacted with the R-site (rhodamine 123 site) [240]. Anthracyclines, such as doxorubicin, are presumed to bind to this site as well, which could help explain the increase of intracellular doxorubicin that was observed. Interestingly, the weak inhibitors **(*R*)-23e** and **(*S*)-23e** with saturated lactone moiety compared to **(*R*)-3** and **(*S*)-3** did also reveal a strong interaction with P-gp and with the same amino acids in the molecular docking studies. This is in contrast to the *in vitro* data of P-gp inhibition and doxorubicin accumulation. Thus, further analyses are necessary to fully elucidate the inhibitory mechanism of goniothalamin derivatives, including studies to elucidate the exact mechanism of inhibition.

In summary, results of the studies of Chapter I (2.1) and Chapter II (2.2) demonstrated the potential of the natural product goniothalamin and derivatives against sensitive and resistant cancer cells. Depending on the structural modifications, the anticancer activities of the derivatives can either be shifted towards cytotoxicity or towards selective inhibition of P-gp transport function. P-gp inhibition seems to be mostly influenced by the phenyl ring and its substitutions, whereas cytotoxicity mainly depends on the lactone moiety and the vinylic double bond.

As a basis for the *in vitro* characterization of goniothalamin derivatives, qPCR screening of a panel of human tumor cell lines was performed (Appendix to Chapter II, 2.2.1). According to these data, cell lines HCT-15, H69AR and MCF-7/MX were chosen for ABC transporter studies and their expression data, which had been published before, could be verified. The

analysis revealed HCT-15 to express high levels of P-gp, while MRP1 and BCRP mRNA levels were low compared to the reference gene GAPDH, which is in accordance with published data [56]. The multidrug-resistant cell line H69AR is known to overexpress the ABC transporter MRP1 in contrast to its parental cell line NCI-H69 [83,241]. Here, a 70-fold higher relative expression of MRP1 in the H69AR cells compared to NCI-H69 was revealed, while expression levels of P-gp and BCRP only differed slightly in both cell lines. The multidrug-resistant cell line MCF-7/MX overexpresses BCRP, whereas its parental cell line MCF-7 exhibits only low expression of this transporter [56]. In accordance, relative expression levels of BCRP in MCF-7/MX cells were over 1000-fold higher compared to parental MCF-7, whereas expression of P-gp and MRP1 was only marginally up- or downregulated in the resistant cells. Furthermore, this in-depth comparative analysis allows identification of intrinsically resistant cancer cell lines, for example, colon carcinoma cell line Caco-2 (elevated P-gp expression), liver carcinoma cell line HepG2 (elevated P-gp and BCRP expression) or pancreas carcinoma cell line Panc-1 (elevated MRP1 and BCRP expression). Liver and pancreas carcinomas both represent aggressive cancers with high mortality rates worldwide and poor prognosis due to the lack of efficacious therapy options [3,242,243]. This can in part be assigned to the inherent chemotherapy resistance caused by ABC transporters. Thus, development of MDR-overcoming therapies might be very beneficial for the treatment of these tumor types. In addition, the data show as well that MDR might not only be caused by overexpression of a single transporter, but can be mediated by interplay of several transporters.

3.1.3 Future Perspectives

Until now, most research focused on the anticancer activities of naturally occurring goniothalamin. Goniothalamin has been shown to induce apoptosis in cancer cells through caspase activation and cell cycle arrest, to inhibit cancer cell migration and to induce production of ROS [179,183,184,244,245]. Furthermore, it inhibits activation of nuclear factor kappa B (NF-κB) [187]. NF-κB, a key transcription factor of inflammation, has been shown to be constitutively activated in different cancer types and it supports tumor progression, invasiveness and therapy resistance [246,247]. Several derivatives were identified with higher cytotoxic activities in different sensitive cancer cell lines and the P-gp expressing NCI-ADR/RES cell line, but most studies did not have a further look into the mechanism of action of these derivatives and did not evaluate their influence on the mechanisms mentioned above in comparison with the natural product

[178,180,182,190,191,248]. Especially in case of compounds killing the resistant cancer cell line, it would be interesting to identify the molecular target as a basis for the development of novel compound candidates. This applies to the novel derivatives that were studied here as well.

The observed P-gp inhibition by goniothalamin derivatives was only of moderate potency compared to other well-characterized inhibitors like valspodar (PSC883) or tariquidar, which even entered clinical trials. The most potent one, derivative **(*R*)-3**, only exhibited full transporter inhibition in a cell-based assay when applied at a concentration of 50 µM and it is questionable if this concentration can be reached *in vivo*. Nevertheless, the promising results of this study support further structure optimization of goniothalamin derivatives towards potentially more efficacious P-gp inhibitors. One starting point could be the introduction of other functional groups at the phenyl ring or variations in the substitution pattern.

The two most potent goniothalamin derivatives identified as selective P-gp inhibitors, derivatives **(*R*)-3** and **(*S*)-3**, displayed none or only weak toxic effects in the tested human cancer cell lines. Their cytotoxicity in normal healthy tissues has not been tested in this study, but this would be indispensable for following *in vivo* experiments and for considering them as potential drug candidates. Naturally occurring goniothalamin has already been administered in mouse and rat models of cancer, inflammation and malaria infection and doses up to 300 mg/kg did not show any signs of toxicity [177,185,186,188,249]. In another study, two aza-goniothalamin derivatives were applied *in vivo* and doses up to 100 mg/kg could be administered without risk [191]. Thus, it is not unlikely that the derivatives **(*R*)-3** and **(*S*)-3** from this study might be safe for *in vivo* use.

After functional optimization and toxicity evaluation, another important step of characterizing the MDR-overcoming activity of novel P-gp inhibitors is applying the compound in *in vivo* studies. Xenograft models can be established by inoculating mice with cells from a P-gp overexpressing cancer cell line. They would then be treated with a chemotherapeutic drug (for example doxorubicin) alone or in combination with the respective test compounds and tumor size and survival would be analyzed. As a more predictive model, patient-derived resistant tumor cells could also be used for xenograft generation and study of MDR and its reversal *in vivo* [250,251]. Advantages of these models are the heterogeneity of the tumors, their growth in a physiologically-relevant environment and the lack of genetic transformations and adaptations of established cell lines gained by *in vitro* culture [252].

3.2 Isocoumarins as Dual Inhibitors of P-gp and BCRP

A second class of natural compounds, which was studied, are the isocoumarins or more precisely 3,4-dihydroisocoumarins. They represent a large group of secondary metabolites with great structural and functional variety from various natural sources, including bacteria, fungi and plants [194]. Although several isocoumarins and 3,4-dihydroisocoumarins with anticancer activities have been identified, they have not been considered as inhibitors of human ABC transporters for the reversal of MDR so far. Thus, the three natural products 6-methoxymellein, angelicoin B and ellagic acid as well as nine novel derivatives were synthesized by our project partners from the *Institute of Bioorganic Chemistry, Heinrich-Heine Universität Düsseldorf* (*M.Sc. Anja Weber, Prof. Dr. Jörg Pietruszka*) and from *MicroCombiChem GmbH, Wiesbaden* (*Dr. Edmond Fleischer, Dr. Anette Klinger*) and characterized in Chapter III (2.3) as potential candidates for reversal of cancer MDR.

3.2.1 Inhibition of P-gp and BCRP Activity by 3,4-Dihydroisocoumarins

All compounds were tested for their potential to inhibit the ABC transporters P-gp, MRP1 and BCRP and three compounds demonstrated dual and dose-dependent inhibition of P-gp and BCRP (Figure 10A). The most potent of these compounds was the pentyl-derivative **16**, which inhibited transport function of both transporters between 80% and 90% at the highest test concentration (50 µM) compared to the respective positive control. This derivate also had the potential to sensitize P-gp expressing HCT-15 cells and BCRP-expressing MCF-7/MX cells to treatment with the respective transporter substrates and chemotherapeutic drugs doxorubicin and mitoxantrone and thereby reverse resistance of these cell lines. In HCT-15 cells, the IC_{50} value of doxorubicin was reduced up to 3.7-fold and in MCF-7/MX cells, the IC_{50} value of mitoxantrone was reduced up to 5.6-fold by co-treatment with derivative **16**.

The *tert*-butyldimethylsilyl (TBS) protected derivatives **(*R*)-19** and **(*S*)-19** demonstrated a weaker activity with relative inhibition up to 40% to 50% compared to the positive controls. For further insights into the SAR of transporter inhibition, data were compared to pentyl-derivative **16a**, which differs from derivative **16** by the methoxy group instead of the hydroxy group at position 8, and the deprotected derivatives **(*R*)-19a** and **(*S*)-19a**. All three derivatives demonstrated reduced inhibitory activity against P-gp and BCRP and the reduction was more pronounced in case of BCRP. In addition, the three natural products 6-methoxymellein (**3**), angelicoin B (**4**) and ellagic acid as well as the tricyclic derivative **21** and the derivatives **14** and **14a** without substituent at position 3 did not inhibit BCRP and were only weak inhibitors

of P-gp with relative inhibition between around 10% and 20% at the highest test concentration. Taking these results together, SAR of P-gp and BCRP inhibition by 3,4-dihydroisocoumarins could be established, which were consistent for both transporters (Figure 10B). Firstly, a hydroxy group at position 8 is indispensable for transporter inhibition and substitution by a methoxy group leads to clearly reduced activity as was seen by comparing derivatives **16** and **16a**. Secondly, the molecule needs an alkyl substituent at position 3 of a certain length. Derivative **14** without substituent as well as methoxymellein (**3**) and angelicoin B (**4**) with a methyl group at position 3 demonstrated significantly decreased inhibition compared to the pentyl-derivative **16**. Lastly, this substituent has to be hydrophobic as was demonstrated by the derivatives with deprotected hydroxy group, **(*R*)-19a** and **(*S*)-19a**, which were less potent than their TBS protected counterparts **(*R*)-19** and **(*S*)-19**.

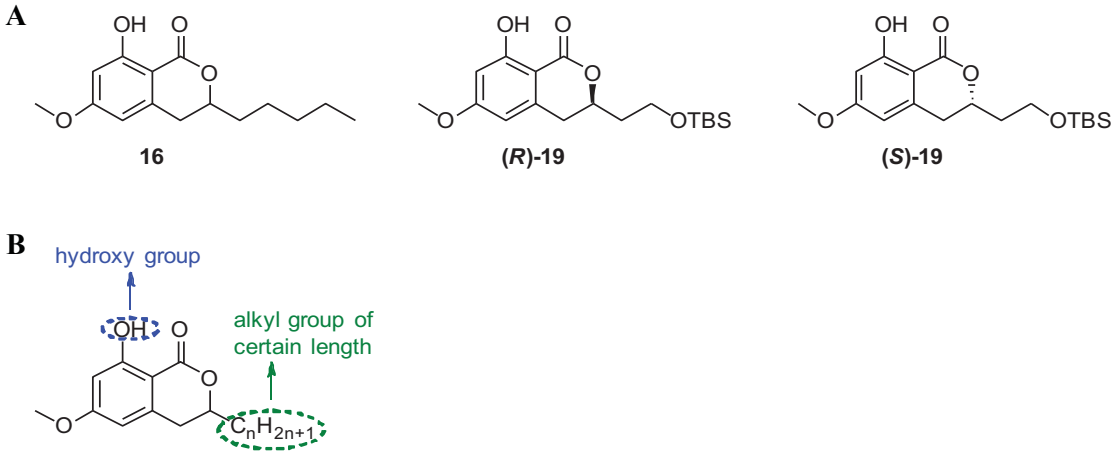

Figure 10. 3,4-dihydroisocoumarins which dually inhibit P-gp and BCRP transport. (A) Three 3,4-dihydroisocoumarins were identified as dual inhibitors of P-gp and BCRP transport function, the pentyl-derivative **16** and the TBS-protected enantiomers **(*R*)-19** and **(*S*)-19**. **(B)** Structural elements which are essential for inhibition of P-gp and BCRP by 3,4-dihydroisocoumarins are the hydroxyl group at position 8 and the hydrophobic alky chain at position 3.

In summary, some novel 3,4-dihydroisocoumarins tested in this study proved to be moderate dual inhibitors of P-gp and BCRP with the potential of further development towards more potent inhibitors. So far, most studies focused on identification and development of selective inhibitors of a certain transporter. On the one hand, advantages of selective inhibitors are reduced side effects that might arise from inhibiting several transporters at once as they are not only expressed in tumor tissues, but are also important for homeostasis of healthy tissues. Clinical trials with first generation P-gp inhibitors had to be discontinued because of the unspecific transporter inhibition by the drugs, for example verapamil, which lead to increased toxicity of the cytotoxic chemotherapy. Another limitation was the low efficacy, which necessitated high and potentially toxic doses of the drugs [113,114]. On the

other hand, most tumors do not solely express a single ABC transporter and MDR is rather caused by interplay of multiple transporters. For instance, concurrent overexpression of P-gp and BCRP has been shown in AML patients and was linked to poor therapy responsiveness and overall survival [253–255]. Furthermore, P-gp and BCRP have a partly overlapping substrate spectrum and several anticancer drugs in clinical practice are translocated by both transporters, for example, mitoxantrone, topotecan, etoposide and TKIs [75,256]. In these cases, selective inhibition of one transporter might not be sufficient to reverse resistance to chemotherapy and dual and potent inhibitors of both transporters seem to be a more efficacious strategy for treatment of MDR. Moreover, P-gp and BCRP are co-expressed at the blood-brain barrier, where they prevent brain penetration of potentially harmful compounds. This protects the sensitive brain, but at the same time limits the efficacy of chemotherapy in the therapy of brain tumors [257]. Expression of P-gp and BCRP in gliomas as well as their contribution to temozolomide resistance, the first-line treatment of glioblastoma multiforme, has also been described [258]. These issues could be addressed by the dual targeting of P-gp and BCRP as well. Thus far, different dual inhibitors have been identified, such as tariquidar and derivatives, aurones and chalcones [259–261]. Especially in case of aurones and chalcones, further development and research is still required to elucidate the mechanism of action and to thoroughly characterize the compounds for potential *in vivo* and clinical use. The 3,4-dihydroisocoumarins of this study might serve as additional candidate compounds for further development of potent, dual inhibitors of P-gp and BCRP.

3.2.2 Cytotoxic Activities of 3,4-Dihydroisocoumarins

Besides transporter inhibition, cytotoxicity of the test compounds was analyzed in sensitive A549 lung cancer cells and in resistant HCT-15 colon cancer cells, H69AR lung cancer cells and MCF-7/MX breast cancer cell. As mentioned in 1.7.2, one strategy to overcome cancer MDR mediated by ABC transporter overexpression is the development of cytotoxic drugs with selective activity against multidrug-resistant cells by exploiting the phenomenon of collateral sensitivity [151]. While most of the tested 3,4-dihydroisocoumarins displayed only weak or no significant cytotoxicity in different human cancer cell lines, derivative **16a** demonstrated exclusive toxicity in the BCRP-expressing MCF-7/MX breast cancer cell line with an IC_{50} value of 10.6 μM. Hence, this compound might be worth further studies of its mechanism of action and cellular target in this resistant cell line. If it does not induce cytotoxicity in the parental, sensitive MCF-7 cell line, it could serve as a promising starting point for the development of drug candidates with selective toxicity in resistant tumors that

overexpress BCRP. Selective activity against BCRP-expressing tumor cells has for example been shown for the natural product curcumin in combination with either ouabain or gramicidin [262]. This combination induces intracellular ATP depletion by stimulating ATP hydrolysis, which leads to caspase-dependent apoptosis.

3.2.3 Future Perspectives

Novel 3,4-dihydroisocoumarins were identified as dual inhibitors of P-gp and BCRP and as the results show, the SAR of the tested compounds is analogous regarding inhibition of P-gp and BCRP. Thus, there is evidence for a similar mechanism of transport inhibition by those compounds. To clarify this, further comparative analyses regarding influence on ATPase activity of both transporters and on intracellular drug accumulation are required. This would provide valuable information if the compounds inhibit transport function in a competitive or non-competitive manner. Furthermore, molecular docking studies of the newly identified inhibitors to homology-modeled human P-gp and to human BCRP can provide insights about the binding sites of the inhibitors at the transporter proteins. As the SAR from the inhibition analyses are comparable for P-gp and BCRP, it is possible that the binding-sites for 3,4-dihydroisocoumarins of both transporters are similar in their structure as well. In case of both transporters, multiple binding sites in the drug-binding domains have been proposed, but the exact numbers and locations still remain elusive. For P-gp, at least four distinct binding sites have been described, whereas for BCRP, a recent study revealed three binding sites [71,102]. In February 2018, the crystal structure of human-mouse chimeric P-gp in complex with the third-generation inhibitor zosuquidar was resolved [69]. It is the first P-gp structure with a fully occluded substrate-binding cavity in an outward-closed confirmation. The structure revealed binding of two closely interacting zosuquidar molecules. However, it still has to be confirmed by molecular docking if two zosuquidar molecules can bind simultaneously and if the same applies to other inhibitors or substrates. Because of the partially overlapping substrate spectrums of P-gp and BCRP, possibly similarities in drug-binding sites are conceivable. Furthermore, inhibitors can bind to the NDBs of the transporter, thereby inhibiting its function in a non-competitive manner by interfering with the catalytic cycle.

The most potent compound, derivative **16**, inhibited P-gp and BCRP transport activity up to 80% to 90%, but relatively high compound concentrations of 50 µM had to be used. As this is the case for the goniothalamin derivatives, it is doubtful if this concentration can be reached in *in vivo* studies for successfully inhibiting P-gp and BCRP in tumors. Therefore, structure modifications based on derivative **16** might provide compounds with a significantly improved

inhibitory profile. These modifications could include prolonged alkyl groups at position 8 and substitutions at other positions of the molecule.

3.3 Colchicine Derivatives as Drug Candidates against Sensitive and Resistant Tumors

The alkaloid colchicine is a highly potent inhibitor of tubulin polymerization and thus, microtubule formation. As microtubules are integral for various cell biological mechanisms, inhibition of microtubule formation leads to cell death and serves as an interesting target in cancer therapy [225]. Approved microtubule-targeting drugs include taxanes (paclitaxel, docetaxel) and *vinca* alkaloids (vinblastine, vincristine, vinorelbine). Colchicine displays strong toxic effects in cancer cells as wells as normal cells and hence, it is not used in the treatment of cancer so far, but is only approved for the treatment of gout. Nevertheless, colchicine remains a promising natural product with potent anticancer activities because of its potent activity as microtubule-formation inhibitor and many studies focus on development of novel colchicine derivatives, prodrugs or formulations with reduced toxicity in healthy tissues as anticancer drug candidates [229,230].

A part of this thesis was the evaluation of novel colchicine-derived triazoles in regard to cytotoxic activities and inhibition of tubulin polymerization (Chapter IV, 2.4) [235]. These compounds were synthesized by our cooperation partners from the *Department of Chemistry, Universität zu Köln* (*Dr. Persefoni Thomopoulou, Prof. Dr. Hans-Günther Schmalz*). Cytotoxicity assays were performed in leukemia cells as well as solid tumor cells of lung and cervix. In a first screening using leukemia cell lines THP-1 (acute monocytic leukemia) and Jurkat (acute lymphoblastic leukemia), several derivatives with up to 5-fold improved cytotoxic activities were identified. Their IC_{50} values were between 2.9 nM and 5.7 nM compared to colchicine with IC_{50} values between 13.5 nM and 20.4 nM in the two cell lines. The three most potent ones, derivatives **3f**, **3o** and **3p** (Figure 11), were further characterized on the solid tumor cell lines and in an *in vitro* tubulin polymerization assay. Especially the 4-fluorobenzyl ester **3o** proved to be a potent cytotoxic compound and results of the tubulin inhibition assay revealed its improved ability to inhibit tubulin polymerization compared to colchicine. Moreover, these results were confirmed by immunofluorescence staining and microscopy. Colchicine-derived triazoles and in particular derivative **3o** might serve as interesting lead compounds, but would need further characterization. On one hand, it is indispensable to analyze toxicity in healthy tissues. On the other hand, as this thesis focuses

on overcoming resistance of tumor to chemotherapeutic therapy, it would be interesting to characterize the colchicine derivatives in this respect.

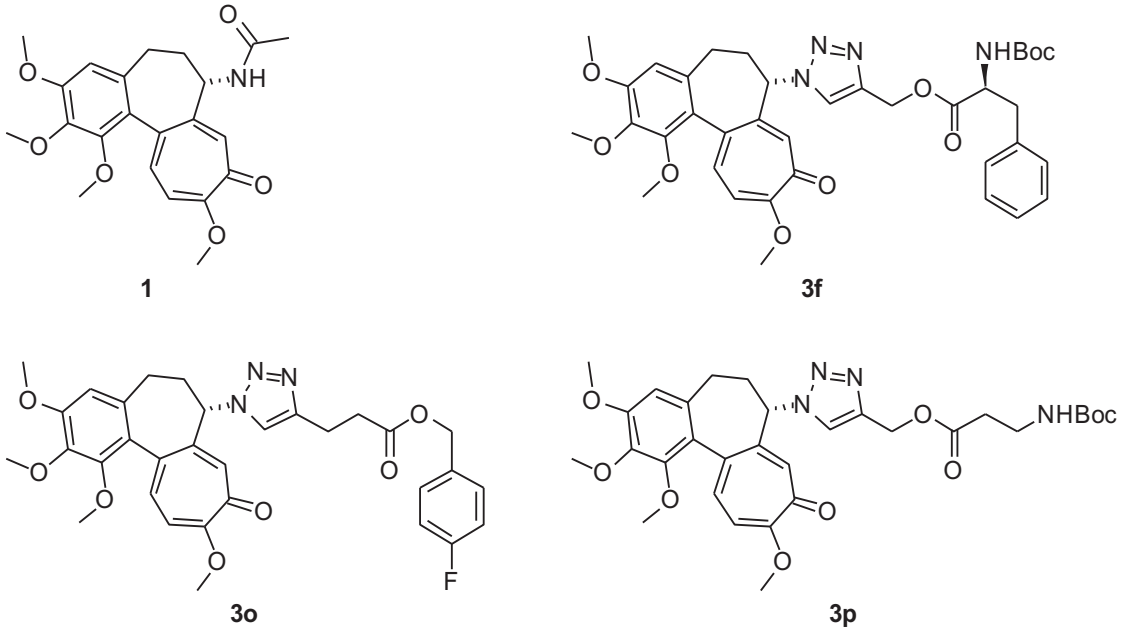

Figure 11. Colchicine derivatives with improved cytotoxicity and inhibition of tubulin polymerization. Three colchicine-derived triazoles were identified which demonstrated to be more potent in inducing cytotoxicity in different human cancer cell lines and in inhibiting tubulin polymerization compared to colchicine **1**, the derivatives **3f**, **3o** and **3p**.

The natural product colchicine is a known substrate of P-gp and an inducer of its expression in cancer cells [231,232]. Regarding this circumstance, it would be of particular interest to examine the ability of the colchicine derivatives to elevate P-gp expression or to be translocated by P-gp. P-gp overexpression is a common mechanism of cancer MDR against other tubulin-targeting drugs, for example, paclitaxel or vinblastine [8,263,264]. Hence, colchicine derivatives that do not act as substrates of P-gp could serve as alternative chemotherapeutic drugs that would allow efficacious treatment of multidrug-resistant tumors despite P-gp overexpression. Furthermore, in the treatment of sensitive tumors, these compounds could prevent emergence of MDR, if they did not induce P-gp expression. Different colchicine derivatives have already been characterized in this respect and promising compounds with these desired features could be identified [234,265,266].

Other mechanisms of resistance to microtubule-targeting drugs are represented by alterations in the drug target [233]. One possibility, which has been demonstrated, is that resistance can be mediated by changes of tubulin isotype expression patterns. In humans, there are eight isotypes of β-tubulin with unique expression patterns in different cell types and tissues [267]. It has been shown that isotype composition influences microtubule dynamics,

stability and drug binding [268]. Especially the βIII-tubulin isotype seems to be a crucial parameter of resistance. Elevated expression of this isotype was identified as an essential mediator of taxane resistance and its expression levels can be correlated with patients' response to treatment and tumor aggressiveness [269–272]. Interestingly, higher expression of βIII-tubulin seems to be a mediator of colchicine resistance as well [273]. As another mechanism, mutations in the different tubulin subtypes have been observed in drug-resistant cell lines, but their clinical impact remains unclear [274]. *In vitro*, mutations lead to changes in microtubule stability or decreased drug-binding affinity [275–277]. In these cases, colchicine derivatives might have the potential to overcome resistance by acting at a different binding site or by having the ability to target other isotypes as has already been shown by different studies [278–280].

Nevertheless, the potential of the colchicine derivatives studied here to overcome resistance to microtubule-targeting anticancer drugs still needs to be evaluated and further improvement of their structure might be necessary on the way to a novel drug candidate for efficacious treatment of sensitive or multidrug-resistant tumors.

3.4 Summary

The objective of this thesis was to evaluate the potential of numerous natural products and derivatives thereof as novel candidates for the treatment of multidrug-resistant tumors. In order to accomplish this aim, cell-based assays were established and optimized and compounds provided by cooperation partners from universities and industry in Düsseldorf, Wiesbaden and Cologne were screened for cytotoxic activity in sensitive and resistant cancer cell lines and for the inhibition of the human ABC transporters P-gp, MRP1 and BCRP. To date, these transporters belong to the main mediators of MDR in cancer.

Among the compound classes, which were studied, two novel, non-toxic derivatives of the natural product goniothalamin were identified as selective and moderate inhibitors of P-gp. Both derivatives were able to sensitize P-gp expressing colon carcinoma cells to doxorubicin treatment. Furthermore, ATPase assays and molecular docking studies indicated them to inhibit P-gp by being alternative transporter substrates. Moreover, novel cytotoxic derivatives were identified and displayed activity in sensitive as well as in resistant cell lines. In both cases, specific SAR could be described. Thus, the present work reveals directed structure modifications of goniothalamin either guiding activity towards P-gp inhibition or towards cytotoxicity.

In a second class of compounds, the 3,4-dihydroisocoumarins, three non-toxic compounds demonstrated dual inhibition of P-gp and BCRP and a distinct SAR for transporter inhibition was observed. To my knowledge, this is the first time that 3,4-dihydroisocoumarins were identified as inhibitors of ABC transporters. The most potent derivative was applied in co-treatment with chemotherapeutic drugs that are transporter substrates and a sensitization of P-gp colon carcinoma cells as well as BCRP expressing breast carcinoma cells to doxorubicin and mitoxantrone, respectively, could be demonstrated. In addition, another derivative with selective cytotoxicity in a BCRP-expressing cell line was identified.

Finally, novel colchicine-derived triazoles were analyzed for cytotoxic activity in several cancer cell lines and derivatives with higher potency in leukemia and solid tumor cell lines compared to the naturally occurring colchicine were identified. Moreover, the three most potent ones displayed improved inhibition of tubulin polymerization, which interferes with vital cellular processes resulting in apoptotic cell death.

In summary, novel natural product derivatives from different compound classes were identified in this thesis. Although additional evaluation of their mechanism of action and pharmacological activities is required, these compounds might serve a putative basis for further development of innovative chemotherapeutic drug candidates aiming at treating resistance to current therapies.

4 References

[1] Hanahan D, Weinberg RA. The hallmarks of cancer. Cell 2000;100:57–70.

[2] Negrini S, Gorgoulis VG, Halazonetis TD. Genomic instability - an evolving hallmark of cancer. Nat Rev Mol Cell Biol 2010;11:220–8.

[3] Fitzmaurice C, Allen C, Barber RM, Barregard L, Bhutta ZA, Brenner H et al. Global, Regional, and National Cancer Incidence, Mortality, Years of Life Lost, Years Lived With Disability, and Disability-Adjusted Life-years for 32 Cancer Groups, 1990 to 2015: A Systematic Analysis for the Global Burden of Disease Study. JAMA Oncol 2017;3:524–48.

[4] Robert Koch-Institut, Gesellschaft der epidemiologischen Krebsregister in Deutschland e.V., editors. Krebs in Deutschland für 2013/2014. Berlin: Robert Koch-Institut; 2017.

[5] Longley DB, Johnston PG. Molecular mechanisms of drug resistance. J Pathol 2005;205:275–92.

[6] Gillet J-P, Gottesman MM. Mechanisms of Multidrug Resistance in Cancer. In: Zhou J, editor. Multi-Drug Resistance in Cancer. Totowa, NJ: Humana Press; 2010. p. 47–76 .

[7] Khamisipour G, Jadidi-Niaragh F, Jahromi AS, Zandi K, Hojjat-Farsangi M. Mechanisms of tumor cell resistance to the current targeted-therapy agents. Tumour Biol 2016;37:10021–39.

[8] Gottesman MM, Fojo T, Bates SE. Multidrug resistance in cancer: Role of ATP-dependent transporters. Nat Rev Cancer 2002;2:48–58.

[9] Danø K. Active outward transport of daunomycin in resistant Ehrlich ascites tumor cells. Biochim Biophys Acta 1973;323:466–83.

[10] Holland IB, editor. ABC proteins: From bacteria to man. San Diego: Academic Press; 2003.

[11] Vasiliou V, Vasiliou K, Nebert DW. Human ATP-binding cassette (ABC) transporter family. Hum Genomics 2008;3:281.

[12] Mimmack ML, Gallagher MP, Pearce SR, Hyde SC, Booth IR, Higgins CF. Energy coupling to periplasmic binding protein-dependent transport systems: Stoichiometry of ATP hydrolysis during transport in vivo. Proc Natl Acad Sci USA 1989;86:8257–61.

[13] Hyde SC, Emsley P, Hartshorn MJ, Mimmack MM, Gileadi U, Pearce SR et al. Structural model of ATP-binding proteins associated with cystic fibrosis, multidrug resistance and bacterial transport. Nature 1990;346:362–5.

[14] Higgins CF, Hiles ID, Salmond GP, Gill DR, Downie JA, Evans IJ et al. A family of related ATP-binding subunits coupled to many distinct biological processes in bacteria. Nature 1986;323:448–50.

[15] Higgins CF, Gallagher MP, Mimmack ML, Pearce SR. A family of closely related ATP-binding subunits from prokaryotic and eukaryotic cells. Bioessays 1988;8:111–6.

[16] ter Beek J, Guskov A, Slotboom DJ. Structural diversity of ABC transporters. J Gen Physiol 2014;143:419–35.

[17] Qu Q, Sharom FJ. FRET analysis indicates that the two ATPase active sites of the P-glycoprotein multidrug transporter are closely associated. Biochemistry 2001;40:1413–22.

[18] Loo TW, Bartlett MC, Clarke DM. The "LSGGQ" motif in each nucleotide-binding domain of human P-glycoprotein is adjacent to the opposing walker A sequence. J Biol Chem 2002;277:41303–6.

[19] Wilkens S. Structure and mechanism of ABC transporters. F1000Prime Rep 2015;7:14.

[20] Jardetzky O. Simple Allosteric Model for Membrane Pumps. Nature 1966;211:969-970.

[21] Johnson ZL, Chen J. ATP Binding Enables Substrate Release from Multidrug Resistance Protein 1. Cell 2018;172:81-89.e10.

[22] Verhalen B, Dastvan R, Thangapandian S, Peskova Y, Koteiche HA, Nakamoto RK et al. Energy transduction and alternating access of the mammalian ABC transporter P-glycoprotein. Nature 2017;543:738–41.

[23] Szöllősi D, Rose-Sperling D, Hellmich UA, Stockner T. Comparison of mechanistic transport cycle models of ABC exporters. Biochim Biophys Acta 2017;1860:818–32.

[24] Higgins CF, Linton KJ. The ATP switch model for ABC transporters. Nat Struct Mol Biol 2004;11:918–26.

[25] Jones PM, George AM. Opening of the ADP-bound active site in the ABC transporter ATPase dimer: Evidence for a constant contact, alternating sites model for the catalytic cycle. Proteins 2009;75:387–96.

[26] Jones PM, George AM. A reciprocating twin-channel model for ABC transporters. Q Rev Biophys 2014;47:189–220.

[27] Langmann T, Mauerer R, Zahn A, Moehle C, Probst M, Stremmel W et al. Real-time reverse transcription-PCR expression profiling of the complete human ATP-binding cassette transporter superfamily in various tissues. Clin Chem 2003;49:230–8.

[28] Gillet J-P, Efferth T, Remacle J. Chemotherapy-induced resistance by ATP-binding cassette transporter genes. Biochim Biophys Acta 2007;1775:237–62.

[29] Leslie EM, Deeley RG, Cole SPC. Multidrug resistance proteins: Role of P-glycoprotein, MRP1, MRP2, and BCRP (ABCG2) in tissue defense. Toxicol Appl Pharmacol 2005;204:216–37.

[30] Sarkadi B, Homolya L, Szakács G, Váradi A. Human multidrug resistance ABCB and ABCG transporters: Participation in a chemoimmunity defense system. Physiol Rev 2006;86:1179–236.

[31] Taipalensuu J, Törnblom H, Lindberg G, Einarsson C, Sjöqvist F, Melhus H et al. Correlation of gene expression of ten drug efflux proteins of the ATP-binding cassette transporter family in normal human jejunum and in human intestinal epithelial Caco-2 cell monolayers. J Pharmacol Exp Ther 2001;299:164–70.

[32] Mahringer A, Fricker G. ABC transporters at the blood-brain barrier. Expert Opin Drug Metab Toxicol 2016;12:499–508.

[33] Cummins CL, Jacobsen W, Benet LZ. Unmasking the dynamic interplay between intestinal P-glycoprotein and CYP3A4. J Pharmacol Exp Ther 2002;300:1036–45.

[34] Glavinas H, Krajcsi P, Cserepes J, Sarkadi B. The role of ABC transporters in drug resistance, metabolism and toxicity. Curr Drug Deliv 2004;1:27–42.

[35] Tweedie D, Polli JW, Berglund EG, Huang SM, Zhang L, Poirier A et al. Transporter studies in drug development: Experience to date and follow-up on decision trees from the International Transporter Consortium. Clin Pharmacol Ther 2013;94:113–25.

[36] Zhou S, Schuetz JD, Bunting KD, Colapietro AM, Sampath J, Morris JJ et al. The ABC transporter Bcrp1/ABCG2 is expressed in a wide variety of stem cells and is a molecular determinant of the side-population phenotype. Nat Med 2001;7:1028–34.

[37] Lin T, Islam O, Heese K. ABC transporters, neural stem cells and neurogenesis-a different perspective. Cell Res 2006;16:857–71.

[38] Eggensperger S, Tampé R. The transporter associated with antigen processing: A key player in adaptive immunity. Biol Chem 2015;396:1059–72.

[39] Ling A, Löfgren-Burström A, Larsson P, Li X, Wikberg ML, Öberg Å et al. TAP1 down-regulation elicits immune escape and poor prognosis in colorectal cancer. Oncoimmunology 2017;6:e1356143.

[40] Riordan, Rommens J, Kerem B, Alon N, Rozmahel R, Grzelczak Z et al. Identification of the cystic fibrosis gene: Cloning and characterization of complementary DNA. Science 1989;245:1066–73.

[41] Cant N, Pollock N, Ford RC. CFTR structure and cystic fibrosis. Int J Biochem Cell Biol 2014;52:15–25.

[42] Rust S, Rosier M, Funke H, Real J, Amoura Z, Piette JC et al. Tangier disease is caused by mutations in the gene encoding ATP-binding cassette transporter 1. Nat Genet 1999;22:352–5.

[43] Allikmets R, Singh N, Sun H, Shroyer NF, Hutchinson A, Chidambaram A et al. A photoreceptor cell-specific ATP-binding transporter gene (ABCR) is mutated in recessive Stargardt macular dystrophy. Nat Genet 1997;15:236–46.

[44] Strautnieks SS, Bull LN, Knisely AS, Kocoshis SA, Dahl N, Arnell H et al. A gene encoding a liver-specific ABC transporter is mutated in progressive familial intrahepatic cholestasis. Nat Genet 1998;20:233–8.

[45] Deleuze JF, Jacquemin E, Dubuisson C, Cresteil D, Dumont M, Erlinger S et al. Defect of multidrug-resistance 3 gene expression in a subtype of progressive familial intrahepatic cholestasis. Hepatology 1996;23:904–8.

[46] El-Awady R, Saleh E, Hashim A, Soliman N, Dallah A, Elrasheed A et al. The Role of Eukaryotic and Prokaryotic ABC Transporter Family in Failure of Chemotherapy. Front Pharmacol 2017;7:535.

[47] Price RN, Uhlemann A-C, Brockman A, McGready R, Ashley E, Phaipun L et al. Mefloquine resistance in *Plasmodium falciparum* and increased pfmdr1 gene copy number. Lancet 2004;364:438–47.

[48] Prasad R, Wergifosse P de, Goffeau A, Balzi E. Molecular cloning and characterization of a novel gene of *Candida albicans*, CDR1, conferring multiple resistance to drugs and antifungals. Curr Genet 1995;27:320–9.

[49] Sanglard D, Ischer F, Monod M, Bille J. Cloning of *Candida albicans* genes conferring resistance to azole antifungal agents: Characterization of CDR2, a new multidrug ABC transporter gene. Microbiology 1997;143:405–16.

[50] Li Y, Atkinson K, Zhang T. Combination of chemotherapy and cancer stem cell targeting agents: Preclinical and clinical studies. Cancer Lett 2017;396:103–9.

[51] Hida K, Kikuchi H, Maishi N, Hida Y. ATP-binding cassette transporters in tumor endothelial cells and resistance to metronomic chemotherapy. Cancer Lett 2017;400:305–10.

[52] Shen DW, Cardarelli C, Hwang J, Cornwell M, Richert N, Ishii S et al. Multiple drug-resistant human KB carcinoma cells independently selected for high-level resistance to colchicine, adriamycin, or vinblastine show changes in expression of specific proteins. J Biol Chem 1986;261:7762–70.

[53] Slovak ML, Ho JP, Bhardwaj G, Kurz EU, Deeley RG, Cole SP. Localization of a novel multidrug resistance-associated gene in the HT1080/DR4 and H69AR human tumor cell lines. Cancer Res 1993;53:3221–5.

[54] Yang CH, Schneider E, Kuo ML, Volk EL, Rocchi E, Chen YC. BCRP/MXR/ABCP expression in topotecan-resistant human breast carcinoma cells. Biochem Pharmacol 2000;60:831–7.

[55] Wang J, Seebacher N, Shi H, Kan Q, Duan Z. Novel strategies to prevent the development of multidrug resistance (MDR) in cancer. Oncotarget 2017;8:84559–71.

[56] Szakács G, Annereau J-P, Lababidi S, Shankavaram U, Arciello A, Bussey KJ et al. Predicting drug sensitivity and resistance: Profiling ABC transporter genes in cancer cells. Cancer cell 2004;6:129–37.

[57] Park S, Shimizu C, Shimoyama T, Takeda M, Ando M, Kohno T et al. Gene expression profiling of ATP-binding cassette (ABC) transporters as a predictor of the pathologic response to neoadjuvant chemotherapy in breast cancer patients. Breast Cancer Res Treat 2006;99:9–17.

[58] Efferth T, Gillet J-P, Sauerbrey A, Zintl F, Bertholet V, Longueville F de et al. Expression profiling of ATP-binding cassette transporters in childhood T-cell acute lymphoblastic leukemia. Molecular cancer therapeutics 2006;5:1986–94.

[59] Leonard GD, Fojo T, Bates SE. The Role of ABC Transporters in Clinical Practice. Oncologist 2003;8:411–24.

[60] Szakács G, Paterson JK, Ludwig JA, Booth-Genthe C, Gottesman MM. Targeting multidrug resistance in cancer. Nat Rev Drug Discov 2006;5:219–34.

[61] Fletcher JI, Haber M, Henderson MJ, Norris MD. ABC transporters in cancer: More than just drug efflux pumps. Nat Rev Cancer 2010;10:147–56.

[62] Begicevic R-R, Falasca M. ABC Transporters in Cancer Stem Cells: Beyond Chemoresistance. Int J Mol Sci 2017;18.

[63] Vander Borght S, Komuta M, Libbrecht L, Katoonizadeh A, Aerts R, Dymarkowski S et al. Expression of multidrug resistance-associated protein 1 in hepatocellular carcinoma is associated with a more aggressive tumour phenotype and may reflect a progenitor cell origin. Liver Int 2008;28:1370–80.

[64] Hanada S, Maeshima A, Matsuno Y, Ohta T, Ohki M, Yoshida T et al. Expression profile of early lung adenocarcinoma: Identification of MRP3 as a molecular marker for early progression. J Pathol 2008;216:75–82.

[65] Henderson MJ, Haber M, Porro A, Munoz MA, Iraci N, Xue C et al. ABCC multidrug transporters in childhood neuroblastoma: Clinical and biological effects independent of cytotoxic drug efflux. J Natl Cancer Inst 2011;103:1236–51.

[66] Juliano RL, Ling V. A surface glycoprotein modulating drug permeability in Chinese hamster ovary cell mutants. Biochim Biophys Acta 1976;455:152–62.

[67] Aller SG, Yu J, Ward A, Weng Y, Chittaboina S, Zhuo R et al. Structure of P-glycoprotein reveals a molecular basis for poly-specific drug binding. Science 2009;323:1718–22.

[68] Li J, Jaimes KF, Aller SG. Refined structures of mouse P-glycoprotein. Protein Sci 2014;23:34–46.

[69] Alam A, Küng R, Kowal J, McLeod RA, Tremp N, Broude EV et al. Structure of a zosuquidar and UIC2-bound human-mouse chimeric ABCB1. Proc Natl Acad Sci USA 2018.

[70] Martin C, Berridge G, Higgins CF, Mistry P, Charlton P, Callaghan R. Communication between multiple drug binding sites on P-glycoprotein. Mol Pharmacol 2000;58:624–32.

[71] Mittra R, Pavy M, Subramanian N, George AM, O'Mara ML, Kerr ID et al. Location of contact residues in pharmacologically distinct drug binding sites on P-glycoprotein. Biochem Pharmacol 2017;123:19–28.

[72] Loo TW, Bartlett MC, Clarke DM. Substrate-induced conformational changes in the transmembrane segments of human P-glycoprotein. Direct evidence for the substrate-induced fit mechanism for drug binding. J Biol Chem 2003;278:13603–6.

[73] Ueda K, Taguchi Y, Morishima M. How does P-glycoprotein recognize its substrates? Semin Cancer Biol 1997;8:151–9.

[74] Montanari F, Ecker GF. Prediction of drug-ABC-transporter interaction—Recent advances and future challenges. Adv Drug Deliv Rev 2015;86:17–26.

[75] Choudhuri S, Klaassen CD. Structure, function, expression, genomic organization, and single nucleotide polymorphisms of human ABCB1 (MDR1), ABCC (MRP), and ABCG2 (BCRP) efflux transporters. Int J Toxicol 2006;25:231–59.

[76] Bugde P, Biswas R, Merien F, Lu J, Liu D-X, Chen M et al. The therapeutic potential of targeting ABC transporters to combat multi-drug resistance. Expert Opin Ther Targets 2017;21:511–30.

[77] Thiebaut F, Tsuruo T, Hamada H, Gottesman MM, Pastan I, Willingham MC. Cellular localization of the multidrug-resistance gene product P-glycoprotein in normal human tissues. Proc Natl Acad Sci USA 1987;84:7735–8.

[78] Cordon-Cardo C, O'Brien JP, Boccia J, Casals D, Bertino JR, Melamed MR. Expression of the multidrug resistance gene product (P-glycoprotein) in human normal and tumor tissues. J Histochem Cytochem 1990;38:1277–87.

[79] Fojo AT, Ueda K, Slamon DJ, Poplack DG, Gottesman MM, Pastan I. Expression of a multidrug-resistance gene in human tumors and tissues. Proc Natl Acad Sci USA 1987;84:265–9.

[80] Goldstein LJ, Galski H, Fojo A, Willingham M, Lai SL, Gazdar A et al. Expression of a multidrug resistance gene in human cancers. J Natl Cancer Inst 1989;81:116–24.

[81] Leith CP, Kopecky KJ, Chen IM, Eijdems L, Slovak ML, McConnell TS et al. Frequency and clinical significance of the expression of the multidrug resistance proteins MDR1/P-glycoprotein, MRP1, and LRP in acute myeloid leukemia: A Southwest Oncology Group Study. Blood 1999;94:1086–99.

[82] Han K, Kahng J, Kim M, Lim J, Kim Y, Cho B et al. Expression of functional markers in acute nonlymphoblastic leukemia. Acta Haematol 2000;104:174–80.

[83] Cole SP, Bhardwaj G, Gerlach JH, Mackie JE, Grant CE, Almquist KC et al. Overexpression of a transporter gene in a multidrug-resistant human lung cancer cell line. Science 1992;258:1650–4.

[84] Bakos E, Evers R, Szakács G, Tusnády GE, Welker E, Szabó K et al. Functional multidrug resistance protein (MRP1) lacking the N-terminal transmembrane domain. J Biol Chem 1998;273:32167–75.

[85] Westlake CJ, Cole SPC, Deeley RG. Role of the NH2-terminal membrane spanning domain of multidrug resistance protein 1/ABCC1 in protein processing and trafficking. Mol Biol Cell 2005;16:2483–92.

[86] Johnson ZL, Chen J. Structural Basis of Substrate Recognition by the Multidrug Resistance Protein MRP1. Cell 2017;168:1075-1085.e9.

[87] Flens MJ, Zaman GJ, van der Valk P, Izquierdo MA, Schroeijers AB, Scheffer GL et al. Tissue distribution of the multidrug resistance protein. Am J Pathol 1996;148:1237–47.

[88] Jedlitschky G, Leier I, Buchholz U, Barnouin K, Kurz G, Keppler D. Transport of glutathione, glucuronate, and sulfate conjugates by the MRP gene-encoded conjugate export pump. Cancer Res 1996;56:988–94.

[89] Rappa G, Lorico A, Flavell RA, Sartorelli AC. Evidence that the multidrug resistance protein (MRP) functions as a co-transporter of glutathione and natural product toxins. Cancer Res 1997;57:5232–7.

[90] He S-M, Li R, R. Kanwar J, Zhou S-F. Structural and Functional Properties of Human Multidrug Resistance Protein 1 (MRP1/ABCC1). Curr Med Chem 2011;18:439–81.

[91] Cole SPC. Targeting multidrug resistance protein 1 (MRP1, ABCC1): Past, present, and future. Annu Rev Pharmacol Toxicol 2014;54:95–117.

[92] Yoh K, Ishii G, Yokose T, Minegishi Y, Tsuta K, Goto K et al. Breast cancer resistance protein impacts clinical outcome in platinum-based chemotherapy for advanced non-small cell lung cancer. Clin Cancer Res 2004;10:1691–7.

[93] Li J, Li Z-N, Yu L-C, Bao Q-L, Wu J-R, Shi S-B et al. Association of expression of MRP1, BCRP, LRP and ERCC1 with outcome of patients with locally advanced non-

small cell lung cancer who received neoadjuvant chemotherapy. Lung Cancer 2010;69:116–22.

[94] Larkin A, O'Driscoll L, Kennedy S, Purcell R, Moran E, Crown J et al. Investigation of MRP-1 protein and MDR-1 P-glycoprotein expression in invasive breast cancer: A prognostic study. Int J Cancer 2004;112:286–94.

[95] Atalay C, Deliloglu Gurhan I, Irkkan C, Gunduz U. Multidrug resistance in locally advanced breast cancer. Tumour Biol 2006;27:309–18.

[96] Haber M, Smith J, Bordow SB, Flemming C, Cohn SL, London WB et al. Association of high-level MRP1 expression with poor clinical outcome in a large prospective study of primary neuroblastoma. J Clin Oncol 2006;24:1546–53.

[97] Doyle LA, Yang W, Abruzzo LV, Krogmann T, Gao Y, Rishi AK et al. A multidrug resistance transporter from human MCF-7 breast cancer cells. Proc Natl Acad Sci USA 1998;95:15665–70.

[98] Allikmets R, Schriml LM, Hutchinson A, Romano-Spica V, Dean M. A human placenta-specific ATP-binding cassette gene (ABCP) on chromosome 4q22 that is involved in multidrug resistance. Cancer Res 1998;58:5337–9.

[99] Miyake K, Mickley L, Litman T, Zhan Z, Robey R, Cristensen B et al. Molecular cloning of cDNAs which are highly overexpressed in mitoxantrone-resistant cells: Demonstration of homology to ABC transport genes. Cancer Res 1999;59:8–13.

[100] Taylor NMI, Manolaridis I, Jackson SM, Kowal J, Stahlberg H, Locher KP. Structure of the human multidrug transporter ABCG2. Nature 2017;546:504–9.

[101] Clark R, Kerr ID, Callaghan R. Multiple drugbinding sites on the R482G isoform of the ABCG2 transporter. Br J Pharmacol 2006;149:506–15.

[102] Ferreira RJ, Bonito CA, Cordeiro MNDS, Ferreira M-JU, dos Santos DJVA. Structure-function relationships in ABCG2: Insights from molecular dynamics simulations and molecular docking studies. Sci Rep 2017;7:15534.

[103] Maliepaard M, Scheffer GL, Faneyte IF, van Gastelen MA, Pijnenborg AC, Schinkel AH et al. Subcellular localization and distribution of the breast cancer resistance protein transporter in normal human tissues. Cancer Res 2001;61:3458–64.

[104] Jani M, Ambrus C, Magnan R, Jakab KT, Beéry E, Zolnerciks JK et al. Structure and function of BCRP, a broad specificity transporter of xenobiotics and endobiotics. Arch Toxicol 2014;88:1205–48.

[105] Robey RW, Ierano C, Zhan Z, Bates SE. The challenge of exploiting ABCG2 in the clinic. Curr Pharm Biotechnol 2011;12:595–608.

[106] Hirschmann-Jax C, Foster AE, Wulf GG, Nuchtern JG, Jax TW, Gobel U et al. A distinct "side population" of cells with high drug efflux capacity in human tumor cells. Proc Natl Acad Sci USA 2004;101:14228–33.

[107] Mo W, Zhang J-T. Human ABCG2: Structure, function, and its role in multidrug resistance. Int J Biochem Mol Bio 2011;3:1–27.

[108] Tsuruo T, Iida H, Tsukagoshi S, Sakurai Y. Overcoming of vincristine resistance in P388 leukemia in vivo and in vitro through enhanced cytotoxicity of vincristine and vinblastine by verapamil. Cancer Res 1981;41:1967–72.

[109] Naito M, Tsuruo T. Competitive inhibition by verapamil of ATP-dependent high affinity vincristine binding to the plasma membrane of multidrug-resistant K562 cells without calcium ion involvement. Cancer Res 1989;49:1452–5.

[110] Zahradníková A, Minarovic I, Zahradník I. Competitive and cooperative effects of Bay K8644 on the L-type calcium channel current inhibition by calcium channel antagonists. J Pharmacol Exp Ther 2007;322:638–45.

[111] Tsuruo T, Iida H, Kitatani Y, Yokota K, Tsukagoshi S, Sakurai Y. Effects of quinidine and related compounds on cytotoxicity and cellular accumulation of vincristine and adriamycin in drug-resistant tumor cells. Cancer Res 1984;44:4303–7.

[112] Slater LM, Sweet P, Stupecky M, Gupta S. Cyclosporin A reverses vincristine and daunorubicin resistance in acute lymphatic leukemia in vitro. J Clin Invest 1986;77:1405–8.

[113] Ozols RF, Cunnion RE, Klecker RW, Hamilton TC, Ostchega Y, Parrillo JE et al. Verapamil and adriamycin in the treatment of drug-resistant ovarian cancer patients. J Clin Oncol 1987;5:641–7.

[114] Warner E, Tobe SW, Andrulis IL, Pei Y, Trachtenberg J, Skorecki KL. Phase I-II study of vinblastine and oral cyclosporin A in metastatic renal cell carcinoma. Am J Clin Oncol 1995;18:251–6.

[115] Twentyman PR, Bleehen NM. Resistance modification by PSC-833, a novel non-immunosuppressive cyclosporin A. Eur J Cancer 1991;27:1639–42.

[116] Germann UA, Shlyakhter D, Mason VS, Zelle RE, Duffy JP, Galullo V et al. Cellular and biochemical characterization of VX-710 as a chemosensitizer: Reversal of P-glycoprotein-mediated multidrug resistance in vitro. Anticancer Drugs 1997;8:125–40.

[117] Baer MR, George SL, Dodge RK, O'Loughlin KL, Minderman H, Caligiuri MA et al. Phase 3 study of the multidrug resistance modulator PSC-833 in previously untreated patients 60 years of age and older with acute myeloid leukemia: Cancer and Leukemia Group B Study 9720. Blood 2002;100:1224–32.

[118] Kolitz JE, George SL, Marcucci G, Vij R, Powell BL, Allen SL et al. P-glycoprotein inhibition using valspodar (PSC-833) does not improve outcomes for patients younger than age 60 years with newly diagnosed acute myeloid leukemia: Cancer and Leukemia Group B study 19808. Blood 2010;116:1413–21.

[119] Gandhi L, Harding MW, Neubauer M, Langer CJ, Moore M, Ross HJ et al. A phase II study of the safety and efficacy of the multidrug resistance inhibitor VX-710 combined with doxorubicin and vincristine in patients with recurrent small cell lung cancer. Cancer 2007;109:924–32.

[120] Wandel C, Kim RB, Kajiji S, Guengerich P, Wilkinson GR, Wood AJ. P-glycoprotein and cytochrome P-450 3A inhibition: Dissociation of inhibitory potencies. Cancer Res 1999;59:3944–8.

[121] Dantzig AH, Shepard RL, Law KL, Tabas L, Pratt S, Gillespie JS et al. Selectivity of the multidrug resistance modulator, LY335979, for P-glycoprotein and effect on cytochrome P-450 activities. J Pharmacol Exp Ther 1999;290:854–62.

[122] Martin C, Berridge G, Mistry P, Higgins C, Charlton P, Callaghan R. The molecular interaction of the high affinity reversal agent XR9576 with P-glycoprotein. Br J Pharmacol 1999;128:403–11.

[123] van Zuylen L, Sparreboom A, van der Gaast A, van der Burg ME, van Beurden V, Bol CJ et al. The orally administered P-glycoprotein inhibitor R101933 does not alter the plasma pharmacokinetics of docetaxel. Clin Cancer Res 2000;6:1365–71.

[124] Pusztai L, Wagner P, Ibrahim N, Rivera E, Theriault R, Booser D et al. Phase II study of tariquidar, a selective P-glycoprotein inhibitor, in patients with chemotherapy-resistant, advanced breast carcinoma. Cancer 2005;104:682–91.

[125] Cripe LD, Uno H, Paietta EM, Litzow MR, Ketterling RP, Bennett JM et al. Zosuquidar, a novel modulator of P-glycoprotein, does not improve the outcome of older patients with newly diagnosed acute myeloid leukemia: A randomized, placebo-controlled trial of the Eastern Cooperative Oncology Group 3999. Blood 2010;116:4077–85.

[126] Kathawala RJ, Gupta P, Ashby CR, Chen Z-S. The modulation of ABC transporter-mediated multidrug resistance in cancer: A review of the past decade. Drug Resist Updat 2015;18:1–17.

[127] Beretta GL, Cassinelli G, Pennati M, Zuco V, Gatti L. Overcoming ABC transporter-mediated multidrug resistance: The dual role of tyrosine kinase inhibitors as multitargeting agents. Eur J Med Chem 2017;142:271–89.

[128] Germann UA, Ford PJ, Shlyakhter D, Mason VS, Harding MW. Chemosensitization and drug accumulation effects of VX-710, verapamil, cyclosporin A, MS-209 and GF120918 in multidrug resistant HL60/ADR cells expressing the multidrug resistance-associated protein MRP. Anticancer Drugs 1997;8:141–55.

[129] Gekeler V, Ise W, Sanders KH, Ulrich WR, Beck J. The leukotriene LTD4 receptor antagonist MK571 specifically modulates MRP associated multidrug resistance. Biochem Biophys Res Commun 1995;208:345–52.

[130] Bakos E, Evers R, Sinkó E, Váradi A, Borst P, Sarkadi B. Interactions of the human multidrug resistance proteins MRP1 and MRP2 with organic anions. Mol Pharmacol 2000;57:760–8.

[131] Norman BH, Lander PA, Gruber JM, Kroin JS, Cohen JD, Jungheim LN et al. Cyclohexyl-linked tricyclic isoxazoles are potent and selective modulators of the multidrug resistance protein (MRP1). Bioorg Med Chem Lett 2005;15:5526–30.

[132] Rabindran SK, Ross DD, Doyle LA, Yang W, Greenberger LM. Fumitremorgin C reverses multidrug resistance in cells transfected with the breast cancer resistance protein. Cancer Res 2000;60:47–50.

[133] Allen JD, van Loevezijn A, Lakhai JM, van der Valk M, van Tellingen O, Reid G et al. Potent and specific inhibition of the breast cancer resistance protein multidrug transporter in vitro and in mouse intestine by a novel analogue of fumitremorgin C. Mol Cancer Ther 2002;1:417–25.

[134] Bruin M de, Miyake K, Litman T, Robey R, Bates SE. Reversal of resistance by GF120918 in cell lines expressing the ABC half-transporter, MXR. Cancer Lett 1999;146:117–26.

[135] Robey RW, Steadman K, Polgar O, Morisaki K, Blayney M, Mistry P et al. Pheophorbide a is a specific probe for ABCG2 function and inhibition. Cancer Res 2004;64:1242–6.

[136] Minderman H, O'Loughlin KL, Pendyala L, Baer MR. VX-710 (biricodar) increases drug retention and enhances chemosensitivity in resistant cells overexpressing P-glycoprotein, multidrug resistance protein, and breast cancer resistance protein. Clin Cancer Res 2004;10:1826–34.

[137] Samalin E, Bouché O, Thézenas S, Francois E, Adenis A, Bennouna J et al. Sorafenib and irinotecan (NEXIRI) as second- or later-line treatment for patients with metastatic colorectal cancer and KRAS-mutated tumours: A multicentre Phase I/II trial. Br J Cancer 2014;110:1148–54.

[138] Pearson JW, Fogler WE, Volker K, Usui N, Goldenberg SK, Gruys E et al. Reversal of Drug Resistance in a Human Colon Cancer Xenograft Expressing MDR1 Complementary DNA by In Vivo Administration of MRK-16 Monoclonal Antibody. J Natl Cancer Inst 1991;83:1386–91.

[139] Mechetner EB, Roninson IB. Efficient inhibition of P-glycoprotein-mediated multidrug resistance with a monoclonal antibody. Proc Natl Acad Sci USA 1992;89:5824–8.

[140] Zhou Y, Gottesman MM, Pastan I. The extracellular loop between TM5 and TM6 of P-glycoprotein is required for reactivity with monoclonal antibody UIC2. Arch Biochem Biophys 1999;367:74–80.

[141] Szalóki G, Krasznai ZT, Tóth Á, Vízkeleti L, Szöllősi AG, Trencsényi G et al. The strong in vivo anti-tumor effect of the UIC2 monoclonal antibody is the combined result of Pgp inhibition and antibody dependent cell-mediated cytotoxicity. PloS one 2014;9:e107875.

[142] Nobili S, Landini I, Giglioni B, Mini E. Pharmacological strategies for overcoming multidrug resistance. Curr Drug Targets 2006;7:861–79.

[143] Bollag DM, McQueney PA, Zhu J, Hensens O, Koupal L, Liesch J et al. Epothilones, a new class of microtubule-stabilizing agents with a taxol-like mechanism of action. Cancer Res 1995;55:2325–33.

[144] Lin B, Catley L, LeBlanc R, Mitsiades C, Burger R, Tai Y-T et al. Patupilone (epothilone B) inhibits growth and survival of multiple myeloma cells in vitro and in vivo. Blood 2005;105:350–7.

[145] Sampath D, Discafani CM, Loganzo F, Beyer C, Liu H, Tan X et al. MAC-321, a novel taxane with greater efficacy than paclitaxel and docetaxel in vitro and in vivo. Mol Cancer Ther 2003;2:873–84.

[146] Minderman H, Brooks TA, O'Loughlin KL, Ojima I, Bernacki RJ, Baer MR. Broad-spectrum modulation of ATP-binding cassette transport proteins by the taxane derivatives ortataxel (IDN-5109, BAY 59-8862) and tRA96023. Cancer Chemother Pharmacol 2004;53:363–9.

[147] Bar-Zeev M, Livney YD, Assaraf YG. Targeted nanomedicine for cancer therapeutics: Towards precision medicine overcoming drug resistance. Drug Resist Updat 2017;31:15–30.

[148] Bell SE, Quinn DM, Kellett GL, Warr JR. 2-Deoxy-D-glucose preferentially kills multidrug-resistant human KB carcinoma cell lines by apoptosis. Br J Cancer 1998;78:1464–70.

[149] Dury L, Nasr R, Lorendeau D, Comsa E, Wong I, Zhu X et al. Flavonoid dimers are highly potent killers of multidrug resistant cancer cells overexpressing MRP1. Biochem Pharmacol 2017;124:10–8.

[150] Füredi A, Tóth S, Szebényi K, Pape VFS, Türk D, Kucsma N et al. Identification and Validation of Compounds Selectively Killing Resistant Cancer: Delineating Cell Line-Specific Effects from P-Glycoprotein-Induced Toxicity. Mol Cancer Ther 2017;16:45–56.

[151] Pluchino KM, Hall MD, Goldsborough AS, Callaghan R, Gottesman MM. Collateral sensitivity as a strategy against cancer multidrug resistance. Drug Resist Updat 2012;15:98–105.

[152] Demain AL, Fang A. The Natural Functions of Secondary Metabolites. In: Fiechter A, editor. History of Modern Biotechnology. Berlin, London: Springer; 2000. p. 1–39 (Advances in Biochemical Engineering/Biotechnology; vol. 69).

[153] Cragg GM, Grothaus PG, Newman DJ. Impact of natural products on developing new anti-cancer agents. Chem Rev 2009;109:3012–43.

[154] Guo Z. The modification of natural products for medical use. Acta Pharm Sin B 2017;7:119–36.

[155] Newman DJ, Cragg GM. Natural products as sources of new drugs from 1981 to 2014. J Nat Prod 2016;79:629–61.

[156] Wani MC, Taylor HL, Wall ME, Coggon P, McPhail AT. Plant antitumor agents. VI. Isolation and structure of taxol, a novel antileukemic and antitumor agent from *Taxus brevifolia*. J Am Chem Soc 1971;93:2325–7.

[157] Johnson IS, Armstrong JG, Gorman M, Burnett JP. The vinca alkaloids: a new class of oncolytic agents. Cancer Res 1963;23:1390–427.

[158] Arcamone F, Cassinelli G, Fantini G, Grein A, Orezzi P, Pol C et al. Adriamycin, 14-hydroxydaunomycin, a new antitumor antibiotic from *S. peucetius* var. *caesius*. Biotechnol Bioeng 1969;11:1101–10.

[159] Long S, Sousa E, Kijjoa A, Pinto MMM. Marine Natural Products as Models to Circumvent Multidrug Resistance. Molecules 2016;21.

[160] Guo Q, Cao H, Qi X, Li H, Ye P, Wang Z et al. Research Progress in Reversal of Tumor Multi-drug Resistance via Natural Products. Anticancer Agents Med Chem 2017;17:1466–76.

[161] Chearwae W, Anuchapreeda S, Nandigama K, Ambudkar SV, Limtrakul P. Biochemical mechanism of modulation of human P-glycoprotein (ABCB1) by curcumin I, II, and III purified from Turmeric powder. Biochem Pharmacol 2004;68:2043–52.

[162] Limtrakul P, Chearwae W, Shukla S, Phisalphong C, Ambudkar SV. Modulation of function of three ABC drug transporters, P-glycoprotein (ABCB1), mitoxantrone resistance protein (ABCG2) and multidrug resistance protein 1 (ABCC1) by tetrahydrocurcumin, a major metabolite of curcumin. Mol Cell Biochem 2007;296:85–95.

[163] Mapoung S, Pitchakarn P, Yodkeeree S, Ovatlarnporn C, Sakorn N, Limtrakul P. Chemosensitizing effects of synthetic curcumin analogs on human multi-drug resistance leukemic cells. Chem Biol Interact 2016;244:140–8.

[164] Rüegger A, Kuhn M, Lichti H, Loosli HR, Huguenin R, Quiquerez C et al. Cyclosporin A, ein immunsuppressiv wirksamer Peptidmetabolit aus *Trichoderma polysporum* (LINK ex PERS.) *Rifai*. Helv Chim Acta 1976;59:1075–92.

[165] Borel JF, Feurer C, Gubler HU, Stähelin H. Biological effects of cyclosporin A: A new antilymphocytic agent. Agents Actions 1976;6:468–75.

[166] Cui CB, Kakeya H, Osada H. Novel mammalian cell cycle inhibitors, tryprostatins A, B and other diketopiperazines produced by *Aspergillus fumigatus*. II. Physico-chemical properties and structures. J Antibiot 1996;49:534–40.

[167] Tan KW, Li Y, Paxton JW, Birch NP, Scheepens A. Identification of novel dietary phytochemicals inhibiting the efflux transporter breast cancer resistance protein (BCRP/ABCG2). Food Chem 2013;138:2267–74.

[168] Kim TH, Shin YJ, Won AJ, Lee BM, Choi WS, Jung JH et al. Resveratrol enhances chemosensitivity of doxorubicin in multidrug-resistant human breast cancer cells via increased cellular influx of doxorubicin. Biochim Biophys Acta 2014;1840:615–25.

[169] Mohana S, Ganesan M, Agilan B, Karthikeyan R, Srithar G, Beaulah Mary R et al. Screening dietary flavonoids for the reversal of P-glycoprotein-mediated multidrug resistance in cancer. Mol Biosyst 2016;12:2458–70.

[170] Hlubucek, JR, Robertson AV. (+)-(5S)-δ-Lactone of 5-hydroxy-7-phenylhepta-2,6-dienoic acid, a natural product from *Cryptocarya caloneura* (Scheff.) Kostermans. Aust J Chem 1967;20:2199–206.

[171] Jewers K, Davis JB, Dougan J, Manchanda AH, Blunden G, Kyi A et al. Goniothalamin and its distribution in four Goniothalamus species. Phytochemistry 1972;11:2025–30.

[172] Seyed MA, Jantan I, Bukhari SNA. Emerging anticancer potentials of goniothalamin and its molecular mechanisms. Biomed Res Int 2014;2014:536508.

[173] Wiart C. Ethnopharmacology of Medicinal Plants: Asia and the Pacific. Totowa, NJ: Humana Press; 2007.

[174] Mosaddik MA, Haque ME. Cytotoxicity and antimicrobial activity of goniothalamin isolated from *Bryonopsis laciniosa*. Phytother Res 2003;17:1155–7.

[175] Fatima A, Martins CV, Resende M de, Ferreira Magalhaes T, Santiago Lima B, Watanabe G et al. Antifungal activity of goniothalamin enantiomers. Lett Drug Des Discov 2008;5:74–8.

[176] Fátima A de, Marquissolo C, Albuquerque S de, Carraro-Abrahão AA, Pilli RA. Trypanocidal activity of 5,6-dihydropyran-2-ones against free trypomastigotes forms of *Trypanosoma cruzi*. Eur J Med Chem 2006;41:1210–3.

[177] Mohd Ridzuan MAR, Ruenruetai U, Noor Rain A, Khozirah S, Zakiah I. Antimalarial properties of Goniothalamin in combination with chloroquine against Plasmodium yoelii and Plasmodium berghei growth in mice. Trop Biomed 2006;23:140–6.

[178] Fátima A de, Kohn LK, Antônio MA, Carvalho JE de, Pilli RA. ®-Goniothalamin: Total syntheses and cytotoxic activity against cancer cell lines. Bioorg Med Chem 2005;13:2927–33.

[179] Chiu C-C, Liu P-L, Huang K-J, Wang H-M, Chang K-F, Chou C-K et al. Goniothalamin inhibits growth of human lung cancer cells through DNA damage, apoptosis, and reduced migration ability. J Agric Food Chem 2011;59:4288–93.

[180] Bruder M, Vendramini-Costa DB, Carvalho JE de, Pilli RA. Design, synthesis and in vitro evaluation against human cancer cells of 5-methyl-5-styryl-2,5-dihydrofuran-2-ones, a new series of goniothalamin analogues. Bioorg Med Chem 2013;21:5107–17.

[181] Innajak S, Mahabusrakum W, Watanapokasin R. Goniothalamin induces apoptosis associated with autophagy activation through MAPK signaling in SK-BR-3 cells. Oncol Rep 2016;35:2851–8.

[182] Boonmuen N, Thongon N, Chairoungdua A, Suksen K, Pompimon W, Tuchinda P et al. 5-Acetyl goniothalamin suppresses proliferation of breast cancer cells via Wnt/β-catenin signaling. Eur J Pharmacol 2016;791:455–64.

[183] Semprebon SC, Marques LA, D'Epiro GFR, Camargo EA de, da Silva GN, Niwa AM et al. Antiproliferative activity of goniothalamin enantiomers involves DNA damage, cell cycle arrest and apoptosis induction in MCF-7 and HB4a cells. Toxicol In Vitro 2015;30:250–63.

[184] Yen C-Y, Chiu C-C, Haung R-W, Yeh C-C, Huang K-J, Chang K-F et al. Antiproliferative effects of goniothalamin on Ca9-22 oral cancer cells through apoptosis, DNA damage and ROS induction. Mutat Res 2012;747:253–8.

[185] Kido LA, Montico F, Sauce R, Macedo AB, Minatel E, Costa DBV et al. Anti-inflammatory therapies in TRAMP mice: Delay in PCa progression. Endocr Relat Cancer 2016;23:235–50.

[186] Vendramini-Costa DB, Francescone R, Posocco D, Hou V, Dmitrieva O, Hensley H et al. Anti-inflammatory natural product goniothalamin reduces colitis-associated and sporadic colorectal tumorigenesis. Carcinogenesis 2017;38:51–63.

[187] Orlikova B, Schumacher M, Juncker T, Yan CC, Inayat-Hussain SH, Hajjouli S et al. Styryl-lactone goniothalamin inhibits TNF-α-induced NF-κB activation. Food Chem Toxicol 2013;59:572–8.

[188] Vendramini-Costa DB, Spindola HM, Mello GC de, Antunes E, Pilli RA, Carvalho JE de. Anti-inflammatory and antinociceptive effects of racemic goniothalamin, a styryl lactone. Life Sci 2015;139:83–90.

[189] Tian Z, Chen S, Zhang Y, Huang M, Shi L, Huang F et al. The cytotoxicity of naturally occurring styryl lactones. Phytomedicine 2006;13:181–6.

[190] Barcelos RC, Pastre JC, Caixeta V, Vendramini-Costa DB, Carvalho JE de, Pilli RA. Synthesis of methoxylated goniothalamin, aza-goniothalamin and γ-pyrones and their in vitro evaluation against human cancer cells. Bioorg Med Chem 2012;20:3635–51.

[191] Barcelos RC, Pastre JC, Vendramini-Costa DB, Caixeta V, Longato GB, Monteiro PA et al. Design and synthesis of N-acylated aza-goniothalamin derivatives and evaluation of their in vitro and in vivo antitumor activity. ChemMedChem 2014;9:2725–43.

[192] Weber A, Döhl K, Sachs J, Nordschild ACM, Schröder D, Kulik A et al. Synthesis and cytotoxic activities of goniothalamins and derivatives. Bioorg Med Chem 2017;25:6115–25.

[193] Sachs J, Kadioglu O, Weber A, Mundorf V, Betz J, Efferth T et al. Selective inhibition of the P-gp transporter by goniothalamin derivatives sensitizes resistant cancer cells to chemotherapy. Phytomedicine 2018;submitted.

[194] Saeed A. Isocoumarins, miraculous natural products blessed with diverse pharmacological activities. Eur J Med Chem 2016;116:290–317.

[195] Verastegui-Omaña B, Rebollar-Ramos D, Pérez-Vásquez A, Martínez AL, Madariaga-Mazón A, Flores-Bocanegra L et al. α-Glucosidase Inhibitors from *Malbranchea flavorosea*. J Nat Prod 2017;80:190–5.

[196] Zhang G-J, Li B, Chen L, Tian Y, Liu S-J, Cui H-M et al. Isocoumarin derivatives and monoterpene glycoside from the seeds of *Orychophragmus violaceus*. Fitoterapia 2018;125:111–6.

[197] Cichewicz RH, Valeriote FA, Crews P. Psymberin, a potent sponge-derived cytotoxin from *Psammocinia* distantly related to the pederin family. Org Lett 2004;6:1951–4.

[198] Abid O-u-R, Khalid M, Hussain MT, Hanif M, Qadeer G, Rama NH et al. Synthesis and anti-cancer, anti-metastatic evaluation of some new fluorinated isocoumarins and 3,4-dihydroisocoumarins. J Fluor Chem 2012;135:240–5.

[199] Guimarães KG, Freitas RP de, Ruiz ALTG, Fiorito GF, Carvalho JE de, da Cunha EFF et al. Synthesis, antiproliferative activities, and computational evaluation of novel isocoumarin and 3,4-dihydroisocoumarin derivatives. Eur J Med Chem 2016;111:103–13.

[200] Arora D, Sharma N, Singamaneni V, Sharma V, Kushwaha M, Abrol V et al. Isolation and characterization of bioactive metabolites from *Xylaria psidii*, an endophytic fungus of the medicinal plant *Aegle marmelos* and their role in mitochondrial dependent apoptosis against pancreatic cancer cells. Phytomedicine 2016;23:1312–20.

[201] Hoepfner D, McNamara CW, Lim CS, Studer C, Riedl R, Aust T et al. Selective and specific inhibition of the *Plasmodium falciparum* lysyl-tRNA synthetase by the fungal secondary metabolite cladosporin. Cell Host Microbe 2012;11:654–63.

[202] Lai D, Wang A, Cao Y, Zhou K, Mao Z, Dong X et al. Bioactive dibenzo-α-pyrone derivatives from the endophytic fungus *Rhizopycnis vagum* Nitaf22. J Nat Prod 2016;79:2022–31.

[203] Simic M, Paunovic N, Boric I, Randjelovic J, Vojnovic S, Nikodinovic-Runic J et al. Functionalised isocoumarins as antifungal compounds: Synthesis and biological studies. Bioorg Med Chem Lett 2016;26:235–9.

[204] Endringer DC, Guimarães KG, Kondratyuk TP, Pezzuto JM, Braga FC. Selective inhibition of aromatase by a dihydroisocoumarin from Xyris pterygoblephara. J Nat Prod 2008;71:1082–4.

[205] Teixeira TSP, Freitas RF, Abrahão O, Devienne KF, Souza LR de, Blaber SI et al. Biological evaluation and docking studies of natural isocoumarins as inhibitors for human kallikrein 5 and 7. Bioorg Med Chem Lett 2011;21:6112–5.

[206] Liang Q, Wu Q, Jiang J, Duan J'a, Wang C, Smith MD et al. Characterization of sparstolonin B, a Chinese herb-derived compound, as a selective Toll-like receptor antagonist with potent anti-inflammatory properties. J Biol Chem 2011;286:26470–9.

[207] Ramanan M, Sinha S, Sudarshan K, Aidhen IS, Doble M. Inhibition of the enzymes in the leukotriene and prostaglandin pathways in inflammation by 3-aryl isocoumarins. Eur J Med Chem 2016;124:428–34.

[208] Matsumoto N, Nakashima T, Isshiki K, Kuboki H, Hirano SI, Kumagai H et al. Synthesis and biological evaluation of cytogenin derivatives. J Antibiot 2001;54:285–96.

[209] Nakashima T, Hirano S, Agata N, Kumagai H, Isshiki K, Yoshioka T et al. Inhibition of angiogenesis by a new isocoumarin, NM-3. J Antibiot 1999;52:426–8.

[210] Reimer CL, Agata N, Tammam JG, Bamberg M, Dickerson WM, Kamphaus GD et al. Antineoplastic effects of chemotherapeutic agents are potentiated by NM-3, an inhibitor of angiogenesis. Cancer Res 2002;62:789–95.

[211] Chen J-L, Zhu J-S, Hong J, Chen M-X, Lu J-L, Chen W-X et al. Effect of 2-(8-hydroxy-6-methoxy-1-oxo-1H-2-benzopyran-3-yl) propionic acid in combination with carboplatin on gastric carcinoma growth in vivo. World J Gastroenterol 2007;13:509–14.

[212] Zhu J-S, Song M-Q, Chen G-Q, Li Q, Sun Q, Zhang Q. Molecular mechanisms of paclitaxel and NM-3 on human gastric cancer in a severe combined immune deficiency mice orthotopic implantation model. World J Gastroenterol 2007;13:4131–5.

[213] Salloum RM, Jaskowiak NT, Mauceri HJ, Seetharam S, Beckett MA, Koons AM et al. NM-3, an isocoumarin, increases the antitumor effects of radiotherapy without toxicity. Cancer Res 2000;60:6958–63.

[214] Barthomeuf C, Grassi J, Demeule M, Fournier C, Boivin D, Béliveau R. Inhibition of P-glycoprotein transport function and reversion of MDR1 multidrug resistance by cnidiadin. Cancer Chemother Pharmacol 2005;56:173–81.

[215] Raad I, Terreux R, Richomme P, Matera E-L, Dumontet C, Raynaud J et al. Structure-activity relationship of natural and synthetic coumarins inhibiting the multidrug transporter P-glycoprotein. Bioorg Med Chem 2006;14:6979–87.

[216] Lee K, Chae SW, Xia Y, Kim NH, Kim HJ, Rhie S et al. Effect of coumarin derivative-mediated inhibition of P-glycoprotein on oral bioavailability and therapeutic efficacy of paclitaxel. Eur J Pharmacol 2014;723:381–8.

[217] Bisi A, Cappadone C, Rampa A, Farruggia G, Sargenti A, Belluti F et al. Coumarin derivatives as potential antitumor agents: Growth inhibition, apoptosis induction and multidrug resistance reverting activity. Eur J Med Chem 2017;127:577–85.

[218] Combes S, Barbier P, Douillard S, McLeer-Florin A, Bourgarel-Rey V, Pierson J-T et al. Synthesis and biological evaluation of 4-arylcoumarin analogues of combretastatins. Part 2. J Med Chem 2011;54:3153–62.

[219] Champelovier P, Barbier P, Daras E, Douillard S, Toussaint B, Persoon V et al. The indolylcoumarin COUFIN exhibits potent activity against renal carcinoma cells without affecting hematopoietic system. Anticancer Agents Med Chem 2014;14:862–71.

[220] Geiger PL. Ueber einige neue giftige organische Alkalien. In: Brandes R, Geiger PL, Liebig J, editors. Annalen der Pharmacie: Meyerschen Hof-Buchh. und der Winterschen Universitäts-Buchh.; 1833. p. 269–80 (vol. 7).

[221] Nuki G, Simkin PA. A concise history of gout and hyperuricemia and their treatment. Arthritis Res Ther 2006;8 Suppl 1:S1.

[222] Weisenberg RC, Borisy GG, Taylor EW. The colchicine-binding protein of mammalian brain and its relation to microtubules. Biochemistry 1968;7:4466–79.

[223] Ravelli RBG, Gigant B, Curmi PA, Jourdain I, Lachkar S, Sobel A et al. Insight into tubulin regulation from a complex with colchicine and a stathmin-like domain. Nature 2004;428:198–202.

[224] Bhattacharyya B, Panda D, Gupta S, Banerjee M. Anti-mitotic activity of colchicine and the structural basis for its interaction with tubulin. Med Res Rev 2008;28:155–83.

[225] Bates D, Eastman A. Microtubule destabilising agents: Far more than just antimitotic anticancer drugs. Br J Clin Pharmacol 2017;83:255–68.

[226] Nicolaou KC, Valiulin RA, Pokorski JK, Chang V, Chen JS. Bio-inspired synthesis and biological evaluation of a colchicine-related compound library. Bioorg Med Chem Lett 2012;22:3776–80.

[227] Zhang X, Kong Y, Zhang J, Su M, Zhou Y, Zang Y et al. Design, synthesis and biological evaluation of colchicine derivatives as novel tubulin and histone deacetylase dual inhibitors. Eur J Med Chem 2015;95:127–35.

[228] Kumar A, Singh B, Mahajan G, Sharma PR, Bharate SB, Mintoo MJ et al. A novel colchicine-based microtubule inhibitor exhibits potent antitumor activity by inducing mitochondrial mediated apoptosis in MIA PaCa-2 pancreatic cancer cells. Tumour Biol 2016;37:13121–36.

[229] Kumar A, Sharma PR, Mondhe DM. Potential anticancer role of colchicine-based derivatives: An overview. Anticancer Drugs 2017;28:250–62.

[230] Ghawanmeh AA, Chong KF, Sarkar SM, Bakar MA, Othaman R, Khalid RM. Colchicine prodrugs and codrugs: Chemistry and bioactivities. Eur J Med Chem 2018;144:229–42.

[231] Roninson IB, Chin JE, Choi KG, Gros P, Housman DE, Fojo A et al. Isolation of human mdr DNA sequences amplified in multidrug-resistant KB carcinoma cells. Proc Natl Acad Sci USA 1986;83:4538–42.

[232] Silva R, Carmo H, Vilas-Boas V, Barbosa DJ, Palmeira A, Sousa E et al. Colchicine effect on P-glycoprotein expression and activity: In silico and in vitro studies. Chem Biol Interact 2014;218:50–62.

[233] Perez EA. Microtubule inhibitors: Differentiating tubulin-inhibiting agents based on mechanisms of action, clinical activity, and resistance. Mol Cancer Ther 2009;8:2086–95.

[234] Singh B, Kumar A, Joshi P, Guru SK, Kumar S, Wani ZA et al. Colchicine derivatives with potent anticancer activity and reduced P-glycoprotein induction liability. Org Biomol Chem 2015;13:5674–89.

[235] Thomopoulou P, Sachs J, Teusch N, Mariappan A, Gopalakrishnan J, Schmalz H-G. New colchicine-derived triazoles and their influence on cytotoxicity and microtubule morphology. ACS Med Chem Lett 2016;7:188–91.

[236] Fátima A de, Modolo LV, Conegero LS, Pilli RA, Ferreira CV, Kohn LK et al. Styryl lactones and their derivatives: Biological activities, mechanisms of action and potential leads for drug design. Curr Med Chem 2006;13:3371–84.

[237] Weiss J, Sauer A, Frank A, Unger M. Extracts and kavalactones of Piper methysticum G. Forst (kava-kava) inhibit P-glycoprotein in vitro. Drug Metab Dispos 2005;33:1580–3.

[238] Litman T, Zeuthen T, Skovsgaard T, Stein WD. Competitive, non-competitive and cooperative interactions between substrates of P-glycoprotein as measured by its ATPase activity. Biochim Biophys Acta 1997;1361:169–76.

[239] Richter O von, Glavinas H, Krajcsi P, Liehner S, Siewert B, Zech K. A novel screening strategy to identify ABCB1 substrates and inhibitors. Naunyn Schmiedebergs Arch Pharmacol 2009;379:11–26.

[240] Ferreira RJ, Ferreira M-JU, dos Santos DJVA. Molecular docking characterizes substrate-binding sites and efflux modulation mechanisms within P-glycoprotein. J Chem Inf Model 2013;53:1747–60.

[241] Mirski SE, Gerlach JH, Cole SP. Multidrug resistance in a human small cell lung cancer cell line selected in adriamycin. Cancer Res 1987;47:2594–8.

[242] Adamska A, Elaskalani O, Emmanouilidi A, Kim M, Abdol Razak NB, Metharom P et al. Molecular and cellular mechanisms of chemoresistance in pancreatic cancer. Adv Biol Regul 2017.

[243] Desai JR, Ochoa S, Prins PA, He AR. Systemic therapy for advanced hepatocellular carcinoma: An update. J Gastrointest Oncol 2017;8:243–55.

[244] Inayat-Hussain SH, Osman AB, Din LB, Ali AM, Snowden RT, MacFarlane M et al. Caspases-3 and -7 are activated in goniothalamin-induced apoptosis in human Jurkat T-cells. FEBS Lett 1999;456:379–83.

[245] Chen W-Y, Wu C-C, Lan Y-H, Chang F-R, Teng C-M, Wu Y-C. Goniothalamin induces cell cycle-specific apoptosis by modulating the redox status in MDA-MB-231 cells. Eur J Pharmacol 2005;522:20–9.

[246] Pires BRB, Silva RCMC, Ferreira GM, Abdelhay E. NF-kappaB: Two Sides of the Same Coin. Genes 2018;9.

[247] Li F, Zhang J, Arfuso F, Chinnathambi A, Zayed ME, Alharbi SA et al. NF-κB in cancer therapy. Arch Toxicol 2015;89:711–31.

[248] Barcelos RC, Pelizzaro-Rocha KJ, Pastre JC, Dias MP, Ferreira-Halder CV, Pilli RA. A new goniothalamin N-acylated aza-derivative strongly downregulates mediators of

signaling transduction associated with pancreatic cancer aggressiveness. Eur J Med Chem 2014;87:745–58.

[249] Vendramini-Costa DB, Castro IBD de, Ruiz ALTG, Marquissolo C, Pilli RA, Carvalho JE de. Effect of goniothalamin on the development of Ehrlich solid tumor in mice. Bioorg Med Chem 2010;18:6742–7.

[250] Arvelo F, Poupon MF, Goguel AF, Lizard G, Bourgeois Y, Arriagada R et al. Response of a multidrug-resistant human small-cell lung cancer xenograft to chemotherapy. J Cancer Res Clin Oncol 1993;120:17–23.

[251] Katayama R, Sakashita T, Yanagitani N, Ninomiya H, Horiike A, Friboulet L et al. P-glycoprotein Mediates Ceritinib Resistance in Anaplastic Lymphoma Kinase-rearranged Non-small Cell Lung Cancer. EBioMedicine 2016;3:54–66.

[252] Jung J, Seol HS, Chang S. The Generation and Application of Patient-Derived Xenograft Model for Cancer Research. Cancer Res Treat 2018;50:1–10.

[253] Benderra Z, Faussat A-M, Sayada L, Perrot J-Y, Chaoui D, Marie J-P et al. Breast cancer resistance protein and P-glycoprotein in 149 adult acute myeloid leukemias. Clin Cancer Res 2004;10:7896–902.

[254] Wilson CS, Davidson GS, Martin SB, Andries E, Potter J, Harvey R et al. Gene expression profiling of adult acute myeloid leukemia identifies novel biologic clusters for risk classification and outcome prediction. Blood 2006;108:685–96.

[255] Ho MM, Hogge DE, Ling V. MDR1 and BCRP1 expression in leukemic progenitors correlates with chemotherapy response in acute myeloid leukemia. Exp Hematol 2008;36:433–42.

[256] Dohse M, Scharenberg C, Shukla S, Robey RW, Volkmann T, Deeken JF et al. Comparison of ATP-binding cassette transporter interactions with the tyrosine kinase inhibitors imatinib, nilotinib, and dasatinib. Drug Metab Dispos 2010;38:1371–80.

[257] Wijaya J, Fukuda Y, Schuetz JD. Obstacles to Brain Tumor Therapy: Key ABC Transporters. Int J Mol Sci 2017;18.

[258] Lin F, Gooijer MC de, Roig EM, Buil LCM, Christner SM, Beumer JH et al. ABCB1, ABCG2, and PTEN determine the response of glioblastoma to temozolomide and ABT-888 therapy. Clin Cancer Res 2014;20:2703–13.

[259] Li X-Q, Wang L, Lei Y, Hu T, Zhang F-L, Cho C-H et al. Reversal of P-gp and BCRP-mediated MDR by tariquidar derivatives. Eur J Med Chem 2015;101:560–72.

[260] Gu X, Ren Z, Peng H, Peng S, Zhang Y. Bifendate-chalcone hybrids: A new class of potential dual inhibitors of P-glycoprotein and breast cancer resistance protein. Biochem Biophys Res Commun 2014;455:318–22.

[261] Sim HM, Loh KY, Yeo WK, Lee CY, Go ML. Aurones as modulators of ABCG2 and ABCB1: Synthesis and structure-activity relationships. ChemMedChem 2011;6:713–24.

[262] Rao DK, Liu H, Ambudkar SV, Mayer M. A combination of curcumin with either gramicidin or ouabain selectively kills cells that express the multidrug resistance-linked ABCG2 transporter. J Biol Chem 2014;289:31397–410.

[263] Licht T, Fiebig HH, Bross KJ, Herrmann F, Berger DP, Shoemaker R et al. Induction of multiple-drug resistance during anti-neoplastic chemotherapy in vitro. Int J Cancer 1991;49:630–7.

[264] Allen JD, Brinkhuis RF, van Deemter L, Wijnholds J, Schinkel AH. Extensive contribution of the multidrug transporters P-glycoprotein and Mrp1 to basal drug resistance. Cancer Res 2000;60:5761–6.

[265] Tang-Wai DF, Brossi A, Arnold LD, Gros P. The nitrogen of the acetamido group of colchicine modulates P-glycoprotein-mediated multidrug resistance. Biochemistry 1993;32:6470–6.

[266] Cosentino L, Redondo-Horcajo M, Zhao Y, Santos AR, Chowdury KF, Vinader V et al. Synthesis and biological evaluation of colchicine B-ring analogues tethered with halogenated benzyl moieties. J Med Chem 2012;55:11062–6.

[267] Ludueña RF, Banerjee A. The Isotypes of Tubulin. In: Fojo T, editor. The Role of Microtubules in Cell Biology, Neurobiology, and Oncology. Totowa, NJ: Humana Press; 2008. p. 123–75 (Cancer Drug Discovery and Development).

[268] Burkhart CA, Kavallaris M, Band Horwitz S. The role of beta-tubulin isotypes in resistance to antimitotic drugs. Biochim Biophys Acta 2001;1471:O1-9.

[269] Kamath K, Wilson L, Cabral F, Jordan MA. βIII-tubulin induces paclitaxel resistance in association with reduced effects on microtubule dynamic instability. J Biol Chem 2005;280:12902–7.

[270] Stengel C, Newman SP, Leese MP, Potter BVL, Reed MJ, Purohit A. Class III beta-tubulin expression and in vitro resistance to microtubule targeting agents. Br J Cancer 2010;102:316–24.

[271] Sève P, Mackey J, Isaac S, Trédan O, Souquet P-J, Pérol M et al. Class III beta-tubulin expression in tumor cells predicts response and outcome in patients with non-small cell lung cancer receiving paclitaxel. Mol Cancer Ther 2005;4:2001–7.

[272] Roque DM, Bellone S, Buza N, Romani C, Cocco E, Bignotti E et al. Class III β-tubulin overexpression in ovarian clear cell and serous carcinoma as a maker for poor overall survival after platinum/taxane chemotherapy and sensitivity to patupilone. Am J Obstet Gynecol 2013;209:62.e1-9.

[273] Rai A, Kapoor S, Naaz A, Kumar Santra M, Panda D. Enhanced stability of microtubules contributes in the development of colchicine resistance in MCF-7 cells. Biochem Pharmacol 2017;132:38–47.

[274] Kavallaris M. Microtubules and resistance to tubulin-binding agents. Nat Rev Cancer 2010;10:194–204.

[275] Giannakakou P, Sackett DL, Kang YK, Zhan Z, Buters JT, Fojo T et al. Paclitaxel-resistant human ovarian cancer cells have mutant beta-tubulins that exhibit impaired paclitaxel-driven polymerization. J Biol Chem 1997;272:17118–25.

[276] Barlow SB, Gonzalez-Garay ML, Cabral F. Paclitaxel-dependent mutants have severely reduced microtubule assembly and reduced tubulin synthesis. J Cell Sci 2002;115:3469–78.

[277] Poruchynsky MS, Kim J-H, Nogales E, Annable T, Loganzo F, Greenberger LM et al. Tumor cells resistant to a microtubule-depolymerizing hemiasterlin analogue, HTI-286, have mutations in alpha- or beta-tubulin and increased microtubule stability. Biochemistry 2004;43:13944–54.

[278] Tseng C-Y, Mane JY, Winter P, Johnson L, Huzil T, Izbicka E et al. Quantitative analysis of the effect of tubulin isotype expression on sensitivity of cancer cell lines to a set of novel colchicine derivatives. Mol Cancer 2010;9:131.

[279] Yeh L-CC, Banerjee A, Prasad V, Tuszynski JA, Weis AL, Bakos T et al. Effect of CH-35, a novel anti-tumor colchicine analogue, on breast cancer cells overexpressing the βIII isotype of tubulin. Invest New Drugs 2016;34:129–37.

[280] Wang RC, Chen X, Parissenti AM, Joy AA, Tuszynski J, Brindley DN et al. Sensitivity of docetaxel-resistant MCF-7 breast cancer cells to microtubule-destabilizing agents including vinca alkaloids and colchicine-site binding agents. PloS one 2017;12:e0182400.

5 Appendix

5.1 List of Test Compounds

5.1.1 Goniothalamin Derivatives

The compounds were synthesized at the *Institute of Bioorganic Chemistry, Heinrich-Heine-Universität Düsseldorf im Forschungszentrum Jülich* (*M.Sc. Anja Weber, Prof. Dr. Jörg Pietruszka*).

Table A1. Goniothalamin derivatives.

Name	Structure	Chemical formula	Molecular weight (g/mol)
***rac*-1**	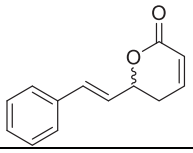	$C_{13}H_{12}O_2$	200.24
(*R*)-1	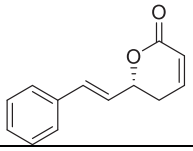	$C_{13}H_{12}O_2$	200.24
(*S*)-1	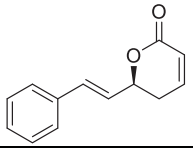	$C_{13}H_{12}O_2$	200.24
(*R*)-23c	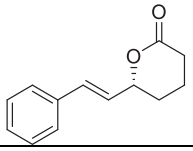	$C_{13}H_{14}O_2$	202.25
(*S*)-23c	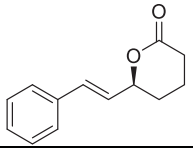	$C_{13}H_{14}O_2$	202.25
(*R*)-2	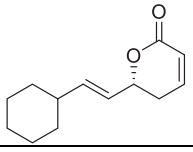	$C_{13}H_{18}O_2$	206.29
(*S*)-2	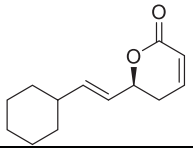	$C_{13}H_{18}O_2$	206.29

(*R*)-25	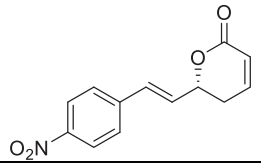	$C_{13}H_{11}NO_4$	245.23
(*S*)-25	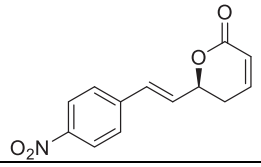	$C_{13}H_{11}NO_4$	245.23
(*R*)-3	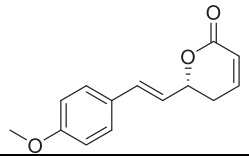	$C_{14}H_{14}O_3$	230.26
(*S*)-3	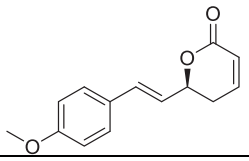	$C_{14}H_{14}O_3$	230.26
(*R*)-23e	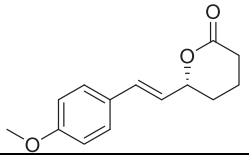	$C_{14}H_{16}O_3$	232.28
(*S*)-23e	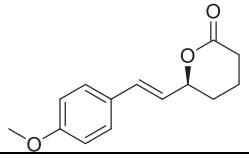	$C_{14}H_{16}O_3$	232.28
(*R*)-24	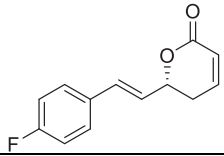	$C_{13}H_{11}FO_2$	218.23
(*S*)-24	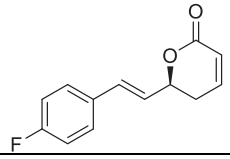	$C_{13}H_{11}FO_2$	218.23
(*R*)-23a	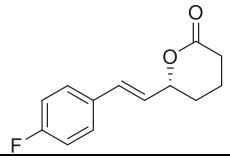	$C_{13}H_{13}FO_2$	220.24
(*S*)-23a	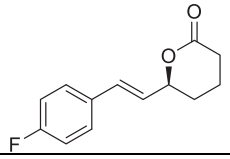	$C_{13}H_{13}FO_2$	220.24
(*R,S,S*)-4	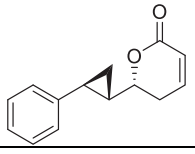	$C_{14}H_{14}O_2$	214.26

(*R*,*R*,*R*)-4	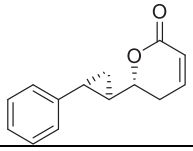	$C_{14}H_{14}O_2$	214.26
(*S*,*S*,*S*)-4	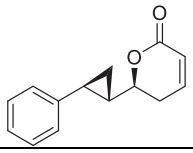	$C_{14}H_{14}O_2$	214.26
(*R*,*R*,*R*)-26	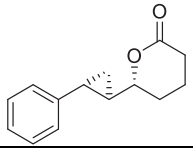	$C_{14}H_{16}O_2$	216.28
(*R*,*R*)-27	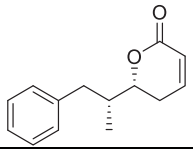	$C_{14}H_{16}O_2$	216.28
(*S*,*S*,*S*)-26	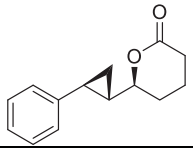	$C_{14}H_{16}O_2$	216.28
(*R*,*S*,*S*)-26	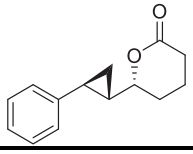	$C_{14}H_{16}O_2$	216.28

5.1.2 Isocoumarin Derivatives

The compounds were synthesized at the *Institute of Bioorganic Chemistry, Heinrich-Heine-Universität Düsseldorf im Forschungszentrum Jülich* (*M.Sc. Anja Weber, Prof. Dr. Jörg Pietruszka*). Ellagic acid was provided by *MicroCombiChem GmbH, Wiesbaden* (*Dr. Edmond Fleischer, Dr. Anette Klinger*).

Table A2. Isocoumarin derivatives.

Name	Structure	Chemical formula	Molecular weight (g/mol)
14	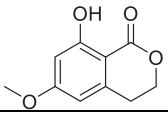	$C_{10}H_{10}O_4$	194.19
14a	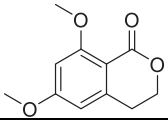	$C_{11}H_{12}O_4$	208.21
6-Methoxymellein (3)	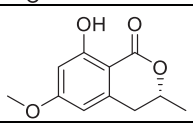	$C_{11}H_{12}O_4$	208.07

Angelicoin B (4)	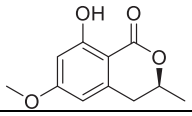	$C_{11}H_{12}O_4$	208.07
16	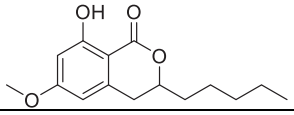	$C_{15}H_{20}O_4$	264.14
16a	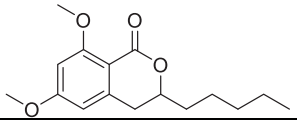	$C_{16}H_{22}O_4$	278.15
(*R*)-19	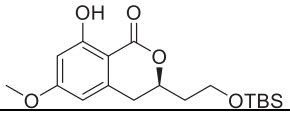	$C_{18}H_{28}O_5Si$	352.17
(*S*)-19	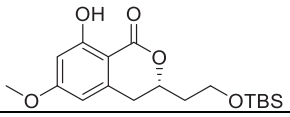	$C_{18}H_{28}O_5Si$	352.17
(*R*)-19a	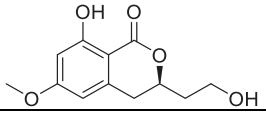	$C_{12}H_{14}O_5$	238.08
(*S*)-19a	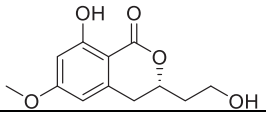	$C_{12}H_{14}O_5$	238.08
21	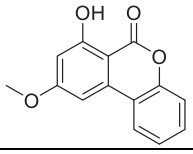	$C_{14}H_{10}O_4$	242.06
Ellagic acid (MCC7348)	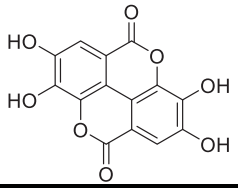	$C_{14}H_6O_8$	302.19

5.1.3 Colchicine Derivatives

The compounds were synthesized at the *Department of Chemistry, Universität zu Köln* (*Dr. Persefoni Thomopoulou, Prof. Dr. Hans-Günther Schmalz*).

Table A3. Colchicine derivatives.

Name	Structure	Chemical formula	Molecular weight (g/mol)
1	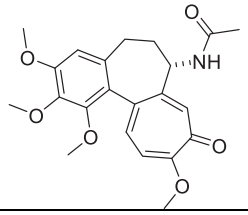	$C_{22}H_{25}NO_6$	399.44

2	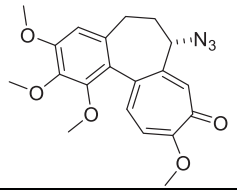	$C_{20}H_{21}N_3O_5$	383.40
3a	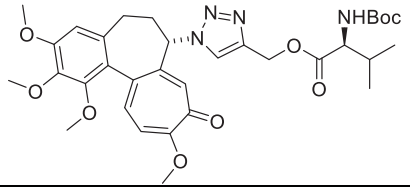	$C_{33}H_{42}N_4O_9$	638.72
3b	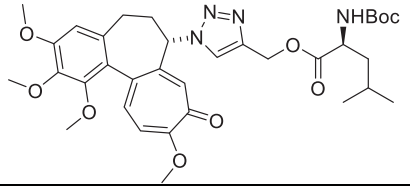	$C_{34}H_{44}N_4O_9$	652.75
3c	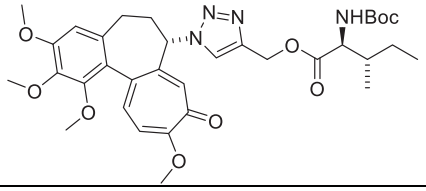	$C_{34}H_{44}N_4O_9$	652.75
3d	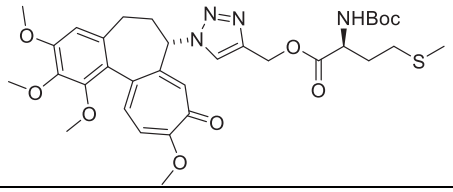	$C_{33}H_{42}N_4O_9S$	670.78
3e	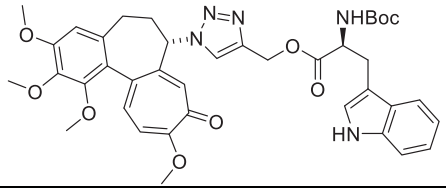	$C_{39}H_{43}N_5O_9$	725.80
3f	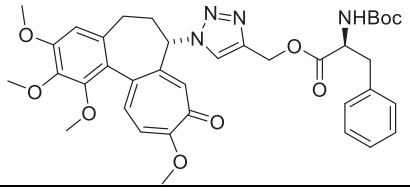	$C_{37}H_{42}N_4O_9$	686.76
3g	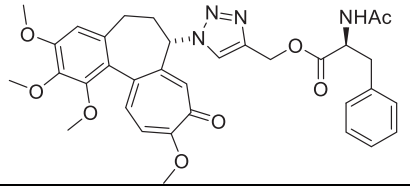	$C_{34}H_{36}N_4O_8$	628.68
3h	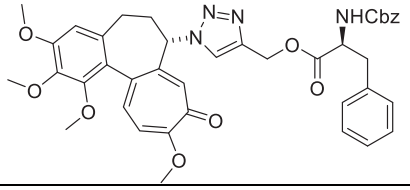	$C_{40}H_{40}N_4O_9$	720.78

3i	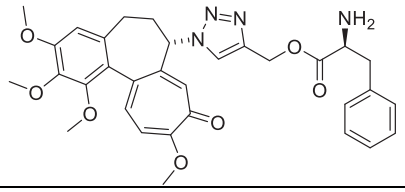	$C_{32}H_{34}N_4O_7$	586.65
3j	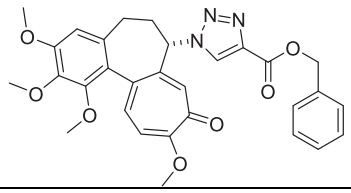	$C_{30}H_{29}N_3O_7$	543.58
3k	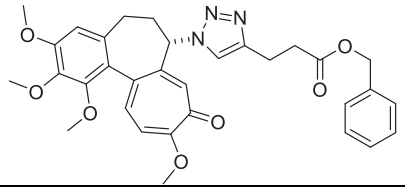	$C_{32}H_{33}N_3O_7$	571.63
3l	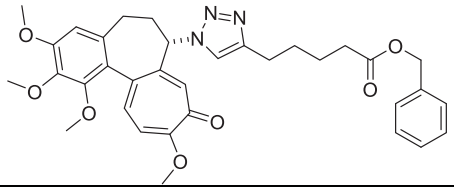	$C_{34}H_{37}N_3O_7$	599.68
3m	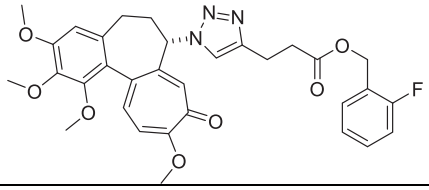	$C_{32}H_{32}FN_3O_7$	589.62
3n	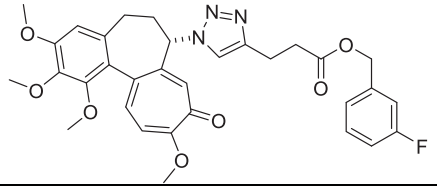	$C_{32}H_{32}FN_3O_7$	589.62
3o	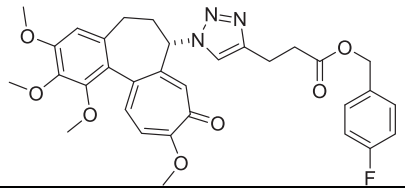	$C_{32}H_{32}FN_3O_7$	589.62
3p	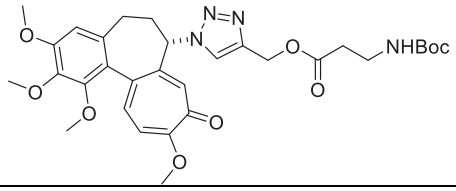	$C_{31}H_{38}N_4O_9$	610.66
3q	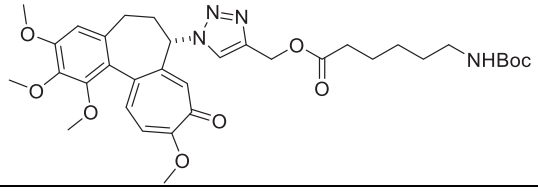	$C_{34}H_{44}N_4O_9$	652.75

3r	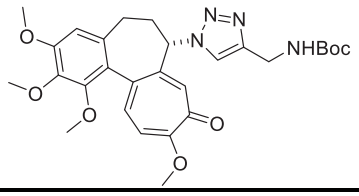	$C_{28}H_{34}N_4O_7$	538.60

Danksagung

Als erstes möchte ich mich bei Prof. Dr. Nicole Teusch bedanken. Ich danke dir, dass ich an diesem interessanten Thema arbeiten durfte, für die Unterstützung während der gesamten Promotion und dass du es mir ermöglicht hast, an Konferenzen, Weiterbildungen und Graduiertenprogrammen teilzunehmen.

Prof. Dr. Lutz Schmitt danke ich herzlich, dass er die Aufgabe des universitären Betreuers übernommen hat.

Ein großer Dank geht an die ZIM-Kooperationspartner. Dr. Anette Klinger und Dr. Edmond Fleischer von der MicroCombiChem GmbH, Katja Döhl und Prof. Dr. Lutz Schmitt vom Institut für Biochemie der Heinrich-Heine-Universität sowie Anja Weber und Prof. Dr. Jörg Pietruszka vom Institut für Bioorganische Chemie der Heinrich-Heine-Universität. Ich möchte mich bei euch und Ihnen für die gute und erfolgreiche Zusammenarbeit in diesem Projekt bedanken. Ebenso danke ich den ehemaligen Projektpartnern Dr. Thomas Fischer und Dr. Yoen Ok Roth von BIO-MAR Düsseldorf.

Ich danke Dr. Persefoni Thomopoulou und Prof. Dr. Hans-Günther von Department für Chemie der Universität zu Köln, die die Colchicin-Derivate zur Verfügung gestellt haben, sowie Dr. Onat Kadioglu und Prof. Dr. Thomas Efferth vom Institut für Pharmazie und Biochemie der Johannes Gutenberg-Universität Mainz, die das molekulare Docking der Goniothalamin-Derivate durchgeführt haben. Vielen Dank für die gute Zusammenarbeit.

Dem Graduiertenprogramm „Pharmacology & Experimental Therapeutics“ der Universität zu Köln und der Bayer AG, dem Graduierteninstitut NRW, Fachgruppe Lebenswissenschaften sowie dem Graduiertenzentrum der TH Köln danke ich für die Unterstützung und Weiterbildungsmöglichkeiten während der Promotion.

Ein großer Dank geht an die fleißigen Studenten, die mich während meiner Arbeit unterstützt haben: meiner Praktikantin Amanda Perozzo aus Kanada, meinen Bachelorstudenten Vanessa Mundorf, Dennis Mittag und Ferdinand Blesse und meinen wissenschaftlichen Hilfskräften Vanessa Mundorf und Janina Betz. Vielen Dank für eure Unterstützung des Projekts, ihr habt tolle Arbeit geleistet und zum Gelingen dieser Arbeit beigetragen. Ich wünsche euch für eure Zukunft alles Gute.

Liebes 5. OG, vielen Dank für die letzten 3,5 Jahre. Es war wirklich schön mit euch und ich hatte eine tolle Zeit mit euch, egal ob im Labor, bei den ausführlichen „Paperbesprechungen“ oder nach der Arbeit. Ihr seid super, ich werde euch alle vermissen. Auch dem Rest der Fakultät 11 danke ich für die gemeinsame Zeit.

Ein besonders großer Dank geht an meine Eltern und meine Schwester für die Unterstützung zu jeder Zeit. Meinem Freund Jörg danke ich, dass er immer für mich da ist, fürs Aufmuntern, Zuhören und Unterstützen, vor allem in den letzten Wochen.

Lebenslauf

Julia Sachs

Ausbildung

seit 09/2014	Technische Hochschule Köln Bio-Pharmazeutische Chemie & Molekulare Pharmakologie Kooperative Promotion mit der Heinrich-Heine-Universität Düsseldorf, Institut für Biochemie Thema: „Pharmacological Characterization of Natural Products as Drug Candidates for the Treatment of Multidrug-Resistant Tumors“ Mitglied im Graduiertenprogramm „Pharmacology & Experimental Therapeutics“, Universität zu Köln & Bayer AG und im Graduierteninstitut NRW, Fachgruppe Lebenswissenschaften
10/2011-09/2013	Medizinische Hochschule Hannover Master of Science, Biomedizin (1,5) Masterarbeit: „Expansion of pluripotent stem cell-derived endodermal progenitor cells: Molecular characterisation and evaluation of their hepatic differentiation capacity“, Translationale Hepatologie & Stammzellbiologie, Medizinische Hochschule Hannover
10/2008-08/2011	Goethe-Universität Frankfurt/Main Bachelor of Science, Biowissenschaften (1,4) Bachelorarbeit: „Characterisation of HsfB1 mutant lines in tomato“, Molekulare Zellbiologie der Pflanzen, Institut für molekulare Biowissenschaften, Goethe-Universität Frankfurt/Main
06/2008	Main-Taunus-Schule Hofheim Abitur (1,8)

Publikationen

2018	**Sachs, J.**, Kadioglu, O., Weber, A., Mundorf, V., Betz, J., Efferth, T., Pietruszka, J., Teusch, N. (2018). Selective inhibition of the P-gp transporter by goniothalamin derivatives sensitizes resistant cancer cells to chemotherapy. Phytomedicine (submitted).
2017	Weber, A., Döhl, K., **Sachs, J.**, Nordschild, A.C.M., Schröder, D., Kulik, A., Fischer, T., Schmitt, L., Teusch, N., Pietruszka, J. (2017). Synthesis and cytotoxic activities of goniothalamins and derivatives. Biorg. Med. Chem. 25, 6115-6125.

2016	Thomopoulou, P., **Sachs, J.**, Teusch, N., Mariappan, A., Gopalakrishnan, J., Schmalz, H.-G. (2016). New colchicine-derived triazoles and their influence on cytotoxicity and microtubule morphology. ACS Med. Chem. Lett. 7, 188-191.

Konferenzteilnahmen

10/2017	Cologne Excellent Women in Science Symposium, Universität zu Köln Poster: „Pharmacological inhibition of the P-gp transporter by goniothalamin derivatives sensitizes resistant cancer cells to chemotherapy“
03/2017	Gordon Research Seminar & Conference „Multi-Drug Efflux Systems“, Galveston, TX, USA Poster & Vortrag: „Pharmacological inhibition of the P-gp transporter by goniothalamin derivatives sensitizes resistant cancer cells to chemotherapy“
12/2016	Cell-VIB Symposium „Hallmarks of Cancer“, Gent, Belgien Poster: „Novel pharmacological activities of the natural product goniothalamin in multidrug-resistant cancer cells“

Vorträge

10/2017	Annual Retreat 2017, Graduiertenprogramm „Pharmacology & Experimental Therapeutics“ Titel: „Pharmacological inhibition of the P-gp transporter by goniothalamin derivatives sensitizes resistant cancer cells to chemotherapy“
03/2017	Gordon Research Conference „Multi-Drug Efflux Systems“, Galveston, TX, USA Titel: „Pharmacological inhibition of the P-gp transporter by goniothalamin derivatives sensitizes resistant cancer cells to chemotherapy“
11/2016	Annual Retreat 2016, Graduiertenprogramm „Pharmacology & Experimental Therapeutics“ Titel: „Natural Compounds as Candidates for the Treatment of Multidrug Resistant Tumors“
11/2015	Annual Retreat 2015, Graduiertenprogramm „Pharmacology & Experimental Therapeutics“ Titel: „Natural Compounds as Candidates for the Treatment of Multidrug Resistant Tumors“

Betreute Abschlussarbeiten

2017	Ferdinand Blesse, Technische Hochschule Köln

	Bachelorarbeit „Identifizierung pflanzlicher Naturstoffe als neue Wirkstoffe zur Behandlung multiresistenter Tumore“
	Dennis Mittag, Technische Hochschule Köln Bachelorarbeit „Charakterisierung pflanzlicher Naturstoffe bezüglich ihrer pharmakologischen Wirkung auf ABC-Transporterproteine in multiresistenten Tumorzellen“
2016	Vanessa Mundorf, Technische Hochschule Köln Bachelorarbeit „Charakterisierung von Naturstoffen und deren Einfluss auf die Aktivität von ABC-Transportern in Tumorzellen“

Eidesstattliche Erklärung

Ich versichere an Eides Statt, dass die Dissertation von mir selbständig und ohne unzulässige fremde Hilfe unter Beachtung der „Grundsätze zur Sicherung guter wissenschaftlicher Praxis an der Heinrich-Heine-Universität Düsseldorf“ erstellt worden ist. Die Dissertation wurde in der vorgelegten oder in ähnlicher Form noch bei keiner anderen Fakultät eingereicht. Ich habe bisher keine erfolglosen und erfolgreichen Promotionsversuche unternommen.

Die Promotion wurde an der Technischen Hochschule Köln, Fakultät für Angewandte Naturwissenschaften in der Arbeitsgruppe „Bio-Pharmazeutische Chemie & Molekulare Pharmakologie“ unter Anleitung von Prof. Dr. Nicole Teusch durchgeführt.

Köln, den 08.03.2018

Julia Sachs